

Inherently chiral calixarenes; methodology and applications

by

Dominic Christian Castell

*Submitted in partial fulfilment of the requirements for the degree
Doctor of Philosophy*



at

Stellenbosch University

Department of Chemistry and Polymer Science
Faculty of Science

Supervisor: Dr. G. E. Arnott

Date: August 2016

DECLARATION

By submitting this thesis electronically, I declare that the entirety of the work contained therein is my own, original work, that I am the owner of the copyright thereof (unless to the extent explicitly stated otherwise) and that I have not previously in its entirety or in part submitted it for obtaining any qualification.

Signature

Name in full

_____/_____/_____
Date

Abstract

The use of chiral directing groups has provided an efficient route to *meta*-functionalised inherently chiral calixarenes. Previously reported ortholithiation methods, incorporating chiral oxazolines have been reexamined, with the aim of revising the individual roles of the three major components of the reaction. The potential mechanistic ramifications of the solvent, additive and alkyllithium structure on the reaction outcomes were individually evaluated. The overarching complexity inherent in this chemistry, coupled with a wide scope of experimental results, point to a number of substrate, solvent and also reagent dependent reaction mechanisms.

In addition to the oxazolines, the *tert*-butyl sulfoxide functional group has also been established as an effective chiral auxiliary for this ortholithiation strategy, yielding enriched diastereomeric mixtures of inherently chiral sulfoxide calixarenes. The absolute stereochemistry of these major and minor products were determined crystallographically. Despite restrictions in electrophile choice, an efficient desulfurization method afforded a route to a new class of *meta*-functionalised inherently chiral compounds.

With the view to evaluating the potential of inherent chirality, oxazoline-directed ortholithiation methods were used to synthesize a new class of inherently chiral phosphine oxazoline ligands. The results from the application studies of these compounds, to both the Tsuji-Trost allylation and asymmetric Suzuki coupling reactions, suggested a definitive relationship between the configurations of the inherent chirality of the calixarene, and central chirality of the oxazoline auxiliary. A model of the π -allyl palladium intermediate responsible for the enantioselection seen in the Tsuji-Trost reaction has been proposed for these calixarene ligands. The model was constructed using previously reported calixarene crystallographic data, in conjunction with numerous solid-state and computational studies of simpler Phox ligand systems. The experimental results obtained for this reaction were found to be in good correlation with the proposed model for the inherently chiral calixarene ligands.

To confirm these observations, two additional inherently chiral Phox ligands, lacking a stereocenter on the oxazoline, were synthesized. Their preliminary application to the Tsuji-Trost allylation also yielded enantiomerically enriched product mixtures. These results point to a significant contribution made by the inherent chirality, toward the overall asymmetric induction observed in the reaction. These findings serve as a positive affirmation of the viability of inherently chiral calixarenes in the field of asymmetric catalysis, and create a platform for further development of new ligands containing this structural property.

Opsomming

Die gebruik van chirale regie groepe verskaf 'n doeltreffende roete tot *meta*-gefunksionaliseerde inherente chirale calixarene. Ortolitiëring metodes wat chirale oksasoliene inkorporeer, waarop daar voorheen verslag gelewer is, is weer ondersoek. Hierdie ondersoek is onderneem om die individuele rolle van die drie hoofkomponente van die reaksie te hersien. Die potensiële meganistiese effek van die oplosmiddel, ligande, en alkiellitiumstruktuur op die reaksie uitkomstes (not sure about uitkomstes, maybe produkte?), is individueel ondersoek. Die oorkoepelende inherente kompleksiteit van hierdie chemie, tesame met die breë omvang van die eksperimentele resultate, dui daarop dat daar 'n hele paar substraat-, oplosmiddel-, en reagensafhanklike reaksiemeganismes teenwoordig is.

Tersiêre-butielsulfoksied funksionele groepe is ook bevestig as 'n effektiewe chirale hulpsgroep vir hierdie ortolitiëstrategie, wat 'n opbrengs van verrykte diastereomeriese mengsels van inherente chirale sulfoksied calixarene lewer. Die absolute stereochemie van die hoof- en byprodukte is bepaal deur die gebruik van kristallografie. Ten spyte van beperkte keuse van elektrofile, is 'n doeltreffende ontswawelingsmetode gebruik om 'n nuwe klas van *meta*-gefunksionaliseerde inherent chirale molekule te produseer.

Oksasolien-gerigte ortolitiëstrategie is gebruik om 'n reeks nuwe inherente chirale fosfiene ligande te sintetiseer, en om sodoende die potensiaal van inherente chiraliteit te evalueer. Die resultate van die toepassingstudies van hierdie molekules op beide die Tsuji-Trost allilering en die asimetriese Suzuki koppelingsreaksies, dui op 'n definitiewe verhouding tussen die konfigurasie van die inherente chiraliteit van die calixarene en die sentrale chiraliteit van die oksasoliene hulpsgroep. 'n Hipotetiese model van die π -alliel palladium intermediêr wat verantwoordelik is vir die enantiomeer seleksie wat tydens Tsuji-Trost reaksie waargeneem word, is vir die calixarene ligande voorgestel. Die model is gebou deur die gebruik van voorheen gerapporteerde kristallografiese data, talle vastetoestand studies en berekeningsstudies van eenvoudige fosfienoksasolienligandsisteme. Die eksperimentele resultate wat vir hierdie reaksie verkry is, het goed gekorreleer met die voorgestelde model vir die inherente chirale calixarene ligande.

Twee addisionele inherent chirale fosfienoksasolienligande waar die stereosentrum op die oksasolien ontbreek, is gesintetiseer om hierdie waarnemings te bevestig. Hul voorlopige toepassing op die Tsuji-Trost allilering het ook enantiomeriese verrykte produkmenngsels opgelewer. Hierdie resultate dui op 'n betekenisvolle bydrae deur die inherente chiraliteit tot die algehele asimetriese induksie wat in die reaksie waargeneem word. Hierdie bevindinge dien as 'n positiewe bevestiging van die moontlike sukses van inherente chirale calixarene in die gebied van asimetriese katalise, en skep 'n fondasie waarop verdere ontwikkeling gedoen kan word van nuwe ligande wat hierdie strukturele eienskap besit.

Acknowledgements

First on my list of thanks are my parents, who have never let me down and given me more than I could ever return. My supervisor, Dr. Gareth Arnott, who has not only put up with me, but has provided the constant support and enthusiasm for this project. Thank you to my fellow students in the GOMOC research group for the support and chemistry related aid when it was needed. A big thank you to technical staff, Mary, Raymond and Debbie, whose efforts go a long way to keeping the cogs turning. Thank you to the NRF and STIAS organizations for providing me with generous financial support, without which none of this would have been possible. Thank you to Stellenbosch University for providing me with the opportunity and to Prof. Jonathan Williams at Bath University for hosting me during my time abroad.

There are many people that have not been mentioned, who deserve so much more than a written thank you (You all know who you are). The three I am going to mention are Prof. Delia Haynes, Dr. Varvara Nikolayenko and Mr. Dylan Ranger. To Delia, your open door policy and positive spin on my never ending rants helped carry me through these many years of study. For Varia, besides being a terrifyingly competent chemist, you made integral contributions to the crystallography component of this dissertation. You have been a constant source of motivation and support throughout this whole process (even when I was grumpy). Finally, thank you to Dylan, who despite not being a scientist, read and edited the entire final draft.

Publications

Herbert, S. A., Arnott, G. E., Clayden, J., Castell, D. C., "Manipulating the Diastereoselectivity of Ortholithiation in Planar Chiral Ferrocenes" *Org. Lett.*, **2013**, 15 (13), pp 3334-3337

Herbert, S. A., Arnott, G. E., Castell, D. C., van Laeren, L. J., "Inherently chiral calix[4]arenes via oxazoline directed ortholithiation: synthesis and probe of chiral space" *Beilstein J. Org. Chem.*, **2014**, 10, pp 2751-2755

Conferences

Frank Warren, **2015**, The Stellenbosch Institute for Advanced Study (STIAS), poster presentation.

Abbreviations

^1H	Proton NMR
^{13}C	Carbon NMR
^{31}P	Phosphorus NMR
<i>de</i>	Diastereomeric excess
<i>ee</i>	Enantiomeric excess
HPLC	High performance liquid chromatography
IR	Infrared spectroscopy
Mp	Melting point
MS	Mass spectrometry
MW	Microwave reaction
NMR	Nuclear magnetic resonance
R_f	Retention factor
R_t	Retention time
Δ	Heat
TLC	Thin layer chromatography
HMPA	Hexamethylphosphoramide
DMPU	1,3-Dimethyl-3,4,5,6-tetrahydro-2-pyrimidinone
PMDTA	<i>N,N,N',N'',N'''</i> -pentamethyldiethylenetriamine
TMEDA	<i>N,N,N',N'</i> -Tetramethylethane-1,2-diamine

Table of contents

1	Chapter 1 - Introduction.....	1
1.1	The history, synthesis and classification of calixarenes.	1
1.1.1	The history of calixarene synthesis.	1
1.1.2	The early synthesis of calixarenes.	3
1.1.3	The structural and conformational properties of calixarenes.....	4
1.1.4	The classification of calixarene conformations.	5
1.1.5	Classification of inherently chiral calixarenes.	6
1.2	The synthesis of inherently chiral calixarenes.....	9
1.2.1	The non-stereoselective synthesis of inherently chiral calixarenes.....	9
1.2.2	The stereoselective synthesis of inherently chiral calixarenes.	16
1.3	The application of inherently chiral calixarenes.....	19
1.3.1	The earliest reports of catalysis.....	19
1.3.2	Relating chirality to catalysis.	19
1.3.3	The application of inherently chiral ligands functionalized on the lower-rim.	21
1.3.4	The application of inherently chiral ligands functionalized on the upper-rim.....	22
1.4	Proposed project and targeted outcomes.	26
1.5	References:.....	27
2	Chapter 2 - Synthesis of calixarene starting materials.....	32
2.1	Introduction.....	32
2.2	Synthesis of the parent <i>tert</i> -butyl calixarene.....	33
2.3	Synthesis of debutylated calixarenes.....	33
2.3.1	Synthesis of tetra-hydroxyl calixarene – 53	33
2.3.2	Synthesis of tetra-propoxy calixarene – 54	34
2.3.3	Synthesis of mono-bromo calixarene – 55	37
2.3.4	Synthesis of carboxyl calixarene – 56	38
2.3.5	Synthesis of the isopropyl oxazoline calixarene – 57	39
2.3.6	Synthesis of <i>tert</i> -butyl oxazoline calixarene – 58	41

2.4	Synthesis of <i>tert</i> -butyl calixarenes.	42
2.4.1	Synthesis of tri-propoxy calixarene – 59	42
2.4.2	Synthesis of tri-propoxy nitro calixarene – 60	43
2.4.3	Synthesis of tetra-propoxy nitro calixarene – 61	44
2.4.4	Synthesis of amino calixarene – 62	45
2.4.5	Synthesis of iodo calixarene – 63	46
2.4.6	Synthesis of carboxyl calixarene – 65	47
2.4.7	The synthesis of butylated isopropyl oxazoline – 66	47
2.4.8	The synthesis of butylated <i>tert</i> -butyl oxazoline – 67	48
2.5	Conclusion	50
2.6	Experimental section.	50
2.7	References:	62
3	Chapter 3 - Ortholithiation of oxazoline calixarene	63
3.1	Introduction.	63
3.2	Preparation of alkyllithium reagents.	64
3.2.1	Synthesis of alkyllithiums.	64
3.2.2	Characterization of the alkyllithium bases – confirmation of structure.	66
3.3	The ortholithiation of isopropyl and <i>tert</i> -butyl oxazoline calixarenes 57 and 58	66
3.3.1	The ortholithiation reaction - a summary of past results.	66
3.3.2	Revisiting the ortholithiation of isopropyl oxazoline - 57	69
3.3.3	Revisiting the ortholithiation of <i>tert</i> -butyl oxazoline – 58	72
3.3.4	The addition and de-aromatization products.	75
3.4	The ortholithiation of <i>tert</i> -butyl oxazoline – 67	79
3.5	Discussion.	80
3.5.1	Introduction – the mechanism of ortholithiation.	80
3.5.2	The general ortholithiation reaction mechanism.	81
3.5.3	The ligand – impacting the activation and aggregation of alkyllithiums.	82
3.5.4	The alkyllithium – the influence of reactivity and steric hindrance.	85
3.5.5	The impact of solvent choice.	89

3.6	Conclusion.....	90
3.7	Experimental section.....	91
3.8	References:.....	100
4	Chapter 4 - Ortholithiation of sulfoxide calixarene.....	102
4.1	Introduction.....	102
4.2	Synthesis of the chiral thiosulfinate ester.....	104
4.3	Synthesis of sulfoxide calixarene.....	105
4.4	Ortholithiation of mono-sulfoxide calixarene – 76	107
4.4.1	Previously reported results.....	107
4.4.1	The nature of the solvent mixture.....	110
4.4.2	Quenching with different electrophiles – an investigation of versatility.....	112
4.5	Determining the absolute configuration of inherently chiral calixarene products.....	113
4.5.1	Configurations of the major and minor product diastereomers.....	113
4.5.2	Assigning the absolute configuration of the diastereomer products.....	118
4.5.3	The crystallographic approach.....	119
4.6	Removal of the sulfoxide group – the desulfurization reaction.....	124
4.7	Discussion – unravelling the ortholithiation of sulfoxide calixarene - 76	125
4.8	Conclusion.....	127
4.9	Experimental section:.....	128
4.10	References:.....	135
5	Chapter 5 – Synthesis of phosphine oxazoline calixarene ligands.....	139
5.1	Introduction.....	139
5.2	First attempts at phosphine oxazoline calixarene synthesis.....	141
5.3	“Taming the beast” that was phosphorus.....	142
5.3.1	Synthesis and ortholithiation of N,N-di-isopropyl benzamide.....	142
5.4	Synthesis of the model phosphine oxazoline ligands.....	144
5.4.1	Selecting a suitable model compound.....	144
5.4.2	Synthesis of isopropyl and tert-butyl model oxazolines – 89 and 90	145
5.4.3	Ortholithiation of the model oxazoline – an optimization study.....	146

5.4.4	Synthesis of the model phosphine oxazoline ligands – 92 and 93 .	148
5.5	Synthesis of calixarene Phox ligands.	150
5.5.1	Preventing phosphine oxidation.	150
5.6	Indirect characterisation of the calixarene Phox ligands.	151
5.7	Conclusion.	153
5.8	Experimental section.	153
5.9	References:	169
6	Chapter 6 - The application of inherently chiral phosphine oxazoline ligands	171
6.1	Introduction.	171
6.2	Asymmetric Tsuji-Trost allylation.	171
6.2.1	Introduction.	171
6.2.2	Results.	171
6.2.3	Discussion.	174
6.2.4	Conclusion.	182
6.3	Asymmetric Heck coupling	182
6.3.1	Introduction.	182
6.3.2	Results and discussion.	182
6.3.3	Conclusion.	184
6.4	Asymmetric Suzuki-Miyaura coupling	184
6.4.1	Introduction.	184
6.4.2	Results.	185
6.4.3	Discussion.	188
6.4.4	Conclusion	189
6.5	A purely inherently chiral phosphine oxazoline ligand	189
6.5.1	Introduction.	189
6.5.2	Synthesis of purely inherently chiral calixarene Phox ligands.	189
6.6	The Tsuji-Trost allylation reaction revisited.	193
6.6.1	Discussion.	193
6.6.2	Conclusion.	195

6.7	Experimental section:.....	195
6.8	References:.....	206
7	Conclusions and future work.....	209
7.1	Conclusions.....	209
7.2	Further developing asymmetric synthesis of inherently chiral calixarenes.....	210
7.2.1	Oxazoline calixarenes.	210
7.2.2	Sulfoxide calixarenes.....	211
7.3	The application of inherently chiral calixarenes.....	212
7.3.1	Calixarene PhOx ligands.....	212
7.3.2	Synthesis of inherently chiral ligands using the sulfoxide chiral auxiliary.....	216
7.4	Final Remarks.....	217
7.5	References:.....	218
8	Additional supporting information.....	220
8.1	General Practices.....	220
8.1.1	Solvents and reagents.	220
8.1.2	Temperature control.	220
8.1.3	Inert conditions.	220
8.1.4	Chromatography.....	220
8.1.5	Characterization.	221
8.2	Reagents required for starting material synthesis.....	221
8.3	Reagents required for ortholithiation studies.....	222
8.4	Reagents required for ligand application studies.....	223
8.5	Single-crystal x-ray diffraction data.....	225

1 Chapter 1 - Introduction

1.1 The history, synthesis and classification of calixarenes.

1.1.1 The history of calixarene synthesis.

Although the chemical structure of calixarene was only confirmed in 1964,¹ the early beginnings of calixarene chemistry can be traced back to the work of Adolf von Baeyer in the 1870s. In 1872 he was interested in the reactions between phenol and formaldehyde in the presence of strong acids. One such reaction produced what he described as a 'cement-like substance'. His most significant observation was the formation of a resinous substance in many of his reactions. Unfortunately, no pure substances were ever isolated from these mixtures, making it impossible for him to propose any chemical structures. His findings were reported in two papers, which are regarded as the first in the field of phenol-formaldehyde chemistry.²

Following in the footsteps of Bayer were a number of chemists, including: Lederer,³ Maneese,⁴ Blumer,^{5,6} Storey⁷ and Luft.⁸ They were interested in the same phenol-formaldehyde chemistry, but were not able to isolate something of value from the thick resinous tars. In the end, they were not able to find any materials of significant commercial value, and as a result interest in the work declined. It was not until Leo Baekeland tried his hand at the phenol-formaldehyde reaction that he managed to isolate a material with useful properties. In 1907 he filed a patent for a synthetic process of a material that he named Bakelite.⁹ Bakelite was the first modern synthetic plastic. The reproducible synthesis of this material resulted in an exponential growth of interest and research in this field. Even though these substances were being commercially synthesized, their exact chemical structures were still unknown at the time. A review on the field, published by Raschig in 1912, proposed that CH_2 and CH_2OCH_2 groups were the most probable linkers between the phenolic groups. He put forward that the resinous tars were a mixture of three potential structural units; resoles, novalaks and dibenzyl ethers (**Figure 1.1**).¹⁰

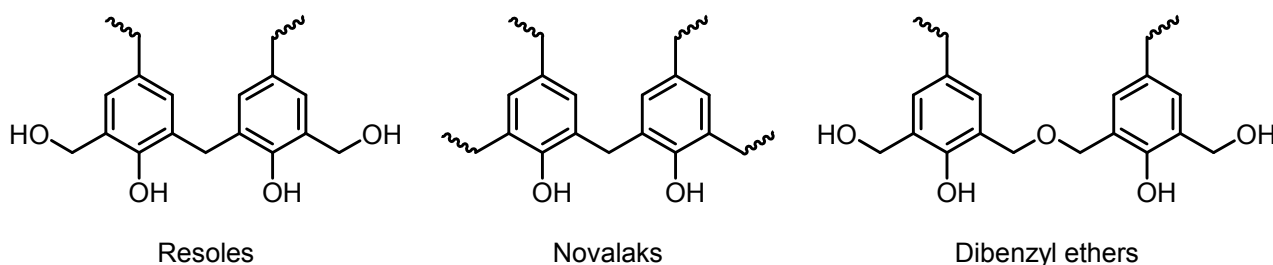


Figure 1.1: The proposed building blocks of the early resinous tars; resoles, novalaks and dibenzyl ethers.¹⁰

Chapter 1: Introduction

In 1942, Alois Zinke managed to cure the resinous tars formed in the phenol-formaldehyde process, thereby making the next significant contribution to the field. He noted that unsubstituted phenols, which react at both the *ortho* and *para*-positions, would result in highly cross linked polymers. So instead, he focused on *para*-substituted phenols, which would only react at the *ortho*-position and reduce the number of potential cross links.^{11,12} Unknowingly, Zinke had synthesized the cyclic calix[4]arene, but he was unable to recognize its cyclic structure. At the same time, Niederal and Vogel proposed a cyclic structure for a similar reaction between aldehydes and resorcinol.¹³ This work served as the basis, on which Zinke later proposed his cyclic tetrameric structure for the base-induced condensation reaction between *para*-substituted phenol and formaldehyde (**Figure 1.2**).¹⁴

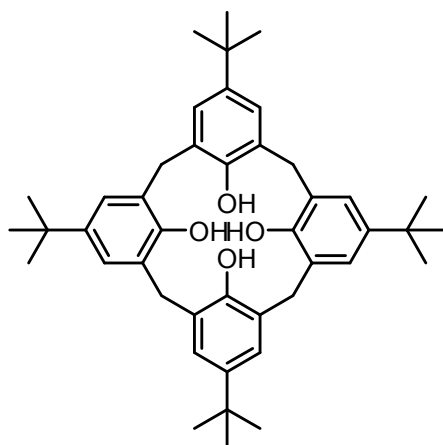


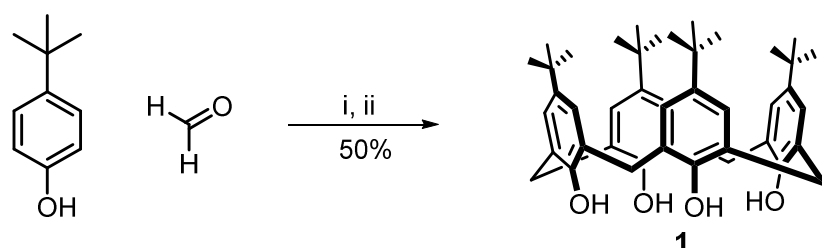
Figure 1.2: Cyclic tetrameric structure proposed by Zinke.¹⁴

Even though the proposed structure was correct, it was not fully characterized and confirmed until modern analytical techniques were developed.^{1,15-19} David Gutsche was responsible for shaping the field of modern calixarene chemistry. His work in the early 1970s was aimed at the development of enzyme mimics based on the unique three dimensional structure of the calix[4]arene. He shifted the commercial focus of the field towards an academic one, and was also responsible for coining the term ‘calixarene’. The name is derived from the Greek word ‘calix’, meaning bowl, and ‘arene’ which refers to the numerous aryl functional groups present in the overall structure.²⁰ To date, calixarenes have been extensively studied in the major fields of chemistry. The reason for this is their unique three-dimensional shape. There are several comprehensive reviews²¹⁻²⁵ and books²⁶⁻²⁹ that cover the many applications and functions of these compounds; including their use for molecular recognition in the solution³⁰⁻³² and gas phase,³³⁻³⁵ solid phase gas storage,³⁶⁻³⁸ application as enzyme mimics,³⁹⁻⁴¹ extensive use in coordination chemistry,⁴²⁻⁴⁴ use as chiral ligands in asymmetric catalysis^{24,44,45} and chemicals sensors.⁴⁶⁻⁴⁸ These are only a few of the reported applications and the growth of academic interest in these compounds has seen the inclusion of calixarenes in chemistry of all types.

Chapter 1: Introduction

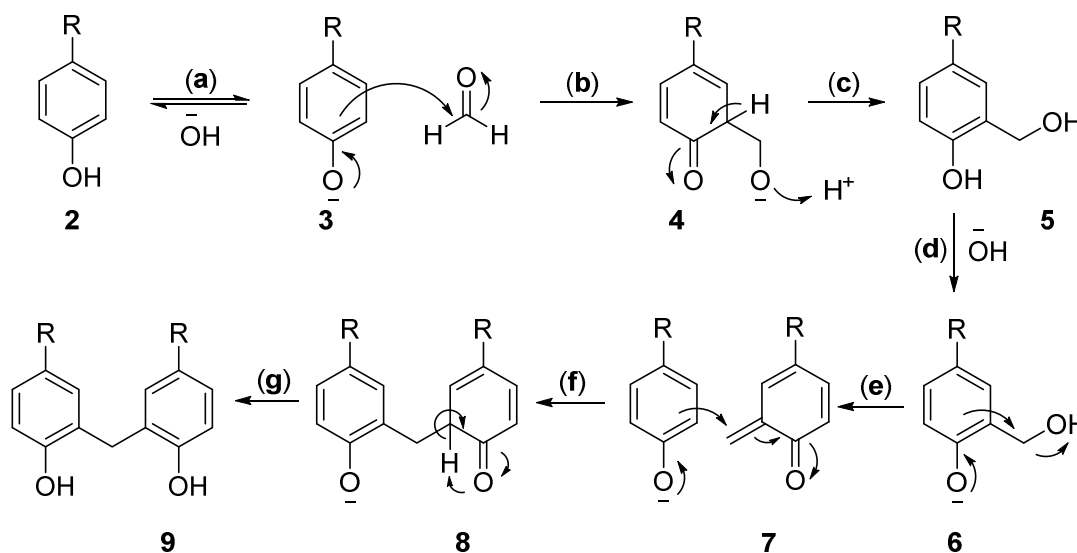
1.1.2 The early synthesis of calixarenes.

For many years the yields reported for the synthesis of the cyclic calix[4]arene tetramers were inconsistent. They would fluctuate wildly in what was thought to be consistent experimental conditions. It was Gutsche who realized that small variations in the amounts of base used at different temperatures were responsible for these inconsistencies.⁴⁹ The standard synthetic procedure for the cyclic calix[4]arene tetramers was originally formulated by Zinke,¹² modified by Cornforth,¹⁵ and finalized by Gutsche (**Scheme 1.1**).



Scheme 1.1: Synthesis of calix[4]arene **1**. Reagents and conditions: i) *p*-*tert*-butyl phenol (1.0 equiv), formaldehyde (1.1 equiv), NaOH (0.045 equiv), 2 h, 110-120 °C; ii) Diphenyl ether, reflux 2-4 h.⁴⁹

The exact reaction mechanism still remains uncertain. It has been studied for years and conclusive proof has been found for several key steps, leading to the eventual proposal of a generally accepted synthetic pathway. The current accepted mechanism follows a base-induced oligomerization pathway (**Scheme 1.2**).



Scheme 1.2: Proposed base-catalyzed oligomerization pathway.²⁷

The first step is the formation of the nucleophilic phenoxide anion **3**, which then attacks the reactive carbonyl group of the formaldehyde, step **(b)**. Studies have shown that under milder conditions the reaction can be stopped at this point, allowing for the resulting hydroxyl methyl phenols to be isolated and characterized.⁵⁰ Under harsher conditions, steps **(c-g)**, the reaction pathway continues to produce diarylmethyl compounds.

Chapter 1: Introduction

Following the deprotonation of the phenol group, step (d), an E1cB pathway kicks out the hydroxide and results in the formation of an *o*-quinone methide intermediate **7**. The existence of this intermediate was proposed as early as 1912,⁵¹ and was later again suggested by Hultzsch⁵² and Euler.⁵³ This intermediate then undergoes a Michael-type attack from one of the deprotonated phenols, step (f). Following this, re-aromatization occurs and the diaryl methyl compound is formed. The process, steps (e-g), then occurs repeatedly, yielding a series of linear oligomers. Depending on the reaction conditions, cyclization of the oligomers results in either a single product or different mixtures of the calix[*n*]arene compounds, where *n* denotes the number of aryl rings in the cyclic structure. The cyclisation and the reasoning behind why specific reaction conditions yield only one calixarene product or a mixture is the most poorly understood element of the overall reaction mechanism. Nevertheless, specific reaction conditions have been established for optimal yields of numerous calixarenes with varied ring sizes (4,5,6 etc). The synthesis of specific ring sizes requires only subtle changes to the base equivalents and reaction temperature, as well as choice of base.²⁷

1.1.3 The structural and conformational properties of calixarenes.

The three-dimensional structure of the calixarene is divided into three regions. The upper (*endo*) rim, lower (*exo*) rim and lastly the methylene bridges (**Figure 1.3**).

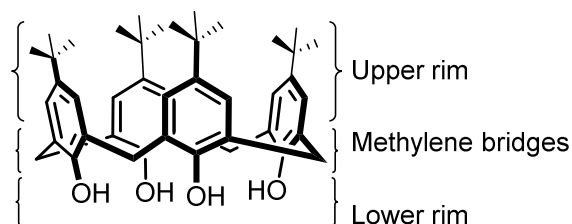
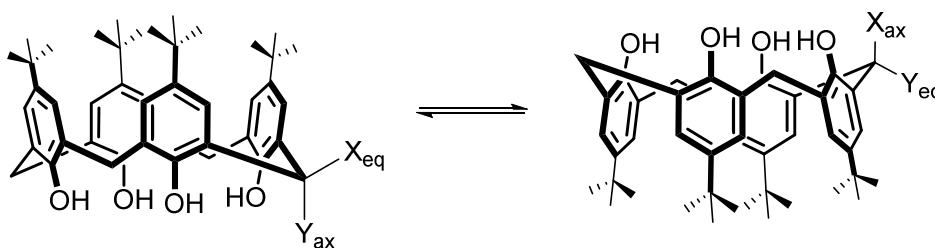


Figure 1.3: Three structural regions of the calixarene.

When in the solid-state, the calixarene exists in the cone conformation (as is depicted in **Figure 1.3**) with near perfect C_4 symmetry. This occurs regardless of the functional groups situated in the *para*-position of the upper-rim of the molecule and can be rationalized by the hydrogen bonding interactions of the phenolic OH groups on the lower-rim.^{54,55} This strong hydrogen bonding interaction also explains the high melting points and thermal stabilities often seen for these compounds.²⁷

Chapter 1: Introduction

Calixarenes are known to undergo rapid inversion of their structure in solution (**Scheme 1.3**). This observation was first reported by Kammerer who used variable temperature ^1H NMR spectroscopy to demonstrate this behaviour.¹⁷



Scheme 1.3: Rapid intra-annular OH inversion of the calixarene in solution.

The ^1H NMR spectrum of the parent calixarene at room temperature showed two broad singlet signals for the axial and equatorial protons. Collecting the spectrum at lower temperatures slowed down the inversion resolving the two proton signals. Throughout the literature this inversion process has been dubbed the ‘oxygen-through-the-annulus-rotation’.

1.1.4 The classification of calixarene conformations.

The calix[4]arene can exist in four possible conformations that were first recognized by Megson, Zinke, Ott and Cornforth.^{15,56,57} The four conformations were named by Gutsche as the cone, partial cone, 1,2-alternate and 1,3-alternate conformations (**Figure 1.4**).

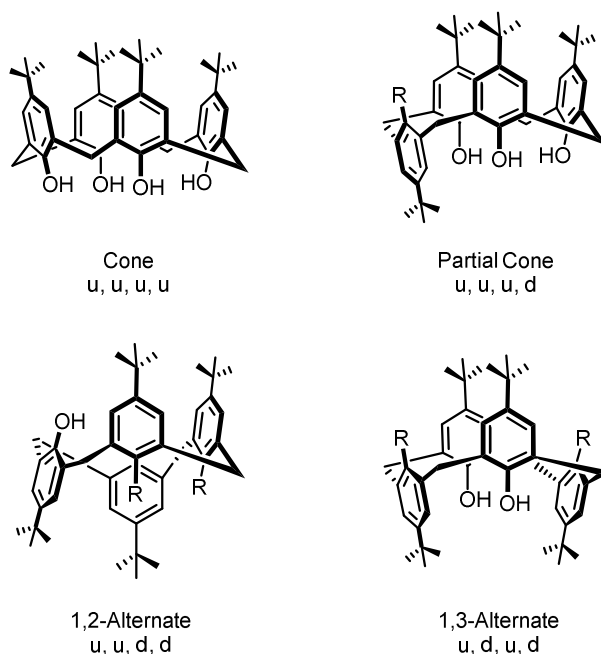


Figure 1.4: Four possible calix[4]arene conformations (u = upper-rim facing up, d = facing down).²⁷

Chapter 1: Introduction

The preference for a particular conformation depends largely on the functional groups present on the phenolic positions of the lower-rim. The driving force behind a specific conformation is often due to the steric strain introduced by these substituents. Other electrostatic interactions, such as hydrogen bonding can also play a role. Among the four major conformations the cone is the most common. Following this are the partial cone and 1,3-alternate, with the 1,2-alternate being the least prevalent.²⁷ The four classic conformations are not absolute and a number of new conformations have since been reported.⁵⁸⁻⁶⁰ Strictly speaking, these conformations are not entirely unique and need to be regarded as sub, or secondary conformations of the existing four and will therefore not be included in the discussion. Synthetic modification of the calixarene usually results in a departure from the true conformations. This occurs when the newly introduced substituents on the aryl groups push one or multiple rings inwards or outward. The most common example of this is sub-division of the cone conformation into the true cone and the pinched cone conformations (**Figure 1.5**).

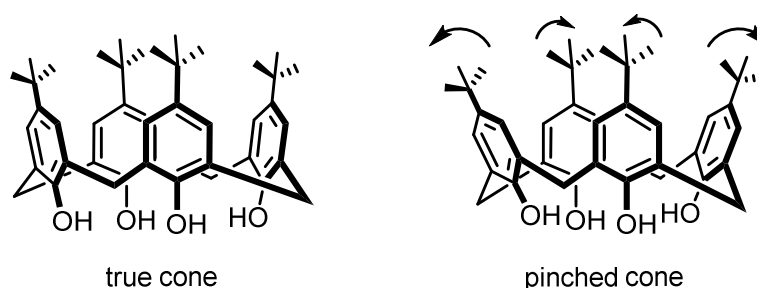


Figure 1.5: The true cone and modified pinched cone conformations of the calixarene.²⁷

¹H NMR spectroscopy is not only useful for investigating the behavior of these compounds in solution: it is the most powerful analytical tool to study the conformations of calixarenes in solution. The true cone conformation is highly symmetrical, with near perfect C_4 symmetry. When in the pinched cone, some of this symmetry is lost and the overall symmetry of the molecule drops to C_2 . This change is evident when comparing the ¹H NMR spectra of C_4 and C_2 symmetric compounds. The differentiation between the true and pinched cone conformations will be covered in **Chapter 2**.

1.1.5 Classification of inherently chiral calixarenes.

As previously mentioned, the interest in calixarene chemistry stems from their three-dimensional cyclic structure. Not only does this bowl shape enable their use in many fields of chemistry, it has an interesting implication from a chiral perspective. Traditionally, chirality in organic chemistry is first thought of as central chirality; a carbon atom bonded to four different functional groups. However, the term chirality has a much broader meaning. It is derived from the Greek work 'chiral', meaning hand, and the concept can be applied to any object with a non-superimposable mirror image.

Chapter 1: Introduction

With the growth and addition of molecular systems, newer systems of classification were required. Over time, new terms to categorize and create order within the growing pool of chiral information emerged. To date, many different forms of chirality have not only been established, they have found use and application in various fields of chemistry. The classification of chirality has evolved rapidly and the following are a few of the more recent examples: axial,⁶¹ planar,⁶² helical,⁶³ supramolecular⁶⁴ and inherent chirality.⁶⁵

In 1994 Böhmer published what can be regarded as the pioneering review on inherent chirality.⁶⁶ Not only was he one of the first to use the term, he also bridged the gap between the academic interest and practical application of this property. After Böhmer, the term 'inherently chiral' was mainly reserved for the calixarene class of compounds. The groups of Mandolini and Schiaffino, together with Szumna have recently proposed a general definition: "Inherent chirality arises from the introduction of a curvature in an ideal planar structure that is devoid of perpendicular symmetry planes in its bi-dimensional representation."⁶⁵ Inherently chiral compounds can either be classified as (*cR*) or (*cS*) where the *c* stands for curvature and the *R* and *S* represent the normal priorities of right and left respectively (**Figure 1.6**). This classification method was proposed by Schiaffino.⁶⁷ Much like central chirality, the bridging carbons are labelled with respect to their chemical priorities which are defined by the sequence rules. The bridges with the lowest priority are then placed facing backwards and can be considered facing into the page. The observer then looks from the front and determines the curvature based on either a clockwise or anticlockwise pattern of the 1st, 2nd and 3rd priority bridges.

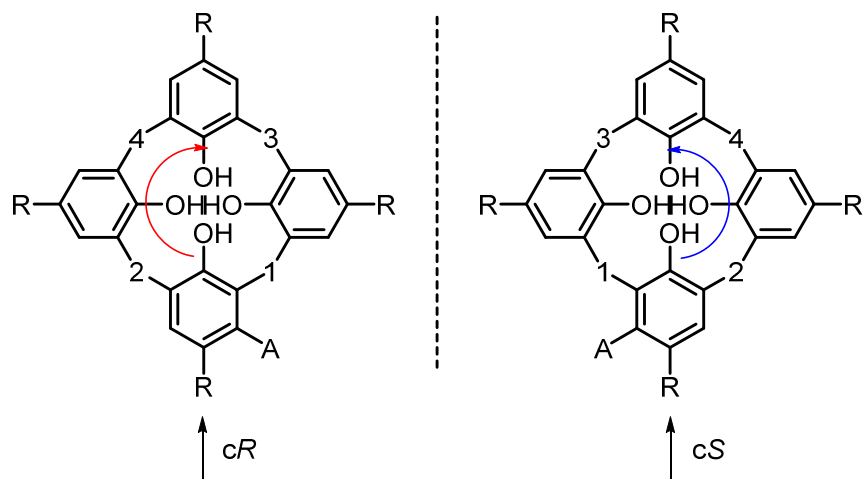


Figure 1.6: Schiaffino's classification of inherent chirality in calixarenes.⁶⁷

In the recent review by Szumna, it was proposed that the (*P*)/(*M*) notation is a more appropriate classification system. Similarly to the (*cR*)/(*cS*) notation, the priorities of the methylene bridges are determined using the standard priority rules. However, the position of the observer changes for this notation, making it more convenient to assign the chiral configuration (**Figure 1.7**).

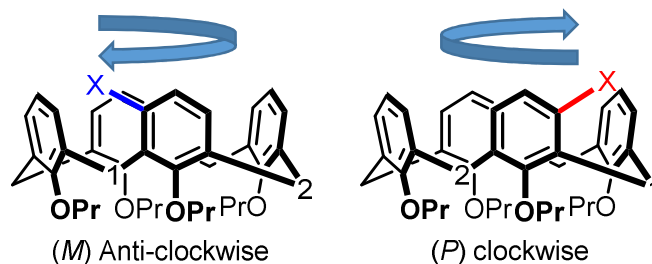


Figure 1.7: The (*M*) and (*P*) notations of inherently chiral calixarenes.

Looking down onto the top rim of the calixarene, and following the priorities, an overall anti-clockwise rotation is seen for the calixarene in the (*M*) configuration. The opposite clockwise rotation is seen for the calixarene in the (*P*) configuration, depicted on the right. This method of classification has been put forward as the better suited notation for inherently chiral molecules and will be used throughout this dissertation.⁶⁵

A basic system for the classification of functionalized calixarenes was proposed by Shinkai (**Figure 1.8**).⁶⁸ By denoting each of the uniquely substituted aryl rings in the cyclic structure with a letter, a shorthand representation of substituted calixarenes was made possible. As depicted in **Figure 1.8**, the R_1 -groups are a representation of a general synthetic modification made to each aryl ring. This classification method is not limited to changes on the upper-rim only, and a synthetic modification can be made to any position of the calixarene and the classification system would still be applicable.

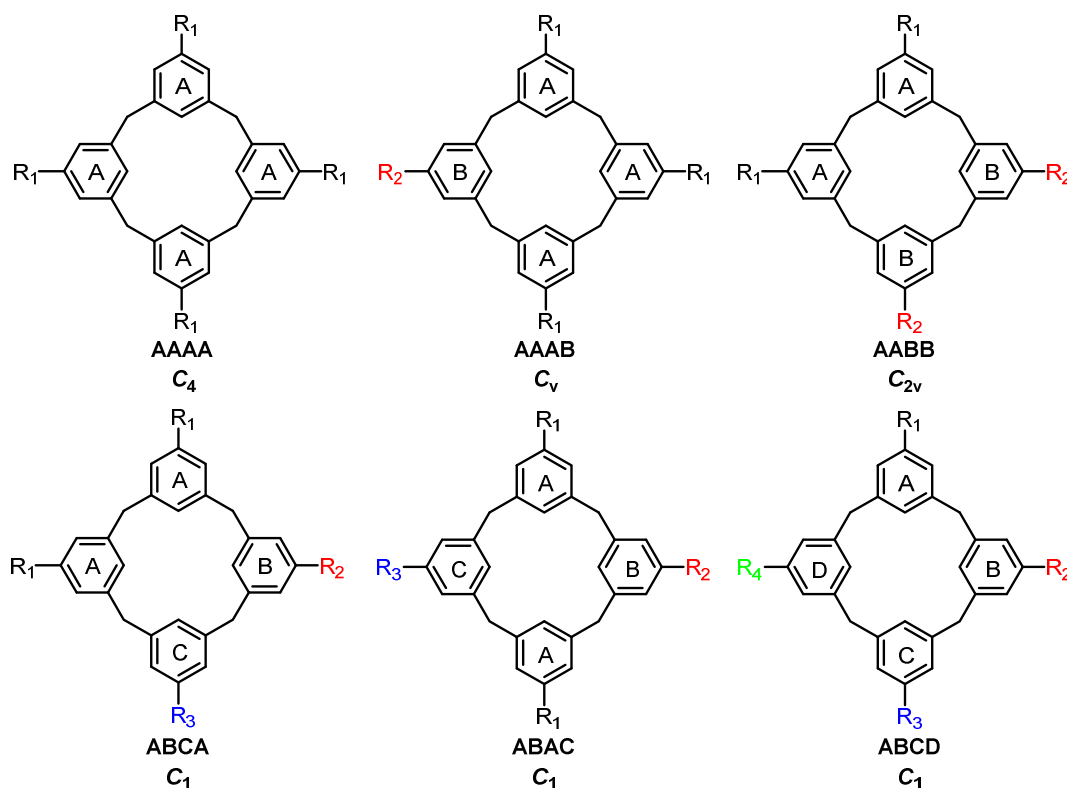


Figure 1.8: Shorthand representation of modified calixarenes proposed by Shinkai.⁶⁸

Chapter 1: Introduction

For a calixarene with four identical sub-units, the molecule is labeled AAAA and has C_4 symmetry. Modification of a single aryl ring changes the substitution pattern to AAAB and the symmetry space group lowers to C_v . Once three of the rings become functionalized, the symmetry space group lowers to C_1 and the molecule no longer has a center of inversion. Therefore, the molecule no longer has a superimposable mirror image and is chiral by definition, or inherently chiral in the case of calixarenes.

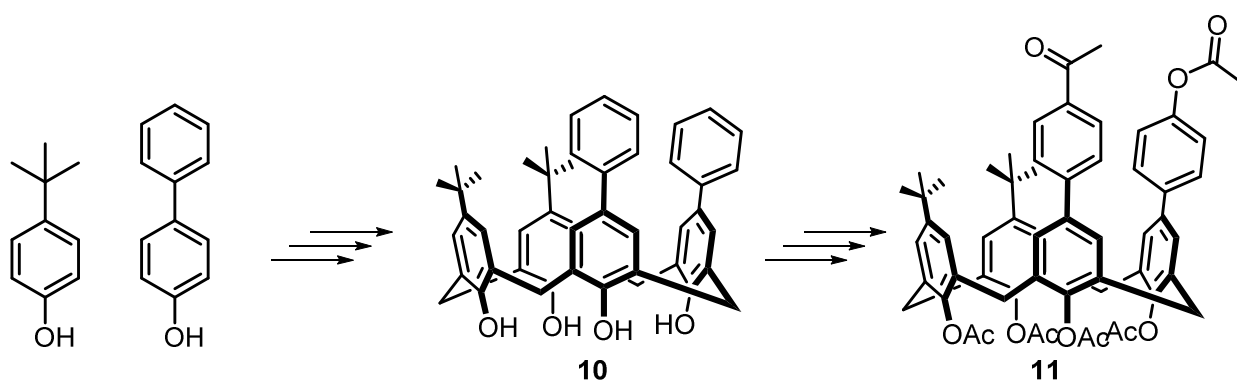
1.2 The synthesis of inherently chiral calixarenes.

The synthesis of calixarenes can be divided into three main groups, depending on which of the three regions are being modified. With regard to the synthesis of inherently chiral calixarenes, changes to the upper and lower-rims have received the most attention with far fewer examples of bridge modifications being reported. However, there are several examples of interesting and innovative instances of chemistry, based on the modification of these bridging carbons, which have been reported.^{69–73} The focus of this work has largely been on fine-tuning conformational and cavity-related properties of calixarenes, thus the modification of bridging carbons will not be covered in detail. Synthetic strategies towards inherently chiral calixarenes have focused on either the upper or lower-rim of the bowl structure. The modification of each of these regions can be further sub-divided into either a stereo or non-stereoselective approach. For the last 35 years an incredible number of inherently chiral calixarenes have been reported, with new examples added to the literature every year.

1.2.1 *The non-stereoselective synthesis of inherently chiral calixarenes.*

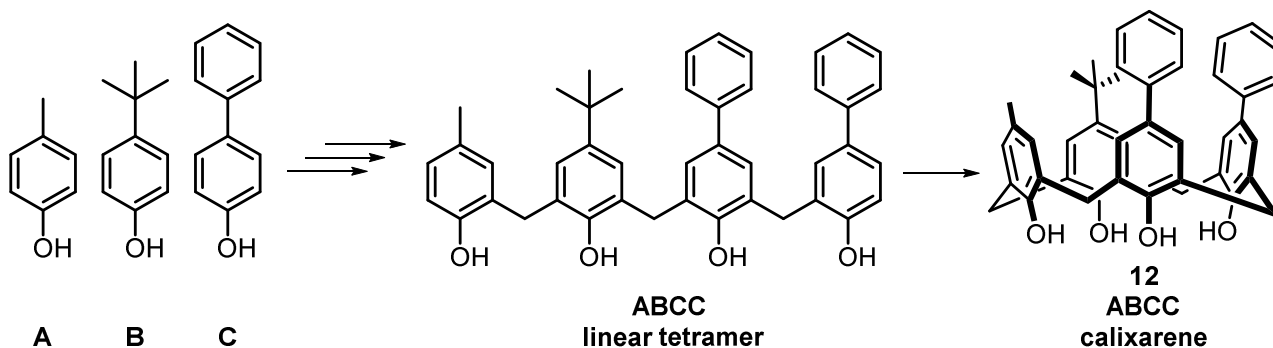
1.2.1.1 *The synthesis of inherently chiral calixarenes – a stepwise approach.*

The earliest synthesis of an inherently chiral calixarene was not strictly a modification of either the upper or lower-rim. Rather, it was a stepwise assembly that can be seen as two parts. Firstly, a stepwise synthesis of a linear tetramer which would then be ring-closed to yield the inherently chiral cyclic tetramer. This was first reported by Gutsche and co-workers in 1982 (**Scheme 1.4**).⁷⁴ Using a four-step sequence calixarene **10**, with reduced symmetry, was first synthesized. Following this, the conformation of the calixarene was locked through esterification of the lower-rims four hydroxyl functional groups. The last two steps were a Friedel-Crafts acylation of the two phenyl functional groups, followed by a selective oxidation of the newly introduced ketone groups. This strategy yielded a racemic mixture of inherently chiral calixarene **11** with an AABC substitution pattern.



Scheme 1.4: First multi-step synthesis of an inherently calixarene.⁷⁴

Apart from being the first of its kind, calixarene **11** was a challenge to synthesize. Many of the steps were unpredictable and often complex mixtures of products had to be separated. The overall yields were low and although it was a first, it was purely an academic venture with little practical application. Another noteworthy example of early work that followed a similar approach was reported by Böhmer in 1987.⁷⁵ Following a stepwise condensation procedure using three different phenolic units, an asymmetric linear tetramer was synthesized using carefully controlled condensation reactions (**Scheme 1.5**). A subsequent cyclisation of the tetramer yielded calixarene **12** in mixed ABC substitution patterns. Again, this approach was generally low yielding. The work was further complicated by the fact that the authors were unable to fix the conformation of the asymmetric calixarenes, as well as having to separate complex product mixtures.



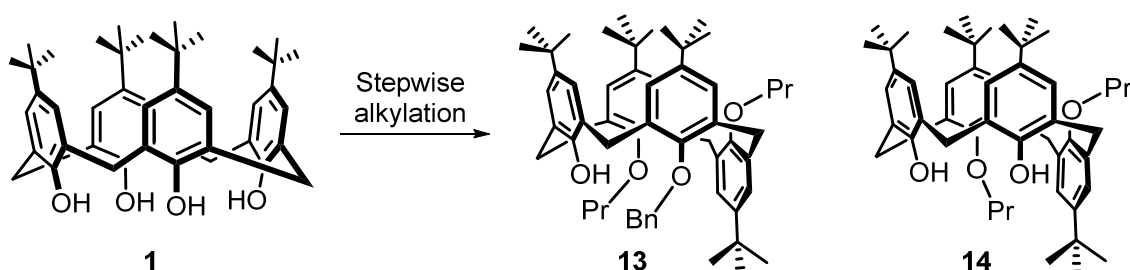
Scheme 1.5: Stepwise non-stereoselective synthesis of inherently chiral calixarenes reported by Böhmer.⁷⁵

Owing to the limited success and tedious nature of this earlier work, these methods were soon replaced by more efficient chiral and achiral strategies aimed at modification of the already formed calixarene molecule. Regardless of this fact, these were significant achievements and the findings sparked interest in this new form of chirality. It wasn't long before new strategies toward inherently chiral calixarenes started appearing throughout the chemical literature.

Chapter 1: Introduction

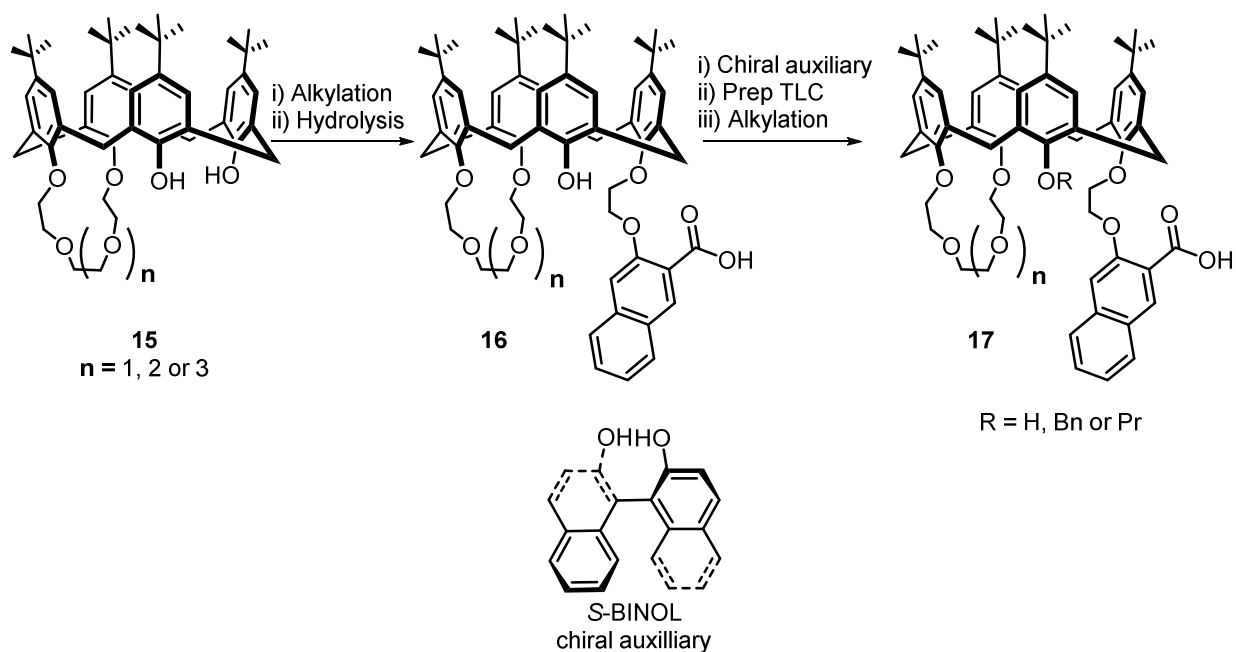
1.2.1.2 Achiral functionalization of the lower-rim.

One of the earlier non-stereoselective functionalization studies on calixarenes was carried out by Shinkai and co-workers (**Scheme 1.6**).⁶⁸ They were able to identify all possible potential isomers resulting from the simultaneous alkylation of select hydroxyl groups on the lower-rim, coupled with fixing the calixarene in one of the four potential conformations discussed earlier. Using their alkylation strategy, several of their proposed compounds were synthesized. Having previously established fixing of the calixarene conformation, propyl, benzyl and 2-methyl pyridine functional groups were added to the lower-rim of the calixarene in a stepwise fashion. By using different bases, the outcome of the calixarene conformation after each step was controlled by the different templating effects introduced by the various base counter ions. The fact that no chiral auxiliary was used in the alkylation steps meant that a mixture of enantiomers was always obtained. Through a process of trial and error, using preparative chiral HPLC, they were able to isolate approximately 20 mg of each enantiomer from their product mixtures. The challenging separation of these enantiomeric product mixtures was an early and unpleasant practical obstacle that remains an issue in the field. Not only is the process of separation troublesome, isolating only 20 mg of a high molecular weight calixarene leaves little room for the development of potential applications.



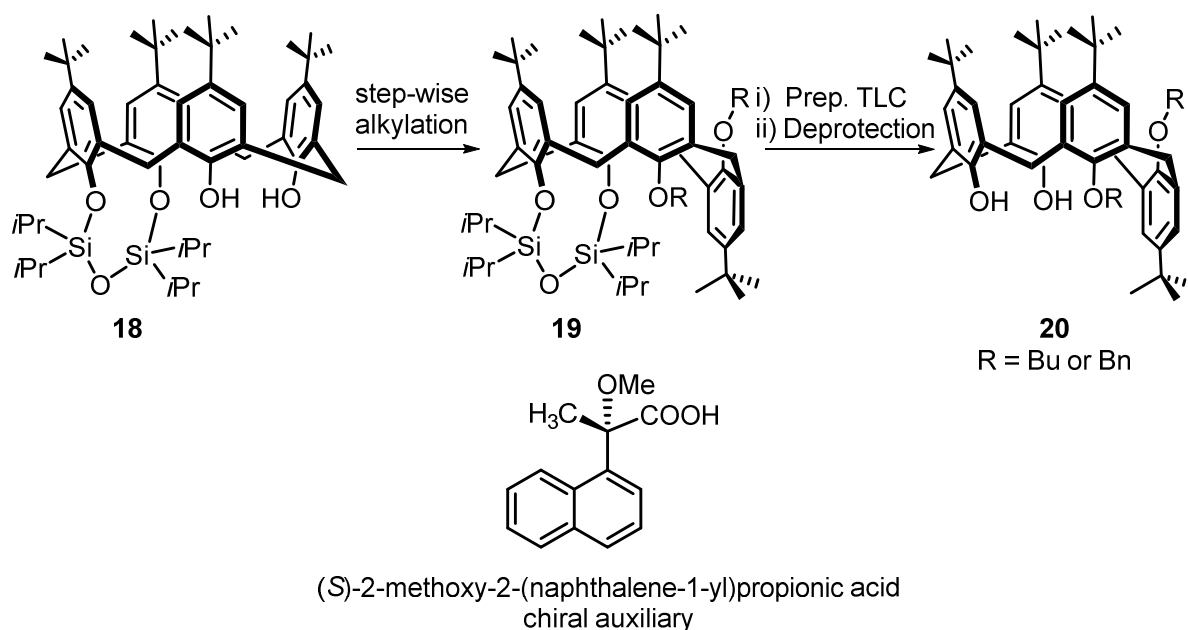
Scheme 1.6: Achiral synthesis of tri-alkylated **13** and di-alkylated **14** inherently chiral calixarenes.⁶⁸

The end result of a non-stereoselective synthetic plan always yielded racemic product mixtures, discouraging further synthetic development. It was not practically feasible to separate enough calixarene material using preparative chiral HPLC for any further application studies. However, a breakthrough was made by Huang's group when they reported the synthesis of a series of tri- and tetra-alkylated inherently chiral calix[4]crown derivatives in 2005 (**Scheme 1.7**).⁷⁶⁻⁷⁹ The inherently chiral calixarenes were synthesized using a sequential alkylation procedure. The process was also non-stereoselective, and a mixture of enantiomers was obtained once again. Calixarene **16** was a 1:1 mixture of products, with the acid attached to either of the available phenolic groups. After the addition of the chiral auxiliary, in their case *S*-BINOL, to the carboxylic acid moiety on the lower-rim, the mixture of enantiomers was changed to a racemic mixture of diastereomers instead. This enabled the separation of the product mixture using preparative TLC, and after removal of the chiral *S*-BINOL auxiliary, yielded the pure inherently chiral calixarene **17** enantiomers.



Scheme 1.7: The achiral synthesis of inherently chiral calixcrown ethers. Separation of the product mixtures was achieved using a chiral auxiliary and preparative TLC.⁷⁶

Even though the use of preparative TLC was a far more efficient separation method than preparative chiral HPLC, it still fell short when considering the quantities of material required for the application of these compounds. The success of Huang's findings were rapidly followed by reports of new procedures involving lower-rim functionalized inherently chiral calixarenes, all based on the strategy of using chiral auxiliaries for the purpose of optical resolution. The groups of Hattori and Narumi also reported a series of inherently chiral calixarenes based on a stepwise, lower-rim functionalization strategy followed by separation using a chiral auxiliary (**Scheme 1.8**).^{80,81} Instead of using a crown-ether, a bridged silyl group was used to protect two of the hydroxyl groups. Stepwise alkylation of calixarene **18**, followed by deprotection of the silyl bridge yielded the inherently chiral calixarenes **20** in the partial cone conformation.

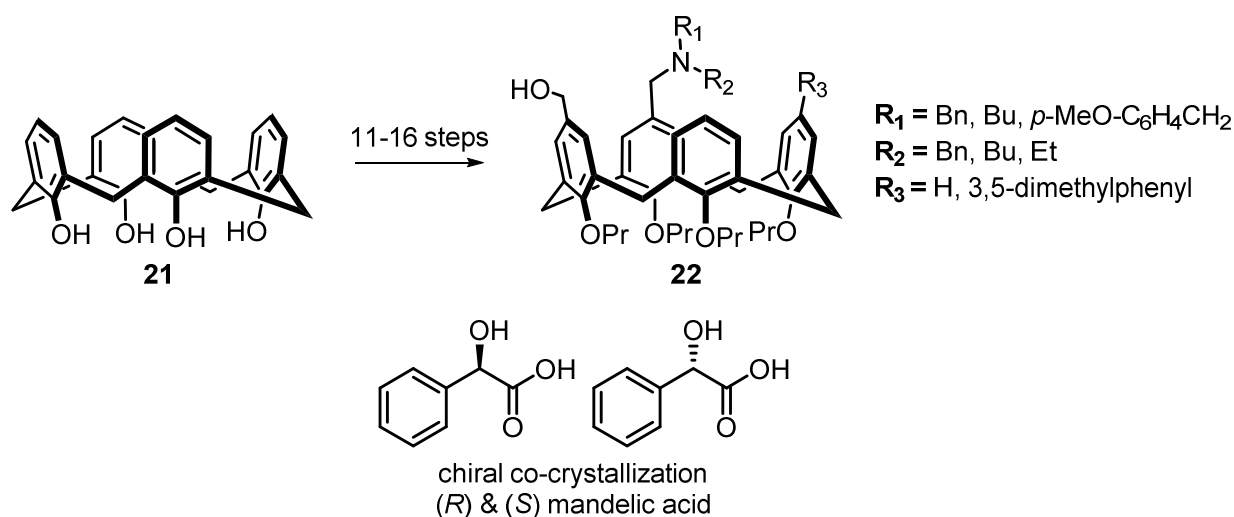


Scheme 1.8: Achiral synthesis of inherently chiral calixarenes using a protection/deprotection strategy. Resolution of the product mixtures was achieved using a chiral auxiliary.⁸¹

Functionalization of the lower-rim is synthetically less challenging than the upper-rim. The hydroxyl groups provide a convenient single point for functionalization on each of the aryl components. On the other hand, the upper-rim has at least two if the *para*-position is occupied, but otherwise three available positions on each of the rings. Despite this, it has been found that chemical resolution of inherently chiral calixarenes functionalized on the upper-rim is less efficient than those with modifications on the lower-rim. A potential rationalization for this observation could be that when situated on the wider upper-rim, the chiral functional groups are spaced further apart which weakens the spatial interactions between them, and in so doing, decreases the degree of differentiation between the diastereomers.²³

1.2.1.3 Achiral functionalization of the upper-rim.

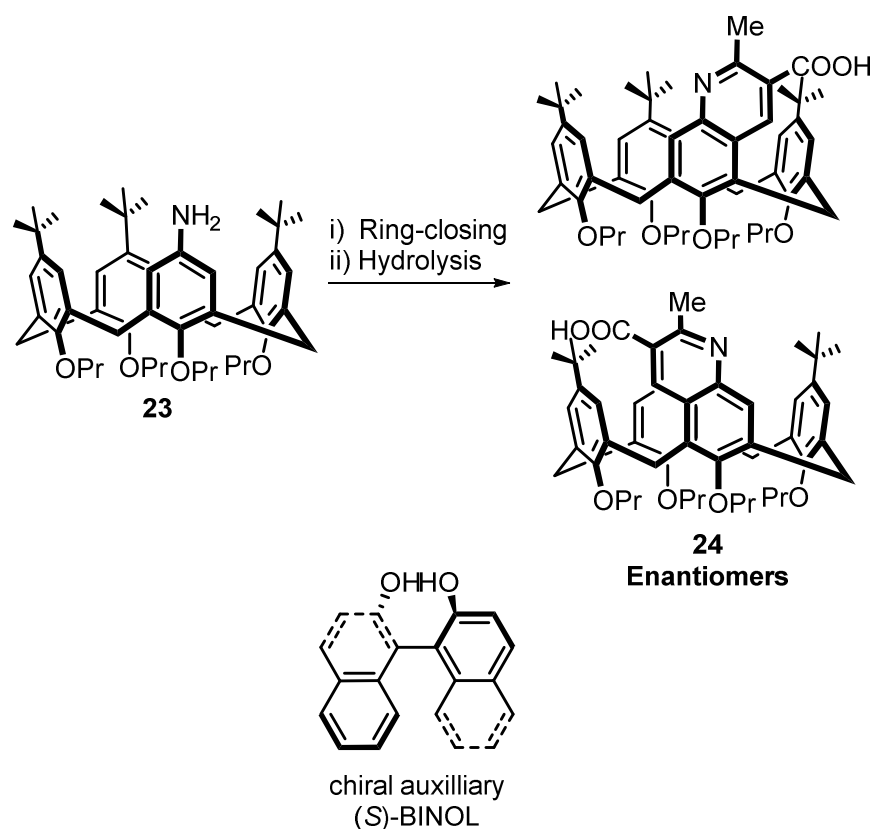
The less common methods of upper-rim functionalization toward inherently chiral calixarene synthesis has been an area of focus for Shimizu and co-workers.^{82–85} To date, they have reported the synthesis and optical resolution of a series of inherently chiral calixarenes that feature variations of amino acid, amino alcohol and aminophenol functional groups on the upper-rim (**Scheme 1.9**). By employing a stepwise synthetic approach, the *para*-positions of the upper-rim of calixarene **21** were sequentially modified. The enantiomeric mixtures of calixarene **22** were separated via a co-crystallization process; the first example of a chiral crystallization process incorporating calixarenes.



Scheme 1.9: The achiral synthesis of inherently chiral calixarenes by stepwise modification of the aryl *para*-positions.⁸⁴

Depending on the structure of the final product, the total synthesis took between 11 and 16 steps, which was a considerable increase when compared to the lower-rim strategies. A major advantage of this method was the ability to separate the diastereomeric mixtures by co-crystallization. Even though this discovery required a considerable amount of trial and error, it allowed for these compounds to be isolated on a much larger scale, which had been a major limiting factor of previously reported methods. It should be noted that the work by Shimizu's group only focused on functionalization of the *para*-positions of the aryl rings.

An alternative path to inherent chirality would be functionalization of the *meta*-position. Huang and Chen used a ring-closing strategy to yield *meta*-functionalized inherently chiral calix[4]quinolones (**Scheme 1.10**).^{86,87} Starting from the *para*-mono-amino calixarene **23**, a single ring-closing reaction using acetoacetate and the Vilsmeier reagent formed the inherently chiral calixarene **24** as a racemic mixture. The use of a chiral auxiliary then enabled the separation of the racemic mixture via column chromatography. The (*S*)-BINOL auxiliary required the presence of a carboxylic acid group to enable its coupling and subsequent hydrolysis after the separation. This requirement placed a limitation on the flexibility of the synthetic method and the same argument can be made for the functional group requirements of all chiral auxiliaries. Even though chemical resolution was necessary, the two-step synthesis from the amino calixarene, coupled with the simple separation procedure afforded an elegant, far more efficient alternative to many of the step-wise strategies. **Scheme 1.10** only represents one of their reported compounds, and a series of inherently chiral calixarenes were synthesized using this strategy. A major advantage of this method was that the chromatographic separation of the inherently chiral products allowed for the gram scale isolation of these materials.



Scheme 1.10: Two-step synthesis of *meta*-functionalized inherently chiral calix[4]quinolines and their subsequent chemical resolution using (S)-BINOL.⁸⁷

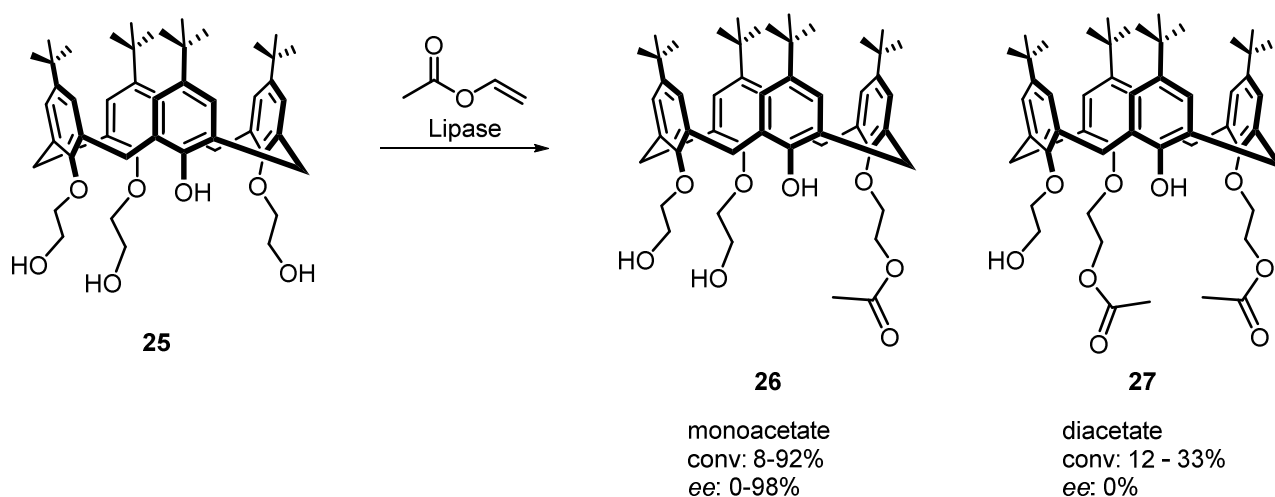
The literature is filled with non-stereoselective synthetic methods toward inherently chiral calixarenes. The examples discussed above are only a select few and there are many more that follow the same general method. Functionalization of the lower-rim has been reported more frequently, as the chemistry on the lower-rim is better understood and easier to control. The stepwise synthetic strategies of both the upper and lower-rim calixarenes are often extremely low yielding, owing to the potential of multiple product mixtures forming along the way. The majority of these methods are not suitable for the synthesis of materials on a scale necessary for further application studies. In addition, the chemical resolution of racemic mixtures is seldom favorable as it limits the design of new compounds by requiring the presence of specific functional groups. A second disadvantage is that the attachment and hydrolysis of a chiral auxiliary always adds two more steps to the synthetic procedure. The efficiency of the separation is often not discussed and often a long process of trial and error is required before an adequate separation is achieved. Frequently a specific set of separation conditions are only suitable for a select few calixarenes. The development of new synthetic strategies is regularly coupled with the need to develop entirely new resolution methods as well. All of these factors only impede the study of the potential application of these compounds. The need for efficient and stereoselective synthesis of inherently chiral calixarenes is thus required to make further study of these compounds practically feasible.

Chapter 1: Introduction

1.2.2 The stereoselective synthesis of inherently chiral calixarenes.

1.2.2.1 Asymmetric functionalization of the lower-rim.

The stereoselective synthesis of inherently chiral calixarenes is defined as the use of either chiral substrates, reagents or asymmetric catalytic processes. In theory, an efficient chiral synthetic process would enable the synthesis of inherently chiral calixarenes on a large scale in high enantiomeric excess. This would eliminate the need for chemical resolution, and potentially require fewer steps than the majority of the existing non-stereoselective methods. One of the first truly asymmetric synthetic strategies toward inherently chiral calixarenes was reported by McKerverey and co-workers in 1998.⁸⁸ In this work, a chiral lipase-catalyzed transesterification reaction, inherently chiral calixarenes **26** and **27** with the AABC configuration were synthesized (**Scheme 1.11**).



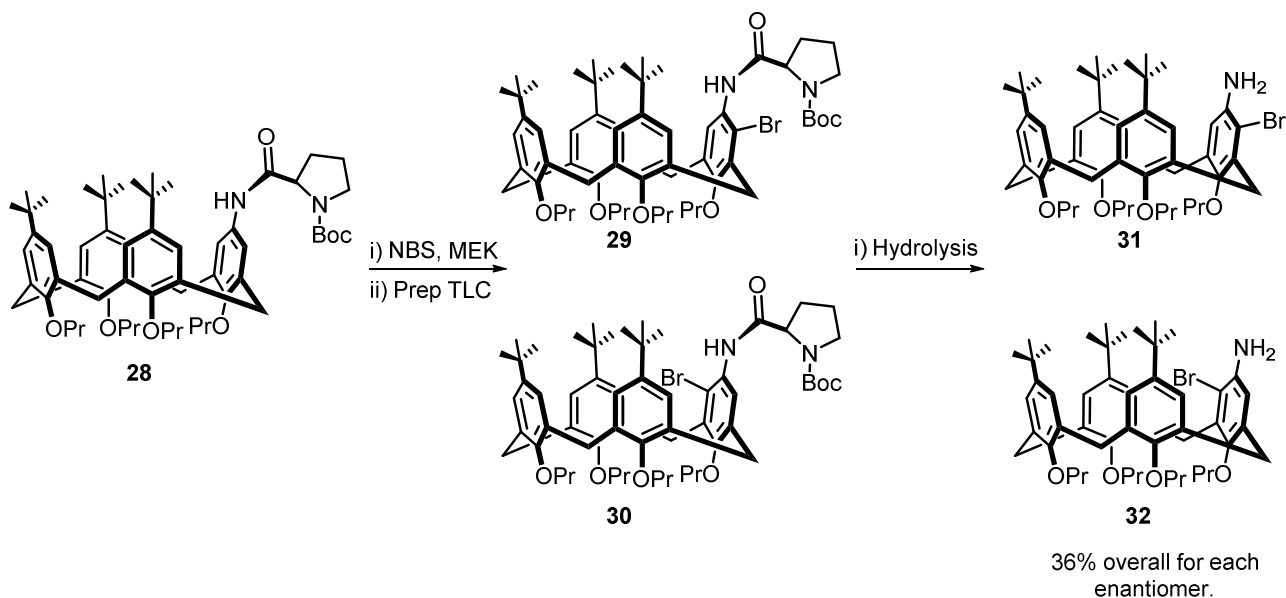
Scheme 1.11: Chiral synthesis of lower-rim inherently chiral calixarenes using lipase enzymes.⁸⁸

Several different lipase enzymes were screened, yielding mixed results. The selective transesterification might seem like a viable method, but the enzyme catalyzed reactions mostly yielded mixtures of mono and diacetate products with inconsistent and varied enantioselectivities. These mixtures required HPLC separation and none of the individual enantiomers were isolated. Besides the issue of isolation, the higher yielding reactions had extremely poor selectivities and the three highly selective reactions had low yields of 8, 14 and 18%.

Chapter 1: Introduction

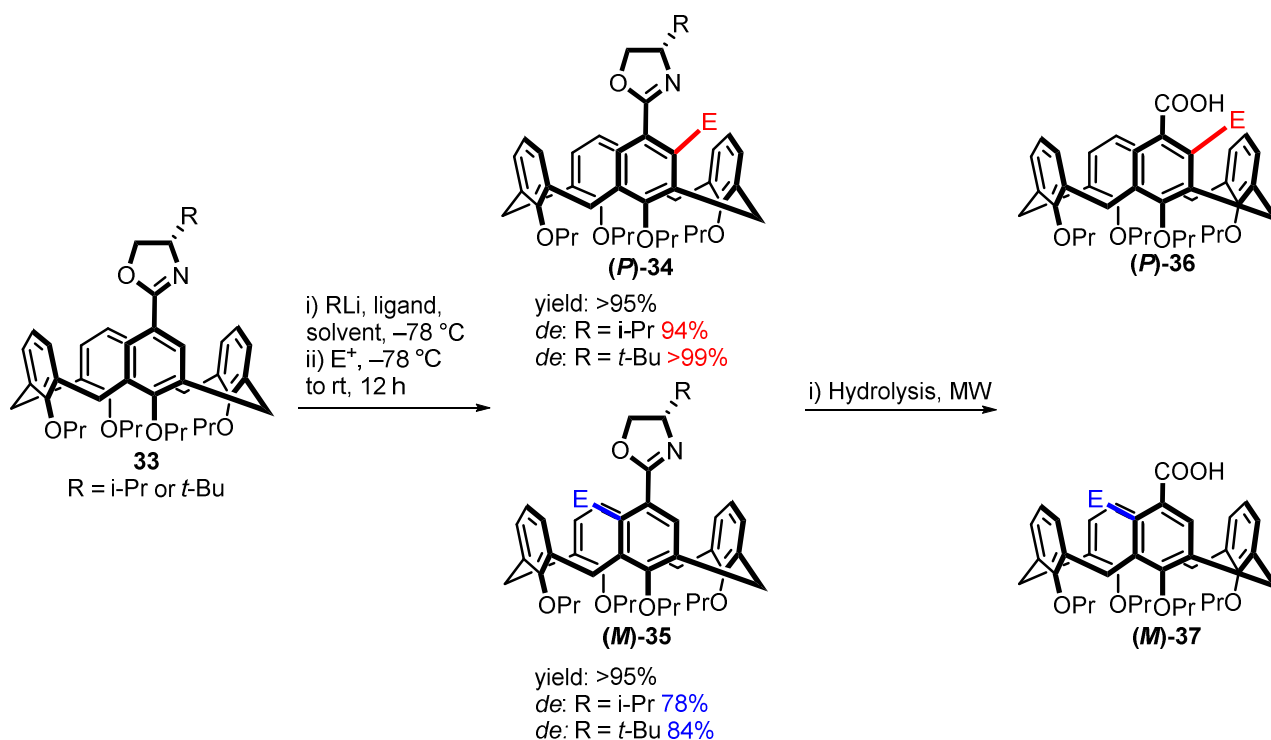
1.2.2.2 Asymmetric functionalization of the upper-rim.

A big step toward the true asymmetric introduction of curvature to the structure of the calixarene was reported by the groups of Huang and Chen in 2008.⁸⁹ Using L-Boc prolinamide as a chiral directing group, they hoped to selectively introduce a new functional group in the *meta*-position on the upper-rim (**Scheme 1.12**). Both electrophilic aromatic nitration and bromination were attempted, but unfortunately no selectivity was observed. A racemic mixture of inherently chiral calixarene diastereomers **29** and **30** were obtained and were separable using preparative TLC. Even though the L-Boc prolinamide failed to induce an asymmetric transformation, it served the dual purpose of activating the ring for the substitution and functioned as a built-in chiral auxiliary, enabling separation. Once the diastereomers were isolated, the prolinamide was hydrolyzed yielding inherently chiral calixarenes **31** and **32** with a new functional group introduced on either *meta*-position of a single aromatic ring.



Scheme 1.12: Attempted asymmetric *meta*-functionalization directed by L-Boc prolinamide.⁸⁹

The first example of a truly asymmetric synthesis toward upper-rim *meta*-functionalized inherently chiral calixarenes was reported by the Arnott group in 2009 (**Scheme 1.13**).^{90,91} Based on a similar strategy that was successful on ferrocene systems, a chiral oxazoline was used to direct a series of asymmetric ortholithiation reactions.^{92–94} Optimization of the method showed that variation of either the solvent, alkyllithium or additives would invert the selectivity of the reaction, and in so doing, provide a means of obtaining enriched product mixtures of both calixarene diastereomers **34** and **35**. Subsequent hydrolysis of the oxazoline functionality then yielded the two purely inherently chiral enantiomers **36** and **37**.



Scheme 1.13: Asymmetric synthesis of inherently chiral calixarenes via directed ortholithiation.^{91,95}

Not only is this some of the latest work in the field, it is also the most promising from an application perspective. The conversions for the ortholithiation reactions were high and the chemistry tolerated numerous electrophiles. The method also enabled the synthesis of enriched mixtures of either diastereomer, giving it significant versatility. Furthermore, the asymmetric nature of the reaction avoids the need for chemical resolution via preparative TLC or chiral HPLC.

One of the disadvantages of this method was that the hydrolysis of the oxazoline required harsh conditions, limiting the electrophile options. The incorporation of sensitive electrophilic functional groups limited the synthesis to diastereomers only. The synthesis of inherently chiral enantiomers would only be possible using stable and unreactive electrophiles that would remain unaffected by the strong aqueous basic and acidic hydrolysis conditions. Despite these disadvantages, the efficient and flexible nature of this reaction made it an ideal candidate for the synthesis of new types of inherently chiral compounds. The results from the preliminary application studies would establish whether or not the improvement of these synthetic methods would be worth pursuing.

1.3 The application of inherently chiral calixarenes.

The growth of calixarene synthesis was invariably coupled with an increased interest in their application. Non-inherently chiral calixarenes have seen use in supramolecular, separation, medicinal and especially metal-organic chemistry (these compounds have been used extensively in the formation of metal complexes).²¹ It should be kept in mind that the synthesis of non-chiral calixarenes is less complex and functional material is conveniently isolated on a large scale. However, the application of inherently chiral calixarenes is not nearly as established and the majority of the current examples are calixarenes functionalized on the lower-rim or simply calixarenes with a chiral functionality attached to it. As mentioned previously, simply attaching chiral functional groups to the ring structure does not fulfill the definition of inherent chirality and the aim of this study is to investigate the impact of the chirality which results from the non-planar structure of the calixarene itself.

1.3.1 *The earliest reports of catalysis.*

The earliest examples of reported science that meet today's general requirements of catalysis were first published in the early 1800s. The term 'catalysis' was first proposed by Jons Jacob Berzelius in 1835. It is a combination of two Greek words 'kata' and 'lycin' which mean 'down' and 'loosen'. Berzelius described the meaning of the term as follows: "The property of exerting on other bodies an action which is very different from chemical affinity. By means of this action they produce decomposition in bodies and form new compounds, into the composition of which they do not enter."⁹⁶ One of the earliest reported catalytic transformations was in the year 1811, where Russian chemist Gottlieb Kirchoff showed that in the presence of sulfuric acid and heat, an aqueous starch solution could be transformed into a mixture of gum, dextrin and raisin sugar.⁹⁷ He noted that the acid remained unmodified throughout the process and by treating the mixture with a basic reagent allowed for the full recovery of all the acid present. Ever since these early discoveries, the field of catalysis has been broadly studied and has grown into what is arguably the largest field of chemistry spanning multiple disciplines.

1.3.2 *Relating chirality to catalysis.*

Whenever a new form of chirality is discovered, catalytic studies quickly follow. The synthesis of chiral ligands and the study of their role in asymmetric transformations have always been one of the fundamental tools used by chemists to understand the nature of new molecular architectures. Two well-known examples of this are the application of the axially chiral BINAP ligands⁶¹ as well as the synthesis of the planar chiral ferrocene ligands (**Figure 1.9**).⁹⁸

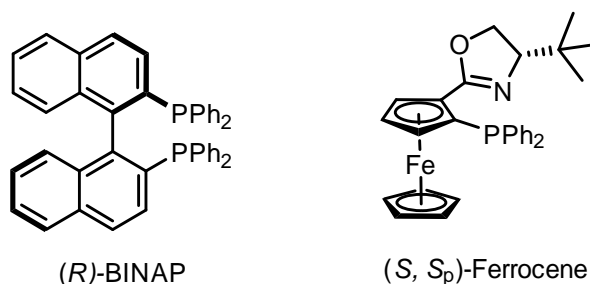


Figure 1.9: The axially chiral BINAP and planar chiral ferrocene phosphine oxazoline ligands.^{61,98}

The incorporation of calixarenes into the field of metal-based catalysis was summarized in a comprehensive review by Redshaw and Homden.²¹ In this work, the collective contribution made by calixarenes over all reaction types was graphically represented (**Figure 1.10**)

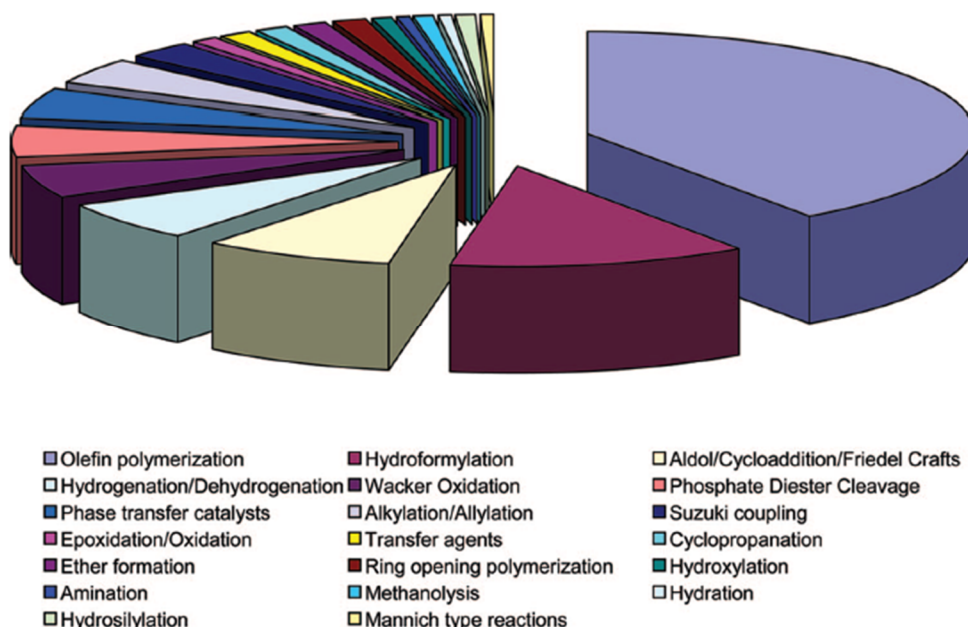


Figure 1.10: A summary of the reaction types incorporating the use of calixarenes in metal-based catalysis, reproduced from the reference.²¹

What this demonstrates is that calixarenes have found use in almost every popular and relevant organic transformation. Their primary contribution to metal-based catalysis has either been for the synthesis of metallo-calixarenes, or their incorporation as ancillary ligands. This is due to several favorable properties of the parent calixarene. It has the ability to form bonds to metals using a number of potential binding sites (**Figure 1.11**).²¹ Additionally, the four oxygen donor atoms exist in a rigid semi-planar geometry, allowing for the development of oxo-surfaces and heterogeneous catalytic systems.⁹⁹ Furthermore, the flexibility of its conformation, as well the ability of the bowl shape to house multiple metal centers are also highly favourable properties.²¹

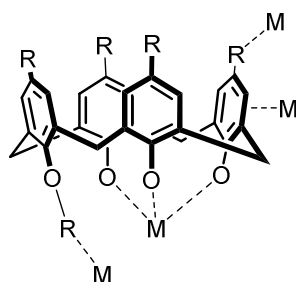
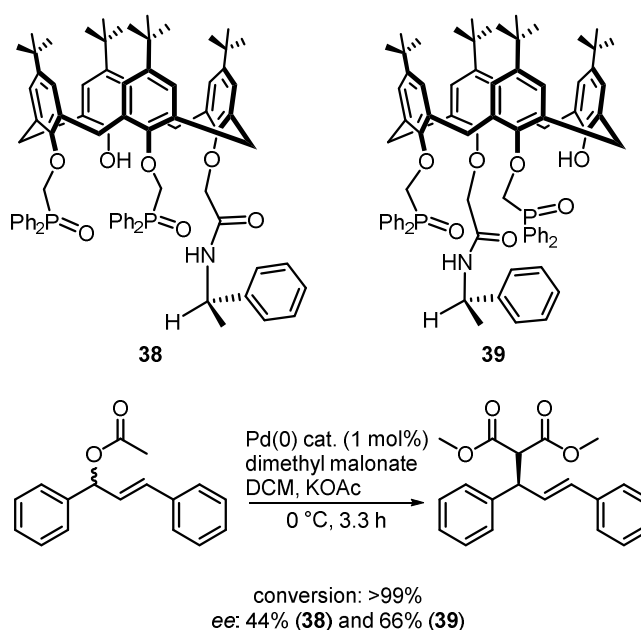


Figure 1.11: The four potential metal binding sites of the parent calixarene.²¹

As a result, less attention has been given to the synthesis of inherently chiral ligands and the majority of these have been functionalized on the lower-rim hydroxyl groups, or the *para*-positions of the upper-rim. As yet, limited applications of inherently chiral calixarenes based on the functionalization of the *meta*-position on the upper-rim have been reported.

1.3.3 The application of inherently chiral ligands functionalized on the lower-rim.

In 2001, a study by Dieleman and co-workers reported the synthesis of a series of inherently chiral calixarenes with the AABC substitution pattern on the lower-rim (**Scheme 1.14**).¹⁰⁰ After separation of the diastereomeric mixtures of **38** and **39**, the two pairs of diastereomeric ligands were tested in the asymmetric Tsuji-Trost allylation reaction. The ligands **38** and **39** yielded the substituted product in complete conversions and were able to induce moderate selectivities of 44% and 66% respectively. Several other non-inherently chiral calixarene ligands were also synthesized for this study. They provided the products in high yields, but their selectivities were significantly lowered. This result suggested that the inherent chirality of the calixarene played a role in the overall transfer of chiral information in the reaction.



Scheme 1.14: The application of inherently chiral phosphine ligands in the asymmetric Tsuji-Trost reaction.¹⁰⁰

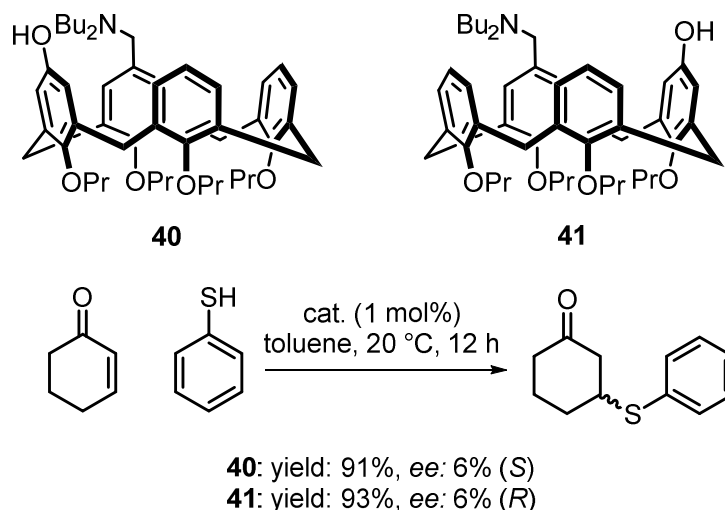
Chapter 1: Introduction

Despite moderate selectivities, this result had an important implication on the application of inherent chirality. It is one of the earliest findings in which the contribution of the inherent chirality in creating a stereo-controlled environment was confirmed. Several other calixarene ligands based on distal phosphine and phosphine oxide groups attached to the lower-rim have also been reported, all of which have similar findings to the compounds discussed above.^{101–104}

1.3.4 The application of inherently chiral ligands functionalized on the upper-rim.

1.3.4.1 Para-functionalized inherently chiral calixarene ligands.

Ligands based on inherently chiral calixarenes functionalized in the *para*-position are rare. One of the only examples was reported by Shimizu and co-workers in 2007.⁸⁴ After the separation of the chiral amino alcohol, calixarenes **40** and **41** were tested as organo-catalysts in an asymmetric Michael addition of thiophenol to 2-cyclohexanone (**Scheme 1.15**).



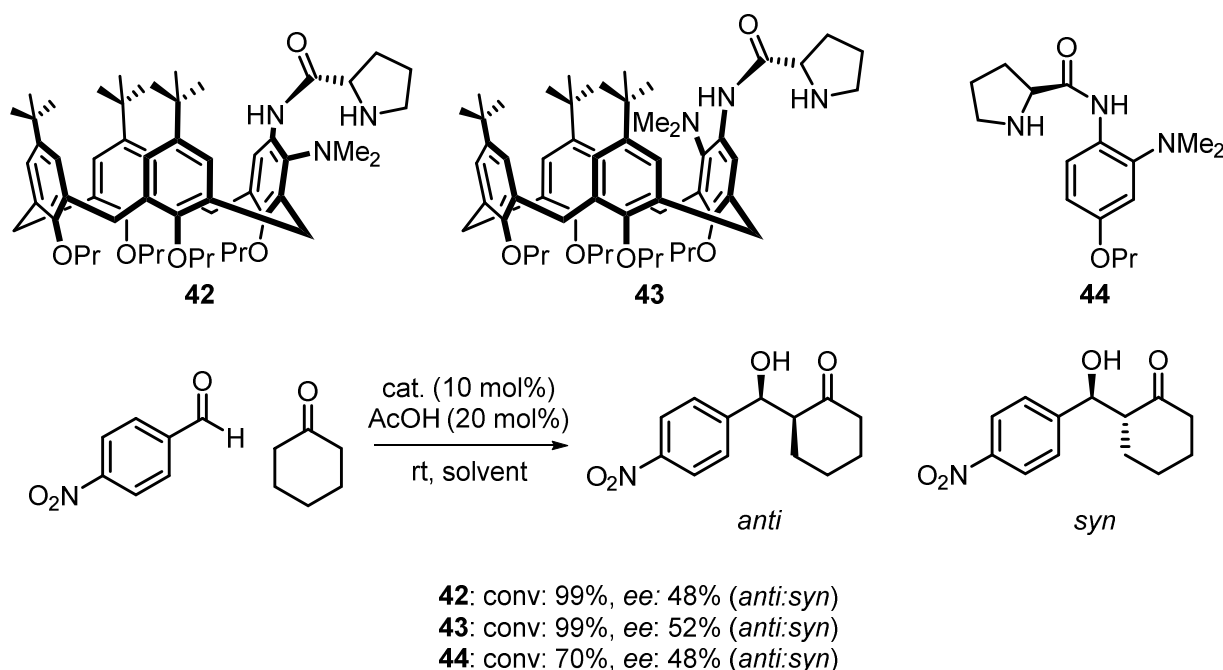
Scheme 1.15: Application of inherently chiral amino alcohols to an asymmetric Michael addition reaction.⁸⁴

The two ligands, **40** and **41**, were the most selective of all of the tested ligands. Both yielded the product in high conversions but with low *ee* values of 6%, each favoring the opposite enantiomer. Again, even though these results might not seem impressive, these were some of the first examples where the stereocontrol in these asymmetric reactions was being generated purely by the chirality of the calixarenes' non-planar structure, rather than a separate source of chirality attached to the ligand.

Chapter 1: Introduction

1.3.4.2 *Meta*-functionalized inherently chiral calixarene ligands.

As discussed previously, Huang's group were one of the first to attempt chiral *meta*-functionalization of the upper-rim. Even though their initial attempts did not go as planned, they were able to synthesize and separate several inherently chiral calixarenes on a large scale. Later work from their group aimed at using these *meta*-functionalized compounds as organo-catalysts in the asymmetric addition of aldehydes to ketones (**Scheme 1.16**).⁸⁹ Inclusion of a model compound in their study provided a means to quantify both the contributions of the point-chirality of the L-prolinamide and the inherent chirality of the calixarene, toward the overall asymmetric induction seen in the reaction.



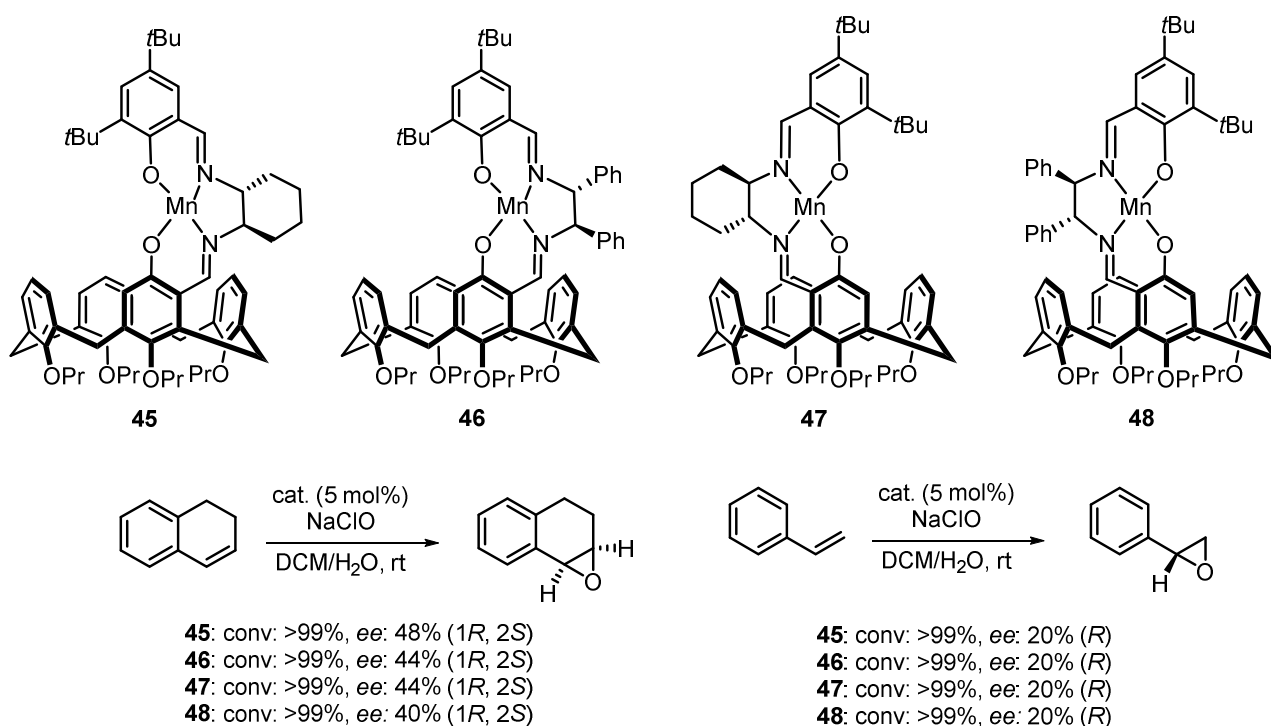
Scheme 1.16: The application of inherently chiral bidentate N/O calixarene ligands in the asymmetric addition of ketones to aldehydes.⁸⁹

The work shown in **Scheme 1.16** represents one of the very few *meta*-functionalized inherently chiral ligand studies. It is worth noting that both calixarenes **42** and **43** gave higher yields for the addition product than the model compound **44**. What was unfortunate was that the selectivity for all three ligands was largely the same, and given that the model compound had no inherent chirality, the selectivity in this reaction can be largely attributed to the central chirality of the L-prolinamide and not the inherent chirality of the calixarene. The selectivity for ligand **43** was slightly improved which could suggest a matched relationship between the two sources of chirality, but it is difficult to say this with certainty, because there is no mismatched relationship seen for ligand **42**.

Chapter 1: Introduction

Another relevant example of upper-rim functionalized calixarene ligands were four (salen)Mn^{III} catalyst complexes synthesized by Tomaselli and co-workers.¹⁰⁵ The compounds were synthesized using an approach similar to that of Huang. Electrophilic aromatic substitution on a calixarene with a single hydroxyl group in the *para*-position on one of the aryl rings, introduced a single salicylaldehyde functional group to either of the *meta*-positions, yielding a racemic mixture of enantiomers. The aldehyde group therefore served as the foundation of the metal binding system.

A subsequent condensation reaction, using two chiral imino-amino components, resulted in the formation of two sets of diastereomeric Schiff base ligands (**Scheme 1.17**). The formation of the diastereomers allowed for their separation via preparative TLC. Lastly, incorporation of Mn(III) yielded the four active catalytic complexes **45-48**.



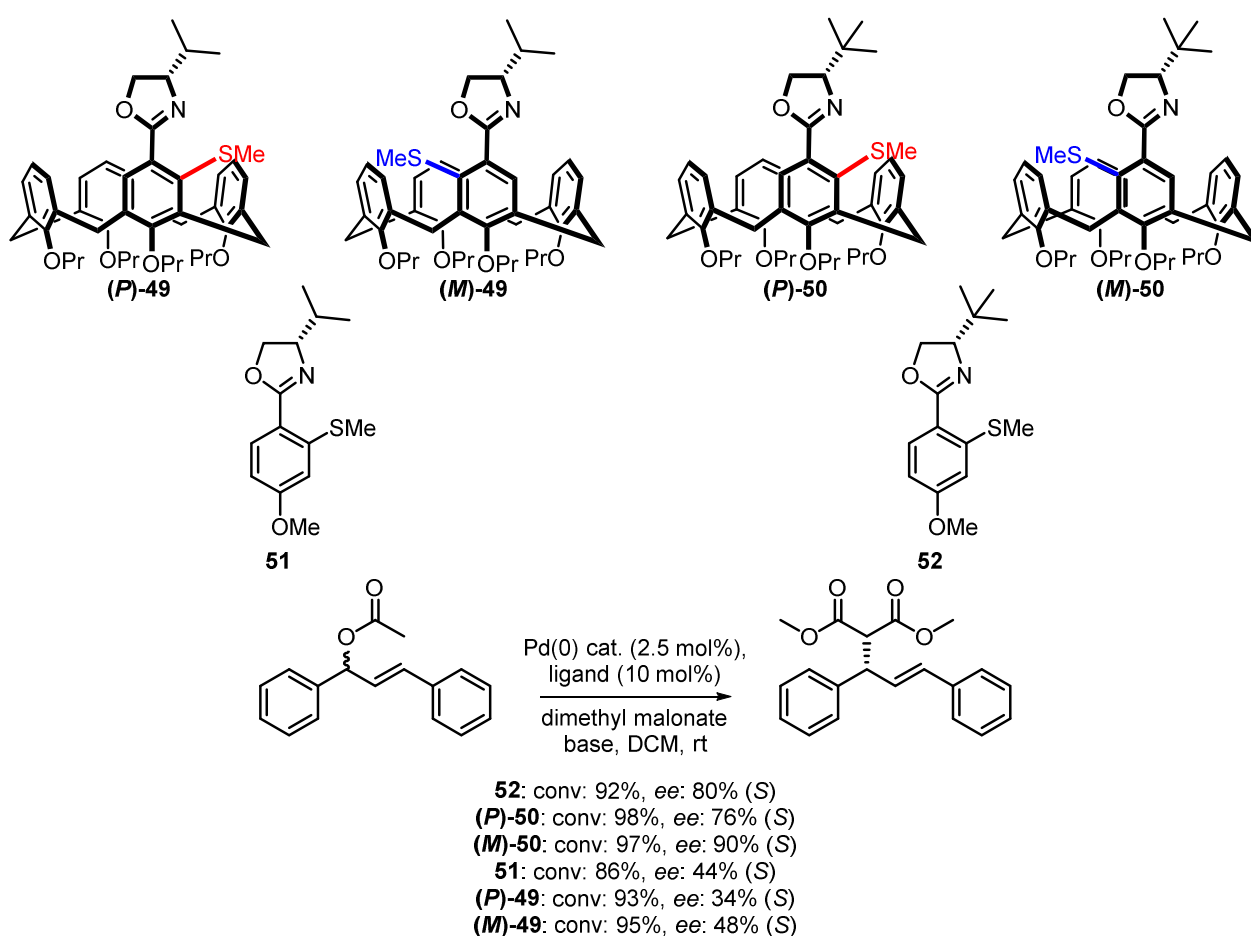
Scheme 1.17: The application of inherently chiral Mn(III) calixarene complexes to asymmetric epoxidation reactions.¹⁰⁵

The four complexes were evaluated with an asymmetric epoxidation reaction. Several different alkene substrates were tested; the two shown above were the only two that had complete conversion into the epoxide product and the conversions for the other substrates ranged between 30-90%. With regards to the application of any chiral ligands, the conversion/yields are important, but the real interest lies in the selectivity of these compounds. Ligands, in which the chiral element is focused on a central carbon, display an inversion of the selectivity when switching between the (*R*) and (*S*) chiral configurations. Therefore, when using the (*P*) and (*M*) versions of inherently chiral ligands, you would expect to see the same outcome. Unfortunately, the four ligands pictured above all yielded largely similar selectivities.

Chapter 1: Introduction

Given that the configuration of the Schiff base component was fixed over all four, it is reasonably safe to conclude that all of the observed selectivity in these reactions is due to induction by the Schiff base component and not the calixarene. There were small deviations in some of the results that might suggest a small contribution from the calixarene, but even so, the contribution is a minor one. Moreover, no model compounds were included in the study, making it difficult to conclusively disregard the role of the calixarene in the reaction.

The first example of an application study, in which the inherent chirality made a notable contribution to the achiral induction of the reaction, was published in 2014 by the Arnott group.¹⁰⁶ A small library of S/N bidentate ligands were synthesized using the asymmetric ortholithation methods developed by Arnott and co-workers.^{91,95} These six ligands were then tested in the asymmetric Tsuji-Trost reaction (**Scheme 1.18**).



Scheme 1.18: The application of inherently chiral bidentate S/N calixarene ligands to the asymmetric Tsuji-Trost reaction.¹⁰⁶

The two model ligands, **51** and **52**, afforded the product with ee values of 44% and 80% respectively, with the improved selectivity of **52** resulting from the bulkier *t*-butyl group attached to the steric center. All four of the calixarene ligands favored the formation of the (*S*) enantiomer. From this it can be concluded that the majority of the steric induction was a result of the stereocenter present on the two oxazoline functional groups.

Chapter 1: Introduction

Despite this fact, the results from the four calixarene ligands show that the inherent chirality does have an impact on the enantiomeric ratio. For the two sets of calixarene ligands, there appears to be a potential matched/mismatched relationship between the inherent chirality of the calixarene and the central chirality of the oxazoline. What this means is that for ligand **(M)-49**, with (*M*) inherent and (*S*) central chirality, the observed selectivity is slightly higher than that of the model compound, indicating that both forms of chirality co-operate and favor the formation of the same diastereomer.

The opposite is seen for ligand **(P)-49**, where the (*P*) inherent chirality of the calixarene seems to slightly favor the (*R*) enantiomer, yielding an enantiomeric mixture lower than that of the model compound. The same trend is seen for ligands **(M)/(P)-50**, and is slightly pronounced. This coincides with similar observations made by Dai and co-workers during the application of their planar chiral ferrocene ligands.⁹⁸ They also noted a matched/mismatched relationship between the planar chirality of their ferrocene backbone and the central chirality of the oxazoline. These preliminary results are some of the first examples illustrating the contribution *meta*-functionalized inherently chiral calixarene ligands have on achieving some degree of chiral induction in an asymmetric transformation.

1.4 Proposed project and targeted outcomes.

The focus of the study will two-fold. Firstly, furthering the development of stereoselective functionalization methods toward inherently chiral calixarenes and secondly, to find applications where the influence of inherent chirality is far more noteworthy.

Currently, the oxazolines have been shown to successfully direct the asymmetric ortholithiation reaction. The goal was to expand on this method by incorporating the chiral sulfoxide directing group. Results from a previous, but incomplete project, showed that the chiral sulfoxide was able to direct lithiation reactions. The aim would be to complete this project and present these findings alongside the oxazoline calixarenes. Despite the oxazoline directed lithiation being well established, numerous underlying questions regarding subtle roles played by the solvent, ligand and alkyllithium used in these reactions remain unanswered. We planned on revisiting this chemistry in order to better understand the individual impacts of these three reaction components.

To date, very few inherently chiral *meta*-functionalized ligands have been reported, none of which have shown inherent chirality being capable of generating an asymmetric environment that affords high ratios of enantiomerically enriched product mixtures. Our aim was to develop a new library of inherently chiral *meta*-functionalized ligands, capable of imparting their inherent chirality on asymmetric catalytic transformations. Currently, we have the means to selectively synthesize these compounds, without the need for optical resolution. In combination with positive results from preliminary application studies, this presents the ideal foundation to further develop the applications of this class of compound.

1.5 References.

- (1) Andreetti, G. D.; Ungaro, R.; Pochini, A. *J. Chem. Soc., Chem. Commun.* **1979**, 1005.
- (2) von Baeyer, A. *Ber. Dtsch. Chem. Ges.* **1872**, 5, 280.
- (3) Lederer, L. *J. Prakt. Chem.* **1894**, 50, 223.
- (4) Manesse, O. *Ber. Dtsch. Chem. Ges.* **1894**, 27, 2409.
- (5) Blumer, L. British Patent. 6823, 1903
- (6) Blumer, L. British Patent. 23880, 1903
- (7) Storey, W. H. British Patent. 8875, 1905
- (8) Luft, A. British Patent. 10218, 1902
- (9) Baekeland, L. H. US Patent. 942699, 1908.
- (10) Raschig, F. *Angew. Chem.* **1912**, 25, 1939.
- (11) Zinke, A.; Ziegler, E. *Chem. Ber.* **1941**, 74, 1729.
- (12) Zinke, A.; Ziegler, E. *Chem. Ber.* **1944**, 77, 264.
- (13) Niederl, J.; Vogel, H. *J. Am. Chem. Soc.* **1940**, 62, 2512.
- (14) Zinke, A.; Zigeuner, G.; Hossinger, K.; Hoffman, G. *Monatsh Chem.* **1952**, 79, 438.
- (15) Cornforth, J. W.; Hart, P. D.; Nicholls, G. A.; Rees, R. J. W.; Stock, J. A. *Br. J. Pharmacol. Chemother.* **1955**, 10, 73.
- (16) Gueniffe, H.; Kammerer, H.; Klepser, E. *Makromol. Chem.* **1972**, 162, 199.
- (17) Kammerer, H.; Happel, G.; Caeser, F. *Makromol. Chem.* **1972**, 162, 179.
- (18) Andreetti, G. D.; Ungaro, R.; Pochini, A. *J. Chem. Soc., Chem. Commun.* **1981**, 2, 533.
- (19) Coruzzi, M.; Andreetti, G. D.; Bocchi, V.; Pochini, A.; Ungaro, R. *J. Chem. Soc., Perkin Trans. 2* **1982**, 1133.
- (20) Gutsche, C. D.; Muthukrisnan, R. *J. Org. Chem.* **1978**, 43, 4905.
- (21) Homden, D. M.; Redshaw, C. *Chem. Rev.* **2008**, 108, 5086.
- (22) McIldowie, M. J.; Mocerino, M.; Ogden, M. I. *Supramol. Chem.* **2010**, 22, 13.
- (23) Zheng, Y. S.; Luo, J. *J. Incl. Phenom. Macrocycl. Chem.* **2011**, 71, 35.

Chapter 1: Introduction

- (24) Li, S-Y.; Xu, Y-W.; Liu, J-M.; Su, C-Y. *Int. J. Mol. Sci.* **2011**, *12*, 429.
- (25) Li, Z-Y.; Chen, J-W.; Liu, Y.; Xia, W.; Wang, L. *Curr. Org. Chem.* **2011**, *15*, 39.
- (26) Vicens, J.; Bohmer, V. *Calixarenes: a versatile class of macrocyclic compounds*; Kluwer Academic Publishers, 1991.
- (27) Gutsche, C. D. *Calixarenes: An Introduction*; The Royal Society of Chemistry: Cambridge, 2008.
- (28) Tobergte, D. R.; Curtis, S. *Calixarenes 2001*; Asfari, Z.; Bohmer, V.; Harrowfield, J.; Vicens, J., Eds.; Kluwer Academic Publishers, 2013; Vol. 53.
- (29) Mandolini, L.; Ungaro, R. *Calixarenes in Action*; 1st ed.; Imperial College Press: London, 2000.
- (30) Zhang, L.; Godinez, L. A.; Lu, T.; Gokel, G. W.; Kaifer, A. E. *Angew. Chem., Int. Ed. Engl.* **1995**, *34*, 235.
- (31) Talanova, G. G.; Elkarim, N. S. A.; Talanov, V. S.; Bartsch, R. A. *Anal. Chem.* **1999**, *71*, 3106.
- (32) Tshikhudo, R. T.; Demuru, D.; Wang, Z.; Brust, M.; Secchi, A.; Arduini, A.; Pochini, A. *Angew. Chem., Int. Ed.* **2005**, *44*, 2913.
- (33) Schalley, C. A. *Mass Spectrom. Rev.* **2001**, *20*, 253.
- (34) Schalley, C. A. *Int. J. Mass Spectrom.* **2000**, *194*, 11.
- (35) Vincenti, M.; Irico, A. *Int. J. Mass Spectrom.* **2002**, *214*, 23.
- (36) Atwood, J. L.; Barbour, L. J.; Thallapally, P. K.; Wirsig, T. B. *Chem. Commun.* **2005**, 51.
- (37) Tian, J.; Thallapally, P. K.; Dalgarno, S. J.; McGrail, P. B.; Atwood, J. L. *Angew. Chem., Int. Ed.* **2009**, *48*, 5492.
- (38) Ananchenko, G. S.; Moudrakovski, I. L.; Coleman, A. W. *Angew. Chem., Int. Ed.* **2008**, *47*, 5616.
- (39) Dong, Z.; Luo, Q.; Liu, J. *Chem. Soc. Rev.* **2012**, *41*, 7890.
- (40) Dospil, G.; Schatz, J. *Tetrahedron Lett.* **2001**, *42*, 7837.
- (41) Molenveld, P.; Engbersen, J. F. J.; Reinhoudt, D. N. *Angew. Chem., Int. Ed.* **1999**, *38*, 3189.
- (42) Lui, M.; Liao, W.; Hu, C.; Du, S.; Zhang, H. *Angew. Chem., Int. Ed.* **2011**, *51*, 1585.
- (43) Kennedy, S.; Karotsis, G.; Beavers, C. M.; Teat, S. J.; Brechin, E. K.; Dalgarno, S. J. *Angew. Chem., Int. Ed.* **2010**, *49*, 4205.
- (44) Gramage-Doria, R.; Armspach, D.; Matt, D. *Coord. Chem. Rev.* **2013**, *257*, 776.
- (45) Roll, W.; Brintzinger, H.-H.; Rieger, B.; Zolk, R. *Angew. Chem., Int. Ed.* **1990**, *29*, 279.

Chapter 1: Introduction

- (46) Diamond, D.; Nolan, K. *Anal. Chem.* **2001**, *73*, 22.
- (47) Filenko, D.; Gotszalk, T.; Kazantseva, Z.; Rabinovych, O.; Koshets, I.; Shirshov, Y.; Kalchenko, V.; Rangelow, I. W. *Sens. Actuators, B.* **2005**, *111–112*, 264.
- (48) Chaabane, R. Ben; Gamoudi, M.; Guillaud, G.; Jouve, C.; Lamartine, R.; Bouazizi, A.; Maaref, H. *Sens. Actuators, B.* **1996**, *31*, 41.
- (49) Gutsche, C. D. *J. Org. Chem.* **1986**, *51*, 742.
- (50) Ullmann, F.; Brittner, K. *Eur. J. Org. Chem.* **1909**, 2539.
- (51) Wohl, A.; Mylo, B. *Ber. Dtsch. Chem. Ges.* **1912**, *45*, 2046.
- (52) Hultzsch, K. *Chem. Ber.* **1941**, *75*, 106.
- (53) Euler, H. V; Adler, E.; Cedwall, O. J.; Torngren, O. *Ark. Mineral. Geol.* **1941**, *15A*.
- (54) Alfieri, C.; Dradi, E.; Pochini, A.; Ungaro, R.; Andreetti, G. D. *J. Chem. Soc., Chem. Commun.* **1983**, 1075.
- (55) Gutsche, C. D.; Bauer, L. J. *J. Am. Chem. Soc.* **1985**, *107*, 6052.
- (56) Megson, N. R. L. *Oesterr. Chem.-Ztg.* **1953**, *54*, 317.
- (57) Zinke, A.; Ott, R. *Oesterr. Chem.-Ztg.* **1954**, *55*, 156.
- (58) Zetta, L.; Wolff, A.; Vogt, W.; Platt, K.-L.; Böhmer, V. *Tetrahedron* **1991**, *47*, 1911.
- (59) Collins, E. M.; McKervey, M. A.; Madigan, E.; Moran, M. B.; Owens, M.; Ferguson, G.; Harris, S. J. *J. Chem. Soc., Perkin Trans. 1* **1991**, *3*, 3137.
- (60) Scheerder, J.; Vreekamp, R. H.; Engbersen, J. F. J.; Verboom, W.; van Duynhoven, J. P. M.; Reinhoudt, D. N. *J. Org. Chem.* **1996**, *61*, 3476.
- (61) Noyori, R.; Takaya, H. *Acc. Chem. Res.* **1990**, *23*, 345.
- (62) Riant, O.; Samuel, O.; Kagan, H. B. *J. Am. Chem. Soc.* **1993**, *115*, 5835.
- (63) Yamamoto, T.; Fukushima, T.; Kosaka, A.; Jin, W.; Yamamoto, Y.; Ishii, N.; Aida, T. *Angew. Chem., Int. Ed.* **2008**, *47*, 1672.
- (64) Prins, L. J.; Huskens, J.; de Jong, F.; Timmerman, P.; Reinhoudt, D. N. *Nature* **1999**, *398*, 498.
- (65) Szumna, A. *Chem. Soc. Rev.* **2010**, *39*, 4274.
- (66) Böhmer, V.; Kraft, D.; Tabatabai, M. *J. Inclusion Phenom. Mol. Recognit. Chem.* **1994**, *19*, 17.

Chapter 1: Introduction

- (67) Cort, A. D.; Mandolini, L.; Pasquini, C.; Schiaffino, L.; Chimica, D.; Sapienza, U. La; Roma, B. *New J. Chem.* **2004**, *28*, 1198.
- (68) Iwamoto, K.; Shimizu, H.; Araki, K.; Shinkai, S. *J. Am. Chem. Soc.* **1993**, *115*, 3997.
- (69) Bergamaschi, M.; Bigi, F.; Lanfranchi, M.; Maggi, R.; Pastorio, A.; Angela, M.; Peri, F.; Porta, C.; Sartorp, G. *Tetrahedron* **1997**, *53*, 13037.
- (70) Scully, P. A.; Hamilton, T. M.; Bennett, J. L. *Org. Lett.* **2001**, *3*, 2741.
- (71) Biali, S. E.; Böhmer, V.; Cohen, S.; Ferguson, G.; Grüttner, C.; Grynszpan, F.; Paulus, E. F.; Thondorf, I.; Vogt, W. *J. Am. Chem. Soc.* **1996**, *118*, 12938.
- (72) Gopalsamuthiram, V.; Predeus, A. V.; Huang, R-H.; Wulff, W. D. *J. Am. Chem. Soc.* **2009**, *131*, 18018.
- (73) Wang, M-X.; Yang, H-B. *J. Am. Chem. Soc.* **2004**, *126*, 15412.
- (74) Hyun, K.; Gutsche, D. *J. Org. Chem.* **1982**, 2713.
- (75) Böhmer, V.; Marschollek, F.; Zettat, L. *J. Org. Chem.* **1987**, *52*, 3200.
- (76) Cao, Y-D.; Luo, J.; Zheng, Q-Y.; Chen, C-F.; Wang, M-X.; Huang, Z-T. *J. Org. Chem.* **2004**, *69*, 206.
- (77) Huang, Z-T.; Chen, C-F.; Zheng, Q-Y.; Luo, J. *Chem. - Eur. J.* **2005**, *11*, 5917.
- (78) Li, S-Y.; Zheng, Q-Y.; Chen, C-F.; Huang, Z-T. *Tetrahedron: Asymmetry* **2005**, *16*, 641.
- (79) Luo, J.; Zheng, Q-Y.; Chen, C-F.; Huang, Z-T. *Tetrahedron* **2005**, *61*, 8517.
- (80) Narumi, F.; Hattori, T.; Yamabuki, W.; Kabuto, C.; Kameyama, H. *Tetrahedron: Asymmetry* **2005**, *16*, 793.
- (81) Narumi, F.; Yamabuki, W.; Hattori, T.; Kameyama, H.; Miyano, S. *Chem. Lett.* **2003**, *32*, 320.
- (82) Shirakawa, S.; Shimizu, S. *New J. Chem.* **2010**, *34*, 1217.
- (83) Shirakawa, S.; Moriyama, A.; Shimizu, S. *Eur. J. Org. Chem.* **2008**, 5957.
- (84) Shirakawa, S.; Moriyama, A.; Shimizu, S. *Org. Lett.* **2007**, *9*, 3117.
- (85) Shirakawa, S.; Kimura, T.; Murata, S.; Shimizu, S. *J. Org. Chem.* **2009**, *74*, 1288.
- (86) Huang, Z-T.; Chen, C-F.; Xu, Z-X.; Miao, R. *Sci. China. Ser. B Chem.* **2009**, *52*, 505.
- (87) Miao, R.; Zheng, Q-Y.; Chen, C-F.; Huang, Z-T. *J. Org. Chem.* **2005**, *70*, 7662.
- (88) Browne, J. K.; McKervey, A. M.; Pitarch, M.; Russel, J. A. *Tetrahedron Lett.* **1998**, *39*, 1787.
- (89) Xu, Z-X.; Li, G-K.; Chen, C-F.; Huang, Z-T. *Tetrahedron* **2008**, *64*, 8668.

Chapter 1: Introduction

- (90) Herbert, S. A. Oxazoline Directed Lithiation of Calix[4]arene and Ferrocene, PhD, Stellenbosch University, 2011.
- (91) Herbert, S. A.; Arnott, G. E. *Org. Lett.* **2009**, *11*, 4986.
- (92) Sammakia, T.; Latham, H. A.; Schaad, D. R. *J. Org. Chem.* **1995**, *60*, 10.
- (93) Sammakia, T.; Latham, H. A. *J. Org. Chem.* **1996**, *61*, 1629.
- (94) Sammakia, T.; Latham, H. A. *J. Org. Chem.* **1995**, *60*, 6002.
- (95) Herbert, S. A.; Arnott, G. E. *Org. Lett.* **2010**, *12*, 4600.
- (96) Lindstrom, B.; Pettersson, L. J. *CATTECH* **2003**, *7*, 130.
- (97) Kirchoff, G. *Mémoires l'Académie impériale des Sci.* **1811**, *27*.
- (98) Dai, L-X.; Tu, T.; You, S-L.; Deng, W-P.; Hou, X-L. *Acc. Chem. Res.* **2003**, *36*, 659.
- (99) Floriani, C.; Floriani Moro, R. *Adv. Organomet. Chem.* **2001**, *47*, 167.
- (100) Dieleman, C.; Steyer, S.; Jeunesse, C.; Matt, D. *J. Chem. Soc., Dalton Trans.* **2001**, *3*, 2508.
- (101) Kuhn, P.; Sémeril, D.; Jeunesse, C.; Matt, D.; Lutz, P. J.; Louis, R.; Neuburger, M. *Dalton Trans.* **2006**, 3647.
- (102) Steyer, S.; Jeunesse, C.; Harrowfield, J.; Matt, D. *Dalton Trans.* **2005**, 1301.
- (103) Wieser, C.; Matt, D.; Harriman, A. *J. Chem. Soc., Dalton Trans.* **1997**, *1*, 2391.
- (104) Sémeril, D.; Jeunesse, C.; Matt, D.; Toupet, L. *Angew. Chem., Int. Ed.* **2006**, *45*, 5810.
- (105) Amato, M. E.; Ballistreri, F. P.; Pappalardo, A.; Tomaselli, G. A.; Toscano, R. M.; Williams, D. J. *Eur. J. Org. Chem.* **2005**, 3562.
- (106) Herbert, S. A.; Van Laeren, L. J.; Castell, D. C.; Arnott, G. E. *Beilstein J. Org. Chem.* **2014**, *10*, 2751.

2 Chapter 2 - Synthesis of calixarene starting materials

2.1 Introduction.

Making use of a chiral auxiliary to asymmetrically direct an ortholithiation reaction has been the key strategy toward the synthesis of inherently chiral calixarenes. To date, the oxazolines have been used on both the debutylated and butylated calixarenes in order to asymmetrically direct the ortholithiation reaction.^{1,2} As is often the case in scientific research, the conclusion of past projects left a number of questions surrounding the ortholithiation of these calixarenes unanswered. The purpose of this study has been two-fold. On the one hand, it has been aimed at finding the answers to the unfinished sections of research presented by past projects. However, the primary goal has been finding an application for these inherently chiral compounds. Due to the fact that this project has incorporated elements of chemistry spanning over several previous projects, many starting material calixarene compounds needed to be synthesized. The aim of this chapter is to clearly present the two major synthetic pathways employed to attain the four target oxazoline calixarenes shown in **Figure 2.1**.

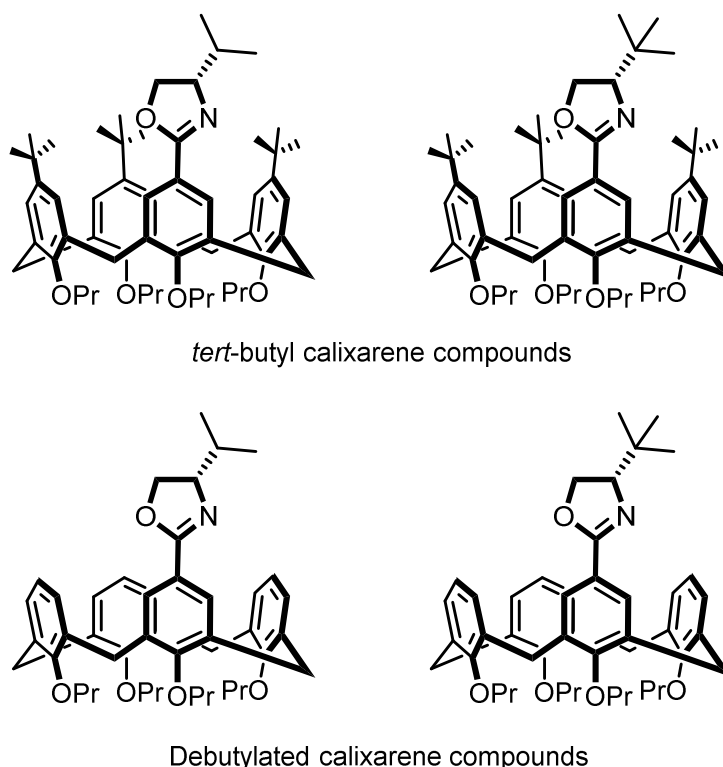


Figure 2.1: Four target oxazoline calixarene starting material compounds.

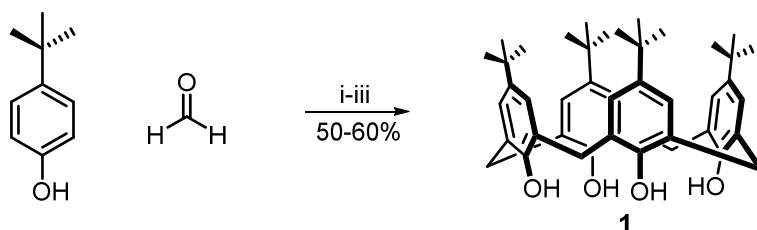
The total synthesis of all the calixarene starting materials can be separated into two distinct branches. One being the *tert*-butyl calixarenes, which still contain the *tert*-butyl groups on the three un-functionalized rings. The other pathway being the debutylated calixarenes, where all of the *tert*-butyl groups have been removed from the upper-rim.

Chapter 2: Synthesis of calixarene starting materials

Both branches have two final products; the isopropyl and *tert*-butyl oxazoline calixarenes. This collection of chemistry largely consists of literature procedures and methods that were developed and optimized by Dr Simon Herbert. These procedures were taken from his thesis, repeated, and minor contributions were made over the course of this study to the optimization process by fine-tuning some of the conditions.¹

2.2 Synthesis of the parent *tert*-butyl calixarene.

The start of any calix[4]arene based project begins with the synthesis of the parent calixarene **1**. Making use of the optimized procedure reported by Gutsche and co-workers,³ the parent calixarene was synthesized via a base-catalyzed condensation reaction between formaldehyde and *para-tert*-butyl phenol (**Scheme 2.1**).



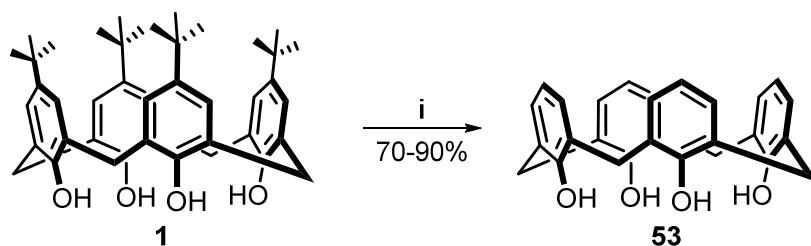
Scheme 2.1: Synthesis of the parent calix[4]arene **1**. Reagents and conditions: i) *p-t*-butyl phenol (1.0 equiv), formaldehyde (1.3 equiv), NaOH (0.05 equiv), H₂O (0.25 equiv), Δ, 35 min. ii) diphenyl ether, 180 °C for 40 min. iii) reflux 260 °C for 4 h.

Once the product was isolated and washed with ethyl acetate, it was of sufficient purity for use in either the tri-propylation or reverse Friedel Crafts de-alkylation reactions that would follow. If necessary, the crude could be further purified by recrystallization from boiling toluene. This was often avoided given the scale of the reaction and the volume of boiling toluene required. Calixarene **1** was obtained in yields between 50-60%, which compared well with the values reported in the literature.³

2.3 Synthesis of debutylated calixarenes.

2.3.1 Synthesis of tetra-hydroxyl calixarene – **53**.

The first step in the non-alkylated calixarene synthetic pathway used a reverse Friedel Crafts de-alkylation reaction; another procedure originally reported by Gutsche.⁴ Aluminum trichloride was employed as a Lewis acid in the presence of phenol to fully dealkylate the upper rim of the calixarene (**Scheme 2.2**).

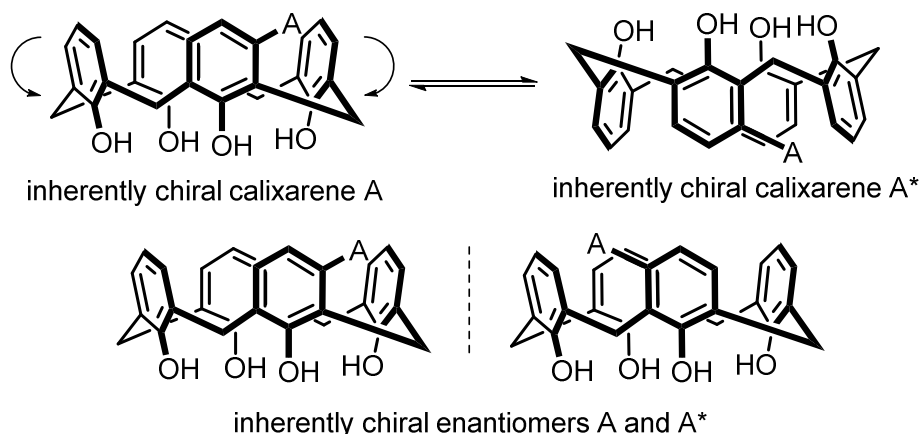


Scheme 2.2: Reverse Friedel-Crafts dealkylation. Reagents and conditions: i) AlCl_3 (5.0 equiv), phenol (2.5 equiv), toluene, rt, 12 h.

Purification was conveniently achieved via trituration from diethyl ether, followed by filtration and drying under high vacuum. The reaction was relatively robust and after several attempts **53** was isolated in yields ranging between 70-90%. A well-known property of the calix[4]arene is the dynamic nature of its conformation in solution.^{5,6} Each of the rings are able to freely rotate through the center of the three dimensional structure. This type of motion or rotation has been dubbed the “*endo*-oxygen-through-the-annulus” inversion and can be seen by the two broad signals for the methylene bridge protons in the ^1H NMR spectrum.⁷

2.3.2 Synthesis of tetra-propoxy calixarene – **54**.

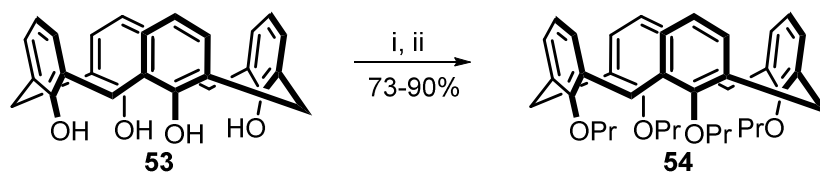
The constant rapid inversion of the calixarene structure poses a problem when considering its implication with regards to inherent chirality. Central inversion of an inherently chiral calixarene would yield the compound's corresponding enantiomer. Without locking the conformation of the calixarene in place, synthesis of an inherently chiral calixarene compound would not be possible. This inversion and its effect on the inherent chirality is depicted by **Scheme 2.3**.



Scheme 2.3: Inversion of the inherently chiral calixarene A, with a side by side comparison of its corresponding enantiomer.

Chapter 2: Synthesis of calixarene starting materials

'Inherently chiral calixarene A' is the simplest theoretical representation of an inherently chiral calixarene, based on the compounds reported in this study. The inversion of calixarene A yields inherently chiral calixarene A*. Rotation of the inverted product and a side by side comparison of A and A* shows that they are enantiomers. Seiji Shinkai is a pioneer in the field of calixarene chemistry, and in the early 1990s published a paper describing the structures and conformations of calixarenes in solution, as well as how they could be immobilized.⁷ After a process of trial and error it was discovered that an *n*-propyl group was the smallest group able to immobilize the conformation. Fully alkylating the lower-rim with this functional group would lock the conformation of the calixarene and prevent any further inversion from taking place (**Scheme 2.4**).



Scheme 2.4: Propylation of **53**. Reagents and conditions: i) NaH (10.0 equiv), DMF, 0 °C, 1 h; ii) iodo-propane (12.0 equiv), rt, 24 h.

The first step of the reaction was a deprotonation at 0 °C, using excess molar equivalents of NaH. Deprotonation of the starting material was complete within an hour, evidenced by the change in the reaction mixture to a characteristic white opaque colour. After the addition of iodo-propane, the reaction took 24 h to reach completion. The excess dimethylformamide was removed with multiple water washes and the crude product was purified by trituration in hot methanol. The fully propylated **54** was isolated in high yields ranging between 73-90%. Due to the mild nature of the reaction conditions, as well as the convenient purification methods, this reaction could be carried out on a large scale, up to 35 g. The ¹H NMR spectrum of **54** depicts some of the structural, as well as conformational properties commonly seen for calixarenes in solution (**Figure 2.2**).

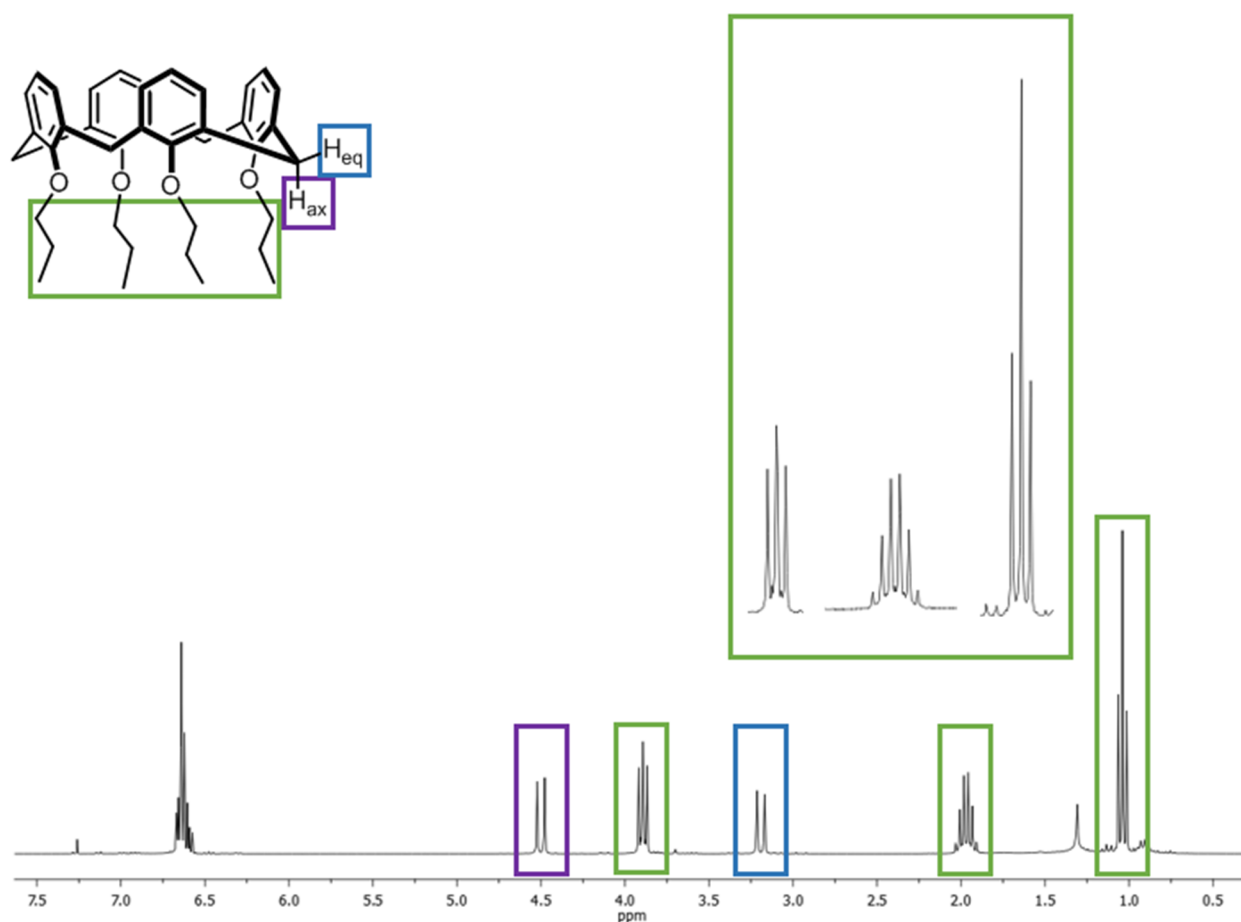


Figure 2.2: ^1H NMR spectrum of calixarene **54**. Signals for the propyl chain are outlined in green, axial methylene protons in purple and the equatorial protons in blue.

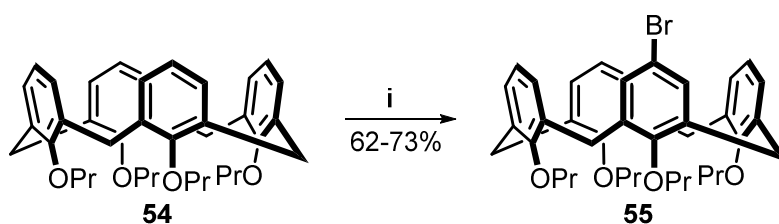
The nature of the magnetic anisotropic effect on the outside of the calixarene affects each of the two methylene bridge protons differently. With the phenolic rings locked in position, the molecule has a rigid three dimensional structure. The axial and equatorial protons are both fixed in position and experience this magnetic field differently. The equatorial protons face upwards and are situated within the magnetic field, whereas the axial protons are facing downwards, away from the field. Therefore, instead of seeing one signal for both protons, the two independent protons have different chemical shifts and are diastereotopic. They couple to one another, which results in two separate doublets (a typical AX spin system). The upfield signal (δ 3.17 ppm) corresponds to the equatorial protons (outlined in blue) and the downfield shift (δ 4.48 ppm) corresponds to the axial protons (outlined in purple). The second group of characteristic signals are the three sets of protons on the propyl chain (all outlined in green). The lower CH_3 (triplet, δ 1.04 ppm), middle CH_2 (sextet, δ 1.96 ppm) and upper CH_2 (triplet, δ 3.90 ppm). The time averaged conformation of **54** in solution resembles a calixarene in the true cone conformation. Without any functional groups on the upper-rim, and with four identical groups on the lower-rim, there is no steric discrepancy that takes place, and all of the aromatic rings share the same position. This means that each of the propyl chains share an equal but averaged position relative to the center of the calixarene.

Chapter 2: Synthesis of calixarene starting materials

These patterns differ significantly as the upper-rim of the calixarene becomes functionalized, which results in the positions of the aromatic rings shifting relative to the center of the bowl to accommodate the newly introduced steric strain. This will be demonstrated and explained in the sections that follow.

2.3.3 Synthesis of mono-bromo calixarene – **55**.

A single bromine was introduced onto the upper-rim of calixarene **54**, using strictly one equivalent of *N*-bromosuccinimide (**Scheme 2.5**). If more than a single equivalent was added, multiple bromination reactions would take place.



Scheme 2.5: Mono-bromination of **54**. Reagents and conditions: i) NBS (1.0 equiv), MEK, rt, 24 h.

Purification of **55** was a challenge. The reaction mixture consisted largely of the mono-bromo calixarene, with negligible amounts of the di, tri, and tetra-bromo calixarenes, as well as some unreacted starting material. The only means of obtaining pure **55** was by using a slow chromatographic separation, owing to the product and starting material having similar R_f values. Even though the brominated calixarenes were crystalline in the solid-state, the starting material, product and all of the brominated by-products recrystallized from the same methanol/DCM mixture. Often multiple columns were required to separate all of **55** from the reaction mixture, which was isolated in yields ranging between 62-73%. The introduction of the bromine atom to the upper-rim resulted in a loss of symmetry in the molecule and a change in conformation to the distorted pinched cone. This change could be seen by the four (two pairs) of diastereotopic doublets for the methylene bridge protons in the ^1H NMR spectrum of the product (**Figure 2.3**).

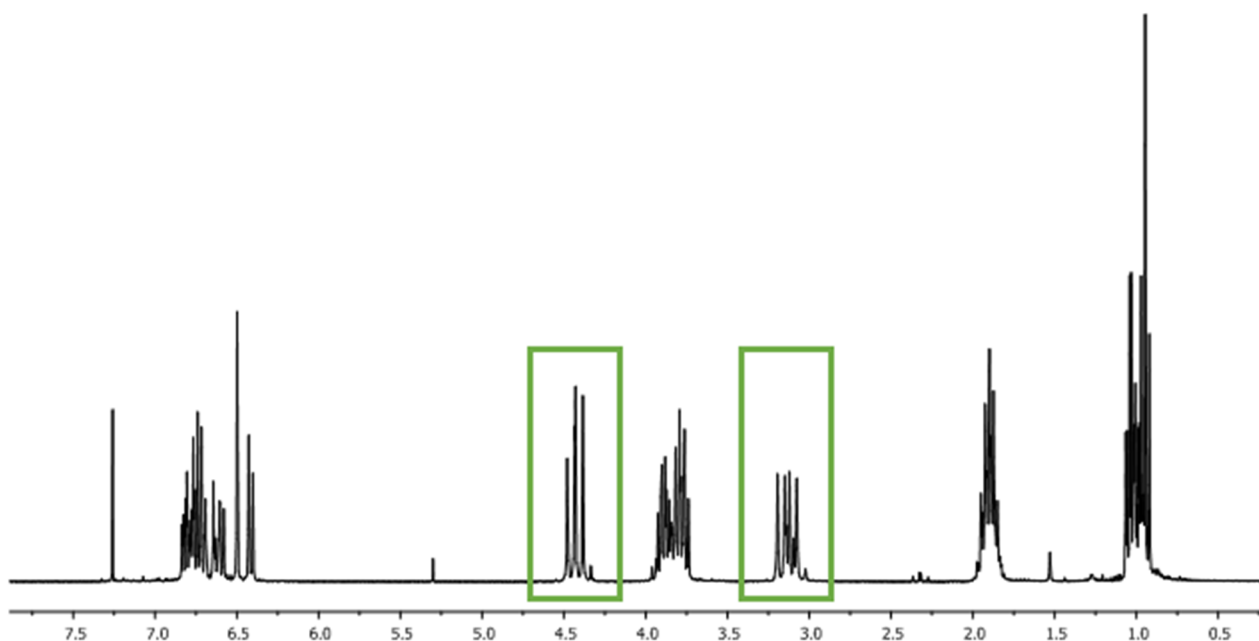
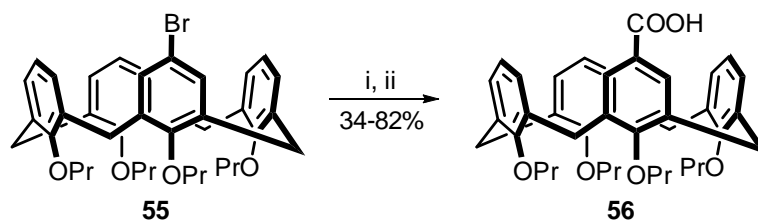


Figure 2.3: ^1H NMR spectrum of the mono-bromo calixarene **55**. The diastereotopic proton signals for the methylene bridge carbons have been outlined in green.

The most common conformation for mono-functionalized calixarenes in solution was the distorted pinched cone. All of the debutylated calixarene starting material structures shared this conformation (See later in **Section 2.4**).

2.3.4 Synthesis of carboxyl calixarene – **56**.

The carboxyl calixarene **56** was a common intermediate for both isopropyl and *tert*-butyl oxazoline calixarenes. Using a lithium halogen exchange reaction at $-78\text{ }^\circ\text{C}$ and quenching with carbon dioxide afforded the mono-carboxyl calixarene **56** (**Scheme 2.6**).



Scheme 2.6: Synthesis of **56** via lithium halogen exchange. Reagents and conditions: i) *n*-BuLi (1.5 equiv), THF, $-78\text{ }^\circ\text{C}$, 10 min; ii) CO_2 (gas, exs), $-78\text{ }^\circ\text{C}$ to rt, 12 h.

It was noted that the method used to quench the reaction with carbon dioxide had a significant impact on the yield. There were three ways in which carbon dioxide was introduced into the reaction mixture. The first was simply pouring the reaction mixture into a beaker filled with freshly collected dry ice.

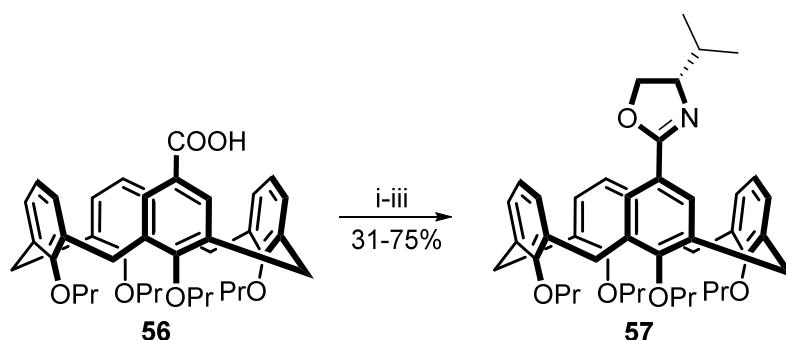
Chapter 2: Synthesis of calixarene starting materials

This had to take place as quickly as possible after the carbon dioxide collection, due to water condensation on the surface of the solid carbon dioxide. Exposing the reaction mixture to any moisture results in a proton quench and the recovery of **54**, essentially taking a step backwards in the synthesis.

The second option was to add solid dry ice directly to the flask. Again, this posed the problem of condensation and the introduction of water to the lithiated (anionic) intermediate. The third, and what was found to be the best option, was bubbling CO₂ gas through the reaction mixture for 5-10 minutes and letting the mixture warm to room temperature under a mild, positive pressure. Bubbling the CO₂ through the reaction mixture gave the highest yields up to 82%, whereas the other two methods resulted in far lower yields that ranged between 35-50%. Introduction of the carboxylic acid significantly changed the polarity of the product, which made column chromatography a convenient method of purification. The **54** by-product was always collected and recycled to synthesize more **55** starting material.

2.3.5 Synthesis of the isopropyl oxazoline calixarene – **57**.

The carboxylic acid **56** was next converted into the oxazoline in three steps (**Scheme 2.7**).



Scheme 2.7: Three-step synthesis of **57**. Reagents and conditions: i) (COCl)₂ (5.0 equiv), DCM, rt, 12 h; ii) L-valinol (1.15 equiv), Et₃N (3.0 equiv), DCM, 0 °C to rt, 12 h; iii) MsCl (3.0 equiv), Et₃N (3.0 equiv), DCM, 0 °C to rt, 12 h.

The synthesis of all oxazoline calixarenes generally followed the same three-step procedure. Firstly, using oxalyl chloride, the carboxylic acid was converted into its acid chloride. The solvent and any excess oxalyl chloride was then removed under reduced pressure. After drying the acid chloride under high vacuum, it was added dropwise to a cooled reaction mixture containing the chiral amino alcohol, which yielded the corresponding amide calixarene. The final step was the cyclization of the amide using mesyl chloride in the presence of a mild and non-nucleophilic base. **Scheme 2.7** depicts a relatively large range for the yield in this reaction. This was due to the fact that the synthesis of both the isopropyl and *tert*-butyl calixarene (following section) presented the same set of difficulties. As soon as the mass of the starting material exceeded 1.0 g, both the formation of the amide and ring closing reactions became problematic. In the case of the amide reaction, calixarene dimers would sometimes form.

Chapter 2: Synthesis of calixarene starting materials

In addition to this, the ring-closing reaction would also struggle to reach completion. Finally, **57** was purified via column chromatography. A vital step in the work-up of these reactions was washing the crude product several times with aqueous 2M potassium hydroxide. Without the base wash, the crude would stick on the column and only fractional amounts of product would be isolated.

This could be explained by the following; one of the by-products in the ring-closing reaction was methanesulfonic acid. It could be that the methanesulfonic acid interacted strongly with the silica and when the product was dry loaded onto the column, the calixarene became trapped by the excess amounts of methanesulfonic acid adhering to the silica. Afterwards, the only way to recover the crude was by flushing the column with a polar 10% MeOH-DCM solvent mixture. It should be noted that the addition of the oxazoline functional group to the calixarene framework added several new signals to the ^1H NMR spectrum (**Figure 2.4**).

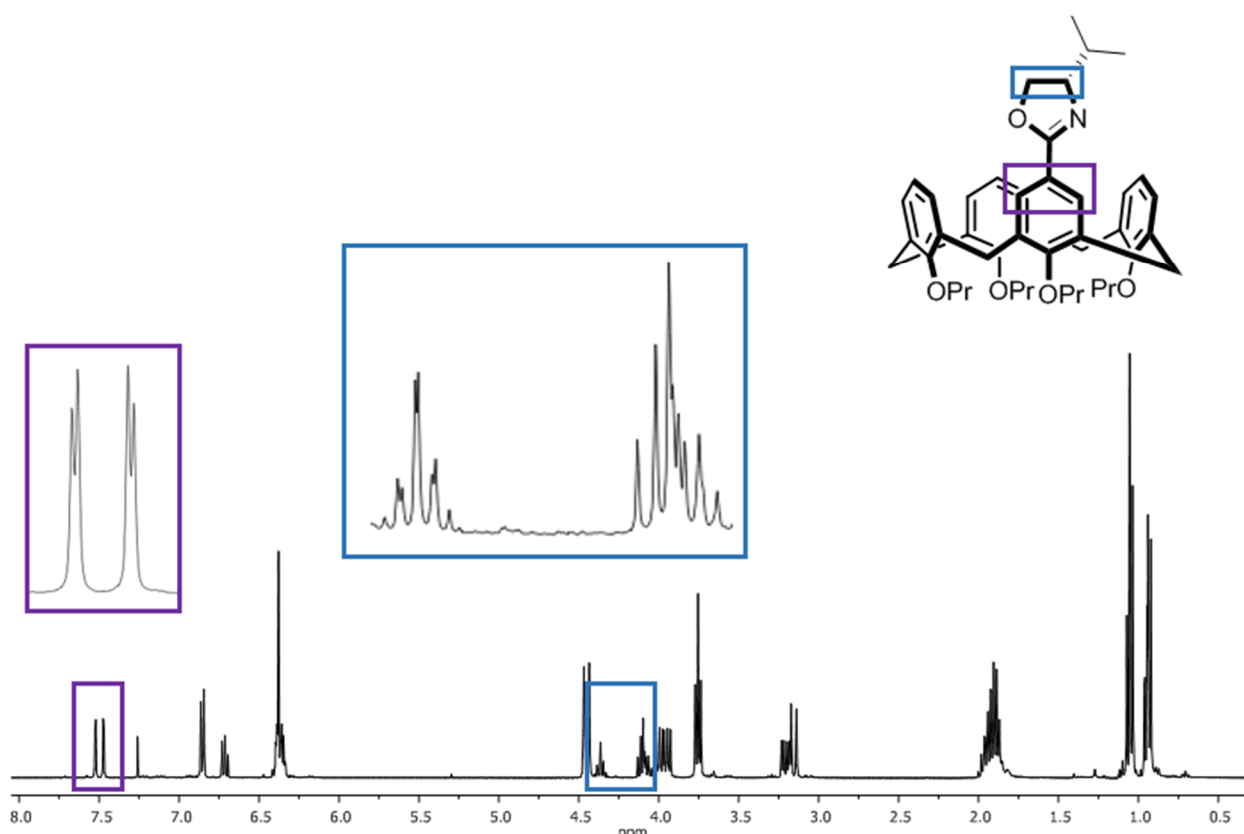


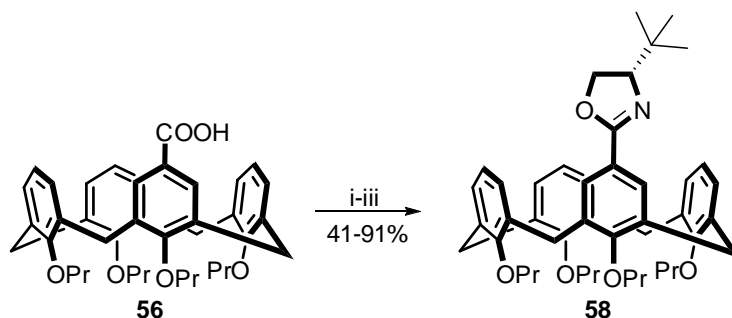
Figure 2.4: ^1H NMR spectrum of **57**. The newly introduced oxazoline signals are outlined in blue and the *ortho*-protons on either side of the oxazoline in purple.

The most notable and important of these signals being the AB doublets (outlined in purple) at δ 7.47 and δ 7.52 ppm ($J = 2.1$ Hz). They correspond to the two protons on the aromatic ring on either side of the oxazoline functional group. The reason why these two small signals were so important was because they were used to determine both the yield and selectivity of the ortholithiation reactions. This will be made clear in the following chapter.

Chapter 2: Synthesis of calixarene starting materials

2.3.6 Synthesis of *tert*-butyl oxazoline calixarene – **58**.

Using a similar procedure, the only difference being the choice of chiral amino alcohol, the *tert*-butyl oxazoline calixarene **58** was synthesized in three steps (**Scheme 2.8**).



Scheme 2.8: Three-step synthesis of **58**. Reagents and conditions: i) $(\text{COCl})_2$ (5.0 equiv), DCM, rt, 12 h; ii) Et_3N (3.0 equiv), *L*-*tert*-Leucinol (1.15 equiv), DCM, 0 °C to rt, 12 h; iii) MsCl (3.0 equiv), Et_3N (3.0 equiv), DCM, 0 °C to rt, 12 h.

Again, any synthesis attempted on anything more than 1.0 g of starting material was met with the same set of problems encountered in the synthesis of the isopropyl oxazoline **57**. The ^1H NMR spectrum for **58** closely resembled that of **57** (**Figure 2.5**).

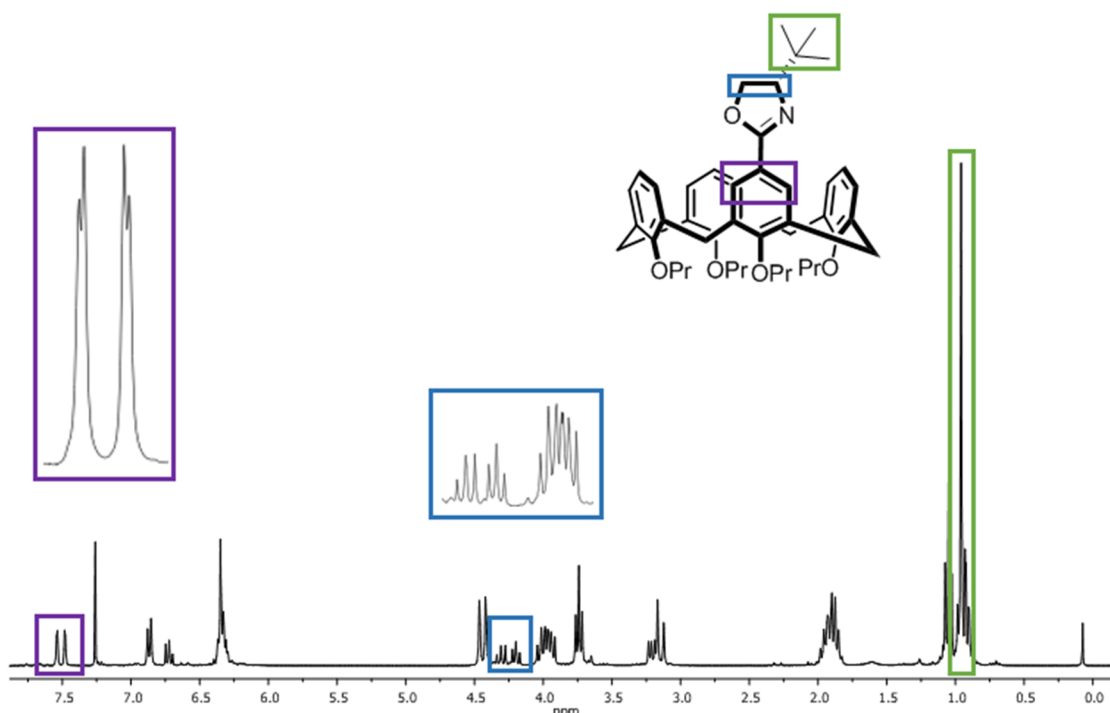


Figure 2.5: ^1H NMR spectrum of **58**. The oxazoline ring signals are outlined in blue, the *ortho*-protons either side of the oxazoline in purple and the oxazoline *tert*-butyl group in green.

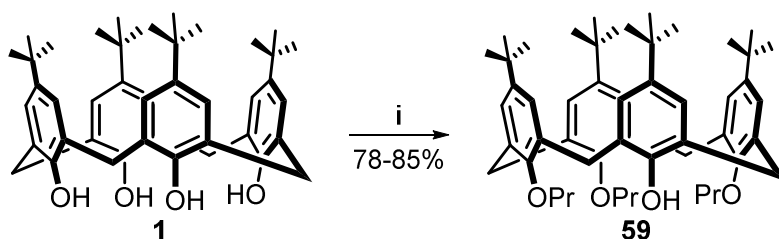
Chapter 2: Synthesis of calixarene starting materials

The ^1H NMR spectrum of **58** also contained the two AB doublets (outlined in purple) with chemical shifts of δ 7.38 and δ 7.44 ppm ($J = 1.8$ Hz). The most notable difference between the two spectra were the signals for the oxazoline R-groups. For **57** these doublet signals overlapped with the CH_3 signals on the propyl chain, while for **58** the *tert*-butyl group was a large singlet with a chemical shift of δ 0.87 ppm (outlined in green).

2.4 Synthesis of *tert*-butyl calixarenes.

2.4.1 Synthesis of tri-propoxy calixarene – **59**.

The first step toward the synthesis of the *tert*-butyl oxazolines was the tri-protection of the lower-rim (**Scheme 2.9**). The aim of this reaction was the activation of the *para*-position of the remaining un-protected aromatic ring. This would allow for selective mono-nitration of only one ring on the calixarene. Following the procedure published by Shinkai and co-workers, a mixture of barium oxide and barium hydroxide octahydrate was used as the base in the presence of a large excess of propyl iodide.⁷



Scheme 2.9: Selective tri-propylation of **1**. Reagents and conditions: i) BaO (3.3 equiv), $\text{Ba}(\text{OH})_2 \cdot 8\text{H}_2\text{O}$, iodo-propane (30.0 equiv), rt, 4 h.

This is one example of a number of “black box” reactions that find use in calixarene synthesis. These reactions are often optimized through a process of trial and error, before the ideal conditions are found. It is also sometimes difficult to fully explain how or why they work. For this selective tri-propylation, it was proposed that the presence of templating counter ions were responsible for generating the selectivity.⁷ The product was purified by recrystallization from a DCM-EtOH mixture, with a yield of up to 78% from the first crystallization. It was possible to isolate the remaining product from a second crystallization in a lower solvent volume. The addition of three propyl chains to the lower-rim significantly altered the conformation seen for the parent calixarene compound. The preferred cone conformation shifted to the pinched cone conformation, which can be seen in the ^1H NMR spectrum of the product (**Figure 2.6**). For **1** there was a single singlet (δ 1.21 ppm) for all four of the *tert*-butyl groups on the upper-rim. However, for **59** the *tert*-butyl signals were split into two distinct groups. The two on either side of the unprotected ring faced inwards, and were more shielded (δ 0.83 ppm, outlined in green), while the remaining two faced outwards and had different chemical shifts (δ 1.33 and δ 1.34 ppm, outlined in purple).

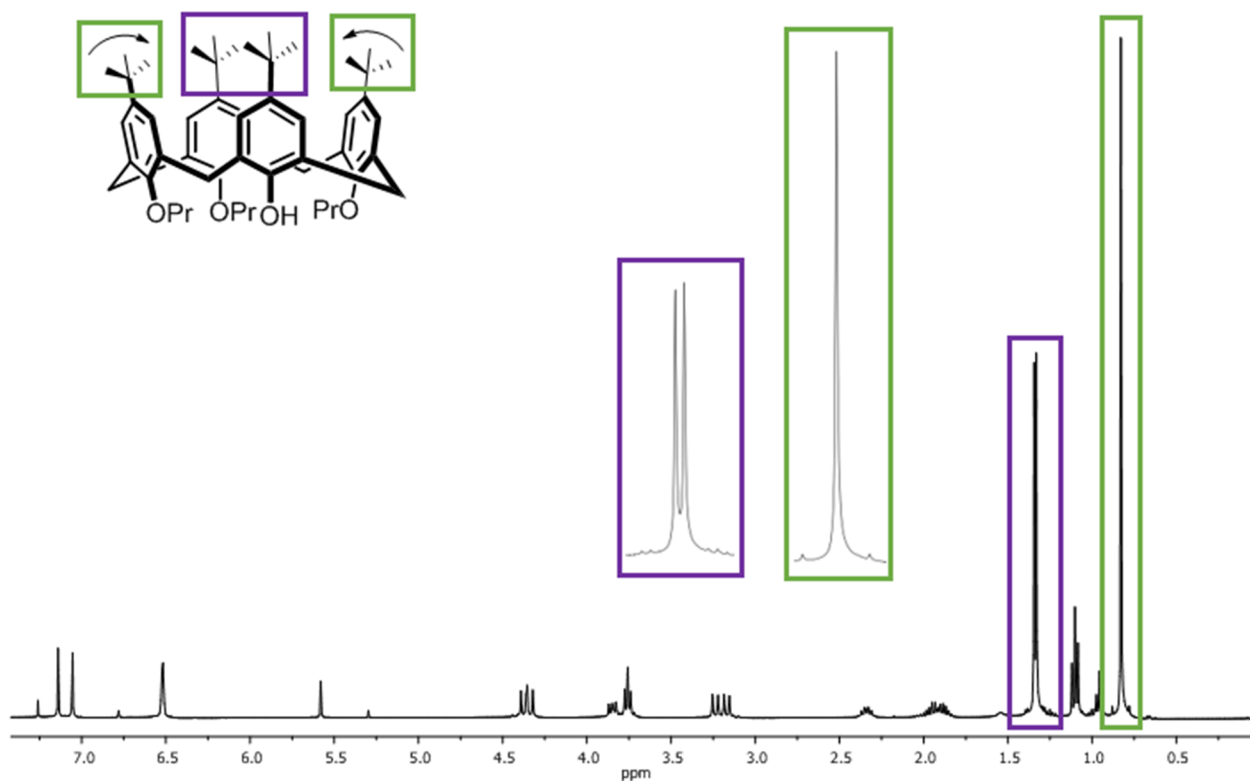
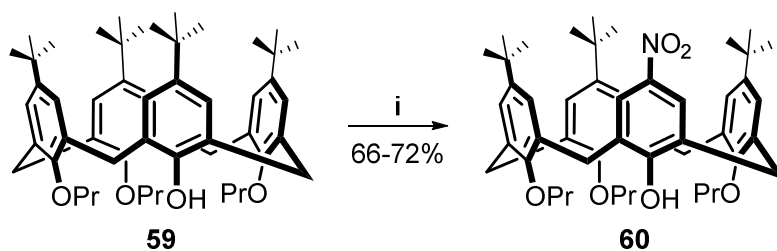


Figure 2.6: ^1H NMR spectrum of **59**. The *tert*-butyl signals are outlined in purple (groups facing outward) and green (groups facing inward).

This difference can be attributed to the slightly different positions of the alkylated and non-alkylated rings relative to the bowl of the calixarene. A steric argument can be used to explain why the phenolic and propoxy groups faced inwards while the two remaining propoxy groups face outwards. The clash over the bottom of the calixarene is minimized with both of the larger groups facing away from one another. An additional reason for this change in conformation was due to the loss of H-bonding on the lower-rim, which was prevalent within the parent calixarene, and was responsible for maintaining its rigid and symmetrical cone conformation in both the solution and solid-state.⁸

2.4.2 Synthesis of tri-propoxy nitro calixarene – **60**.

Activating one of the aromatic rings enabled the selective nitration on the *para*-position (**Scheme 2.10**).⁹ The nitro-product was isolated in generally good yields (66-72%), especially when taking the nature of the reaction into consideration. It had to be monitored carefully. Immediately after the consumption of the starting material, multiple side products would form due to rapid over-nitration taking place. To prevent this, the reaction had to be stopped by dilution with water.

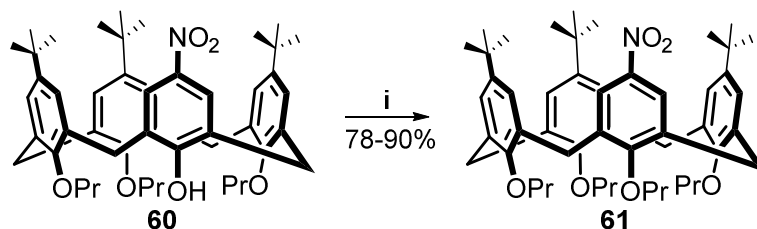


Scheme 2.10: Selective nitration of **59**. Reagents and conditions: i) HNO_3 (7.2 equiv), acetic acid (exs), DCM, 0°C , 8-15 min.

The bulk of the product could be purified via crystallization. Any remaining compound in the mother liquor had to be separated using column chromatography. A low concentration of product in an abundance of impurities prevented a second recrystallization. Fortunately, column chromatography was a sufficient means to separate the product from the mixture of minimal amounts of unreacted starting material and trace quantities of other nitration products. The ^1H NMR spectrum of **60** confirmed similar conformational properties to that of **59**, as both are present in the distorted pinched cone conformation. Once again, this can be attributed to the nature of the steric environment present on the lower-rim of the calixarene. Steric congestion is minimized when the OH group and its opposing propoxy group face inwards, with the two remaining propoxy groups facing outward.

2.4.3 Synthesis of tetra-propoxy nitro calixarene – **61**.

The final propyl group was added using sodium carbonate as a base, with an excess of iodo-propane in acetonitrile under reflux conditions. Unlike previous propylations, a minimum of 48 h was required for the reaction to reach completion (**Scheme 2.11**).



Scheme 2.11: Propylation of **60**. Reagents and conditions: Na_2CO_3 (2.0 equiv), iodo-propane (20.0 equiv), ACN, reflux, 48 h.

The product was again purified via recrystallization, this time from a DCM-EtOH (20:80) mixture, affording the product as pale yellow crystals in a high yield. Interestingly, a conformational change was induced by the addition of the last propyl group. With all four of the functional groups on the lower-rim being identical, the steric discrepancy now took place on the upper-rim of the molecule instead.

Chapter 2: Synthesis of calixarene starting materials

As the nitro group is the smallest functional group, it now faced inwards, along with its *tert*-butyl counterpart. The two remaining *tert*-butyl groups faced outward, away from each other in order to minimize the steric clash over the upper-rim. Again, this was confirmed by the chemical shifts of the three *tert*-butyl groups in the ^1H NMR spectrum (**Figure 2.7**).

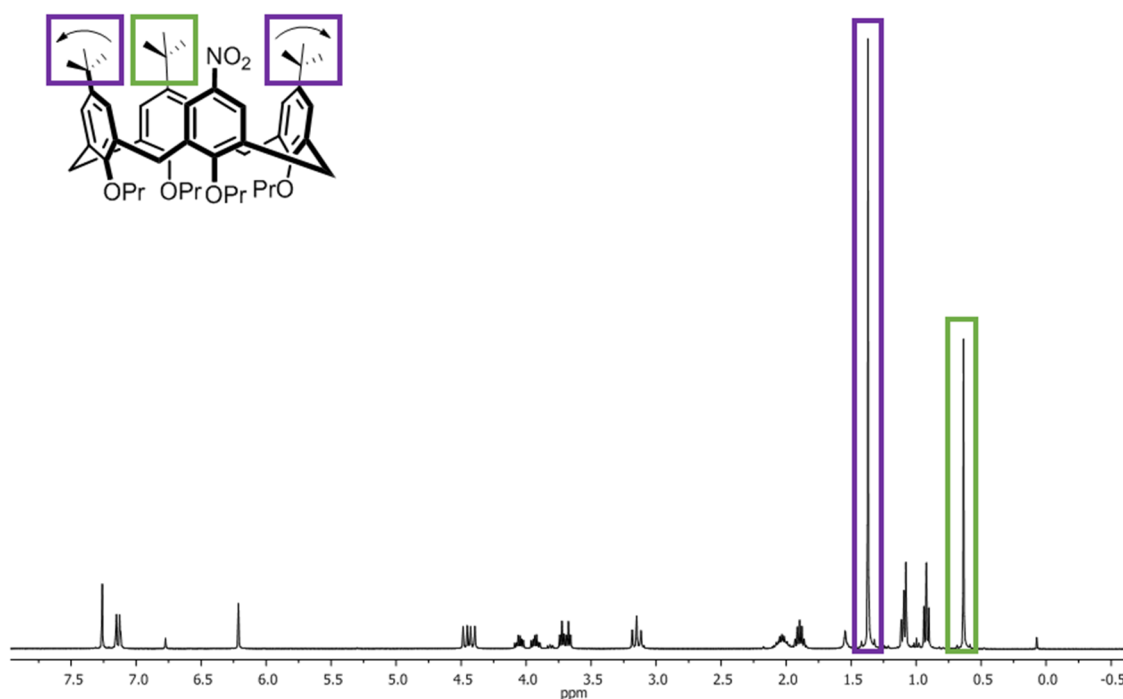
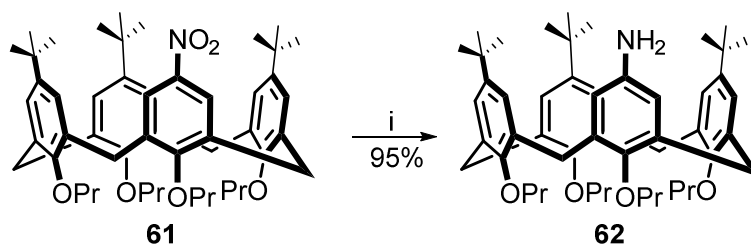


Figure 2.7: ^1H NMR spectrum of **61**. The *tert*-butyl signals are outlined in purple (facing outward) and green (facing inward).

The positions of the *tert*-butyl functional group signals seen for the previous two calixarenes **59** and **60**, were now reversed. The *tert*-butyl group opposite the nitrated ring was now more up-field (δ 0.64 ppm, outlined in green) and faced inwards. The two *tert*-butyl signals on either side were more down-field (δ 1.37 ppm, outlined in purple) and faced away from the center of the ring.

2.4.4 Synthesis of amino calixarene – **62**.

An amine was required for the Sandmeyer reaction which was to follow. This was achieved by the reduction of the nitro group, using a classic transfer hydrogenation reaction with palladium on carbon as catalyst and hydrazine hydrate as the hydrogen source (**Scheme 2.12**).¹⁰

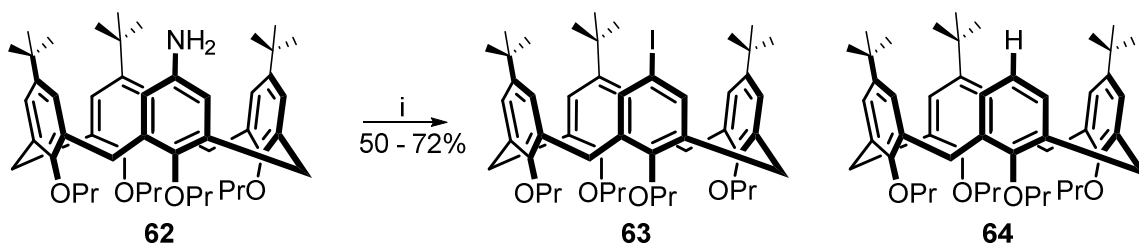


Scheme 2.12: Reduction of **61**. Reagents and conditions: i) Pd-C cat. (10 mol%), hydrazine hydrate (2.6 equiv), EtOH, reflux, 2 h.

The conversion for this reaction was consistently near quantitative within two hours. The crude product was always remarkably clean and barely required additional purification. If deemed necessary, the product was purified by trituration from a DCM-EtOH mixture, which yielded fine white crystals in a 95% yield. The ^1H NMR spectrum for **62** was much like that of calixarene **61** and the conformation of the calixarene remained unchanged.

2.4.5 Synthesis of iodo calixarene – **63**.

Substitution of the amine with iodine was accomplished using a procedure published by Knochel and co-workers (**Scheme 2.13**).¹¹ The reaction had several favourable characteristics, such as ease of experimental set up and mild reaction conditions. There was only one downside, the formation of a protonated by-product **64**.



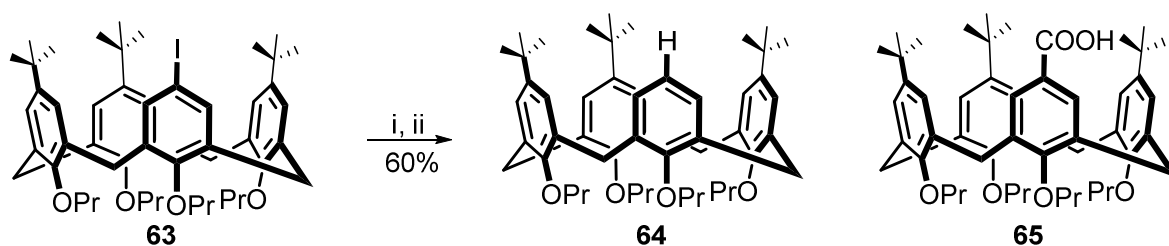
Scheme 2.13: Synthesis of **63** and **64**. Reagents and conditions: i) *p*-toluene sulfonic acid (3.0 equiv), NaNO_2 (2.0 equiv), KI (2.45 equiv), ACN, 0 °C to rt 2 h.

At first this was somewhat confusing, as the by-product **64** and the iodo-calixarene **63** shared the same R_f value and also crystallized from the same solvent mixture. Side product **64** was first identified in the ^1H NMR spectrum of what was thought to be a pure compound **63** after a single spot was isolated from the column. The conversion of the reaction was determined by comparing the areas of two known signals corresponding to each of the compounds. The conformations of **63** and **64** were the same as the amine calixarene **62**. Fortunately, the presence of **64** as a mixture with the starting material had no detrimental effect on the following reaction.

Chapter 2: Synthesis of calixarene starting materials

2.4.6 Synthesis of carboxyl calixarene – **65**.

Initially this reaction presented some difficulty. Iodine is known to undergo rapid lithium halogen exchange, with a much higher rate relative to bromine. Earlier work showed that when attempting the standard lithium halogen exchange conditions, the same conditions used for all of the brominated calixarene compounds, extremely poor conversions were repeatedly obtained. Instead, a viable alternative was established by using a magnesium halogen exchange reaction (**Scheme 2.14**).

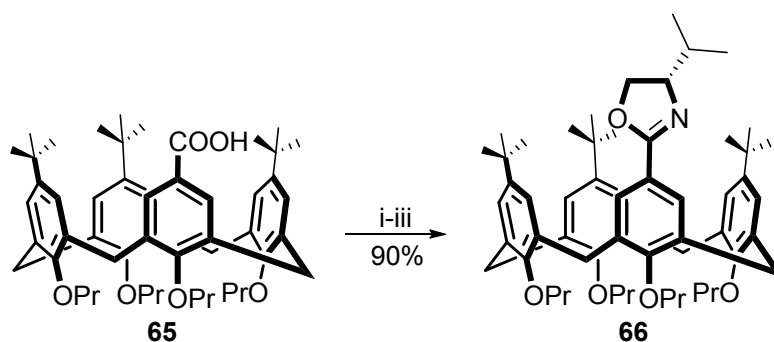


Scheme 2.14: The synthesis of **64** and **65**. Reagents and conditions: i) $i\text{-PrMgCl}\cdot\text{LiCl}$ (4.0 equiv), THF, $0\text{ }^{\circ}\text{C}$ to rt 2 h; ii) CO_2 gas (exs), $-78\text{ }^{\circ}\text{C}$ to rt, 12 h.

As discussed previously, when quenching with carbon dioxide, a protonated by-product was an inevitability. Fortunately the large difference in polarity between the carboxyl and protonated compounds made separation via column chromatography a viable purification method. The formation of **64** was by no means a waste, and all of the protonated by-product that formed during the synthesis of **63** and **65** was pooled and used to synthesise more starting material.

2.4.7 The synthesis of butylated isopropyl oxazoline – **66**.

The oxazoline calixarene **66** was synthesised in three steps, with an overall procedure analogous to the synthesis of **57** and **58** (**Scheme 2.15**).¹²



Scheme 2.15: Synthesis of **66**. Reagents and conditions: i) SOCl_2 (exs), rt, 2 h; ii) L-valinol, Et_3N (4.7 equiv), DCM, $0\text{ }^{\circ}\text{C}$ to rt, 12 h; iii) SOCl_2 , DCM, rt, 3 h.

Chapter 2: Synthesis of calixarene starting materials

First came the conversion of the carboxyl functional group into its acid chloride using thionyl chloride. After removing all of the excess thionyl chloride, the next step was the synthesis of the chiral calixarene amide, which was accomplished by coupling the acid chloride to the chiral amino alcohol. Unlike the previously mentioned isopropyl oxazoline **57**, the synthesis of **66** was far more robust and less sensitive to factors such as concentration or rate of reagent addition. None of the dimer by-products formed, and it was not necessary to isolate the amide to ensure an improved yield for the ring-closing step. After a standard aqueous work-up, the crude amide was treated with thionyl chloride which promptly formed the oxazoline ring. The addition of the oxazoline and conformation of **65** are made clear by the ^1H NMR spectrum (**Figure 2.8**).

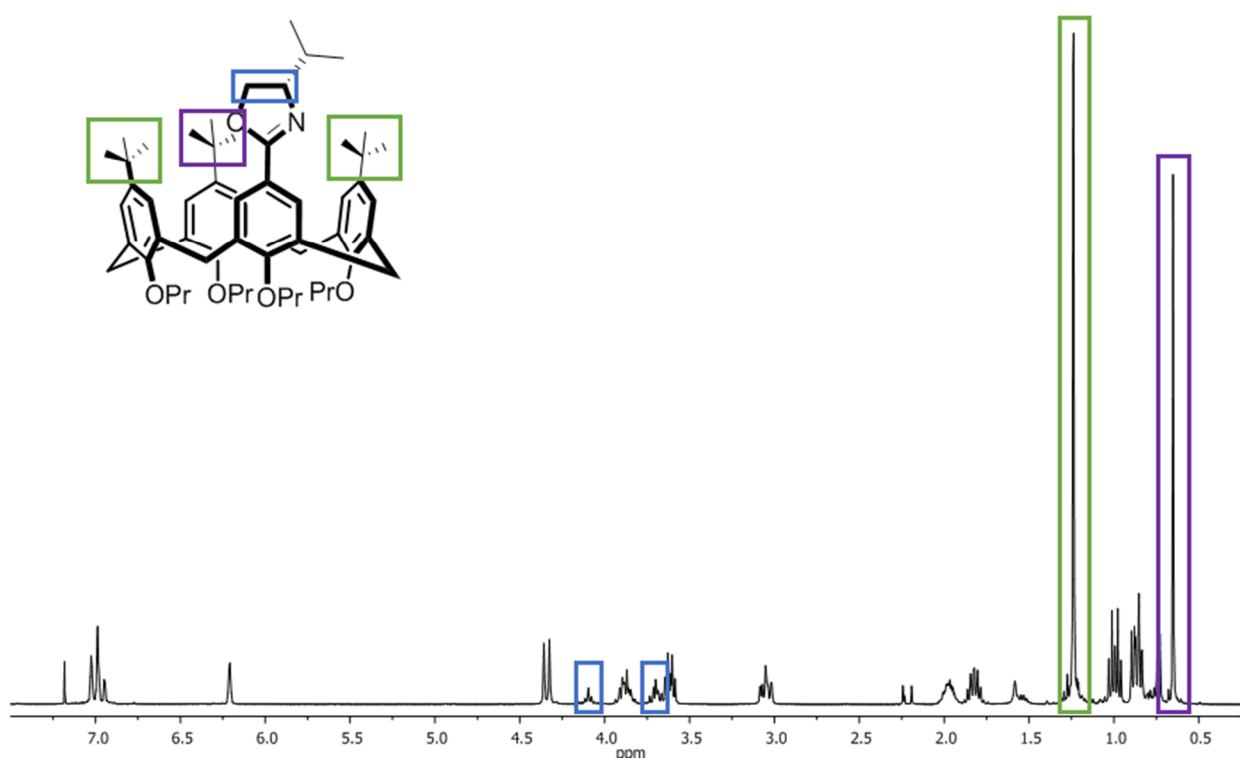
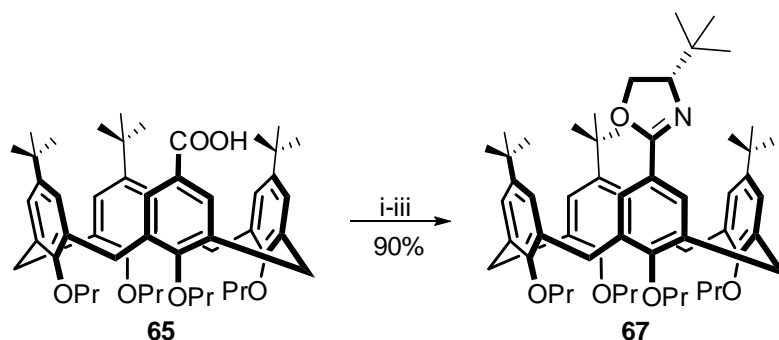


Figure 2.8: ^1H NMR spectrum of **66**. The oxazoline ring protons are outlined in blue and the *tert*-butyl groups of the upper-rim in green and purple.

The multiplet signals for the protons on the oxazoline ring (outlined in blue) had chemical shift ranges of δ 3.66-3.81 and δ 4.16-4.19 ppm. The chemical shifts of three *tert*-butyl signals confirmed that **65** also adopted a distorted pinch cone conformation. The oxazoline and the opposing *tert*-butyl group (outlined in purple) faced inwards (δ 0.73 ppm) and the remaining two *tert*-butyl groups (outlined in green) faced outwards (δ 1.32 ppm).

2.4.8 The synthesis of butylated *tert*-butyl oxazoline – **67**.

The same three step procedure for the synthesis of **67** was used to synthesize **66** (**Scheme 2.16**). The only difference being the structure of the chiral amino alcohol used in step two.



Scheme 2.16: Synthesis of **67**. Reagents and conditions: i) SOCl_2 (exs), rt, 2 h; ii) *L-tert-leucinol* (1.15 equiv), Et_3N (4.7 equiv), DCM, 0 °C to rt 12 h; iii) SOCl_2 (exs), DCM, rt, 3 h.

The two oxazoline compounds had the same conformation, as well as the addition of similar characteristic oxazoline signals to the ^1H NMR spectrum (**Figure 2.9**).

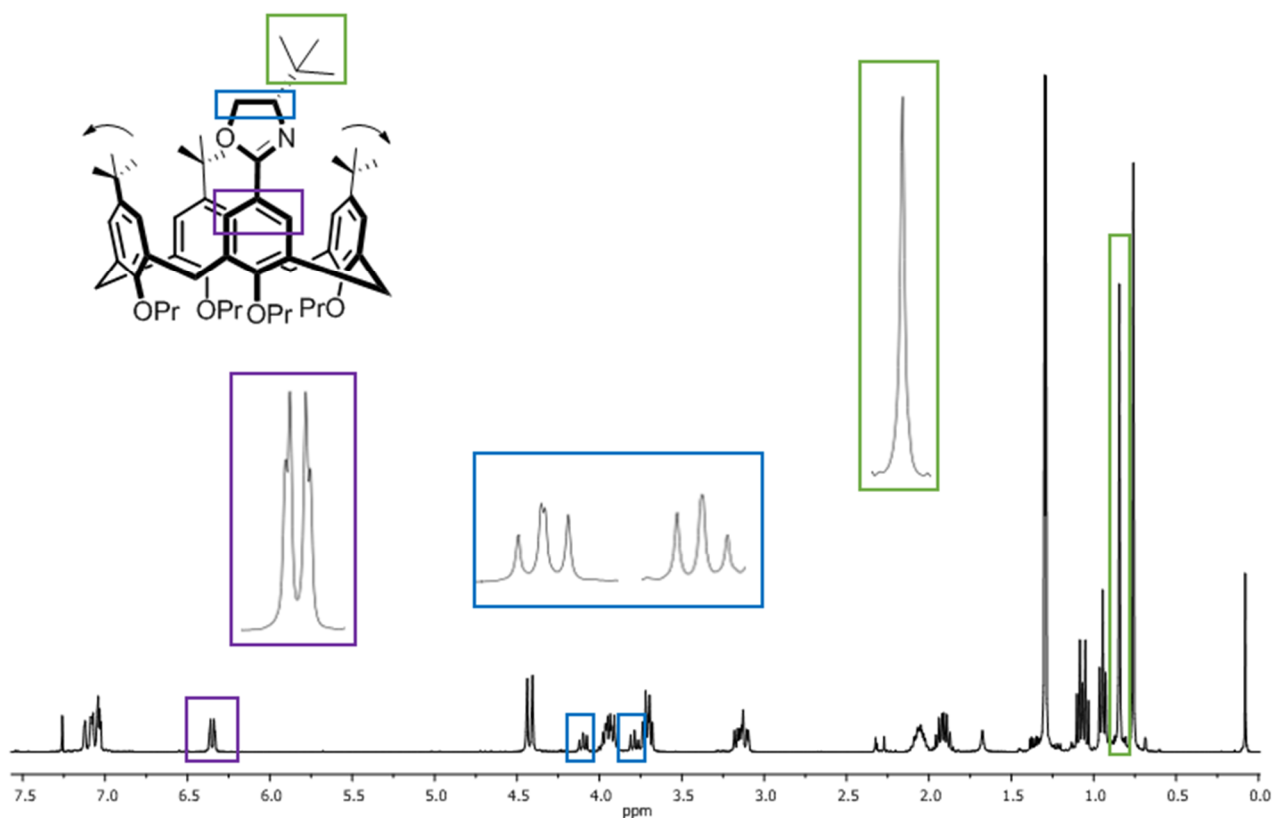


Figure 2.9: ^1H NMR spectrum of **67**. The oxazoline ring protons are outlined in blue, *tert*-butyl group in green and the *ortho*-protons on either side of the oxazoline in purple.

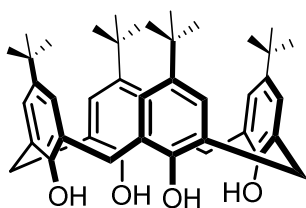
The singlet for the *tert*-butyl group of the oxazoline (outlined in green) had a chemical shift of δ 0.84 ppm. The three diastereotopic singlets of the protons of the oxazoline back-bone had chemical shifts of δ 3.79, 3.94 and 4.10 ppm. Two of these signals have been outlined in blue, and the third (δ 3.94 ppm) overlapped with the OCH_2 signal of the propyl chain. Finally, the characteristic pair of AB doublets in the aromatic region had chemical shifts of δ 6.33 and 6.37 ppm ($J = 2.4$ Hz).

2.5 Conclusion.

Using a combination of previously optimized reactions and procedures reported in the literature, the four oxazoline calixarene starting materials were successfully synthesized in preparation for the ortholithiation studies to follow. During the synthesis of these compounds, a few of the procedures were fine-tuned and several small improvements were made to these experimental conditions.

2.6 Experimental section.

2.6.1 5,11,17,23-tetra-*tert*-butyl-calix[4]arene – **1**.¹³

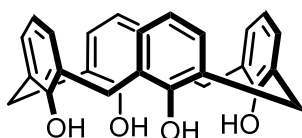


A three necked round bottom flask was fitted with a mechanical stirrer and heating mantle. *p-tert*-butyl phenol (100 g, 665 mmol), formaldehyde (62.9 ml, 864 mmol, 1.3 equiv) and NaOH (1.36 g, 34.0 mmol) dissolved in H₂O (3.0 ml) were all added. While vigorously stirring, the flask was gradually heated to 115 °C. After stirring at 115 °C for approximately an hour; a solid, yellow, foamy mass formed. The flask was quickly removed from the heat source. Once cool, the content of the flask was dissolved in diphenyl ether (800 ml). The mixture was warmed to 120 °C for an hour in order to drive off excess water. After removing the water, the mixture was heated to reflux (approximately 260 °C) for 4 h. The flask was again cooled to room temperature and ethyl acetate (1000 ml) was added, and the contents stirred for a further 30 min. The precipitate was filtered and washed once with ethyl acetate (150 ml) and twice with acetone (2 × 100 ml). The product was purified via recrystallization from a minimum amount of boiling toluene, yielding a calixarene-toluene complex (59.0 g, 48%), *R_f* = 0.6 (DCM:PET, 50:50).

The characterisation data collected for this compound compared well with the reported literature values.¹³

¹H NMR (300 MHz, CHLOROFORM-*d*) δ 1.21 (s, 36H, C(CH₃)₃), 3.48-3.51 (m, 4H, ArCH₂^{eq}Ar), 4.24-4.28 (m, 4H, ArCH₂^{ax}Ar), 7.05 (s, 8H, ArH), 10.34 (s, 4H, ArOH) ppm.

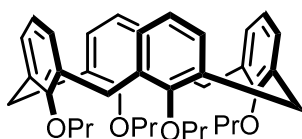
Chapter 2: Synthesis of calixarene starting materials

2.6.2 25,26,27,28-tetrahydroxycalix[4]arene - **53**.¹⁴

Calixarene **1** (15.0 g, 23.1 mmol) was added to dry toluene (100 ml) in a two necked round bottom flask fitted with a mechanical stirrer. Phenol (2.72 g, 27.9 mmol, 1.2 equiv) was added and the contents was stirred at room temperature for 15 min. AlCl_3 (15.0 g, 114 mmol, 5 equiv) was added all at once. The mixture went yellow/orange immediately and a characteristic thick, brown sludge formed on the bottom soon after. The mixture was stirred for 3 h at room temperature, after which the content of the flask was poured into a beaker filled with ice. The product was extracted using DCM (250 ml) and washed with 1M HCl (2×150 ml). Purification was achieved via trituration from hot methanol, yielding a white solid (6.70 g, 70 %).

The characterisation data collected for this compound compared well with the reported literature values.¹⁴

^1H NMR (300 MHz, CHLOROFORM-*d*) δ 3.59 (br s, 4H $\text{ArCH}_2^{\text{eq}}\text{Ar}$), 4.29 (br s, 4H $\text{ArCH}_2^{\text{ax}}\text{Ar}$), 6.77 (t, $J = 7.6$ Hz, 4H, ArH), 7.09 (d, 4H, $J = 7.6$ Hz, 8H, ArH), 10.24 (s, 4H, ArOH) ppm.

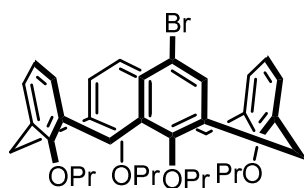
2.6.3 25,26,27,28-tetrapropoxycalix[4]arene - **54**.¹⁵

NaH (9.60 g, 160 mmol, 11.0 equiv) was added to an oven dried two necked round bottom flask and washed with petroleum ether (3×15 ml). DMF (250 ml) was then added and the mixture was cooled (0°C). Calixarene **53** (6.00 g, 14.2 mmol) was added in small portions, taking care as H_2 gas was rapidly given off. Once all of the calixarene had been added, the mixture was stirred for 20 minutes, after which, it had thickened and turned a white opaque colour. Iodo-propane (14.2 ml, 146 mmol, 10 equiv) was then added in one portion. The mixture was given time to warm to room temperature and left to stir overnight (14 h). After which, the colour had changed to a light yellow. The reaction was quenched with cold (0°C) 2 M HCl (20 ml), yielding a yellow precipitate which was collected and stirred in warm methanol (50°C) for 30 minutes, before being cooled in the freezer for 4 h. A white powder (6.74 g, 80%) was collected from the methanol via filtration and dried under vacuum.

The characterisation data collected for this compound compared well with the reported literature values.¹⁵

^1H NMR (300 MHz, CHLOROFORM-*d*) δ 1.02 (t, $J = 7.5$ Hz, 12H, $\text{OCH}_2\text{CH}_2\text{CH}_3$), 1.89-2.01 (m, 8 H, $\text{OCH}_2\text{CH}_2\text{CH}_3$), 3.17 (d, $J = 13.4$ Hz, 4H, $\text{ArCH}_2^{\text{eq}}\text{Ar}$), 3.85-3.90 (m, 8H, $\text{OCH}_2\text{CH}_2\text{CH}_3$), 4.47 (d, $J = 13.4$ Hz, 4H, $\text{ArCH}_2^{\text{ax}}\text{Ar}$), 6.56-6.65 (m, 12H, ArH) ppm.

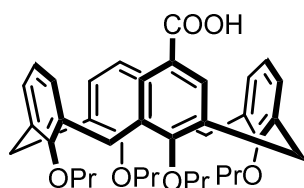
Chapter 2: Synthesis of calixarene starting materials

2.6.4 5-bromo-25,26,27,28-tetrapropoxycalix[4]arene - **55**.¹⁶

Calixarene **54** (5.00 g, 8.40 mmol) was added to dry methyl ethyl ketone (40 ml) at room temperature. *N*-bromosuccinimide (1.40 g, 8.40 mmol, 1.0 equiv) was added all at once, turning the mixture a clear yellow almost immediately. The flask was covered in foil and stirred for 24 h. During this time the yellow mixture darkened to orange. The content of the flask was transferred to a separating funnel, and the organic layer was washed with 10% sodium thiosulfate (3 × 100 ml) and dried over MgSO₄. The excess solvent was removed under reduced pressure and purification was achieved via silica gel column chromatography (DCM:PET, 10:90), yielding a white solid (3.82 g, 68%).

The characterisation data collected for this compound compared well with the reported literature values.¹⁶

¹H NMR (300 MHz, CHLOROFORM-*d*) δ 0.95 (t, *J* = 7.5 Hz, 6H, OCH₂CH₂CH₃), 1.03 (t, *J* = 7.5 Hz, 3H, OCH₂CH₂CH₃), 1.04 (t, *J* = 7.5 Hz, 3H, OCH₂CH₂CH₃), 1.83-1.98 (m, 8H, OCH₂CH₂CH₃), 3.14 (d, *J* = 13.5 Hz, 2H, ArCH₂^{eq}Ar), 3.17 (d, *J* = 13.5 Hz, 2H, ArCH₂^{eq}Ar) 3.74-3.82 (m, 4H, OCH₂CH₂CH₃), 3.84-3.94 (m, 4H, OCH₂CH₂CH₃), 4.41 (d, *J* = 13.5 Hz, 2H, ArCH₂^{ax}Ar), 4.45 (d, *J* = 13.5 Hz, 2H, ArCH₂^{ax}Ar), 6.42 (d, *J* = 7.5 Hz, 2H, ArH), 6.58-6.84 (m, 9H, ArH) ppm.

2.6.5 5-carboxyl-25,26,27,28-tetrapropoxycalix[4]arene - **56**.²

Mono-bromo calixarene **55** (15.0 g, 23.3 mmol) was added to dry THF (250 ml) and cooled to -78 °C. *n*-BuLi (14.4 ml, 33.5 mmol, 1.5 equiv) was carefully added, turning the colourless mixture a clear yellow. After stirring at -78 °C for 20 minutes, CO₂ was bubbled through the mixture for 10 min. The reaction mixture was then given time to slowly warm to room temperature. Once at room temperature, the yellow colour had almost completely disappeared.

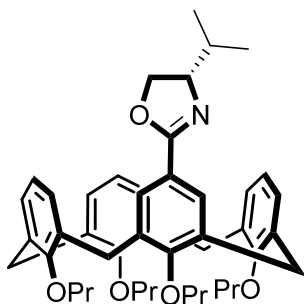
The reaction was finally quenched with the addition of 1M HCl. The product was extracted using EtOAc (150 ml), which was washed with 1 M HCl (100 ml), dried over MgSO₄ and the excess solvent was removed under reduced pressure. Purification was achieved via silica gel column chromatography (EtOAc:PET, 20:80 with <0.1 % Acetic Acid) yielding a white solid (11.6 g, 81.5% Yield). *R*_f = 0.72 (EtOAc:PET, 40:60).

Chapter 2: Synthesis of calixarene starting materials

The characterisation data collected for this compound compared well with the reported literature values.²

¹H NMR (300 MHz, CHLOROFORM-*d*) δ 0.96-1.03 (m, 12H, OCH₂CH₂CH₃), 1.84-1.97 (m, 8H, OCH₂CH₂CH₃), 3.15 (d, *J* = 13.5 Hz, 2H, ArCH₂^{eq}Ar), 3.20 (d, *J* = 13.5 Hz, 2H ArCH₂^{eq}Ar), 3.79-3.88 (m, 6H, OCH₂CH₂CH₃), 3.92 (t, *J* = 7.5 Hz, 2H, OCH₂CH₂CH₃), 4.43 (d, *J* = 13.5 Hz, 2H, ArCH₂^{ax}Ar), 4.46 (d, *J* = 13.5 Hz, 2H, ArCH₂^{ax}Ar), 6.46-6.67 (m, 9H, ArH), 7.30 (br s, 2H, ArH) ppm.

2.6.6 5-((*S*)-4-isopropyl-4,5-dihydrooxazol-2-yl)-25,26,27,28-tetrapropoxycalix[4]arene - **57**.²

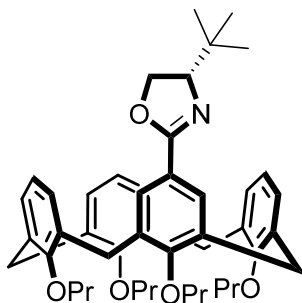


Calixarene **56** (550 mg, 0.930 mmol) was added to dry DCM (15 ml) under argon. Oxalyl chloride (0.340 ml, 4.65 mmol, 5.0 equiv) was added all at once at room temperature, turning the colourless mixture a dark clear orange. The mixture was allowed to stir overnight. The excess solvent and oxalyl chloride were then removed under reduced pressure yielding a yellow/orange foam that was dried under high vacuum for 1 h. Et₃N (0.300 ml, 2.12 mmol, 6.0 equiv) and L-valinol (103 mg, 1.00 mmol, 1.2 equiv) were added to dry DCM (5 ml) and cooled (0 °C). The acid chloride was dissolved in dry DCM (5 ml) which was added at 10 ml/h to the cooled stirring mixture. The reaction mixture was left to stir over night, after which, the content of the flask was transferred to a separating funnel and additional DCM (20 ml) was added. The organic layer was then washed with 1 M HCl (50 ml) and dried over MgSO₄. The excess solvent was removed under reduced pressure, yielding a yellow solid for the crude amide intermediate product. Mesyl chloride (0.200 ml, 2.30 mmol, 2.7 equiv) and Et₃N (0.700 ml, 4.70 mmol, 5.5 equiv) were added to dry DCM (5 ml) forming a clear orange mixture. The crude amide was dissolved in dry DCM (5 ml) and carefully added to the stirring orange mixture at room temperature. The mixture was then left to stir over night. Additional DCM (15 ml) was added to the flask and the content was transferred to a separating funnel. The organic layer was washed with 2 M NaOH (2 × 50 ml) and dried over MgSO₄. The excess solvent was removed under reduced pressure. The final product was purified using silica gel column chromatography (EtOAc:PET, 10:90) affording a white solid (470 mg, 75 %) as the final product.

The characterisation data collected for this compound compared well with the reported literature values.²

Chapter 2: Synthesis of calixarene starting materials

^1H NMR (300 MHz, CHLOROFORM-*d*) δ 0.91-0.96 (m, 9H, $\text{OCH}_2\text{CH}_2\text{CH}_3$, $\text{CH}(\text{CH}_3)_2$), 1.02-1.07 (m, 9H, $\text{OCH}_2\text{CH}_2\text{CH}_3$, $\text{CH}(\text{CH}_3)_2$), 1.82-2.00 (m, 9H, $\text{OCH}_2\text{CH}_2\text{CH}_3$, $\text{CH}(\text{CH}_3)_2$), 3.14 (d, $J = 13.5$ Hz, 2H, $\text{ArCH}_2^{\text{eq}}\text{Ar}$), 3.19 (d, $J = 13.5$ Hz, 1H, $\text{ArCH}_2^{\text{eq}}\text{Ar}$), 3.21 (d, $J = 13.5$ Hz, 1H, $\text{ArCH}_2^{\text{eq}}\text{Ar}$), 3.74 (t, $J = 7.1$ Hz, 4H, $\text{OCH}_2\text{CH}_2\text{CH}_3$), 3.91-4.01 (m, 4H, $\text{OCH}_2\text{CH}_2\text{CH}_3$), 4.03-4.14 (m, 2H, OCH_2CHN), 4.34-4.39 (m, 1H, OCH_2CHN), 4.45 (d, $J = 13.5$ Hz, 4H, $\text{ArCH}_2^{\text{ax}}\text{Ar}$), 6.31-6.38 (m, 6H, ArH), 6.71 (t, $J = 7.5$ Hz, 1H, ArH), 6.85 (d, $J = 7.3$ Hz, 2H, ArH), 7.47 (d, $J = 2.0$ Hz, 1H, ArH), 7.52 (d, 1H, $J = 2.0$ Hz, ArH) ppm.

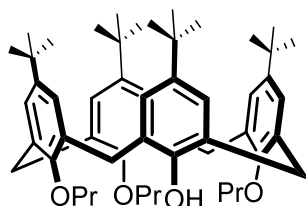
2.6.7 5-((*S*)-4-*tert*-butyl-4,5-dihydrooxazol-2-yl)-25,26,27,28-tetrapropoxycalix[4]arene – **58**.¹⁷

Calixarene **56** (1.50 g, 2.27 mmol), oxalyl chloride (1.00 ml, 11.4 mmol, 5.0 equiv) and DCM (20 ml) were added to an oven dried flask and stirred at room temperature for 3 h. The excess solvent and remaining oxalyl chloride were then removed under reduced pressure yielding an orange/yellow foam. The acid chloride was dissolved in dry DCM (5 ml) and slowly added to a mixture of *L-tert*-leucinol (319 mg, 2.70 mmol, 1.2 equiv) and Et_3N (1.60 ml, 11.4 mmol, 5.0 equiv) in DCM (20 ml) at 0 °C. The mixture was given time to slowly warm to room temperature and stirred overnight. Mesityl chloride (0.50 ml, 8.30 mmol, 3.0 equiv) was carefully added and the flask stirred for a further 3 h, following which, H_2O (5 ml) and DCM (20 ml) were added. The layers separated and the aqueous layer washed with DCM (15 ml). The organic phases were combined, dried over MgSO_4 , and the solvent removed under reduced pressure. Purification was achieved via silica gel column chromatography (EtOAc:PET, 5:95) affording a white foam (1.21 g, 0.290 mmol, 75% yield). $R_f = 0.52$ (EtOAc:PET, 10:90).

The characterisation data collected for this compound compared well with the reported literature values.¹⁷

^1H NMR (300 MHz, CHLOROFORM-*d*) δ 0.90-0.99 (m, 15H, $\text{C}(\text{CH}_3)_3$, $\text{OCH}_2\text{CH}_2\text{CH}_3$), 1.06 (t, $J = 7.4$ Hz, 6H, $\text{OCH}_2\text{CH}_2\text{CH}_3$), 1.82-2.03 (m, 8H, $\text{OCH}_2\text{CH}_2\text{CH}_3$), 3.15 (d, $J = 13.5$, 2H, $\text{ArCH}_2^{\text{eq}}\text{Ar}$), 3.19 (d, $J = 13.5$ Hz, 1H, $\text{ArCH}_2^{\text{eq}}\text{Ar}$), 3.22 (d, $J = 13.5$ Hz, 1H, $\text{ArCH}_2^{\text{eq}}\text{Ar}$), 3.77 (t, $J = 7.0$ Hz, 4H, $\text{OCH}_2\text{CH}_2\text{CH}_3$), 3.91-4.07 (m, 5H, $\text{OCH}_2\text{CH}_2\text{CH}_3$, OCH_2CHN), 4.20 (t, $J = 7.7$ Hz, 1H, OCH_2CHN), 4.32 (d, $J = 8.6$ Hz, 1H, OCH_2CHN), 4.46 (d, $J = 13.5$ Hz, 4H, $\text{ArCH}_2^{\text{ax}}\text{Ar}$), 6.31-6.45 (m, 6H, ArH), 6.71 (dd, $J = 9.6, 1.2$ Hz, 1H, ArH), 6.85-6.89 (m, 2H, ArH), 7.49 (d, $J = 2.1$ Hz, 1H, ArH), 7.53 (d, $J = 2.1$ Hz, 1H, ArH) ppm.

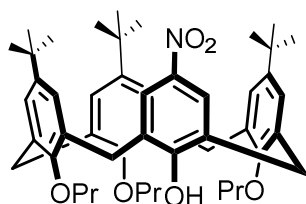
Chapter 2: Synthesis of calixarene starting materials

2.6.8 5,7,11,23-tetra-tert-butyl-26,27,28-tripropoxycalix[4]arene - **59**.⁷

BaO (8.26 g, 53.9 mmol, 7), Ba(OH)₂·8H₂O (8.50 g, 27.0 mmol, 3.5 equiv) and calixarene **1** (5.00 g, 7.70 mmol) were all added to dry DMF (150 ml). The mixture was stirred at room temperature for 1 h, after which the solution had turned cloudy and viscous. Iodo-propane (19.3 ml, 193 mmol 25.0 equiv) was added all at once and after 30 min of stirring the mixture turned yellow/orange. After 2 h the reaction was quenched with 1M HCl. The product was extracted with EtOAc (250 ml), which was washed with 1M HCl (50 ml) and H₂O (2 × 200 ml). The organic layer was dried over MgSO₄ and the excess solvent was removed under reduced pressure, affording pale yellow foam as the crude product. The crude product was purified by recrystallization from a DCM/EtOH mixture (8:25 ml), yielding pale yellow crystals (4.50 g, 77%) *R_f* = 0.62 (DCM:PET, 50:50)

The characterisation data collected for this compound compared well with the reported literature values.⁷

¹H NMR (300 MHz, CHLOROFORM-*d*) δ 0.83 (s, 18H, C(CH₃)₃), 0.96 (t, *J* = 7.5 Hz, 3H, OCH₂CH₂CH₃), 1.10 (t, *J* = 7.3 Hz, 6H, 2 × OCH₂CH₂CH₃), 1.33 (s, 9H, C(CH₃)₃), 1.34 (s, 9H, C(CH₃)₃), 1.82-2.06 (m, 4H, 2 × OCH₂CH₂CH₃), 2.29-2.39 (m, 2H, OCH₂CH₂CH₃), 3.17 (d, *J* = 12.6 Hz, 2H, ArCH₂^{eq}Ar), 3.23 (d, *J* = 13.2 Hz, 2H, ArCH₂^{eq}Ar), 3.74-3.78 (t, *J* = 6.9 Hz, 4H, OCH₂CH₂CH₃), 3.83-3.87 (m, 2H, OCH₂CH₂CH₃), 4.32 (d, *J* = 13.2 Hz, 2H, ArCH₂^{ax}Ar), 4.38 (d, *J* = 12.6 Hz, 2H, ArCH₂^{ax}Ar), 5.58 (s, 1H, ArOH), 6.48-6.56 (m, 4H, ArH), 7.05 (s, 2H, ArH), 7.14 (s, 2H, ArH) ppm.

2.6.9 11,17,23-tri-tert-butyl-5-nitro-26,27,28-tripropoxycalix[4]arene – **60**.¹⁸

Calixarene **59** (2.20 g, 2.83 mmol) and acetic acid (14.3 ml, excess) were added to dry DCM (8 ml) and cooled (0 °C). After stirring for 10 min, HNO₃ (1.50 ml, 20.4 mmol, 7.2 equiv) was carefully added and the mixture was allowed to warm to room temperature. The progress of the reaction needed to be carefully monitored via TLC in order to avoid over-nitration. The reaction was diluted with distilled H₂O (5 ml) after approximately 6 min. (The reaction took anywhere between 6-12 min, depending on the temperature and concentration).

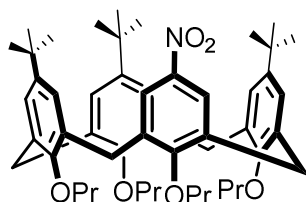
Chapter 2: Synthesis of calixarene starting materials

The product was extracted with DCM (50 ml) and washed with successive portions of H₂O (100 ml) and sat. NaHCO₃ (2 × 100 ml). The organic layer was dried over MgSO₄ and the excess solvent was removed under reduced pressure. Purification was achieved via slow crystallization from a DCM/EtOH mixture (8:35 ml), yielding light orange crystals (1.30 g, 70%). The yields obtained for this reaction ranged from 60-75%.

The characterisation data collected for this compound compared well with the reported literature values.¹⁸

¹H NMR (300 MHz, CHLOROFORM-*d*) δ 0.83 (s, 18H, C(CH₃)₃), 0.95 (t, *J* = 7.5 Hz, 3H, OCH₂CH₂CH₃), 1.10 (t, *J* = 7.5 Hz, 6H, OCH₂CH₂CH₃), 1.35 (s, 9H, C(CH₃)₃), 1.83-2.03 (m, 4H, OCH₂CH₂CH₃), 2.23-2.33 (m, 2H, OCH₂CH₂CH₃), 3.19 (d, *J* = 12.6 Hz, 2H, ArCH₂^{eq}Ar), 3.39 (d, *J* = 13.5 Hz, 2H, ArCH₂^{eq}Ar), 3.71-3.85 (m, 6H, OCH₂CH₂CH₃), 4.31 (d, *J* = 13.5 Hz, 2H, ArCH₂^{ax}Ar), 4.34 (d, *J* = 12.6 Hz, 2H, ArCH₂^{ax}Ar), 6.46 (d, *J* = 1.9 Hz, 2H, ArH), 6.60 (d, *J* = 1.9 Hz, 2H, ArH), 7.16 (s, 2H, ArH), 7.23 (s, 1H, ArOH), 8.06 (s, 2H, ArH) ppm.

2.6.10 11,17,23-tri-*tert*-butyl-5-nitro-25,26,27,28-tetrapropoxycalix[4]arene – **61**.²

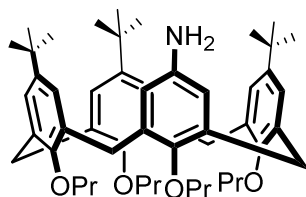


Calixarene **60** (7.60 g, 10.0 mmol) and sodium carbonate (2.10 g, 20.0 mmol, 2.0 equiv) were added to dry acetonitrile (120 ml). The mixture was heated to reflux. After stirring at reflux for 90 min, the iodopropane (19.9 ml, 200 mmol, 20.0 equiv) was added. Reflux conditions were maintained for 48 h. The reaction was quenched with H₂O (20 ml) and the product was extracted with EtOAc (150 ml). The organic layer was washed with 1M HCl (100 ml), brine (100 ml) and dried over MgSO₄. The excess solvent was removed under reduced pressure and the purification was achieved by recrystallization from a DCM/EtOH mixture (20:60 ml), yielding pale yellow crystals (7.21 g, 89%). Yields for this reaction ranged between 75-90%.

The characterisation data collected for this compound compared well with the reported literature values.²

¹H NMR (300 MHz, CHLOROFORM-*d*) δ 0.64 (s, 9H, C(CH₃)₃), 0.92 (t, *J* = 7.5 Hz, 6H, OCH₂CH₂CH₃), 1.09 (t, *J* = 7.4 Hz, 3H, OCH₂CH₂CH₃), 1.10 (t, *J* = 7.4 Hz, 3H, OCH₂CH₂CH₃), 1.37 (s, 18H, C(CH₃)₃), 1.84-1.95 (m, 4H, OCH₂CH₂CH₃), 1.96-2.11 (m, 4H, OCH₂CH₂CH₃), 3.13 (d, *J* = 12.9 Hz, 2H, ArCH₂^{eq}Ar), 3.17 (d, *J* = 12.9 Hz, 2H, ArCH₂^{eq}Ar), 3.67 (t, *J* = 6.9 Hz, 2H, OCH₂CH₂CH₃), 3.72 (t, *J* = 6.9 Hz, 2H, OCH₂CH₂CH₃), 3.89-3.96 (m, 2H, OCH₂CH₂CH₃), 4.01-4.09 (m, 2H, OCH₂CH₂CH₃), 4.41 (d, *J* = 12.9 Hz, 2H, ArCH₂^{ax}Ar), 4.46 (d, *J* = 12.9 Hz, 2H, ArCH₂^{ax}Ar), 6.21 (s, 2H, ArH), 7.12 (d, *J* = 2.4 Hz, 2H, ArH), 7.15 (d, *J* = 2.4 Hz, 2H, ArH), 7.26 (s, 2H, ArH) ppm.

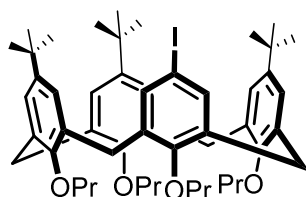
Chapter 2: Synthesis of calixarene starting materials

2.6.11 11,17,23-tri-tert-butyl-5-amino-25,26,27,28-tetrapropoxycalix[4]arene – **62**.¹⁰

Calixarene **61** (3.20 g, 4.00 mmol) and 10% Pd-C cat. (450 mg, 0.400 mmol, 0.1 equiv) were added to dry EtOH (50 ml). The mixture was heated to reflux. Hydrazine hydrate (0.500 ml, 10.4 mmol, 2.6 equiv) was then added drop-wise. Reflux was maintained for 3 h, after which the contents of the flask were filtered through a pad of celite. The Celite was washed with DCM (2 × 30 ml) and the excess solvent was removed under reduced pressure, affording a white solid as the crude product. The products of two separate reactions were combined and recrystallized from a DCM/EtOH (20:60 ml) mixture yielding fine white crystals (6.10 g, 95% combined yield from two separate reactions). Yields for this reaction varied between 90-98%.

The characterisation data collected for this compound compared well with the reported literature values.¹⁰

¹H NMR (300 MHz, CHLOROFORM-*d*) δ 0.79 (s, 9H, C(CH₃)₃), 0.91 (t, *J* = 7.5 Hz, 6H, OCH₂CH₂CH₃), 1.02-1.11 (m, 6H, OCH₂CH₂CH₃), 1.33 (s, 18H, C(CH₃)₃), 1.81-1.96 (m, 4H, OCH₂CH₂CH₃), 1.98-2.11 (m, 4H, OCH₂CH₂CH₃), 3.00 (d, *J* = 12.7 Hz, 2H, ArCH₂^{eq}Ar), 3.12 (d, *J* = 12.7 Hz, 2H, ArCH₂^{eq}Ar), 3.60 (t, *J* = 7.0 Hz, 2H, OCH₂CH₂CH₃), 3.72 (t, *J* = 7.0 Hz, 2H, OCH₂CH₂CH₃), 3.94-4.00 (m, 4H, OCH₂CH₂CH₃), 4.36 (d, *J* = 12.7 Hz, 2H, ArCH₂^{ax}Ar), 4.45 (d, *J* = 12.7 Hz, 2H, ArCH₂^{ax}Ar), 5.69 (s, 2H, ArH), 6.28 (s, 2H, ArH), 7.00 (d, *J* = 2.4 Hz, 2H, ArH), 7.08 (d, *J* = 2.4 Hz, 2H, ArH) ppm.

2.6.12 11,17,23-tri-tert-butyl-5-iodo-25,26,27,28-tetrapropoxycalix[4]arene – **63**.¹¹

Calixarene **62** (2.10 g, 2.71 mmol) and *p*-toluene sulfonic acid (1.42 g, 8.30 mmol, 3.0 equiv) were added to dry acetonitrile (10 ml) and stirred at room temperature for 15 min. The mixture was cooled (0 °C) and NaNO₂ (400 mg, 5.40 mmol, 2.0 equiv) was added, turning the mixture a cloudy yellow. KI (1.10 g, 6.62 mmol, 2.5 equiv), dissolved in water (1.6 ml), was added drop-wise, immediately turning the yellow mixture a dark brown colour. The reaction was allowed to warm to room temperature and was stirred for 1.5 h. The product was extracted using DCM (60 ml), which was washed with 10 % Na₂SO₃ (60 ml) and sat. NaHCO₃ (100 ml).

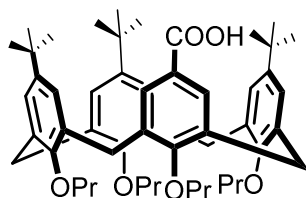
Chapter 2: Synthesis of calixarene starting materials

The products of two separate reactions were combined and purified by silica gel column chromatography (PET, 100) yielding a pale yellow solid (3.8 g, 72%). Yields obtained for this reaction ranged from 68-75%. The ^1H NMR spectrum of this compound is a mixture of the iodo and protonated **64** calixarene by-product.

The characterisation data collected for this compound compared well with the reported literature values.¹¹

^1H NMR (300 MHz, CHLOROFORM-*d*) δ 0.87 (s, 9H, C(CH₃)₃), 0.92 (t, *J* = 7.5 Hz, 6H, OCH₂CH₂CH₃), 1.05-1.11 (m, 6H, OCH₂CH₂CH₃), 1.32 (s, 18H, C(CH₃)₃), 1.82-1.94 (m, 4H, OCH₂CH₂CH₃), 1.97-2.11 (m, 4H, OCH₂CH₂CH₃), 3.05 (d, *J* = 12.6 Hz, 2H, ArCH₂^{eq}Ar), 3.14 (d, *J* = 12.6 Hz, 2H, ArCH₂^{eq}Ar), 3.64 (t, *J* = 7.0 Hz, 2H, OCH₂CH₂CH₃), 3.70 (t, *J* = 7.0 Hz, 2H, OCH₂CH₂CH₃), 3.90-4.02 (m, 4H, OCH₂CH₂CH₃), 4.35 (d, *J* = 12.6 Hz, 2H, ArCH₂^{ax}Ar), 4.42 (d, *J* = 12.6 Hz, 2H, ArCH₂^{ax}Ar), 6.35 (s, 2H, ArH), 6.71 (s, 2H, ArH), 6.97 (d, *J* = 2.4 Hz, 2H, ArH), 7.10 (d, *J* = 2.4 Hz, 2H, ArH) ppm.

2.6.13 11,17,23-tri-*tert*-butyl-5-carboxy-25,26,27,28-tetrapropoxycalix[4]arene – **65**.²

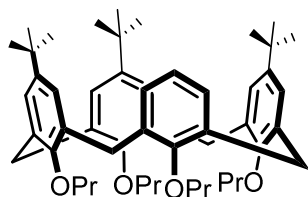


Pre-drying: Iodo calixarene **63** (3.50 g, 3.94 mmol) added to dry THF which was then removed under reduced pressure. The flask was left on high vacuum for an additional hour. The flask was cooled (0 °C) and *i*-PrMgCl·LiCl (24.5 ml, THF, 15.8 mmol, 4.0 equiv) was carefully added all at once. The black/dark grey mixture was allowed to warm to room temperature and stirred for 2 h. The flask was then cooled again (–78 °C) and CO₂ gas was bubbled through the mixture for 30 min, after which it was given 1 h to warm to room temperature. The reaction was finally quenched by the addition of H₂O (30 ml). The product was extracted with DCM (150 ml) which was washed with 1M HCl (100 ml). The organic layer was dried over MgSO₄ and the excess solvent was removed under reduced pressure, affording a pale yellow solid as the crude product. Purification was achieved via silica gel column chromatography (EtOAc:PET, 10:90) yielding two compounds; the protonated calixarene **64** (895 mg, 36%) and the carboxyl calixarene **65** (1.90 g, 60%).

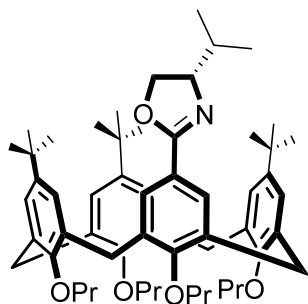
The characterisation data collected for this compound compared well with the reported literature values.²

^1H NMR (300 MHz, CHLOROFORM-*d*) δ 0.68 (s, 9H, C(CH₃)₃), 0.92 (t, *J* = 7.5 Hz, 6H, OCH₂CH₂CH₃), 1.07 (t, *J* = 7.4 Hz, 3H, OCH₂CH₂CH₃), 1.09 (t, *J* = 7.4 Hz, 3H, OCH₂CH₂CH₃), 1.34 (s, 18H, C(CH₃)₃), 1.89 (t, *J* = 7.2 Hz, 2H, OCH₂CH₂CH₃), 1.91 (t, *J* = 7.2 Hz, 2H, OCH₂CH₂CH₃), 1.98-2.11 (m, 4H, OCH₂CH₂CH₃), 3.11 (d, *J* = 12.2, 2H, ArCH₂^{eq}Ar), 3.15 (d, *J* = 12.2 Hz, 2H, ArCH₂^{eq}Ar), 3.69 (t, *J* = 6.8 Hz, 2H, OCH₂CH₂CH₃), 3.71 (t, *J* = 6.8 Hz, 2H, OCH₂CH₂CH₃), 3.89-4.05 (m, 4H, OCH₂CH₂CH₃), 4.41 (d, *J* = 12.2 Hz, 2H, ArCH₂^{ax}Ar), 4.45 (d, *J* = 12.2 Hz, 2H, ArCH₂^{ax}Ar), 6.25 (s, 2H, ArH), 7.09 (br. s. 4H, ArH), 7.16 (s, 2H, ArH) ppm.

Chapter 2: Synthesis of calixarene starting materials

2.6.14 11,17,23-tri-tert-butyl-25,26,27,28-tetrapropoxycalix[4]arene – **64**.

^1H NMR (300 MHz, CHLOROFORM-*d*) δ 0.78 (s, 9H, , C(CH₃)₃), 0.91 (t, J = 7.6 Hz, 6H, OCH₂CH₂CH₃), 1.06-1.12 (m, 6H, OCH₂CH₂CH₃), 1.35 (s, 18H, C(CH₃)₃), 1.83-1.95 (m, 4H, OCH₂CH₂CH₃), 1.97-2.10 (m, 4H, OCH₂CH₂CH₃), 3.11 (d, J = 12.9 Hz, 2H, ArCH₂^{eq}Ar), 3.12 (d, J = 12.9 Hz, 2H, ArCH₂^{eq}Ar), 3.64-3.70 (m, 4H, OCH₂CH₂CH₃), 3.96-4.01 (m, 4H, OCH₂CH₂CH₃), 4.43 (d, J = 12.9 Hz, 2H, ArCH₂^{ax}Ar), 4.45 (d, J = 12.9 Hz, 2H, ArCH₂^{ax}Ar), 6.20 (s, 2H, ArH), 6.25 (s, 3H, ArH), 7.05 (d, J = 2.4 Hz, 2H, ArH), 7.10 (d, J = 2.4 Hz, 2H, ArH) ppm.

2.6.15 11,17,23-tri-tert-butyl-5-((*S*)-4-isopropyl-4,5-dihydrooxazol-yl)-25,26,27,28-tetrapropoxycalix[4]arene – **66**.¹²

Calixarene **65** (1.00 g, 1.22 mmol) was added to SOCl₂ (5 ml) under argon at room temperature, forming a clear yellow mixture. The reaction was stirred at room temperature for 15 minutes, after which it was heated to reflux for 2 h. The mixture was given time to slowly cool to room temperature and was stirred overnight. The excess SOCl₂ was removed under reduced pressure, affording an orange/yellow foam that was left to dry under high vacuum for 4 h. L-valinol (188 mg, 1.80 mmol, 1.5 equiv) and Et₃N (0.800 ml, 5.70 mmol, 4.7 equiv) were added to dry DCM (10 ml) under argon at room temperature and cooled (0 °C). The dry acid chloride was added to DCM (10 ml) and slowly added to the cooled mixture at 10 ml/h using a syringe pump. Additional DCM (40 ml) was added to the mixture and the contents of the flask was transferred to a separating funnel. The organic layer was washed with sat. NaHCO₃ (50 ml) and H₂O (50 ml). After drying over MgSO₄ the excess solvent was removed under reduced pressure. The crude amide was dried under high vacuum for 3 h, after which it was dissolved in dry DCM (15 ml). SOCl₂ was then added at room temperature and the mixture was stirred for 12 h. The reaction was quenched by adding distilled H₂O (10 ml). The crude product was extracted with DCM (50 ml) that was washed with sat. NaHCO₃ (50 ml) and dried over MgSO₄. The excess solvent was removed under reduced pressure, yielding a yellow semi-solid as the crude product.

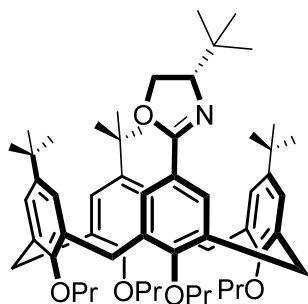
Chapter 2: Synthesis of calixarene starting materials

Purification was achieved via silica gel column chromatography (EtOAc:PET, 5:95), yielding a white foam (952 mg, 90%) as the final product. $R_f = 0.64$ (EtOAc:PET, 10:90).

The characterisation data collected for this compound compared well with the reported literature values.¹²

^1H NMR (300 MHz, CHLOROFORM-*d*) δ 0.73 (s, 9H, C(CH₃)₃), 0.81 (d, $J = 6.7$ Hz, 3H, CH(CH₃)₂), 0.88-0.97 (m, 9H, OCH₂CH₂CH₃, CH(CH₃)₂), 1.06 (t, $J = 6.7$ Hz, 3H, OCH₂CH₂CH₃), 1.09 (t, $J = 6.7$ Hz, 3H, OCH₂CH₂CH₃), 1.32 (s, 9H, C(CH₃)₃), 1.32 (s, 9H, C(CH₃)₃), 1.84-1.96 (m, 4H, OCH₂CH₂CH₃), 1.99-2.12 (m, 4H, OCH₂CH₂CH₃), 3.09-3.16 (m, 4H, ArCH₂^{eq}Ar), 3.66-3.81 (m, 6H, OCH₂CH₂CH₃, OCH₂CHN, OCH₂CHN), 3.91-4.01 (m, 4H, OCH₂CH₂CH₃), 4.16-4.19 (m 1H, OCH₂CHN), 4.42 (d, $J = 12.8$ Hz, 4H, ArCH₂^{ax}Ar), 6.30 (m, 2H, ArH), 7.03 (d, $J = 1.9$ Hz, 2H, ArH), 7.07 (m, 2H, ArH), 7.10 (m, 2H, ArH) ppm.

2.6.16 11,17,23-tri-*tert*-butyl-5-((*S*)-4-*tert*-butyl-4,5-dihydrooxazol-yl)-25,26,27,28-tetrapropoxycalix[4]arene – **67**.¹⁷



Calixarene **65** (1.00 g, 1.22 mmol) was added to SOCl₂ (5 ml) under argon at room temperature, forming a clear yellow mixture. The mixture was stirred at room temperature for 15 minutes, after which, it was heated to reflux for 2 h. The mixture was given time to slowly cool to room temperature and was stirred overnight. The excess SOCl₂ was removed under reduced pressure, affording an orange/yellow foam that was dried under high vacuum for 4 h. *L*-*tert*-Leucinol (214 mg, 1.82 mmol, 1.5 equiv) and Et₃N (0.80 ml, 5.73 mmol, 4.7 equiv) were added to dry DCM (10 ml) under argon at room temperature and cooled (0 °C). The acid chloride was dissolved in DCM (10 ml) and slowly added to the cooled mixture at 10 ml/h using the syringe pump. Additional DCM (40 ml) was added to the mixture and the content of the flask was transferred to a separating funnel. The organic layer was washed with sat. NaHCO₃ (50 ml) and H₂O (50 ml). After drying over MgSO₄, the excess solvent was removed under reduced pressure. The crude amide was dried under high vacuum for 3 h, after which it was added to DCM (15 ml). SOCl₂ was then added at room temperature and the mixture was stirred for 12 h. The reaction was quenched by adding distilled H₂O (10 ml). The crude product was extracted with DCM (50 ml) that was washed with sat. NaHCO₃ (50 ml) and dried over MgSO₄. The excess solvent was removed under reduced pressure yielding a yellow semi-solid as the crude product. Purification was achieved via silica gel column chromatography (EtOAc:PET, 5:95), yielding a white foam (973 mg, 90%) as the final product. $R_f = 0.78$ (EtOAc:PET, 10:90).

Chapter 2: Synthesis of calixarene starting materials

The characterisation data collected for this compound compared well with the reported literature values.¹⁷

¹H NMR (300 MHz, CHLOROFORM-*d*) δ 0.76 (s, 9H, C(CH₃)₃), 0.84 (s, 9H, C(CH₃)₃), 0.95 (t, *J* = 7.5 Hz, 6H, OCH₂CH₂CH₃), 1.05 (t, *J* = 6.8 Hz, 3H, OCH₂CH₂CH₃), 1.08 (t, *J* = 6.8 Hz, 3H, OCH₂CH₂CH₃), 1.29 (s, 9H, C(CH₃)₃), 1.30 (s, 9H, C(CH₃)₃), 1.85-1.98 (m, 4H, OCH₂CH₂CH₃), 2.01-2.10 (m, 4H, OCH₂CH₂CH₃), 3.10-3.18 (m, 4H, ArCH₂^eAr), 3.68-3.74 (m, 4H, OCH₂CH₂CH₃), 3.76-3.81 (m, 1H, NCHCH₂), 3.89-3.99 (m, 5H, OCH₂CH₂CH₃, OCH₂CHN), 4.10 (d, *J* = 10.3 Hz, 1H, OCH₂CHN), 4.42 (d, *J* = 12.7 Hz, 4H, ArCH₂^aAr), 6.34 (d, *J* = 2.3 Hz, 1H, ArH), 6.37 (d, *J* = 2.3 Hz, 1H, ArH), 7.03-7.05 (m, 3H, ArH), 7.07-7.09 (m, 2H, ArH), 7.12 (d, *J* = 1.9 Hz, 1H, ArH) ppm.

2.7 References.

- (1) Herbert, S. A. Oxazoline Directed Lithiation of Calix[4]arene and Ferrocene, PhD, Stellenbosch University, 2011.
- (2) Herbert, S. A.; Arnott, G. E. *Org. Lett.* **2010**, *12*, 4600.
- (3) Gutsche, C. D. *Calixarenes: An Introduction*; The Royal Society of Chemistry: Cambridge, 2008.
- (4) Gutsche, C. D.; Pagoria, P. F. *J. Org. Chem.* **1985**, *50*, 5795.
- (5) Gutsche, C. D.; Iqbal, M.; Nam, K. S.; See, K.; Alam, I. *Pure Appl. Chem.* **1988**, *60*, 483.
- (6) Gutsche, C. D. *Angew. Chem., Int. Ed.* **2008**, *34*, 3782.
- (7) Iwamoto, K.; Araki, K.; Shinkai, S. *J. Org. Chem.* **1991**, *29*, 4955.
- (8) Gutsche, C. D.; Bauer, L. J. *J. Am. Chem. Soc.* **1985**, *107*, 6052.
- (9) Dahan, E.; Bialio, S. E. *J. Org. Chem.* **1991**, *56*, 7269.
- (10) Bitter, I.; Grun, A.; Toth, G.; Szollosy, A.; Horvath, G.; Agai, B.; Toke, L. *Tetrahedron* **1996**, *52*, 639.
- (11) Krasnokutskaya, E.; Semenischeva, N.; Filimonov, V.; Knochel, P. *SYNTHESIS* **2007**, *81*.
- (12) Herbert, S. A.; Arnott, G. E. *Org. Lett.* **2009**, *11*, 4986.
- (13) Gutsche, C. D.; Iqbal, M. *Org. Synth.* **1990**, *68*, 234.
- (14) Gutsche, C. D.; Lin, L.; Louis, S. *Tetrahedron* **1986**, *42*, 1633.
- (15) Dondoni, A.; Marra, A.; Scherrmann, M.-C.; Casnati, A.; Sansone, F.; Ungaro, R. *Chem. - A Eur. J.* **1997**, *3*, 1774.
- (16) Ikeda, A.; Yoshimura, M.; Lhotak, P.; Shinkai, S. *J. Chem. Soc. Perkin Trans. 1* **1996**, 1945.
- (17) Herbert, S. A.; Van Laeren, L. J.; Castell, D. C.; Arnott, G. E. *Beilstein J. Org. Chem.* **2014**, *10*, 2751.
- (18) Verboom, W.; Durie, A.; Egberink, R. J. M.; Asfari, Z.; Reinhoudt, D. N. *J. Org. Chem.* **1992**, *11*, 1313.

3 Chapter 3 - Ortholithiation of oxazoline calixarenes

3.1 Introduction.

There are scant examples of high yielding and practical synthetic methods toward inherently chiral calixarenes. One of the first strategies capable of yielding enriched diastereomeric mixtures of *ortho*-functionalized inherently chiral calixarenes was reported by the Arnott group in 2009.^{1,2} Up until now, the principal focus of this research has been aimed at method optimization. Preliminary application studies were carried out by a previous MSc student, Miss L. van Laeren, which yielded encouraging results.³ In order to further the studies for the application of these compounds, the challenging synthetic techniques associated with these methods had to be mastered.

Ever since the initial independent discoveries made by Gilman⁴ and Wittig⁵ in the late 1930's, the mechanistic complexities behind directed metalation have been thoroughly investigated. As of yet, the details behind the simplest directed lithiation reactions lack agreement amongst peers. However, there are several steps of the overall process that have become widely accepted. By reviewing the literature, we aimed to apply some of the most relevant findings, with the view to better understanding the detail of the chemistry reported here.

This study was initially carried out by Dr. Simon Herbert.⁶ To summarize, the motivation for continuing with this work was as follows; firstly, the oxazoline-directed asymmetric ortholithiation of calixarenes is currently the most efficient method of synthesizing *ortho*-functionalised inherently chiral calixarenes in enriched diastereomeric mixtures. Experimental proficiency in this chemistry was key to furthering any application studies of inherent chirality. Secondly, we aimed to achieve an improved understanding of the roles played by each of the reaction components. Besides the nature of the starting material, the *ortho*-directed lithiation reaction has three major components; the ligand/additive, solvent and alkyllithium. The various combinations of these three parameters have been shown to dictate the outcome of the reaction. Therefore, understanding the individual roles played by each of these factors was vital when choosing a set of experimental conditions aimed at synthesizing specific calixarene compounds. Lastly, purification was a major practical challenge associated with this chemistry. Given that the ultimate goal was to use this chemistry to develop new ligand compounds, effective purification methods had to be established.

3.2 Preparation of alkyllithium reagents.

3.2.1 Synthesis of alkyllithiums.

The choice of lithium base was one of three key parameters in the ortholithiation reaction. Obtaining these reagents commercially proved to be problematic for two reasons; they were shipped on a biannual basis and many, barring the standard *n*, *s*, and *t*-BuLi, were either overly expensive or simply not available for purchase. This required preparation of these reagents in-house. The yields and selectivities of the ortholithiation reactions were considerably varied depending on the oxazoline starting material and the choice of alkyllithium base.^{1,2,7,8} Therefore, testing the largest possible range of these reagents has always been of primary interest. In the past, a substantial number of bases had been screened, however, a few still remained unchecked. Thus, synthesizing a small library of these reagents was a necessity. Besides the interest in testing new alkyllithiums, several different alkyllithiums were required to synthesize the four inherently chiral calixarenes with the highest selectivities.

The synthesis for the majority of these compounds was achieved using the same general procedure reported by Gilman in 1932.⁹ This process involved mixing the lithium metal with the corresponding alkyl halide in pentane, while maintaining reflux conditions for 3-8 hours. Following this, the reaction mixture was filtered (under inert conditions) which yielded the alkyllithium in a pentane solution. The synthesis of these reagents is summarised in **Table 3.1**.

Table 3.1: Synthesis of the alkyllithium bases.

$$\text{R-Cl} \xrightarrow{\text{i)}} \text{R-Li}$$

Entry	R	Lithium (equiv)	Conditions	Conc. (mmol/ml)
1	<i>s</i> -Butyl	Granules (3.0)	Pentane, Δ	1.63
2	<i>t</i> -Butyl	Powder (15)	Pentane, Δ	0.40
3	<i>i</i> -Butyl	Granules (3)	Pentane, Δ	1.05
4	<i>i</i> -Propyl	Granules (3)	Pentane, Δ	1.45
5	<i>c</i> -Pentyl	Granules (3)	Pentane, Δ	1.14
6	<i>c</i> -Hexyl	Powder (3)	Toluene, Δ	0.08
7	<i>c</i> -Hexyl	Granules (3)	Toluene, Δ	0.05

Reagents and conditions: i) RCl, solvent, reflux 3-6 h. Alkyllithium bases were titrated using either a mixture of *n*-benzylbenzamide in THF ($-20\text{ }^{\circ}\text{C}$ to $0\text{ }^{\circ}\text{C}$) or methanol and 2,2-bipyridine in THF ($0\text{ }^{\circ}\text{C}$).

Despite the synthesis for the majority of these reagents following a well-established procedure, a number of factors merit discussion. The nature of the lithium metal, solvent used and purification methods each effected the reaction outcome. The lithium metal was available in two forms; either as granules or a much finer lithium powder, both of which were suitable for the synthesis of all the alkyllithium bases. This excluded the synthesis of *t*-BuLi, which required the more reactive lithium powder.

Chapter 3 – Ortholithation of oxazoline calixarenes

Fortunately, *t*-BuLi and *n*-BuLi were both commercially available, which meant the use of the lithium powder could be avoided, as the handling and quenching of the excess metal was far more dangerous in comparison to the pellets. Even though the use of lithium granules was safer and generally more convenient, they too presented several experimental challenges. Any exposure of the pellets to the atmosphere resulted in the rapid oxidation of the outer metal layer. This light grey/blue LiOH crust would prevent the formation of the alkyllithium base and result in low or negligible reaction yields. In order to prevent this, the granules had to be treated with a preparation procedure. To date, several preparation techniques for lithium metal have been reported,^{10,11} one of them being the formation of lithium sand.¹¹ This required melting the lithium granules in silicon oil and rapidly stirring the mixture to form lithium sand. After rapidly cooling the mixture, the oil was removed and the sand washed with freshly distilled pentane. An alternative procedure, which proved to be more practical, was the removal of the entire outer oxidised layer by a stepwise oxidation and sonication procedure.¹⁰ This was accomplished by briefly exposing the lithium metal to dry isopropyl alcohol (IPA). The brief exposure rapidly oxidised the outer layer of the metal, forming a thicker and more uniform lithium-isopropoxide crust. The excess IPA was then removed and the oxidized pellets dried under vacuum. Once dry, the pellets were suspended in freshly distilled pentane and the outer layer was removed by sonication. The lithium pellets now had a pure metallic surface and after a final wash they were ready for use. A clean and non-oxidized metallic surface was critical to the formation of the alkyllithium bases in high yields.

The lithium bases in Entries 1-5 were synthesized using the procedure reported by Gilman.⁹ The exothermic reaction required the slow addition of the alkyl halide as a diluted solution in pentane. The reaction was initiated by adding a small volume, usually 2.0 to 3.0 ml of this solution, and then adding the rest drop-wise, over a three hour period. The initiation of the reaction could be seen when the mixture turned a dark purple colour. This colour change was characteristic for all of the synthesized alkyllithiums and had to hold throughout the synthesis. If this change never took place, or the colour faded over the duration of the reaction, negligible yields of the base were always obtained.

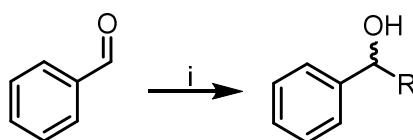
Initially, when attempting Gilman's reaction conditions for the preparation of *c*-HexLi, none of the product was isolated. It was speculated that the competing elimination reaction was taking place over the formation of the base, which yielded the unwanted cyclohexene. For this reason alkylchlorides were preferentially used over alkyl-bromides, as bromine is a better leaving group, making the alkylbromides more susceptible to elimination. Instead, an alternative method was found in which toluene was replaced as the solvent (entries 6 & 7).^{12,13} Despite still obtaining low yields for this reaction, the *c*-HexLi solutions were concentrated under vacuum. The *c*-HexLi solution in toluene could be concentrated to a maximum of 0.24 M at room temperature, before precipitation took place.

Chapter 3 – Ortholithiation of oxazoline calixarenes

Conveniently, both the *c*-PentLi and *c*-HexLi reagents were crystalline at higher temperatures and in lower concentrations in comparison to the linear alkyllithium bases. This allowed for their purification via recrystallization. Cooling the *c*-PentLi solution to $-20\text{ }^{\circ}\text{C}$ overnight resulted in the growth of colourless plate-like crystals. While maintaining low temperatures and inert conditions, the excess solvent was removed. After washing the crystals with additional cooled ($0\text{ }^{\circ}\text{C}$) and freshly distilled pentane, they were transferred to a clean flask and dissolved in freshly collected pentane at room temperature. A similar procedure was followed for the *c*-HexLi in toluene, but this required a lower temperature of $-80\text{ }^{\circ}\text{C}$.

3.2.2 Characterization of the alkyllithium bases – confirmation of structure.

The structures of the alkyllithium bases were confirmed through quenching with a known electrophile at a low temperature (**Scheme 3.1**). Benzaldehyde was found to be suitable and was used to characterize these reagents. By adding a slight excess of the base to the aldehyde, the corresponding alcohol was quantitatively obtained as the quenched product. ^1H NMR spectroscopic analysis of the crude products was used to identify the characteristic alkyl signals added by the lithium base.



Scheme 3.1: Characterization of the alkyllithium bases. Reagents and conditions: i) benzaldehyde (1.0 equiv), RLi (1.1 equiv), THF, $-78\text{ }^{\circ}\text{C}$, 2 h.

The use of benzaldehyde had several benefits, it was both inexpensive and the corresponding alcohol was easily visualized on TLC. Most importantly, the aromatic component of the aldehyde added no signals to the alkyl region of the ^1H NMR spectrum, making it easy to identify the characteristic alkyl signals of the different lithium bases.

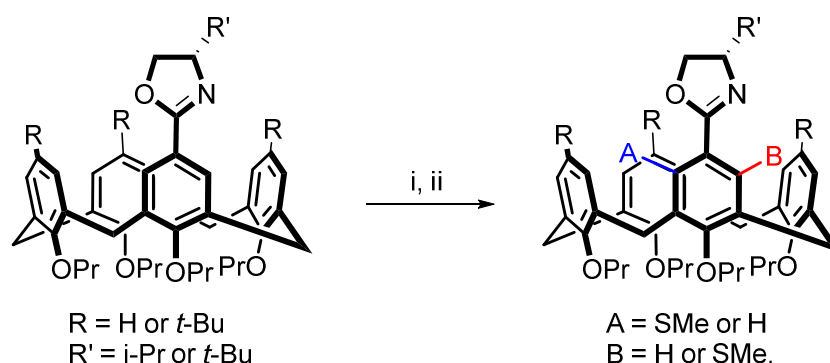
3.3 The ortholithiation of isopropyl and *tert*-butyl oxazoline calixarenes **57** and **58**.

3.3.1 The ortholithiation reaction - a summary of past results.

The asymmetric functionalization of all four oxazoline calixarene (**57**, **58**, **66** and **67**) scaffolds had been previously optimized and reported by Dr. S. Herbert (**Scheme 3.2**).^{1,2} The key to this strategy involved the use of a chiral auxiliary to direct an asymmetric *ortho*-metalation reaction. Across the four oxazoline compounds, it was shown that variations of the solvent, alkyllithium and ligand were responsible for generating different degrees of chiral induction. None of the scaffolds were found to adhere to a standard set of conditions.

Chapter 3 – Ortholithiation of oxazoline calixarenes

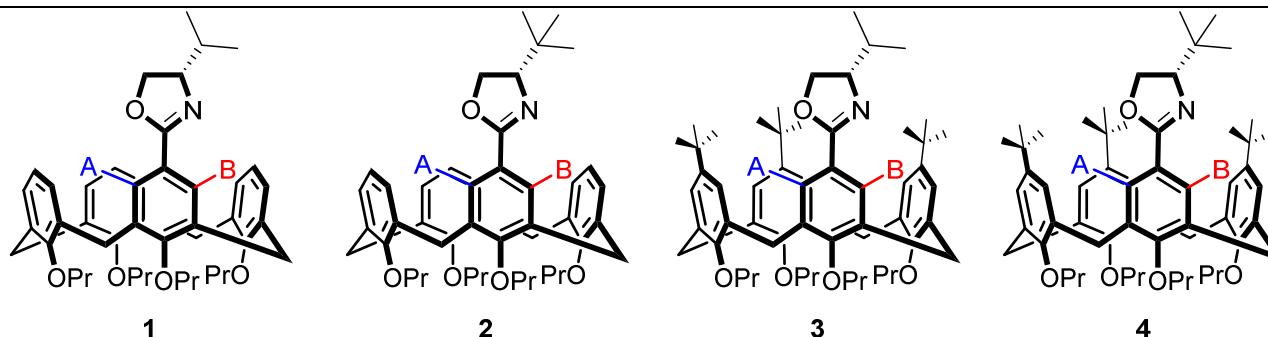
On top of this, the selectivities and conversions would vary considerably for each of the compounds over the same set of conditions. All of the oxazoline calixarenes required a unique and specific set of reaction conditions to obtain the desired diastereomer in the highest yield and selectivity.



Scheme 3.2: The general ortholithiation reaction conditions: i) RLi (5.0 equiv), ligand (10 equiv), solvent, $-78\text{ }^{\circ}\text{C}$, 7-48 h; ii) E (exs), $-78\text{ }^{\circ}\text{C}$ to rt 12 h. Lithiation times for the de-alkylated ($R = \text{H}$) calixarenes were notably faster 7-24 h. For the $t\text{-Bu}$ calixarenes lithiation reaction times were significantly longer 24-48 h.

In this previous study it was established that selecting a specific set of reaction conditions would enable the selective synthesis of either diastereomer for each of the oxazoline calixarenes. To demonstrate the extent and versatility of the reaction, a summary of the entire study carried out by Dr. S. Herbert can be seen in **Table 3.2**. The above mentioned variation in performance is clearly depicted when considering the results for any of the entries, from left to right, over the four different oxazoline compounds. The reaction conditions of interest were those that afforded the two diastereomers in the best yields and highest selectivities (entries 2, 3, 7, 8, 9 and 14) seeing as these would be used to synthesize the new inherently chiral compounds to be used in an application study. A sizable number of alkyllithiums were tested and reported in the ortholithiation study carried out by Dr. S. Herbert. The findings from this project had been published and it was considered to be largely complete.^{2,3,8} Despite this, there were a few unanswered questions with the potential to yield interesting results, and so a second look at the ortholithiation of isopropyl and *tert*-butyl oxazoline calixarene was deemed necessary. Several of these conditions were considered interesting owing to their unique outcome (entries 2, 3 and 4). The reason for this interest will be explained and discussed further on in the chapter, where the outcomes of these reactions were revisited. For all of the oxazoline directed lithiation reactions, the effect of different alkyllithiums on the outcome of both selectivity and yield was one of the most interesting aspects of the study. In addition, as already mentioned, even though a comprehensive body of work had already been reported, a few lithium bases remained untested. Before the reaction was attempted with any of the newly synthesized alkyllithiums, the necessary experimental preparations and inert synthetic techniques had to be acquired.

Chapter 3: Ortholithiation of oxazoline calixarenes

Table 3.2: A summary of the ortholithiation study first reported by Dr. S. Herbert.⁷

Entry	Solvent	RLi	Ligand	1		2		3		4	
				Conv (%)	de (%)	Conv (%)	de (%)	Conv (%)	de (%)	Conv (%)	de (%)
1	Et ₂ O	<i>n</i> -BuLi	TMEDA	50	96 (B)	18	71 (B)	0	-	<5	-
2	Et ₂ O	<i>s</i> -BuLi	TMEDA	95	86 (B)	94	78 (B)	73	50 (B)	80	>99 (B)
3	Et ₂ O	<i>t</i> -BuLi	TMEDA	70	0	75	84 (A)	<5	-	61	97 (A)
4	Et ₂ O	<i>c</i> -PentLi	TMEDA	90	86 (B)	80	91 (B)	64	92 (B)	30	>99 (B)
5	Et ₂ O	<i>i</i> -PrLi	TMEDA	90	94 (B)	92	98 (B)	65	83 (B)	25	>99 (B)
6	Pentane	<i>n</i> -BuLi	TMEDA	47	96 (B)	<5	-	0	-	<5	-
7	Pentane	<i>s</i> -BuLi	TMEDA	97	86 (B)	95	>99 (B)	8	33 (B)	46	>99 (B)
8	Pentane	<i>t</i> -BuLi	TMEDA	95	66 (B)	50	82 (A)	<5	-	<5	-
9	Pentane	<i>c</i> -PentLi	TMEDA	93	94 (B)	67	98 (B)	<5	-	<5	-
10	Pentane	<i>i</i> -PrLi	TMEDA	95	94 (B)	67	>99 (B)	<5	-	<5	-
11	Pentane	<i>s</i> -BuLi	DGME	95	50 (A)	38	0	0	-	<5	-
12	Pentane	<i>t</i> -BuLi	DGME	25	33 (A)	17	67 (A)			<5	-
13	Pentane	<i>i</i> -PrLi	DGME	24	0	<5	-			<5	-
14	Pentane	<i>s</i> -BuLi	(<i>t</i> Bu) ₂ -DGME	95	78 (A)	33	50 (A)			12	50 (A)
15	Et ₂ O	<i>s</i> -BuLi	-	93	0	88	0	-	-	26	50 (B)
16	THF	<i>n</i> -BuLi	-	<5	-	<5	-	<5	-	<5	-
17	THF	<i>t</i> -BuLi	-	<5	-	<5	-	<5	-	<5	-
18	THF	<i>s</i> -BuLi	-	93	0	88	0	49	33 (A)	26	50 (B)

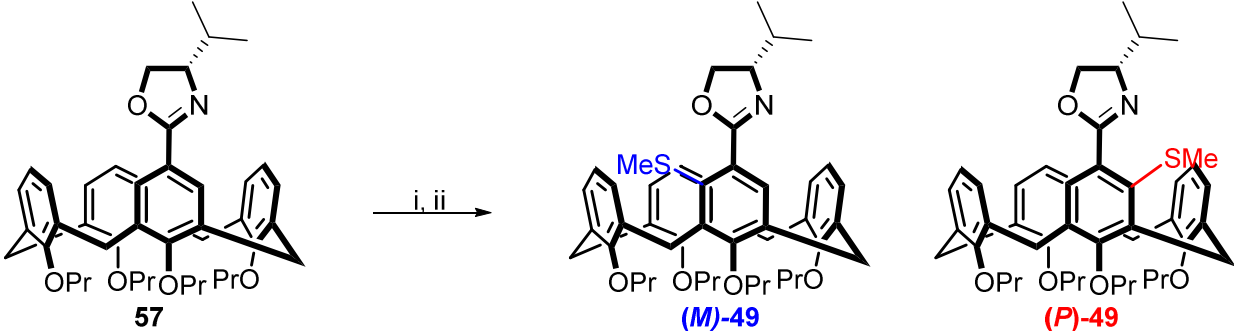
A and B are placeholders for the electrophiles used in the original study.

Chapter 3: Ortholithiation of oxazoline calixarenes

3.3.2 Revisiting the ortholithiation of isopropyl oxazoline - 57.

Early attempts at the ortholithiation reaction resulted in frustratingly low yields. A totally inert experimental setup was crucial and over time an optimal reaction protocol was developed. Only once the successful ortholithiation of **57** had become routine, was the use of new alkylolithiums attempted. In addition to testing a new alkylolithium base, the major and minor diastereomer products of this reaction needed to be fully characterized. The newly collected data towards these aims are summarized in **Table 3.3**.

Table 3.3: The ortholithiation of isopropyl oxazoline – **57**.



Entry	RLi	Ligand	Solvent	Conversion (%) ^a	de (%) ^a
1	<i>s</i> -BuLi	di- <i>t</i> Bu-diglyme	Pentane	98	80
2	<i>c</i> -PentLi	TMEDA	Pentane	97	94
3	<i>i</i> -BuLi	TMEDA	Pentane	0	-
4	<i>i</i> -BuLi	TMEDA	Et ₂ O	0	-
5	<i>c</i> -PentLi	TMEDA	Et ₂ O	96	94
6	<i>t</i> -BuLi	TMEDA	Et ₂ O	90	0

Reagents and conditions: i) RLi (5.0 equiv), ligand (10.0 equiv), solvent, -78 °C, 7-24 h; ii) Me₂S₂, -78 °C to rt, 24 h. ^aConversions and *de* values were determined using ¹H NMR spectroscopy.

Using a *c*-PentLi/TMEDA mixture (entries 2 and 5), thioether (**(P)**-49) was synthesized in high conversions when using both pentane (97%) and diethyl ether (96%) as the solvent. The corresponding *de* values for both of these reactions were both calculated as 94%. In order to synthesize the opposing diastereomer (**(M)**-49 (entry 1), a mixture of *s*-BuLi/di-*t*Bu-diglyme in pentane was used instead. The conversion and *de* for the reaction were calculated as 98% and 80% respectively. These were the optimal conditions for the synthesis of both diastereomers.

Ortholithiation with *i*-BuLi had not been previously reported and the reaction was attempted using an excess of the standard *i*-BuLi/TMEDA mixture (entries 3 and 4) in both pentane and Et₂O. Frustratingly, none of the thio-ether product mixture was formed. Generally speaking, lithiation chemistry was found to be sensitive and prone to failure. To confirm that the experimental setup was not responsible, the reactions were attempted multiple times in both solvents and only the starting material was recovered.

Both of the thioether calixarene diastereomers (**(M)**-49 and **(P)**-49) were particularly difficult to characterize. The reason for this was that they shared *R_f* values with the starting material **57**. These ortholithiation reactions therefore always yielded a mixture of diastereomers.

Chapter 3: Ortholithiation of oxazoline calixarenes

The addition of the small thio-methyl functional group to the large and quite non-polar calixarene barely affected its overall polarity. This posed a serious problem with regards to purification of the product mixtures. Conventional column chromatographic separation techniques were unable to separate the diastereomers from each other or the starting material. Unfortunately, preparative HPLC methods were unavailable and the characterization of these compounds required a different approach.

The pure thio-ether products thus had to be characterized as a mixture of diastereomers. The product mixtures resulting from entries 1 and 2 were optimal for this purpose when taking both selectivity and conversion into consideration. The highest selectivity for the reaction was originally obtained using an *n*-BuLi/TMEDA mixture in either pentane or Et₂O (Table 3.2, entries 1 and 6) but the conversions were low. The product mixture from entry 2 was therefore purified using column chromatography. This effectively removed the impurities that were present in the crude ¹H NMR spectrum, with only minor amounts of the opposite diastereomer and unreacted starting material remaining (Figure 3.1).

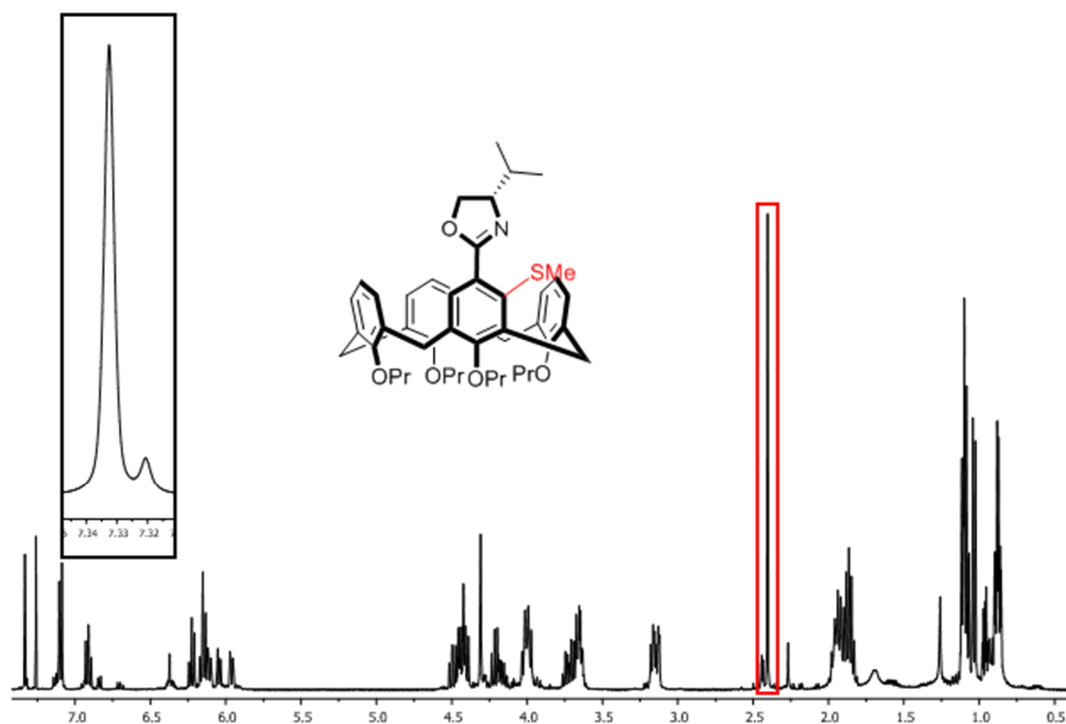


Figure 3.1: ¹H NMR spectrum of thio-ether calixarene (*P*)-49. The signal for the thio-methyl group is outlined in red.

The two diastereomers are structurally very similar and shared an almost identical ¹H NMR spectrum. The only small, but also extremely significant difference, was the chemical shifts for the single remaining *ortho*-proton next to the oxazoline on the functionalized aryl ring. The starting material **57** *ortho*-proton's signals were two diastereotopic doublets, with chemical shifts of δ 7.47 and δ 7.52 ppm respectively.

Chapter 3: Ortholithiation of oxazoline calixarenes

The introduction of a new functional group to the ring left one proton remaining, and these doublets were then replaced by a singlet. The chemical shift for the remaining aromatic proton on thio-ether (**P**)-**49** was δ 7.35 ppm (This region is expanded on the ^1H NMR spectrum) and the much smaller signal at δ 7.33 ppm represents the opposite thio-ether diastereomer (**M**)-**49**. The conversions for these reactions were calculated by comparing the total area of the two diastereomer signals to the remaining doublet signals of the starting material. Similarly, the selectivity of the reaction was calculated by comparing the areas of the two diastereomer singlets.

Besides the issues associated with the separation of the product mixture, purification of calixarene (**M**)-**49** posed an additional challenge. After column chromatography, the ^1H NMR spectrum still contained large amounts of the diglyme ligand. The di-*t*Bu-diglyme ligand was also required in vast excess to ensure a high conversion to the thio-ether product, within a reasonable amount of time. It was not possible to remove the ligand during the work-up, or by using column chromatography. Another column with a lower polarity solvent mixture was attempted with the aim of first washing off the ligand, and then later increasing the polarity to isolate the product, but this was also unsuccessful. During the synthesis of the diglyme ligand, it was purified via vacuum distillation, and so it could be potentially removed in the same way. After heating the calixarene product mixture to 60 °C under high vacuum conditions for 24 h, the ^1H NMR for the product mixture was recollected. The new spectrum confirmed that the majority of the diglyme ligand had been removed. Importantly, no degradation of the thio-ether product had taken place. The compound was submitted to the same conditions and left for a total of 48 h, after which the ^1H NMR spectrum confirmed that none of the ligand remained (**Figure 3.2**).

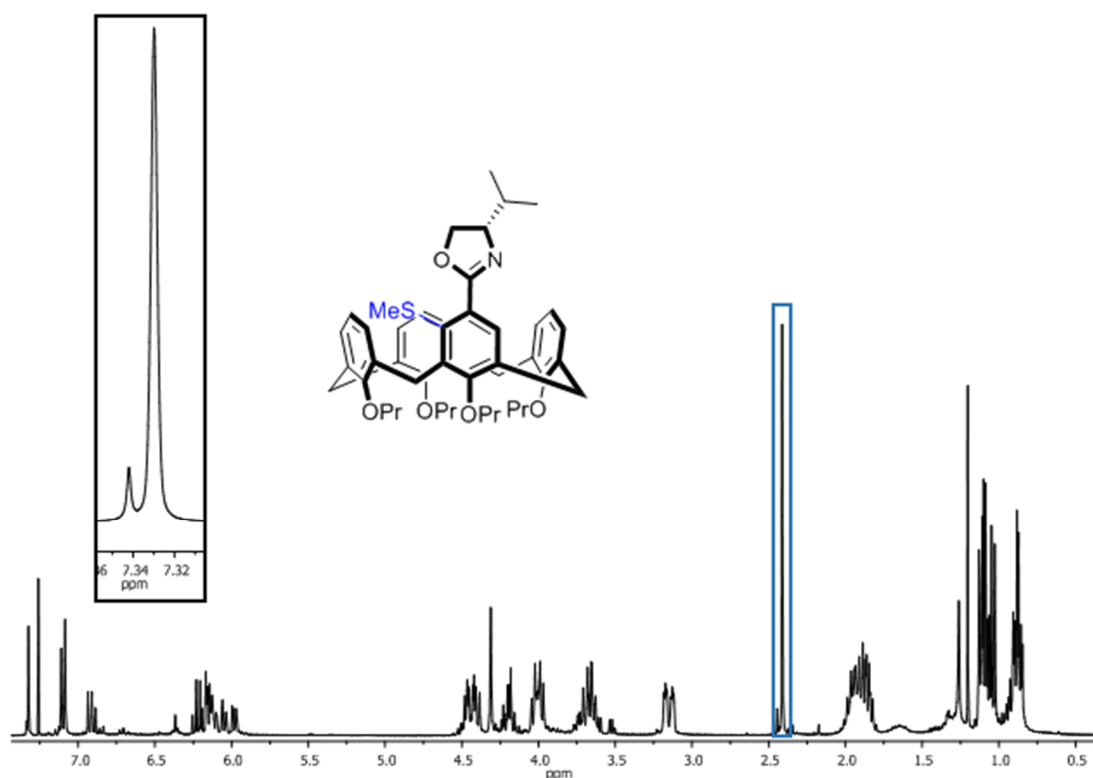
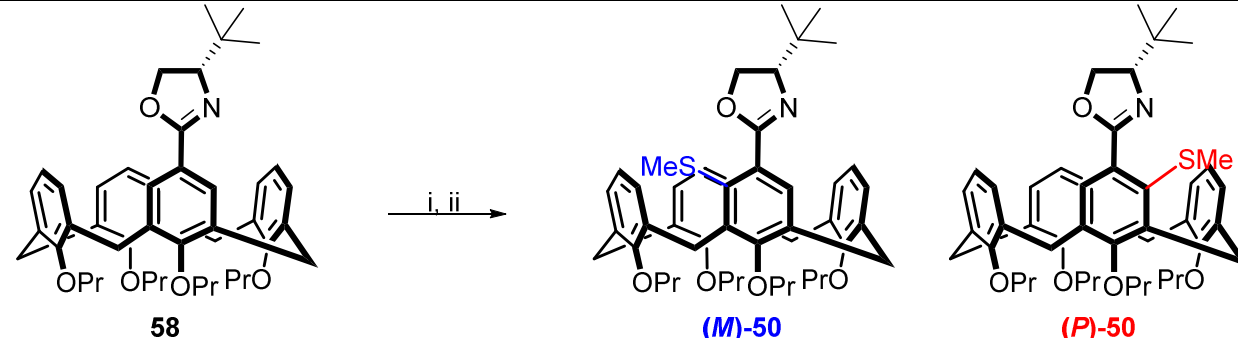


Figure 3.2: ^1H NMR spectrum of thio-ether calixarene (**M**)-49. The signal for the thio-methyl group is outlined in blue.

The ^1H NMR spectrum for thio-ether (**M**)-49 was very similar to that of (**P**)-49. Comparison of the two expanded regions shows the major and minor signals for each of the diastereomers. The chemical shift for the aromatic singlet of (**M**)-49 is slightly more up-field with a chemical shift of δ 7.35 ppm. For both **Figure 3.1** and **Figure 3.2**, the signals for the newly introduced thio-methyl functional groups are outlined in red and blue respectively. This signal overlapped for both diastereomers and they both shared a chemical shift of δ 2.40 ppm. It would have been convenient if the chemical shifts differed, as these values could have been used to corroborate the product ratios calculated from the aromatic signals.

3.3.3 Revisiting the ortholithiation of *tert*-butyl oxazoline – 58.

Much like with the isopropyl oxazoline, the aim here was to take a second look at past results, as well as adding to the existing data set by synthesizing new alkyl lithium bases and studying their impact on the ortholithiation reaction. The previously established experimental preparations, set up, and general procedure were kept consistent for the *tert*-butyl oxazoline scaffold. The newly reported data are summarized in **Table 3.4**.

Table 3.4: The ortholithiation of *tert*-butyl oxazoline – **58**.


Entry	R _{Li}	Ligand	Solvent	Conversion (%) ^a	<i>de</i> (%) ^b
1	<i>s</i> -BuLi	TMEDA	Pentane	99	>99
2	<i>t</i> -BuLi	TMEDA	Pentane	99	82
3	<i>c</i> -PentLi	TMEDA	Pentane	98	97
4	<i>i</i> -BuLi	TMEDA	Pentane	0	-
5	<i>c</i> -HexLi	TMEDA	Pentane	96	95
6	<i>i</i> -BuLi	TMEDA	Et ₂ O	0	-
7	<i>c</i> -HexLi	TMEDA	Et ₂ O	97	94
8	<i>t</i> -BuLi	TMEDA	Et ₂ O	*	-
9	<i>s</i> -BuLi	TMEDA	Et ₂ O	95	78

Reagents and conditions: i) R_{Li} (5.0 equiv), ligand (10.0 equiv), solvent, –78 °C, 24 h; ii) Me₂S₂, –78 °C to rt, 24 h. ^aConversions for these reactions were determined using ¹H NMR spectroscopy. ^bSelectivities were determined using either ¹H NMR spectroscopy or HPLC analysis.

The successful ortholithiation of *tert*-butyl calixarene was achieved using the previously reported methods. Thio-ethers (**(M)-50** and **(P)-50**) were synthesized using conditions that were previously optimised (entries 1 and 2). An excess *s*-BuLi/TMEDA mixture in pentane yielded **(P)-50** in a near quantitative yield of 99% and a *de* of >99%. The opposite diastereomer **(M)-50**, was synthesized using a *t*-BuLi/TMEDA mixture in pentane with a conversion of 99% and *de* of 82%. The near quantitative conversion for both of these reactions was ideal for the characterization of both diastereomers. Similarly to the isopropyl diastereomers, the product mixtures shared an *R_f* value with the starting material, and silica gel column chromatography was used to remove any impurities resulting from the crude product mixture. Unlike **(M)-49**, the synthesis of **(M)-50** did not require the use of the diglyme ligand. The switch in selectivity for the *t*-butyl oxazoline calixarenes occurred when the bulkier *t*-BuLi was used. This observation was the most unusual difference between the reactivity of the two oxazoline starting materials. These results prompted a thorough investigation of the literature surrounding directed metalation chemistry and will be covered in detail in the discussion section to follow. Lithiation using an *i*-BuLi/TMEDA mixture was also attempted for **58** (entries 4 and 6). After attempting the reaction multiple times in both pentane and Et₂O, none of the thio-ether product was isolated. The fact that no product was obtained for both oxazolines was a strong indication that *i*-BuLi was an unsuitable alkylolithium for these reactions. However, ortholithiation using a *c*-HexLi/TMEDA mixture (entries 5 and 7) yielded good results, affording **(P)-50** in high conversions for both pentane (96%) and diethyl ether (96%), with similar selectivities of 95% and 94%, respectively.

Chapter 3: Ortholithiation of oxazoline calixarenes

Much like the isopropyl oxazoline diastereomers, The ^1H NMR spectra for (*P*)-**50** (Figure 3.3) and (*M*)-**50** (Figure 3.4) were almost identical, the most notable and important difference being the chemical shifts of the singlet for the last remaining proton on the functionalised aromatic ring.

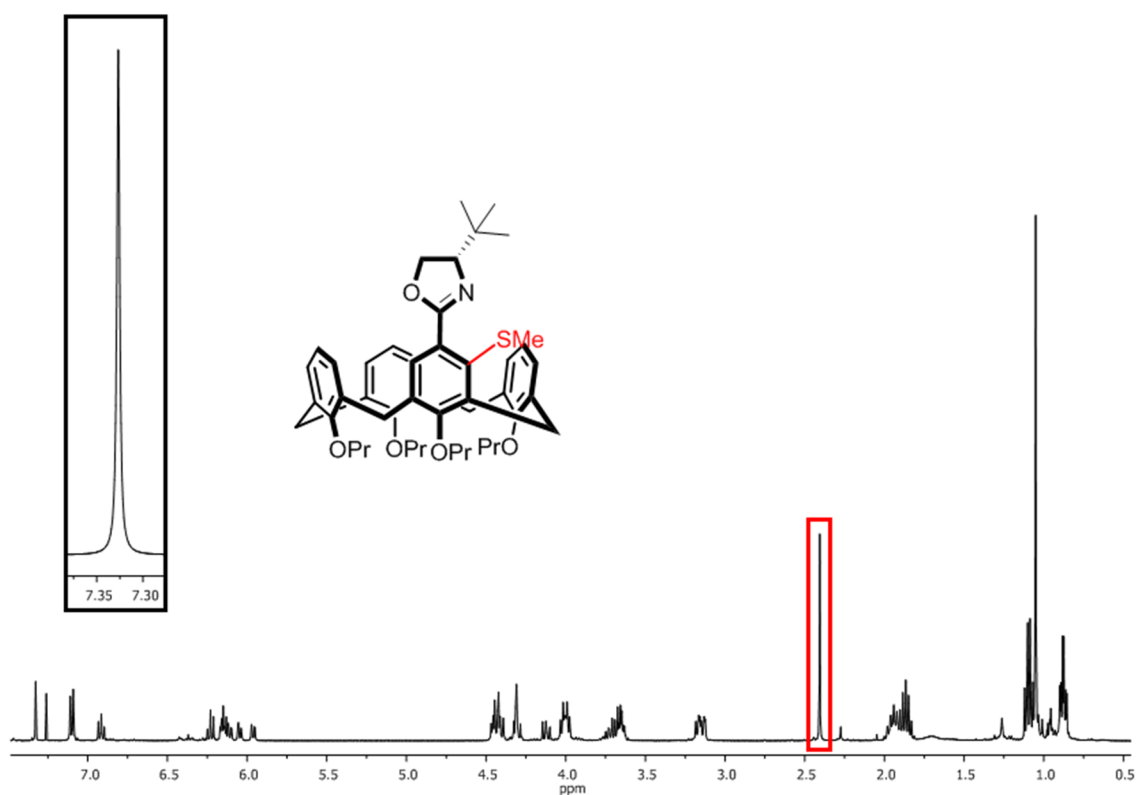


Figure 3.3: ^1H NMR spectrum of thio-ether (*P*)-**50**. The signal for the thio-methyl group is outlined in red.

The ^1H NMR spectrum of calixarene (*P*)-**50** was unique in the sense that there appeared to be only a single diastereomer signal with a chemical shift of δ 7.32 ppm. This was due to the fact that the selectivity for the reaction was so high (>99%) that the amount of minor diastereomer present was below the limit of detection for ^1H NMR spectroscopy. When the *de* of these reactions exceeded 95%, quantification via ^1H NMR spectroscopy was unreliable as the signals for the minor diastereomers were too small to be calculated accurately. In these cases quantification via HPLC was necessary. Even though the diastereomers looked like a single spot on TLC, they were separable on a normal phase HPLC column. The major and minor diastereomers eluted close after one another and the peaks were never fully resolved in the chromatograms. These peaks were resolved and integrated using a combination of both SigmaPlot and PeakFit. The conversions for these reactions were also calculated by comparison of the areas of the product and starting material aromatic signals. The signal for the thio-methyl peak also had the same chemical shift of δ 2.40 ppm and is outlined in red on the spectrum above.

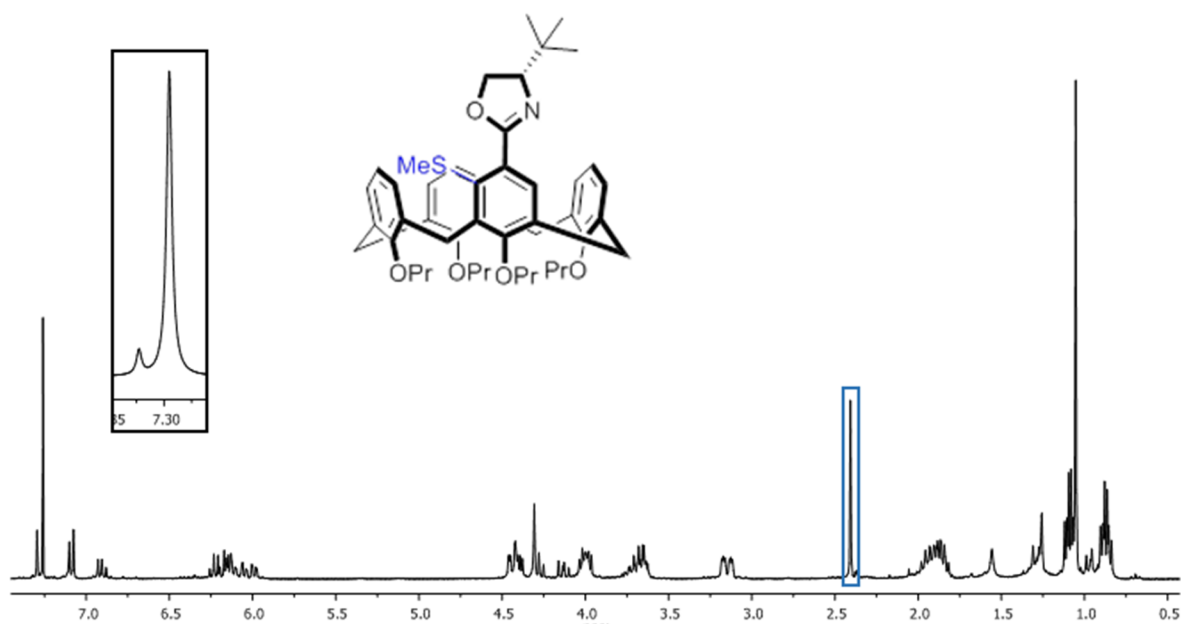
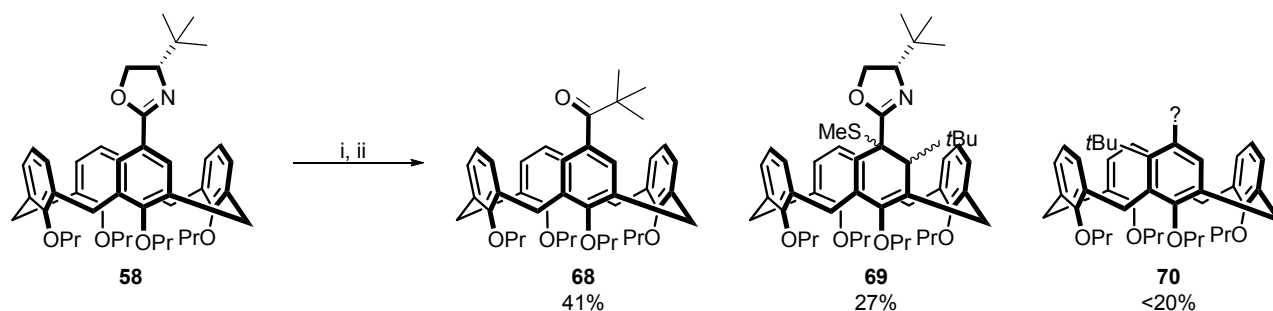


Figure 3.4: ^1H NMR spectrum of calixarene (**M**)-**50**. The signal for the thio-methyl group is outlined in blue.

The remaining aromatic singlet for thio-ether (**M**)-**50** was slightly more up-field and had a chemical shift of δ 7.30 ppm. The selectivity for this reaction was considerably lower and could be calculated by comparing the areas of the major and minor singlets in the ^1H NMR spectrum. The thio-methyl signal had the same chemical shift of δ 2.40 ppm and is outlined in blue.

3.3.4 The addition and de-aromatization products.

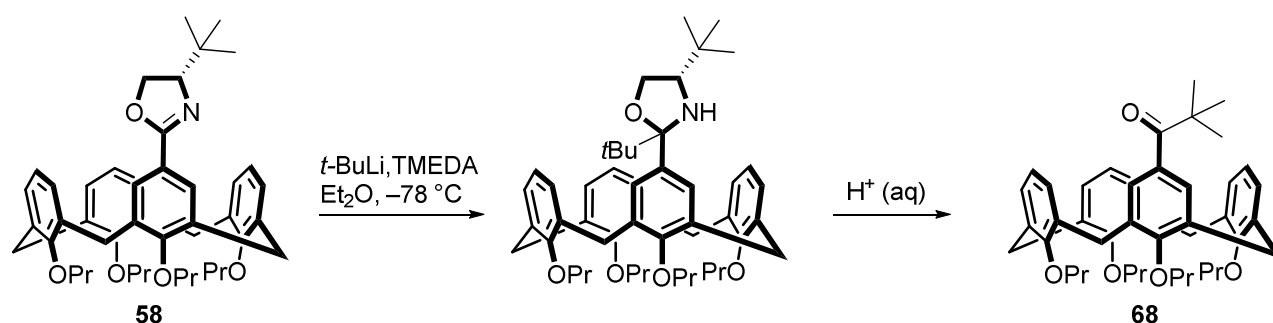
When attempting the reaction with a *t*-BuLi/TMEDA mixture in pure Et_2O (**Table 3.4**, entry 8), several new and unexpected products formed. TLC analysis showed the formation of three new products, each with a unique R_f values different to that of the starting material. This was unusual as the *tert*-butyl thio-ether calixarenes also always shared an R_f with the starting material. Initially the scale of the reaction was too low to isolate any of these compounds. Using the same conditions, and taking care to replicate procedure exactly, the reaction was carried out on a much larger scale (**Scheme 3.3**). TLC analysis of the reaction mixture confirmed the formation of the same three products. The R_f values were relatively close to one another and the three products were isolated by making use of a very slow chromatographic separation.



Scheme 3.3: The synthesis of products **68-70**. Reagents and conditions: i) *t*-BuLi (5.0 equiv), TMEDA (10.0 equiv), Et₂O, -78 °C, 24 h; ii) S₂Me₂ (exs), -78 °C to rt 12 h.

The formation of these three products only occurred with a subtle difference in the reaction conditions. If the pentane from the *t*-BuLi solution was not removed, and the reaction was carried out in an Et₂O/pentane mixture instead, then only the expected ortholithiated (**M**)-**50** was formed. However, when the pentane from the *t*-BuLi was removed and the reaction was carried out in pure Et₂O, none of (**M**)-**50** was obtained and the reaction yielded the three new products instead.

The formation of **68** can be explained by addition of *t*-BuLi to the imidate center on the oxazoline functional group, forming an *N,O* acetal (**Scheme 3.4**). The acetal was likely hydrolysed to the ketone during the acidic aqueous work-up.



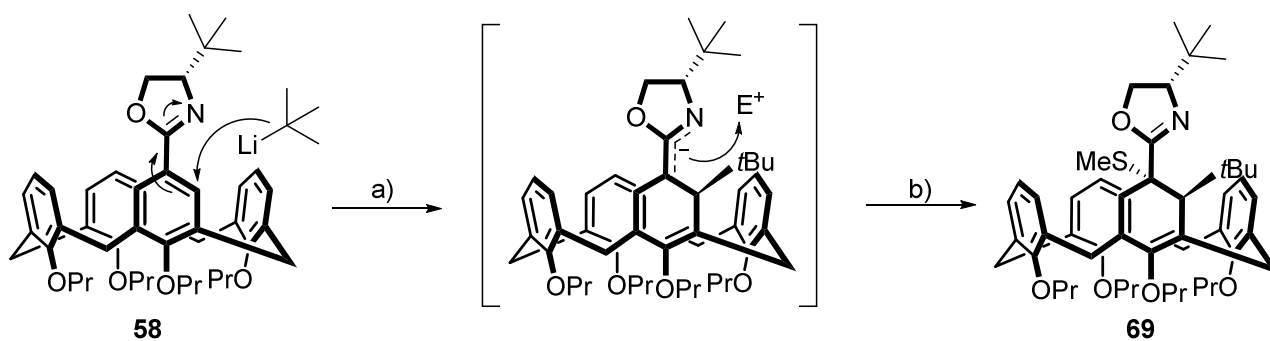
Scheme 3.4: The proposed reaction sequence for the formation of **68**.

The same observation was made by Herbert when attempting the ortholithiation of *tert*-butyl isopropyl calixarene **66** under similar conditions.⁷ Similarly, the addition product only formed when the reaction was carried out in pure Et₂O, but in temperatures above -78 °C. In that case, only a mixture the *N,O* acetal and ketone was seen. The acetal was also isolated and its structure was confirmed by MS and NMR spectroscopy. None of the other products formed and the *tert*-butyl ketone was the only isolated product following the hydrolysis of the acetal functional group.

A possible explanation for the formation of the de-aromatized product **69** is through the attack of *t*-BuLi on the *p*-propoxyphenyl ring containing the oxazoline directing group. This type of chemistry is known for aryl oxazoline systems, and the direct nucleophilic addition of alkylolithiums to π -systems was first reported on naphthyl oxazolines by Meyers and co-workers.¹⁴

Chapter 3: Ortholithiation of oxazoline calixarenes

More recently, a similar finding was made by Clayden and co-workers where the de-aromatization of a series of simple aryl-oxazolines was reported.¹⁵ A potential mechanism for the formation of this product is proposed below (**Scheme 3.5**).



Scheme 3.5: A mechanism for the formation of the de-aromatized calixarene 69.

The first step (a) is the nucleophilic attack of the *t*-BuLi on the *ortho*-position of the aryl ring, forming an anionic intermediate with a delocalized pair of electrons over the aryl-carbon and nitrogen-carbon bonds. In the second step (b) the anionic intermediate is quenched with an electrophilic source. Given that S₂Me₂ was the electrophile used in the attempted ortholithiation reaction, a thio-methyl group was introduced onto the *ipso*-position of the aryl ring. The formation of this de-aromatized product introduced two new central chiral centers to the molecule, as well as forming a new type of inherently chiral calixarene. The combination of inherent and multiple points of central chirality automatically complicates the situation with respect to assigning the absolute configuration of the product. In the report by Meyers and co-workers, they found the sequential addition of the nucleophile and subsequent electrophilic quench to take place exclusively in a *trans*-fashion.¹⁴ The formation of the two enantiomer products in their study was directed by the facial selectivity of the nucleophilic addition.

In the case of the calixarene, it is difficult to say for certain what was responsible for directing the addition. Arguments for both the central chirality on the oxazoline, or the calixarene's three-dimensional bowl shape could be made. Taking the distance of the chiral center from the point of addition into account, we suspected that it is more likely that the addition was directed by the shape of the calixarene. The nucleophile had the option of adding to either the front (from outside the bowl) or the back (from inside the bowl) of the planar aryl ring. The inside of the calixarene bowl was thought to present a more sterically hindered environment, and therefore the attack on the less hindered front would be more likely. If this was indeed the case, it would preferentially yield the diastereomer with the *tert*-butyl group facing outwards as the major product, and the opposite diastereomer with the thio-methyl facing outwards as the minor product (**Figure 3.5**).

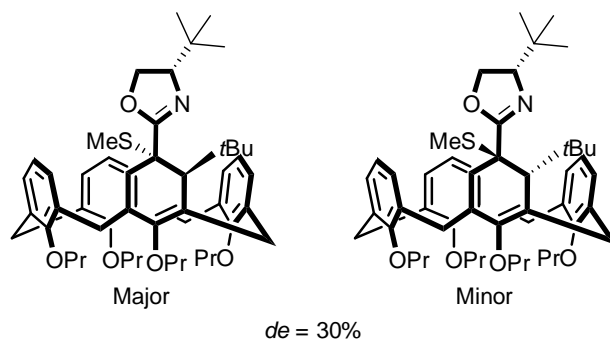


Figure 3.5: The proposed major (left) and minor (right) de-aromatized diastereomers.

Compound **69** presented with a complex ^1H NMR spectrum (**Figure 3.6**), indicating a mixture of diastereomers. Closer inspection revealed two signals for each of the three singlets representing the thio-methyl (δ 2.37 and δ 2.38 ppm, outlined in blue), two *tert*-butyl functional groups (δ 1.31 and δ 1.28 ppm, outlined in green) and (δ 0.99 and 0.96 ppm, outlined in purple) respectively. By comparing the areas of these three signals, the de for this reaction was found to be 30%.*

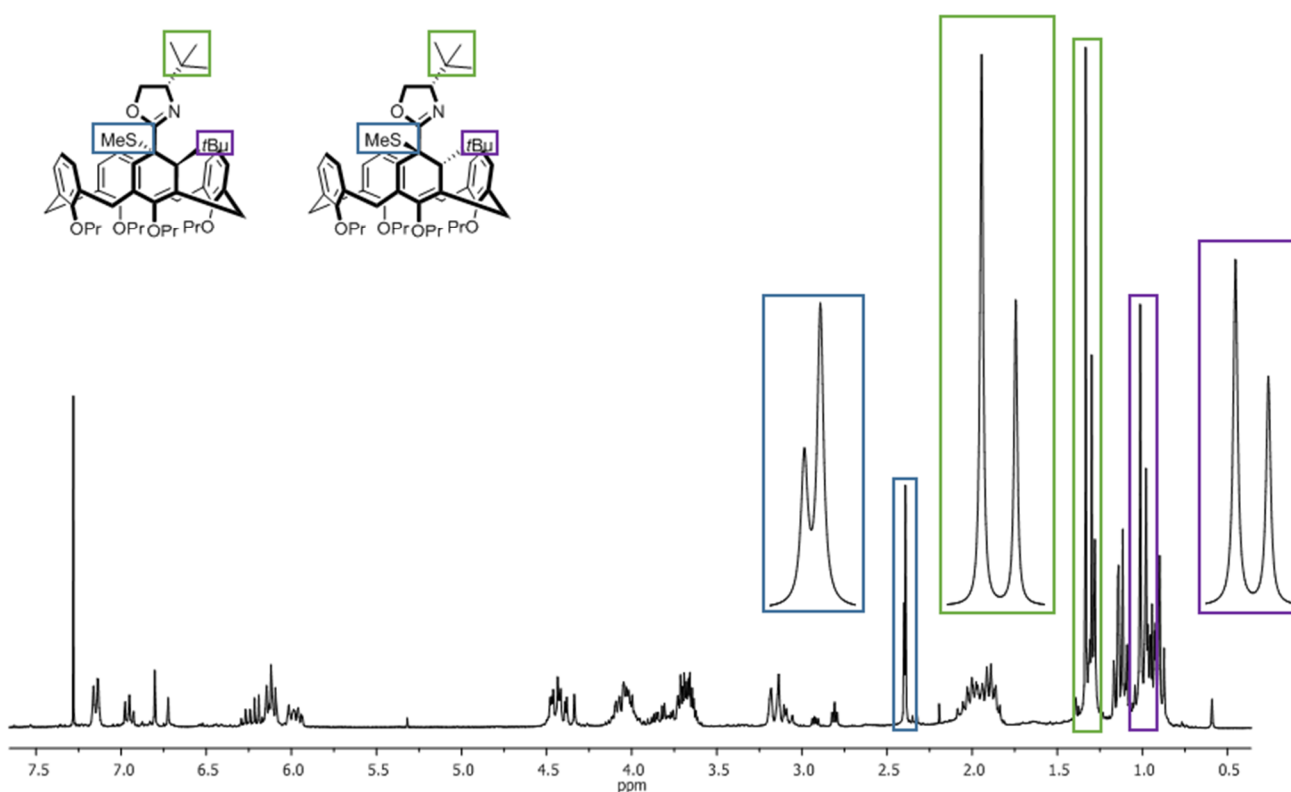


Figure 3.6: ^1H NMR spectrum of the mixture of thio-ether addition product **69** diastereomers. The thio-methyl signals are outlined in blue, the oxazoline *tert*-butyl signals in green and the calixarene *tert*-butyl signals in purple.

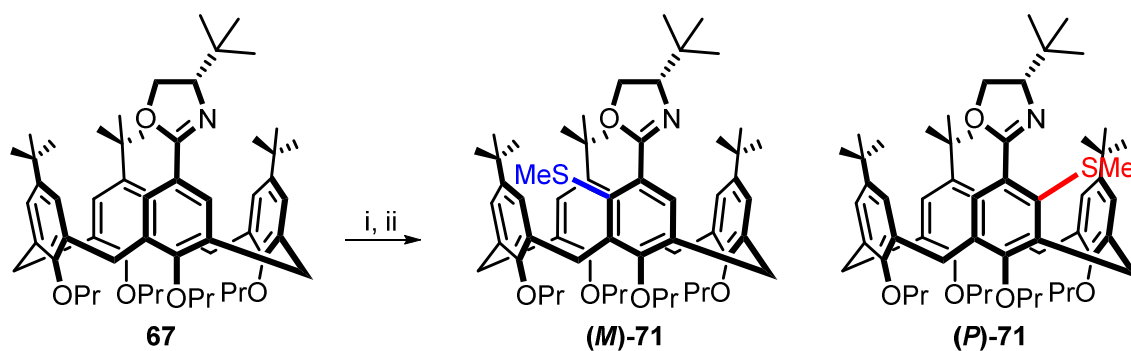
* The ^{13}C NMR spectrum was extremely complex. Not all of the signals for the two diastereomers were resolved, many overlapped and we attempted to assign a single set of signals for just the major compound.

Chapter 3: Ortholithiation of oxazoline calixarenes

A third product was also isolated from the reaction mixture. A full set of characterization data was collected for all three products. The combination of these analytical techniques conclusively confirmed the structures of the ketone **68** and de-aromatized products **69**. However, the structure of the third product **70** remained elusive. Perplexingly the NMR spectroscopic data point to the presence of certain functional groups but then the corresponding MS and IR data did not match these suggestions. Added to this disparity was the fact that the IR spectrum added little new information. Usually a characterisation problem occurs when the quality of the data is poor. This was not the case here and all of the data collected for **70** was for a single pure compound. This made the fact that the structure could not be determined all the more frustrating. Despite this, there were a few structural elements of this compound that were clear. Firstly, a *tert*-butyl functional group was definitely present, but there was a lack of evidence for both the ketone and oxazoline. The singlet (δ 7.53 ppm) which integrated for a single proton coupled to the fact that there were a total of 10 aromatic protons, suggested a product similar to the usual ortholithiated thio-ether, in the sense that it contained two functional groups on one of the aromatic rings. This singlet would correspond to the proton on the functionalized ring, with the remaining 9 protons present on the other three aryl rings. The lack of oxazoline signals, ketone and thio-methyl functionalities was confirmed by both the ^1H and ^{13}C NMR spectra, which only further complicated the assignment. The mass spectrum provided evidence of a single molecular ion with a mass of 722.42. The data has been reviewed and studied extensively, but unfortunately the structure of this compound remains a mystery and efforts towards elucidation of this structure are still underway.

3.4 The ortholithiation of *tert*-butyl oxazoline – 67.

Previously, compounds (**M**)-**71** and (**P**)-**71** were evaluated as potential bidentate S/N ligands in the asymmetric Tsuji-Trost reaction.³ They were unable to catalyze the reaction and in the study it was noted that soon after the addition of the ligands to the palladium catalyst, palladium black would precipitate from the solution. (**M**)-**71** had previously not been fully characterized, hindering the publication of these findings. Given their poor performance as ligands, they were not considered to be suitable candidates for further application studies and the two diastereomers were synthesized solely for the purpose of characterization (**Scheme 3.6**).



Scheme 3.6: Ortholithiation of calixarene **67**. Reagents and conditions: Calixarene (**M**)-**71**, *t*-BuLi (5.0 equiv), TMEDA (10.0 equiv), Et₂O, -78 °C, 48 h; ii) S₂Me₂ (excess), -78 °C to rt, 24 h. Calixarene (**P**)-**71**, *s*-BuLi (5.0 equiv), TMEDA (10.0 equiv), Et₂O, -78 °C, 48 h. ii) S₂Me₂ (exs), -78 °C to rt, 24 h.

The ortholithiation chemistry for the butylated *tert*-butyl oxazolines was almost identical to their non-alkylated counterparts. The same preparative and experimental procedures were required. The only major difference being the lithiation reaction time, a minimum of 48 h was necessary ensure a high yield. It has been speculated that the presence of the *tert*-butyl groups around the upper rim creates a sterically congested environment that hinders the approach of the lithium base. Interestingly, the alkylated thio-ether oxazoline compounds did not share an *R_f* value with the starting material. Even though the difference was slight, this enabled the separation of both diastereomers from the starting material by using a relatively non-polar mobile phase and slow separation. The purification of (**M**)-**71** was successful and was fully characterised by 1D and 2D NMR, IR, and mass spectrometry. This enabled the publication of the results from a previous application study carried out by the group. This was the first look at the use of oxazoline directed ortholithiation toward the synthesis and application of inherently chiral ligands.³

3.5 Discussion.

3.5.1 Introduction – the mechanism of ortholithiation.

The first examples of directed lithiation were independently reported by Wittig⁵ and Gilman⁴ in the late 1930s. They discovered that the metalation of anisole took place preferentially on the *ortho*-position. This discovery served as the foundation for a new field of aromatic substitution chemistry. Directed orthometalation has since developed into a popular and routinely used organic reaction. Even though it has been widely reported throughout the literature, a great deal of debate and disagreement still surrounds the finer details of the reaction mechanism. To date, a large body of work in this field has been generated. The focus of which can be subdivided into three categories; the role played by the solvent,^{16–19} ligand,^{20–23} and alkylolithium^{21,22} during the metalation process. Given the complex nature of even the simplest systems, these three parts tend to be investigated and reported individually.

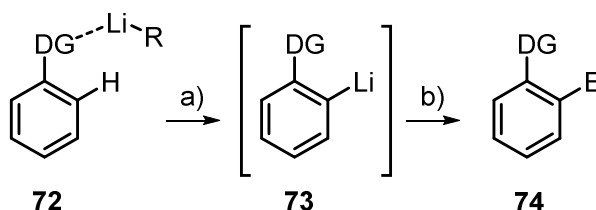
Chapter 3: Ortholithiation of oxazoline calixarenes

The ortholithiation mechanism has been the primary interest for a number of research groups worldwide. David Collum has reported a substantial body of work. His publications are widely cited and generally serve as good starting point when trying to explain new observations made in this field. Where applicable, the relevant findings in the literature will be applied to the studies carried out by the Arnott group, with the view to improving the understanding behind the reasons for these observations.

We lack the experimental depth to understand the finer points of the chemistry taking place during the calixarene lithiation process. To propose an overall ortholithiation reaction mechanism would not be the best approach. There are too many variables and irregularities within the study to make the proposal of a single mechanism realistic. We can, however, still postulate and suggest possible explanations for these results. Instead, drawing from the literature, the roles played by the solvent, ligand, and alkyllithium were assessed individually in the hopes of establishing a better understanding of the contributions made by each for these results. This discussion section can be sub-divided into four sections; what is currently known and generally accepted about the mechanism, followed by the contributions made by each of the three reaction components. The newly acquired results have been added to the initial study, and this collective will serve as the basis for this analysis. The ortholithiation study focused primarily on the isopropyl and *tert*-butyl oxazolines (**57** and **58**) and only these findings will be used for this discussion.

3.5.2 The general ortholithiation reaction mechanism.

In a comprehensive review on the subject, Snieckus described the directed *ortho*-metalation as a three-step sequence.²⁶ A simplified sequence of this process is depicted in **Scheme 3.7**. Firstly, the alkyllithium aggregate coordinates to a hetero-atom present on the directing group in compound **72**. This is followed by a deprotonation step (a) to yield the anionic ortholithiated intermediate **73**. The final step (b), is the reaction of this intermediate with an electrophile yielding the product **74**.



Scheme 3.7: The simplified stepwise ortholithiation sequence proposed by Snieckus.²⁶

At first glance this might come across as a simple, stepwise procedure but the mechanistic detail of each step is yet to be conclusively agreed upon. Even though this general Li sequence of coordination, deprotonation and quench is widely accepted, many conflicting mechanistic arguments and hypotheses have been proposed for the coordination and deprotonation steps, suggesting a great deal of mechanistic complexity. The two points most widely debated are the necessity for the formation of intermediate complexes before and/or during the rate limiting deprotonation step, as well as their potential structure.^{24,27,28}

Chapter 3: Ortholithiation of oxazoline calixarenes

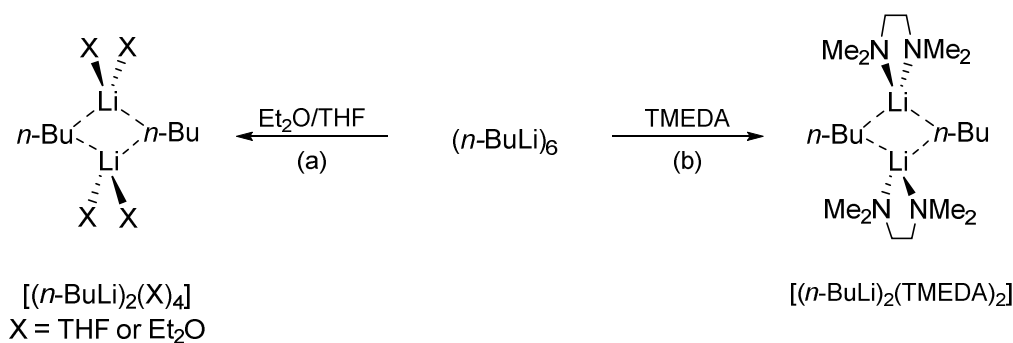
Secondly, there are some questions regarding the details behind why the *ortho*-protons, which are being abstracted, are activated.^{26,29,30} With regards to the first point, there are two opposing views being argued. One group claims that ortholithiation is a one-step reaction under strict kinetic control.^{24,28,31} A second group advocates a stepwise process known as the Roberts and Curtin mechanism,²⁷ in which an initial pre-lithiation complex is formed, followed by the rate-limiting intramolecular deprotonation. To begin a detailed comparative analysis of these two opposing views is a little above the aim of this discussion. The goal of proposing an accurate mechanism or model for the ortholithiation of the oxazoline calixarene already seems like a stretch. To understand how the diastereoselectivity for each of the alkyllithium/ligand mixtures is generated would require a detailed understanding of the co-ordination and proton abstraction processes. It is during this step that the ratio of lithiated intermediates are formed and currently the exact details behind even the simplest ortholithiation reactions are not agreed upon.^{26,32,33} On top of this, several publications have indicated that there could potentially be a number of independent lithiation mechanisms dependent on the nature of the substrate, base, solvent and ligands used.^{31,34,35} Instead, the aim of this discussion is shifted towards relating what is known about this reaction, specifically with respect to the roles played by the solvent, additive/ligand, and finally the choice of alkyllithium. Specifically focusing on how these three factors have contributed to the results obtained here.

3.5.3 The ligand – impacting the activation and aggregation of alkyllithiums.

The choice of additive was found to be essential for the successful ortholithiation of calixarenes in good yields and with high diastereoselectivity. The two ligands that were key to this study were TMEDA and di-*t*Bu-diglyme. Without the presence of any additive (**Table 3.2**, entries 15-18), generally negligible product yields or low selectivities were obtained. The presence of TMEDA thus played a key role towards steric induction during these reactions. TMEDA's behavior as a coordinating ligand during ortholithiation reactions has been extensively studied by David Collum.^{23,33,36,37} The use of TMEDA is almost ubiquitous throughout the lithiation literature, and has found application in many *ortho*-directed lithiation studies on a wide range of substrates, with varied directing groups. The book, *Organolithiums: Selectivity for Synthesis*, by Clayden outlines the scope of this chemistry and reports many of these commonly used directing groups and additives.³⁸ Collum's research has primarily focused on dissecting the ortholithiation reaction piece by piece in an attempt to understand finer details of the mechanism. An aspect that has received a substantial amount of attention by many researchers is the ability of coordinating ligands to change the aggregation states of alkyllithiums in solution, which in turn, effects the way they take part in the reaction.^{16,20,24,25,39} When thinking about how a lithium base approaches the substrate, it is easy to assume that a single molecule of the alkyllithium, as it is drawn, is taking part in the reaction. However, this is not the case, and alkyllithium reagents are known to exist in several aggregation states.

Chapter 3: Ortholithiation of oxazoline calixarenes

This aggregation state is not dependent on the steric properties of the base itself, or the solvent it is stored in, but can be manipulated and controlled with the use of coordinating ligands such as TMEDA. An example of this behavior is represented in **Scheme 3.8**.^{23,33}



Scheme 3.8: The de-aggregation of hexameric *n*-BuLi to solvated dimers in the presence of donor solvents/ligands.^{23,33}

In the presence of coordinating ligands, the aggregation states of the lithium bases are usually lowered. Both (a) and (b) in **Scheme 3.8** represent the same de-aggregation process, i.e. the ability of compounds with donor capabilities to form the lower monomer, dimer and tetramer aggregates from their corresponding higher aggregate states in non-donor environments. It has been proposed that these lower aggregates are more reactive and could also be responsible for generating the selectivity seen for oxazoline-directed metalations.²⁰ This was not only true for the oxazoline calixarenes,^{1,2} and the same was found for the metalation of ferrocene oxazolines.⁸ Even though TMEDA is a widely used ligand in alkyllithium chemistry, many other donor ligands have been established as effective additives.³⁸ The example above demonstrates the de-aggregation of *n*-BuLi in the presence of different donor ligands. It exists as a hexamer aggregate in a non-donating hydrocarbon solution, but in the presence of donor ligands a solvated dimer-aggregate is preferred. Similar behavior has been found for all of the major alkyllithium bases and their behavior in non-donor hydrocarbon as well as donor solvents has been extensively investigated.

Considering the experimental care that is required during the synthesis and use of alkyllithium compounds, detailed analysis of their properties is understandably challenging. So far the investigation of their structural and reactive properties has been limited to inert low temperature NMR spectroscopy, IR spectroscopy, X-ray diffraction and computational calculations. Unlike *n*-BuLi,⁴⁰ the behavior of *s*-BuLi and *t*-BuLi is a little more complex. When coordinated to TMEDA, *s*-BuLi remains a tetramer in hydrocarbon solvents, but the aggregation lowers to a dimer in the presence of THF and Et₂O.³⁸ *t*-BuLi exists as a tetramer in hydrocarbon solvents and as a dimer in Et₂O, but in the presence of THF, it exists as a temperature dependent mixture between a monomer and dimer aggregates.⁴¹

Chapter 3: Ortholithiation of oxazoline calixarenes

The function of TMEDA during the ortholithiation of the calixarenes is two-fold; not only does it act as a donor ligand to form the more reactive lower aggregate states, it also seems to play a unique role in generating the selectivity of these reactions for each of the alkyllithiums. It is not simply any lower aggregate combination of donor/base that yields ortholithiated products in enriched diastereomeric ratios.

The role played by TMEDA was found to be unique, a number of other additives were investigated by Herbert, the majority of which gave results much poorer in terms of both product yields and selectivities, when compared to TMEDA. Et₂O is has also been established as a suitable donor for alkyllithiums, yet when used in place of TMEDA, ortholithiation took place with little to no selectivity (**Table 3.2**, entry 15). Another interesting observation was that the highest selectivities obtained for the four oxazoline calixarenes made use of three different TMEDA/alkyllithium combinations. Both *tert*-butyl oxazolines required the *s*-BuLi/TMEDA mixture, whereas isopropyl calixarenes **57** and **66** required the use of *c*-PentLi/TMEDA and *n*-BuLi/TMEDA mixtures respectively (**Table 3.2**, entries 1 and 4).

TMEDA was not the only successful additive found for this chemistry, since a significant library of alkyllithium additives have been established over the years, including HMPA, PMPTA, DMPU and TBME.³⁸ These are only a scant few, and recently a new ligand was reported by the Arnott group.⁸ The bulky diglyme-based ligand (di-*t*Bu-diglyme) was not only a suitable ligand, it was able to effectively switch the selectivity when used instead of TMEDA, for calixarene **57** only, and yielded the opposing diastereomer (**M**)-**50** in a 95% yield and *de* of 78% (**Table 3.2**, entries 11-14). These results suggest a directly proportional correlation between the selectivity and the steric bulk of the ligand. As the bulk of the ligand increased, the *de* of the reaction improved from 0% to 78%. Perplexingly, the diglyme ligands showed very little success with the *tert*-butyl oxazolines in terms of both reactivity and their ability towards asymmetric induction. The yields for these reactions did not exceed 40% and they were unable switch the selectivity of the analogous TMEDA reactions. The electronic and structural difference between the isopropyl **57** and *tert*-butyl oxazoline **58** calixarenes is arguably small, almost negligible, so why the completely different results?

These points lend support to the previously mentioned suggestions of substrate-dependent mechanisms. When trying to determine the source of chiral induction, a steric explanation is often first considered. If one compares the results for the same alkyllithium/TMEDA mixtures over the two calixarenes, none of the results correlate well with each other, i.e. the selectivities and conversions vary considerably when the same alkyllithium/TMEDA mixtures are used. Surely, if the same reaction mechanism was taking place, and the only difference between the substrates was the steric clash of the two oxazoline R-groups, these numbers would be comparable? As it stands, all evidence provided by the different effects of the ligands in these reactions point to a number of different reaction mechanisms.

Chapter 3: Ortholithiation of oxazoline calixarenes

3.5.4 The alkylolithium – the influence of reactivity and steric hindrance.

When considering the influence of the bulk of the oxazoline-directing group on the reaction mechanism, there was only a small difference between the isopropyl and *tert*-butyl groups to compare. On the other hand, the steric properties of all the different alkylolithiums used in the study covered a much wider range, creating sizable pool of data from which to work.

It was hoped that we could somehow correlate the selectivity of these reactions with the steric properties of each of the alkylolithiums. Without a kinetic and computational study behind each result there was little else left to consider. Before the influence of steric strain could be determined, a vital concern was the accurate quantification and measurement of steric bulk. A recent paper, published by Sigman and co-workers in 2012 reviewed a number of widely used classic and modern steric parameters, all of which are used to measure the steric properties for several different classes of compounds.⁴² Rather than review each of these, only those relevant to this study will be discussed. One of the earliest examples is the Taft parameter. Taft attempted to define the steric properties of different reagents in such a way that they remained unaffected by any additional electronic and inductive effects that were present on the molecule. To do so, he determined the rates of ester hydrolysis for a range of different OR groups.⁴³ Using these rate values as a basis, he calculated a numerical measurement for each of the varying R-groups. Taft hypothesized that “under acid catalyzed conditions, the preservation of charge through a rate-determining step would diminish any inductive or resonance electronic distributions from the R-substituents. Thus, any variation in the rate of hydrolysis would be proportional to the steric repulsion of the approaching nucleophile.”⁴²

Following these results, Charton made use of Taft’s findings to establish a refined set of steric measurements. Taking the experimental values determined by Taft, Charton was able to correlate the experimental results with the van der Waals radii of each R-group. In so doing, a new set of values was established, which was supported by both experimental and computational evidence.⁴⁴

The majority of this study was carried out using almost exclusively one ligand (TMEDA), and only two solvents (pentane and Et₂O). What varied most was the steric properties of the alkylolithiums. One of the most interesting aspects of this chemistry was the degree to which the selectivities and yields varied over the range of alkylolithiums. Besides their differences in basicity and reactivity, the most notable discrepancy was their difference in structure. Earlier, the various aggregation states of alkylolithiums in the presence of different solvents and/or donor ligands, was discussed. Given that these solvated coordination structures have been proposed as the reactive components for the lithiation reaction, it became important to consider how the steric properties of the aggregates related to the steric parameters assigned to the R-group. Given the lack of literature for this question, there was no way to conclude whether or not the steric parameters for the individual R-groups would be consistent over the alkylolithiums varied states of aggregation.

Chapter 3: Ortholithiation of oxazoline calixarenes

For example: the steric bulk of the *n*-butyl R-group in the $[(n\text{-BuLi})_2(\text{TMEDA})_2]$ dimer might be completely different to the *n*-butyl functional group on its own. Unfortunately, there was no way to correlate or correct these parameters with the structural properties of the aggregates, and it had to be assumed that these measurements would remain generally constant.

The results for all of the reported ortholithiations of **57** were pooled, and the Charton values for each of the alkyllithiums was plotted against the corresponding selectivity (**Figure 3.7**). As a means to provide an improved and refined representation of the selectivity of these reactions, the Gibbs free energy for the distribution of the lithiated diastereomer intermediates was calculated using the Boltzmann distribution equation ($\Delta\Delta G^\ddagger = -RT\ln K$). In so doing, the selectivities for these reactions could be represented as an energy value, rather than a product ratio. The calculated energy values created the potential of establishing a linear free energy relationship between the observed selectivity of these reactions and the steric bulk of the lithium base.

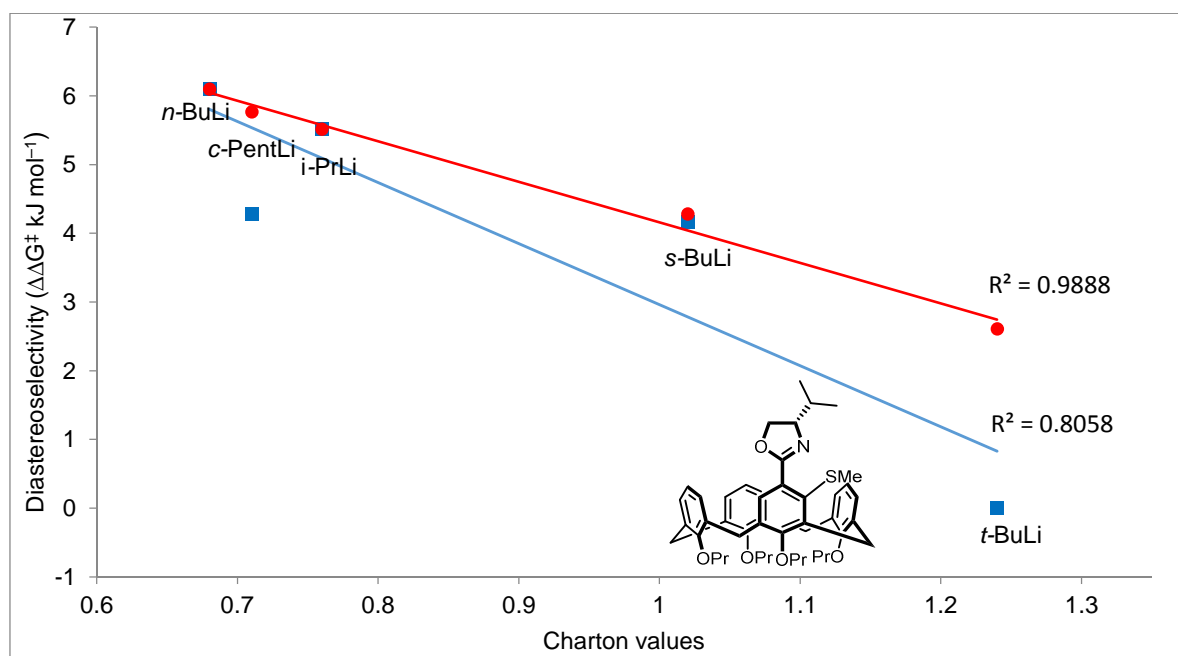


Figure 3.7: The Gibbs free energy (selectivity) vs Charton values (alkyllithium) for the ortholithiation of **57** in pentane (red) and Et₂O (blue).

The two data sets (red and blue) plotted for **57** represent the selectivities of the reaction in pentane and Et₂O respectively. Interestingly, the selectivities over the two solvents were generally comparable, with *t*-BuLi being the only discrepancy. Originally, the results for *c*-PentLi in pentane and Et₂O also differed considerably. The selectivity in Et₂O was first reported as being significantly lower than that of pentane. For the majority of the alkyllithiums, the selectivities in Et₂O were only marginally lower. To verify this, the experiment was carried out again (**Table 3.3**, entry 5). The selectivity was found to be much closer to the result obtained in pentane, than was originally reported.

Chapter 3: Ortholithiation of oxazoline calixarenes

This suggested that the same had occurred for *t*-BuLi, so this experiment was also repeated (Table 3.3, entry 6). In this case the repeated experiment matched the result of original study. Generally, for the reactions performed in both solvents, there was a clear and gradual linear decrease in the selectivity as the steric bulk of the alkyllithium increased. This was an interesting observation, as the general trend seen for chiral induction in asymmetric reactions is often the opposite.

Usually, an increase in steric bulk is used to further push the chiral induction in asymmetric reactions towards an increase in selectivity. A possible explanation for these observations is simply the kinetic difference between reaction rates of the different aggregates. Higher reaction rates would result in poorer kinetic control. Alternatively, it could be that each of the alkyllithium aggregates possess an independent reaction mechanism. Not knowing whether or not the mechanism is substrate or alkyllithium dependent only further complicates the matter. The Gibbs free energy for the selectivities for the ortholithiation of **58** were also calculated and plotted against the Charton values corresponding to each of the alkyllithiums used in the study (Figure 3.8)[†]

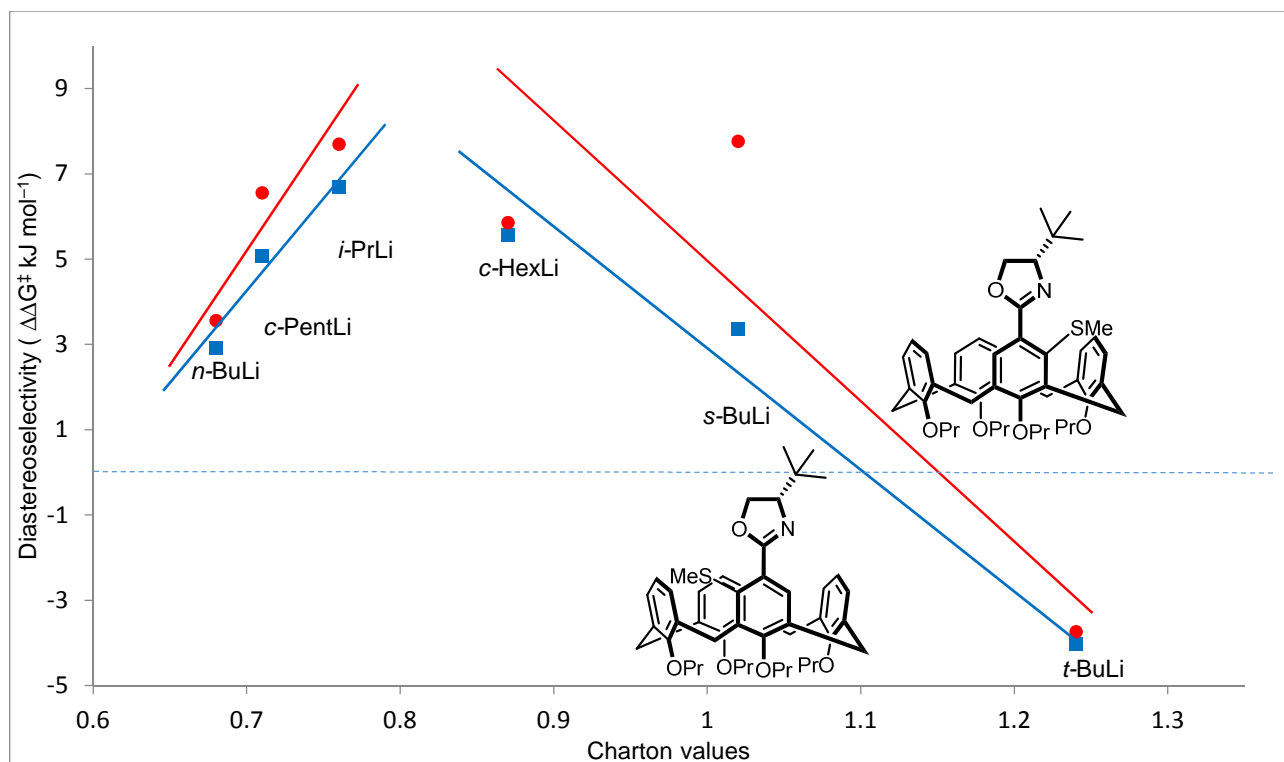


Figure 3.8: The Gibbs free energy (selectivity) vs Charton values (alkyllithium) for the ortholithiation of **58** in pentane (red) and Et₂O (blue).

[†]The straight lines depicted on this graph were not actual trend lines, but rather rough approximations of what appeared to be two potential separate linear trends.

Chapter 3: Ortholithiation of oxazoline calixarenes

Unlike the data for **57**, there was no linear trend for the selectivity of these reactions when performed in either Et₂O or pentane. Again, the selectivities between the two solvents were similar. However, the difference between almost all of the plotted points was greater in comparison to **57**. The linear trend in **Figure 3.7** indicates that a linear free energy relationship exists between the steric bulk of the alkyllithium and the asymmetric induction seen for these reactions, which could be considered evidence for a single substrate dependent mechanism. It could be that the reaction mechanism for the ortholithiation of **57**, over all of the alkyllithiums, was the same, and the differences in the steric properties of the alkyllithium aggregates were responsible for the varied results.

However, the ortholithiation of **58** suggested something completely different. Firstly, the selectivity increases from *n*-BuLi to *i*-PrLi (an increase in steric bulk) and the opposite is seen for **57**. When the steric bulk increased from *c*-PentLi to *t*-BuLi the selectivity dropped significantly (the *s*-BuLi/Pentane TMEDA being the exception), even to the point of investing the selectivity entirely with *t*-BuLi. Previously, *c*-HexLi hadn't been investigated and these results (**Table 3.4**, entries 5 and 7) were also added to the existing data set. Considering the large differences between the selectivities observed for *s*-BuLi in pentane and Et₂O, these experiments were also repeated. The same was carried out for *c*-PentLi. These repeated results (**Table 3.4**, entries 1, 3 and 9) agreed with past results confirming the generally larger differences in the selectivities between pentane and Et₂O.

This could be indicative of at least two different reaction mechanisms determined by the steric properties of the alkyllithiums. The first is selective for the formation of diastereomer (**P**)-**50**, but only for alkyllithiums within a specific steric range. When the bulk of the alkyllithium exceeds this range, a different reaction mechanism is favoured, one which is selective for diastereomer (**M**)-**50**. One of the most confusing results was the inversion of selectivity when *t*-BuLi was used (**Table 3.4**, entry 8). The results between pentane and Et₂O varied to the point where it was considered that all of the speculation regarding a single or multiple reaction mechanism(s) could be completely incorrect. Instead, every aggregate could have had a unique mode of action depending on both the substrate and the solvent. The fact that there was a shift from a *de* of >99% to the opposing 80%, simply by changing the alkyllithium from *s*-BuLi to *t*-BuLi suggests completely different reaction mechanisms taking place.

The behavior of the two oxazolines was significantly different over a uniform set of reaction conditions. For example, *s*-BuLi gave the highest selectivity for **58** and a relatively low selectivity for **57**. This is just a single example and overall there were far more differences than similarities when comparing these results. Overall, it would be safe to put forward that there are multiple lithiation mechanisms at play, dependent on the nature of the substrate, solvent, ligand, and alkyllithium. The lack of a detailed speciation, kinetic and computational study for every set of reaction conditions, leaves room for little more than speculation.

Chapter 3: Ortholithiation of oxazoline calixarenes

3.5.5 The impact of solvent choice.

As discussed previously, the behavior of the different alkyllithium bases in different solvents alone is at times varied and complex. The subtlety behind the choice of solvent in a reaction often goes unnoticed, but for the ortholithiation reaction it was found to play a significant role. Generally speaking, donor solvents formed alkyllithium mixtures with lower aggregation states. Several different solvents were tested by Herbert, with THF, Et₂O and pentane being the three most popular.

Like Et₂O, THF is known to function as an efficient ligand for alkyllithium bases,⁴⁵ but all of the reactions carried out in THF yielded poor selectivities for all four oxazolines (**Table 3.2**, entries 16-18) and unlike TMEDA it was unable to yield either of the diastereomers in a high selectivity.

Across all four oxazoline substrates, the use of pentane and Et₂O formed the large bulk of the study. A general increase in the reaction rate was noted when pure Et₂O was used for all of the oxazoline compounds. The selectivities were often slightly lower in Et₂O for the isopropyl oxazoline and even more so for *tert*-butyl oxazoline. This observation fit with the model of kinetic control originally proposed by Herbert. A similar finding was noted in his related study on the oxazoline directed asymmetric synthesis of planar chiral ferrocenes.⁸

Differences in the results for the non-donating pentane and the donating Et₂O indicated that Et₂O was able to compete with TMEDA for coordination to the alkyllithium. The lower selectivities observed in Et₂O could be a combination of the increased reaction rate, as well as structural differences between the solvated [(*n*-BuLi)₂(Et₂O)₄]₂ and [(*n*-BuLi)₂(TMEDA)₂]₂ dimers. An interesting observation was noted when the reactions were performed in a mixture of pentane and Et₂O, i.e. if the solvent from the alkyllithium was not removed before it was added to the reaction mixture. In all of these cases the selectivity matched the selectivity when pure pentane was used. This suggested that for the Et₂O to compete with TMEDA for coordination, none or perhaps minimal amounts of the pentane could be present. The most interesting difference in the reactivity between Et₂O and pentane was the formation of the addition products (**68**, **69** and **70**) for **58**. The same reaction conditions were replicated for **57** (**Table 3.3**, entry 6) to see if the isopropyl oxazoline functional group, and calixarene would undergo the addition and de-aromatization reactions. This was not the case and the same result reported previously, a racemic mixture of diastereomers, was obtained.

The collected data from all three parameters strongly points to multiple ortholithiation mechanisms. The solvent effect can be easily overlooked, as the two solvents generally gave similar results, but then again the formation of the addition products, coupled with the discrepancies between the several of the alkyllithiums for **58**, and *t*-BuLi for **57** suggests otherwise.

3.6 Conclusion.

The results reported for this ortholithiation chemistry do contain irregularities, which are difficult to rationalize without additional information. The mechanistic study of ortholithiation mechanisms is an extremely challenging area of research. Besides the theoretical intricacies and experimental difficulties, a broad application of disciplines is required to fully grasp the detail behind this chemical process. The first step towards unravelling these complexities is a speciation study aimed at identifying all potential intermediates involved over the course of the reaction. This would require the use of inert and low temperature IR and NMR spectroscopic analysis of these reactions. Once a number of intermediates have been identified, individual kinetic studies would be needed to determine their respective rates of formation and subsequent reactivity. Finally, the results of the kinetic and speciation studies would have to be scrutinized computationally. The combination of all of this data would then be used to formulate a potential reaction mechanism.

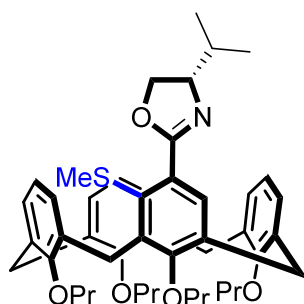
A large body of literature was reviewed with the aim finding an explanation for these results. During this process, it was quickly realized that not only was the theoretical detail of this chemistry daunting and challenging to understand, but most of the conclusions surrounding this chemistry are uncertain. There are often conflicts in the data and there is still a lack of consensus for even the simplest metalation systems. Even though the finer details of this chemistry remain elusive, the methods reported here are a powerful and useful synthetic tool. The chemistry reported by Dr. S. Herbert has provided the first synthetic route toward inherently chiral calixarenes, without the necessity of chemical resolution. From a practical perspective, the chemistry itself requires little further development, but there is still substantial scope for further methodology studies.

3.7 Experimental section.

3.7.1 General ortholithiation procedure.

The alkyllithium was added to an oven dried Schlenk tube under argon at room temperature and cooled (0 °C). The excess solvent was then removed under reduced pressure. The reaction solvent was then added to the alkyllithium and the solution was cooled (-78 °C). The ligand was then added and the reaction mixture was stirred for 15-30 min. The calixarene was then dissolved in dry solvent and carefully added last, dropwise, to the cooled alkyllithium/ligand mixture. Shortly after, a yellow/orange precipitate would form. If this precipitate disappeared before the electrophile was added, it almost certainly meant that the reaction was quenched. The mixture was stirred for either 24 or 72 h, at -78 °C, following which the electrophile was added. The reaction mixture was then given time to warm to room temperature overnight, and was finally quenched with 1M HCl at room temperature. The product was extracted with either EtOAc or DCM and washed with 1M HCl and brine. Finally, after drying the organic layer over MgSO₄, the excess solvent was removed under reduced pressure.

3.7.2 (*M*)-5-((*S*)-4-Isopropyl-4,5-dihydrooxazol-2-yl)-4-methylthio-25,26,27,28-tetrapropoxycalix[4]arene – **49**.⁸



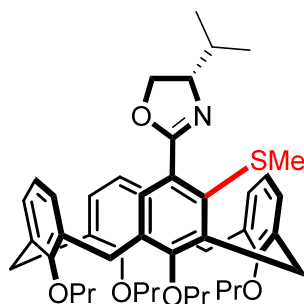
Calixarene (**M**)-**49** was synthesized according to the general ortholithiation procedure. Oxazoline calixarene **57** (20.0 mg, 0.0280 mmol), *s*-BuLi (0.141 mmol, 5.0 equiv), di-*t*Bu-diglyme (0.0620 ml, 0.280 mmol, 10.0 equiv), pentane (0.5 ml) and dimethyl disulfide (0.0500 ml, exs) with a reaction time of 7 h. The product was purified via filtration through a silica plug. The di-*t*Bu-diglyme was removed by heating the product to 60 °C under high vacuum for 48 h. (Conversion: 95%, *de*: 80%).

The characterisation data collected for this compound compared well with the reported literature values.⁸

Chapter 3: Ortholithiation of oxazoline calixarenes

^1H NMR (300 MHz, CHLOROFORM-*d*) δ 0.85-0.92 (m, 6H, $\text{OCH}_2\text{CH}_2\text{CH}_3$), 1.03 (d, $J = 6.7$ Hz, 3H, $\text{CH}(\text{CH}_3)_2$), 1.06-1.14 (m, 9H, CH_2CH_3 , $\text{CH}(\text{CH}_3)_2$), 1.81-2.02 (m, 9H, $\text{OCH}_2\text{CH}_2\text{CH}_3$, $\text{CH}(\text{CH}_3)_2$), 2.41 (s, 3H, SCH_3), 3.10-3.19 (m, 3H, $\text{ArCH}_2^{\text{eq}}\text{Ar}$), 3.61-3.75 (m, 4H, $\text{OCH}_2\text{CH}_2\text{CH}_3$), 3.95-4.06 (m, 4H, $\text{OCH}_2\text{CH}_2\text{CH}_3$), 4.14-4.24 (m, 2H, $\text{ArCH}_2^{\text{ax}}\text{Ar}$, OCH_2CHN), 4.29-4.33 (m, 2H, OCH_2CHN), 4.36-4.50 (m, 4H, $\text{ArCH}_2^{\text{ax}}\text{Ar}$), 5.98 (d, $J = 7.3$ Hz, 1H, ArH), 6.04 (d, $J = 7.3$ Hz, 1H, ArH), 6.08-6.18 (m, 3H, ArH), 6.22 (d, $J = 7.3$ Hz, 1H, ArH), 6.91 (t, $J = 7.3$ Hz, 1H, ArH), 7.10 (d, $J = 7.4$ Hz, 2H, ArH), 7.32 (s, 1H, ArH) ppm.

3.7.3 (*P*)-5-((*S*)-4-Isopropyl-4,5-dihydrooxazol-2-yl)-4-methylthio-25,26,27,28-tetrapropoxycalix[4]arene – **49**.⁸

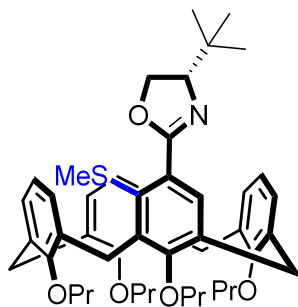


Calixarene (**P**)-**49** was synthesized according to the general ortholithiation procedure. Oxazoline calixarene **57** (20.0 mg, 0.028 mmol), *c*-PentLi (0.141 mmol, 5.0 equiv), TMEDA (0.0440 ml, 0.280 mmol, 10.0 equiv), pentane (0.5 ml) and dimethyl disulfide (0.05 ml, exs) with a reaction time of 7 h. The product was purified via filtration through a silica plug. (Conversion: 98%, *de*: 94%).

The characterisation data collected for this compound compared well with the reported literature values.⁸

^1H NMR (300 MHz, CHLOROFORM-*d*) δ 0.85-0.92 (m, 6H, $\text{OCH}_2\text{CH}_2\text{CH}_3$), 1.03 (d, $J = 6.7$ Hz, 3H, $\text{CH}(\text{CH}_3)_2$), 1.06-1.14 (m, 9H, $\text{OCH}_2\text{CH}_2\text{CH}_3$, $\text{CH}(\text{CH}_3)_2$), 1.81-2.02 (m, 9H, $\text{OCH}_2\text{CH}_2\text{CH}_3$, $\text{CH}(\text{CH}_3)_2$), 2.41 (s, 3H, SCH_3), 3.10-3.19 (m, 3H, $\text{ArCH}_2^{\text{eq}}\text{Ar}$), 3.61-3.75 (m, 4H, $\text{OCH}_2\text{CH}_2\text{CH}_3$), 3.95-4.06 (m, 4H, $\text{OCH}_2\text{CH}_2\text{CH}_3$), 4.14-4.24 (m, 2H, ArCH_2Ar , OCH_2CHN), 4.29-4.33 (m, 2H, OCH_2CHN), 4.36-4.50 (m, 4H, ArCH_2Ar), 5.98 (d, $J = 7.3$ Hz, 1H, ArH), 6.04 (d, $J = 7.3$ Hz, 1H, ArH), 6.08-6.18 (m, 3H, ArH), 6.22 (d, $J = 7.3$ Hz, 1H, ArH), 6.91 (t, $J = 7.3$ Hz, 1H, ArH), 7.10 (d, $J = 7.4$ Hz, 2H, ArH), 7.35 (s, 1H, ArH) ppm.

Chapter 3: Ortholithiation of oxazoline calixarenes

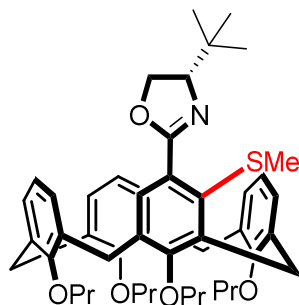
3.7.4 (M)-5-((S)-4-tert-butyl-4,5-dihydrooxazol-2-yl)-4-methylthio-25,26,27,28-tetrapropoxycalix[4]arene – **50**.³

Calixarene (**M**)-**50** was synthesized according to the general ortholithiation procedure. Oxazoline calixarene **58** (80.0 mg, 0.0900 mmol), *t*-BuLi (0.451 mmol, 5.0 equiv), TMEDA (0.170 ml, 0.900 mmol, 10.0 equiv), pentane (2 ml) and dimethyl disulfide (0.20 ml, exs) with a reaction time of 24 h. Purification was achieved via silica gel column chromatography (EtOAc:PET, 2:98) yielding a white solid (71.0 mg, 83%, *de*: 82%). $R_f = 0.52$ (EtOAc:PET, 10:90).

The characterisation data collected for this compound compared well with the reported literature values.³

(300 MHz, CHLOROFORM-*d*) δ 0.84-0.91 (m, 6H, OCH₂CH₂CH₃), 1.06 (s, 9H, C(CH₃)₃), 1.07-1.12 (m, 6H, OCH₂CH₂CH₃), 1.82-1.98 (m, 8H, OCH₂CH₂CH₃), 2.41 (s, 3H, SCH₃), 3.12-3.18 (m, 3H, ArCH₂^{eq}Ar), 3.63-3.74 (m, 5H, ArCH₂^{eq}Ar, OCH₂CH₂CH₃), 3.96-4.04 (m, 4H, OCH₂CH₂CH₃), 4.13 (dd, *J* = 10.1, 8.3 Hz, 1H, OCH₂CHN), 4.25-4.31 (m, 2H, OCH₂CHN), 4.38-4.46 (m, 4H, ArCH₂^{ax}Ar), 5.98 (dd, *J* = 7.3, 1.3 Hz, 1H, ArH), 6.05 (dd, *J* = 7.5, 1.3 Hz, 1H, ArH), 6.10-6.20 (m, 3H, ArH), 6.23 (t, *J* = 7.4 Hz, 1H, ArH), 6.91 (t, *J* = 7.5 Hz, 1H, ArH), 7.09 (d, *J* = 7.5 Hz, 2H, ArH), 7.31 (s, 1H, ArH) ppm.

Chapter 3: Ortholithiation of oxazoline calixarenes

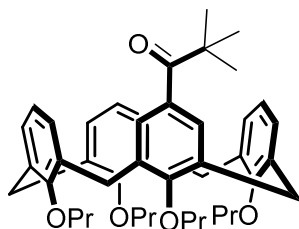
3.7.5 (P)-5-((S)-4-tert-butyl-4,5-dihydrooxazol-2-yl)-4-methylthio-25,26,27,28-tetrapropoxycalix[4]arene – **50**.³

Calixarene (**P**)-**50** was synthesised according to the general procedure. Oxazoline calixarene **58** (20.0 mg, 0.0230 mmol), *c*-HexLi (0.115 mmol, 5.0 equiv), TMEDA (0.0400 ml, 0.230 mmol, 10 equiv), Et₂O (0.5 ml) and dimethyl disulfide (1.0 mmol, excess) with a reaction time of 24 h (Conversion: 97%, *de*: 94%). *R_f* = 0.52 (EtOAc:PET, 10:90).

The characterisation data collected for this compound compared well with the reported literature values.³

¹H NMR (400 MHz, CHLOROFORM-*d*) δ 0.87 (t, *J* = 7.4 Hz, 3H, OCH₂CH₂CH₃), 0.88 (t, *J* = 7.4 Hz, 3H, OCH₂CH₂CH₃), 1.06 (s, 9H, C(CH₃)₃), 1.07-1.12 (m, 6H, OCH₂CH₂CH₃), 1.81-2.02 (m, 8H, OCH₂CH₂CH₃), 2.42 (s, 3H, SCH₃), 3.12-3.22 (m, 3H, ArCH₂^{eq}Ar), 3.62-3.78 (m, 5H, ArCH₂^{eq}Ar, OCH₂CH₂CH₃), 4.01 (m, 4H, OCH₂CH₂CH₃), 4.13 (dd, *J* = 10.2, 8.2 Hz, 1H, OCH₂CHN), 4.29-4.35 (m, 2H, OCH₂CHN), 4.39-4.50 (m, 4H, ArCH₂^{ax}Ar), 5.97 (dd, *J* = 7.4, 1.4 Hz, 1H, ArH), 6.06 (dd, *J* = 7.7, 1.4 Hz, 1H, ArH), 6.10-6.19 (m, 3H, ArH), 6.24 (t, *J* = 7.6, 1H, ArH), 6.92 (t, *J* = 7.6, 1H, ArH), 7.11 (d, *J* = 7.4 Hz, 2H, ArH), 7.34 (s, 1 H, ArH) ppm.

Chapter 3: Ortholithiation of oxazoline calixarenes

3.7.6 5-(2,2-dimethylpropanone)-25,26,27,28-tetrapropoxycalix[4]arene – **68**.

Calixarene **68**, **70** and a third unidentified calixarene compound **70** were synthesized according to the general ortholithiation procedure (The pentane from the *t*-BuLi was removed). Oxazoline calixarene **58** (243 mg, 0.338 mmol), *t*-BuLi (1.70 mmol, 5.0 equiv), TMEDA (0.500 ml, 3.38 mmol, 10.0 equiv), Et₂O (2.3 ml) and dimethyl disulfide (0.05 ml, exs) with a reaction time of 24 hours. The products were purified using silica gel column chromatography (EtOAc: PET, 1:99) yielding white solids; **68** (97.0 mg, 41%), **69** (75.0 mg, 27%), and the unknown **70** (24.0 mg).

¹H NMR (300 MHz, CHLOROFORM-*d*) δ 0.97 (t, *J* = 7.5 Hz, 6H, OCH₂CH₂CH₃), 1.04 (t, *J* = 7.4 Hz, 3H, OCH₂CH₂CH₃), 1.06 (t, *J* = 7.4 Hz, 3H, OCH₂CH₂CH₃), 1.11 (s, 9H, C(CH₃)₃), 1.85-2.03 (m, 8H, OCH₂CH₂CH₃), 3.15 (d, *J* = 13.2 Hz, 2H, ArCH₂^{eq}Ar), 3.17 (d, *J* = 13.2 Hz, 2H, ArCH₂^{eq}Ar), 3.75-3.98 (m, 8H, OCH₂CH₂CH₃), 4.44 (d, *J* = 13.2 Hz, 2H, ArCH₂^{ax}Ar), 4.46 (d, *J* = 13.2 Hz, 2H, ArCH₂^{ax}Ar), 6.33-6.38 (m, 1H, ArH), 6.42-6.44 (m, 2H, ArH), 6.69-6.74 (m, 2H, ArH), 6.80-6.83 (m, 3H, ArH), 7.02 (br s, 2H, ArH) ppm.

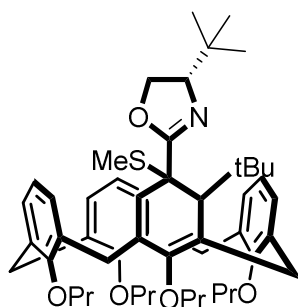
¹³C NMR (75 MHz, CHLOROFORM-*d*) δ 10.3, 10.6, 10.7, 23.3, 23.5, 23.6, 28.5, 31.1, 31.2, 43.8, 76.8, 77.1, 77.2, 122.2, 122.3, 128.0, 128.5, 128.9, 129.3, 131.1, 134.2, 134.6, 136.0, 156.0, 157.0, 159.1, 207.0 ppm.

IR (ATR) cm⁻¹: 2965 (m, -CH), 2876 (s, -CH stretch), 1667 (s, C=O stretch), 1481 (s, C=C stretch), 985 (m, C-H oop bend), 758 (s, C-H oop bend).

HRMS-TOF MS ESI+: *m/z* [M+Na]⁺ calculated for C₄₆H₅₆O₅Na: 699.4025; found: 699.4022.

Chapter 3: Ortholithiation of oxazoline calixarenes

3.7.7 5-(2,2-dimethylpropanone)-25,26,27,28-tetrapropoxycalix[4]arene – 69.



^1H NMR (300 MHz, CHLOROFORM-*d*) δ 0.85-0.94 (m, 6H, $\text{OCH}_2\text{CH}_2\text{CH}_3$), 0.96 (s, 9H, $\text{C}(\text{CH}_3)_3$), 1.07-1.14 (m, 6H, $\text{OCH}_2\text{CH}_2\text{CH}_3$), 1.28 (s, 9H, $\text{C}(\text{CH}_3)_3$), 1.81-2.04 (m, 8H, $\text{OCH}_2\text{CH}_2\text{CH}_3$), 2.38 (s, 3H, SCH_3), 2.90 (dd, $J = 6.6$, 3.6 Hz, 1H, $\text{CHC}(\text{CH}_3)_3$), 3.06 (d, $J = 13.5$ Hz, 1H, $\text{ArCH}_2^{\text{eq}}\text{Ar}$), 3.15 (d, $J = 13.5$ Hz, 3H, $\text{ArCH}_2^{\text{eq}}\text{Ar}$), 3.61-3.77 (m, 4H, $\text{OCH}_2\text{CH}_2\text{CH}_3$), 3.86 (dd, $J = 10.2$, 6.6 Hz, 2H, OCH_2CHN), 3.93-4.11 (m, 4H, $\text{OCH}_2\text{CH}_2\text{CH}_3$), 4.34 (d, $J = 13.5$ Hz, 1H, OCH_2CHN), 4.42 (d, $J = 13.3$ Hz, 1H, $\text{ArCH}_2^{\text{ax}}\text{Ar}$), 4.46 (d, $J = 13.3$ Hz, 3H, $\text{ArCH}_2^{\text{ax}}\text{Ar}$), 5.54-5.99 (m, 2H, ArH), 6.07-6.15 (m, 3H, ArH), 6.25 (t, $J = 7.4$ Hz, 1H, ArH), 6.70 (s, 1H, ArH), 6.94 (t, $J = 7.5$ Hz, 1H, ArH), 7.11-7.14 (m, 2H, ArH) ppm.

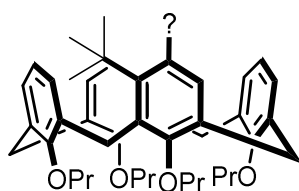
^{13}C NMR (75 MHz, CHLOROFORM-*d*) δ 10.0, 10.1, 11.0, 11.1, 21.6, 21.7, 23.1, 23.3, 23.6, 23.7, 23.8, 27.6, 27.7, 27.9, 28.0, 28.2, 28.9, 29.0, 30.1, 30.7, 30.8, 31.1, 31.2, 34.4, 34.9, 41.0, 41.8, 63.7, 64.1, 70.1, 76.6, 76.9, 77.1, 77.4, 121.9, 122.2, 122.4, 126.6, 126.8, 127.0, 127.4, 127.7, 127.8, 128.2, 128.3, 128.9, 129.1, 132.3, 132.6, 132.8, 133.1, 133.2, 133.3, 133.4, 133.6, 135.9, 136.6, 137.0, 137.4, 141.0, 141.2, 154.9, 155.0, 155.1, 155.2, 155.3, 158.3, 158.8, 158.9, 179.4, 180.9 ppm.

IR (ATR) cm^{-1} : 2965 (m, -CH), 2876 (s, -CH stretch), 1635 (s, C=N stretch), 1120 (m, C-O stretch), 982 (m, C-H oop bend), 762 (s, C-H oop bend).

HRMS-TOF MS ESI+: m/z $[\text{M}+\text{H}]^+$ calculated for $\text{C}_{52}\text{H}_{72}\text{NO}_5\text{S}$: 822.5131; found: 822.5132.

Chapter 3: Ortholithiation of oxazoline calixarenes

3.7.8 Unknown calixarene – 70.



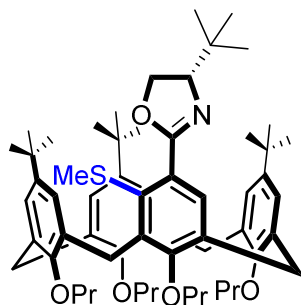
^1H NMR (300 MHz, CHLOROFORM-*d*) δ 0.94 (t, $J = 7.4$ Hz, 3H, $\text{OCH}_2\text{CH}_2\text{CH}_3$), 0.95 (t, $J = 7.4$ Hz, 3H, $\text{OCH}_2\text{CH}_2\text{CH}_3$), 1.04 (t, $J = 7.4$ Hz, 3H, $\text{OCH}_2\text{CH}_2\text{CH}_3$), 1.06 (t, $J = 7.4$ Hz, 3H, $\text{OCH}_2\text{CH}_2\text{CH}_3$), 1.45 (s, 9H, $\text{C}(\text{CH}_3)_3$), 1.84-2.01 (m, 8H, $\text{OCH}_2\text{CH}_2\text{CH}_3$), 3.14 (d, $J = 13.5$ Hz, 2H, $\text{ArCH}_2^{\text{eq}}\text{Ar}$), 3.29 (d, $J = 13.5$ Hz, 1H, $\text{ArCH}_2^{\text{eq}}\text{Ar}$), 3.48 (d, $J = 13.5$ Hz, 1H, $\text{ArCH}_2^{\text{eq}}\text{Ar}$), 3.73-3.87 (m, 4H, $\text{OCH}_2\text{CH}_2\text{CH}_3$), 3.88-4.04 (m, 4H, $\text{OCH}_2\text{CH}_2\text{CH}_3$), 4.44 (d, $J = 13.5$ Hz, 1H, $\text{ArCH}_2^{\text{ax}}\text{Ar}$), 4.47 (d, $J = 13.5$ Hz, 1H, $\text{ArCH}_2^{\text{ax}}\text{Ar}$), 4.57 (d, $J = 13.5$ Hz, 1H, $\text{ArCH}_2^{\text{ax}}\text{Ar}$), 4.64 (d, $J = 4.64$ Hz, 1H, $\text{ArCH}_2^{\text{ax}}\text{Ar}$), 6.35-6.38 (m, 4H, ArH), 6.50-6.62 (m, 2H, ArH), 6.69-6.77 (m, 2H, ArH), 6.90 (s, 1H, ArH), 7.53 (s, 1H, ArH) ppm.

^{13}C NMR (75 MHz, CHLOROFORM-*d*) δ 10.2, 10.3, 10.7, 10.8, 23.2, 23.3, 23.4, 23.6, 29.9, 30.2, 30.5, 31.1, 31.2, 31.9, 34.6, 76.7, 76.9, 77.0, 77.4, 117.6, 121.7, 122.0, 122.1, 124.1, 127.7, 128.0, 128.2, 128.3, 128.5, 129.8, 132.9, 133.0, 133.2, 134.4, 134.5, 134.6, 136.0, 136.3, 141.2, 145.8, 153.8, 156.1, 157.4 ppm.

IR (ATR) cm^{-1} : 2965 (m, -CH), 2876 (s, -CH stretch), 1490 (s, C=C stretch), 995 (m, C-H oop bend), 760 (s, C-H oop bend). (No C-O or C=N frequencies, IR spectrum looks to be only aromatic and hydrocarbon in nature).

HRMS-TOF MS ESI+: m/z $[\text{M}]^+$ found: 722.4250.

Chapter 3: Ortholithiation of oxazoline calixarenes

3.7.9 (*M*)-11,17,23-tri-*tert*-butyl-5-((*S*)-4-*tert*-butyl-4,5-dihydrooxazol-2-yl)-4-methylthio-25,26,27,28-tetrapropoxycalix[4]arene – **71**.

Thioether calixarene (**M**)-**71** was synthesized according to the general procedure. Oxazoline calixarene **67** (117 mg, 0.132 mmol), *t*-BuLi (0.659 mmol, 5.0 equiv), TMEDA (0.200 ml, 1.32 mmol, 10.0 equiv), Et₂O (1 ml) and dimethyl disulfide (0.2 ml, exs) with a reaction time of 72 h. The product was purified using silica gel column chromatography (EtOAc:PET, 1.5:98.5) yielding a white solid (61.0 mg, 50%, *de*: 97%).

¹H NMR (300 MHz, BENZENE-*d*) δ 0.87-0.99 (m, 12 H, OCH₂CH₂CH₃), 0.98 (s, 9 H, C(CH₃)₃), 1.23 (s, 9H, C(CH₃)₃), 1.26 (s, 9H, C(CH₃)₃), 1.29 (s, 9H, C(CH₃)₃), 1.82-1.96 (m, 4H, OCH₂CH₂CH₃), 1.98-2.12 (m, 4H, OCH₂CH₂CH₃), 2.29 (s, 3H, SCH₃), 3.15 (d, *J* = 12.7 Hz, 1H, ArCH₂^{eq}Ar), 3.30 (d, *J* = 12.7 Hz, 1H, ArCH₂^{eq}Ar), 3.66-3.74 (m, 1H, OCH₂CH₂CH₃), 3.80-4.03 (m, 10H, OCH₂CH₂CH₃, OCH₂CHN, OCH₂CHN), 4.51-4.66 (m, 4H, ArCH₂^{ax}Ar), 6.98-7.03 (m, 4H, ArH), 7.06 (d, *J* = 2.4 Hz, 1H, ArH), 7.37 (d, *J* = 2.4 Hz, 1H, ArH), 7.62 (br. s, 1H, ArH) ppm.

¹³C NMR (75 MHz, BENZENE-*d*) δ 10.4 (OCH₂CH₂CH₃), 10.5 (OCH₂CH₂CH₃), 10.6 (OCH₂CH₂CH₃), 10.7 (OCH₂CH₂CH₃), 22.0 (OCH₂CH₂CH₃), 23.3 (OCH₂CH₂CH₃), 23.5 (OCH₂CH₂CH₃), 23.8(OCH₂CH₂CH₃), 26.2 (C(CH₃)₃^{ox}), 29.7 (ArCH₂Ar), 30.2 (ArCH₂Ar), 31.0 (ArCH₂Ar), 31.8 (OCH₂CHN^{ox}), 31.9 (C(CH₃)₃^{Ar}), 32.0(C(CH₃)₃^{Ar}), 32.2(C(CH₃)₃^{Ar}), 34.1 (C(CH₃)₃^{Ar}), 34.2 (2 × C(CH₃)₃^{Ar}), 34.3 (C(CH₃)₃^{Ar}), 68.3 (OCH₂CHN^{ox}), 76.8 (OCH₂CH₂CH₃), 77.1 (OCH₂CH₂CH₃), 77.2 (OCH₂CH₂CH₃), 77.7 (OCH₂CH₂CH₃), 125.2 (C_{Ar}H), 125.4 (C_{Ar}H), 125.7 (C_{Ar}H), 125.8 (C_{Ar}H), 126.0 (C_{Ar}H), 130.8 (C_{Ar}C), 131.3 (C_{Ar}C), 132.8 (C_{Ar}C), 132.9 (C_{Ar}C), 133.0 (C_{Ar}C), 133.9 (C_{Ar}C), 134.2 (C_{Ar}-CSMe), 134.4 (C_{Ar}C), 134.9 (C_{Ar}C), 136.0 (C_{Ar}C), 141.4 (C_{Ar}C), 144.3 (C_{Ar}C), 145.0 (C_{Ar}C), 154.3 (C_{Ar}O), 154.5 (C_{Ar}O), 154.6 (C_{Ar}O), 159.1 (C_{Ar}O), 164.4 (OCN) ppm.

¹H, ¹H COSY (300/300 MHz 278 K, BENZENE-*d*): δ¹H/δ¹H = 2.00 / 0.88 (OCH₂CH₂CH₃ / OCH₂CH₂CH₃), 3.99 / 2.00 (OCH₂CH₂CH₃ / OCH₂CH₂CH₂), 4.70, 4.60 / 3.36, 3.26 (ArCH₂^{eq}Ar / ArCH₂^{ax}Ar), 7.08 / 6.96 (ArH / ArH) ppm.

Chapter 3: Ortholithiation of oxazoline calixarenes

^1H , ^{13}C HSQC (300/75 MHz, 278 K, BENZENE-*d*) $\delta^1\text{H} / \delta^{13}\text{C} = 0.88 / 10.4$ ($\text{OCH}_2\text{CH}_2\text{CH}_3 / \text{OCH}_2\text{CH}_2\text{CH}_3$), 0.91 / 10.5 ($\text{OCH}_2\text{CH}_2\text{CH}_3 / \text{OCH}_2\text{CH}_2\text{CH}_3$), 0.98 / 10.6 ($\text{OCH}_2\text{CH}_2\text{CH}_3 / \text{OCH}_2\text{CH}_2\text{CH}_3$), 0.96 / 26.2 ($\text{C}(\text{CH}_3)_3^{\text{ox}} / \text{C}(\text{CH}_3)_3^{\text{ox}}$), 1.23 / 31.8 ($\text{C}(\text{CH}_3)_3^{\text{Ar}} / \text{C}(\text{CH}_3)_3^{\text{Ar}}$), 1.25 / 31.9 ($\text{C}(\text{CH}_3)_3^{\text{Ar}} / \text{C}(\text{CH}_3)_3^{\text{Ar}}$), 1.27 / 31.3 ($\text{C}(\text{CH}_3)_3^{\text{Ar}} / \text{C}(\text{CH}_3)_3^{\text{Ar}}$), 1.88 / 23.3 ($\text{OCH}_2\text{CH}_2\text{CH}_3 / \text{OCH}_2\text{CH}_2\text{CH}_3$), 3.15 / 29.7 ($\text{ArCH}_2^{\text{eqAr}} / \text{ArCH}_2^{\text{eqAr}}$), 3.16 / 31.0 ($\text{ArCH}_2^{\text{eqAr}} / \text{ArCH}_2^{\text{eqAr}}$), 3.30 / 31.0 ($\text{ArCH}_2^{\text{eqAr}} / \text{ArCH}_2^{\text{eqAr}}$), 3.30 / 30.2 ($\text{ArCH}_2^{\text{eqAr}} / \text{ArCH}_2^{\text{eqAr}}$), 3.82 / 77.2 ($\text{OCH}_2\text{CH}_2\text{CH}_3 / \text{OCH}_2\text{CH}_2\text{CH}_3$), 3.84 / 77.1 ($\text{OCH}_2\text{CH}_2\text{CH}_3 / \text{OCH}_2\text{CH}_2\text{CH}_3$), 3.91 / 77.1 ($\text{OCH}_2\text{CH}_2\text{CH}_3 / \text{OCH}_2\text{CH}_2\text{CH}_3$), 3.93 / 76.8 ($\text{OCH}_2\text{CH}_2 / \text{OCH}_2\text{CH}_2$), 3.99 / 68.30 ($\text{OCH}_2\text{CHN}^{\text{ox}} / \text{OCH}_2\text{CHN}^{\text{ox}}$), 4.50 / 30.2 ($\text{ArCH}_2^{\text{axAr}} / \text{ArCH}_2^{\text{axAr}}$), 4.54 / 30.2 ($\text{ArCH}_2^{\text{axAr}} / \text{ArCH}_2^{\text{axAr}}$), 4.56 / 31.8 ($\text{OCH}_2\text{CHN}^{\text{ox}} / \text{OCH}_2\text{CHN}^{\text{ox}}$), 4.61 / 31.0 ($\text{ArCH}_2^{\text{axAr}} / \text{ArCH}_2^{\text{axAr}}$), 4.65 / 31.2 ($\text{ArCH}_2^{\text{axAr}} / \text{ArCH}_2^{\text{axAr}}$), 6.97 / 125.2 ($\text{C}_{\text{ArH}} / \text{C}_{\text{ArH}}$), 7.05 / 125.4 ($\text{C}_{\text{ArH}} / \text{C}_{\text{ArH}}$), 7.37 / 126.0 ($\text{C}_{\text{ArH}} / \text{C}_{\text{ArH}}$), 7.60 / 130.8 ($\text{C}_{\text{ArH}} / \text{C}_{\text{ArH}}$) ppm.

^1H , ^{13}C HMBC (300/75 MHz, 278 K, C_6D_6) $\delta^1\text{H} / \delta^{13}\text{C}$ 0.88 / 23.5, 77.2 ($\text{OCH}_2\text{CH}_2\text{CH}_3 / \text{OCH}_2\text{CH}_2\text{CH}_3$, $\text{OCH}_2\text{CH}_2\text{CH}_3$), 0.89 / 23.4, 77.1 ($\text{OCH}_2\text{CH}_2\text{CH}_3 / \text{OCH}_2\text{CH}_2\text{CH}_3$, $\text{OCH}_2\text{CH}_2\text{CH}_3$), 0.92 / 23.4, 77.1 ($\text{OCH}_2\text{CH}_2\text{CH}_3 / \text{OCH}_2\text{CH}_2\text{CH}_3$, $\text{OCH}_2\text{CH}_2\text{CH}_3$), 0.95 / 23.5, 77.1 ($\text{OCH}_2\text{CH}_2\text{CH}_3 / \text{OCH}_2\text{CH}_2\text{CH}_3$, $\text{OCH}_2\text{CH}_2\text{CH}_3$), 0.97 / 26.2, 34.1 ($\text{C}(\text{CH}_3)_3^{\text{ox}} / (\text{C}(\text{CH}_3)_3^{\text{ox}}, \text{OCH}_2\text{CHN}^{\text{ox}})$), 1.23 / 34.3 ($\text{C}(\text{CH}_3)_3^{\text{Ar}} / (\text{C}(\text{CH}_3)_3^{\text{Ar}}$), 1.26 / 34.1, ($\text{C}(\text{CH}_3)_3^{\text{Ar}} / (\text{C}(\text{CH}_3)_3^{\text{Ar}}$), 1.29 / 34.2 ($\text{C}(\text{CH}_3)_3^{\text{Ar}} / (\text{C}(\text{CH}_3)_3^{\text{Ar}}$), 1.90 / 10.4, 76.8 ($\text{OCH}_2\text{CH}_2\text{CH}_3 / \text{OCH}_2\text{CH}_2\text{CH}_3$, $\text{OCH}_2\text{CH}_2\text{CH}_3$), 2.04 / 10.4, 77.1 ($\text{OCH}_2\text{CH}_2\text{CH}_3 / \text{OCH}_2\text{CH}_2\text{CH}_3$, $\text{OCH}_2\text{CH}_2\text{CH}_3$) 2.29 / 134.2 ($\text{SCH}_3 / \text{C}_{\text{ArSMe}}$), 3.15 / 125.4, 131.3, 132.8, 136.0, 154.3, 159.1 ($\text{ArCH}_2^{\text{eqAr}} / \text{C}_{\text{ArH}}, \text{C}_{\text{ArH}}, \text{C}_{\text{ArC}}, \text{C}_{\text{ArC}}, \text{C}_{\text{ArO}}, \text{C}_{\text{ArO}}$), 3.17 / 125.4, 131.3, 136.0, 154.3, 159.1 ($\text{ArCH}_2^{\text{eqAr}} / \text{C}_{\text{ArH}}, \text{C}_{\text{ArH}}, \text{C}_{\text{ArC}}, \text{C}_{\text{ArC}}, \text{C}_{\text{ArO}}, \text{C}_{\text{ArO}}$), 3.30 / 125.7, 134.2, 154.5 ($\text{ArCH}_2^{\text{eqAr}} / \text{C}_{\text{ArH}}, \text{C}_{\text{ArC}}, \text{C}_{\text{ArO}}$), 3.31 / 125.7, 134.4, 154.5 ($\text{ArCH}_2^{\text{eqAr}} / \text{C}_{\text{ArH}}, \text{C}_{\text{ArC}}, \text{C}_{\text{ArO}}$), 3.84 / 10.4, 23.3, 154.3 ($\text{OCH}_2\text{CH}_2\text{CH}_3 / \text{OCH}_2\text{CH}_2\text{CH}_3$, $\text{OCH}_2\text{CH}_2\text{CH}_3$, C_{ArO}), 3.85 / 10.4, 23.3, 159.1 ($\text{OCH}_2\text{CH}_2\text{CH}_3 / \text{OCH}_2\text{CH}_2\text{CH}_3$, $\text{OCH}_2\text{CH}_2\text{CH}_3$, C_{ArO}), 3.91 / 26.2, 68.3, 164.4 ($\text{OCH}_2\text{CHN}^{\text{ox}} / \text{C}(\text{CH}_3)_3$, $\text{OCH}_2\text{CHN}^{\text{ox}}$, OCN), 4.50 / 125.4, 131.3, 133.9, 154.3, 159.1 ($\text{ArCH}_2^{\text{axAr}} / \text{C}_{\text{ArH}}, \text{C}_{\text{ArH}}, \text{C}_{\text{ArC}}, \text{C}_{\text{ArC}}, \text{C}_{\text{ArO}}, \text{C}_{\text{ArO}}$), 4.54 / 125.4, 132.9, 136.0, 141.4, 154.3, 159.1 ($\text{ArCH}_2^{\text{axAr}} / \text{C}_{\text{ArH}}, \text{C}_{\text{ArH}}, \text{C}_{\text{ArC}}, \text{C}_{\text{ArC}}, \text{C}_{\text{ArO}}, \text{C}_{\text{ArO}}$), 6.98 / 32.0, 125.2, 154.5 ($\text{ArH} / \text{C}(\text{CH}_3)_3$, $\text{C}_{\text{ArH}}, \text{C}_{\text{ArO}}$), 6.99 / 34.1, 125.7, 154.5 ($\text{ArH} / \text{C}(\text{CH}_3)_3$, $\text{C}_{\text{ArH}}, \text{C}_{\text{ArO}}$), 7.03 / 32.2, 125.4, 154.3 ($\text{ArH} / \text{C}(\text{CH}_3)_3$, $\text{C}_{\text{ArH}}, \text{C}_{\text{ArO}}$), 7.05 / 31.8, 125.2, 154.5 ($\text{ArH} / \text{C}(\text{CH}_3)_3$, $\text{C}_{\text{ArH}}, \text{C}_{\text{ArO}}$), 7.35 / 125.8, 154.6 ($\text{ArH} / \text{C}_{\text{ArH}}, \text{C}_{\text{ArO}}$), 7.60 / 31.0, 134.2, 159.1, 164.4 ($\text{ArH} / \text{ArCH}_2\text{Ar}$, C_{ArSMe} , C_{ArO} , OCN) ppm.

IR (film) cm^{-1} : 2961 (s, CH), 1651 (s, C=N), 1481 (s, C=C), 1130 (m, C-O stretch), 980 (m, C-H oop bend), 760 (s, C-H oop bend).

HRMS-TOF MS ESI⁺: m/z $[\text{M}+\text{H}]^+$ calculated for $\text{C}_{60}\text{H}_{86}\text{NO}_5\text{S}$ 932.6227; found: 932.6257.

3.8 References.

- (1) Herbert, S. A.; Arnott, G. E. *Org. Lett.* **2010**, *12*, 4600.
- (2) Herbert, S. A.; Arnott, G. E. *Org. Lett.* **2009**, *11*, 4986.
- (3) Herbert, S. A.; van Laeren, L. J.; Castell, D. C.; Arnott, G. E. *Beilstein J. Org. Chem.* **2014**, *10*, 2751.
- (4) Gilman, H.; Bebb, R, L. *J. Am. Chem. Soc.* **1939**, *61*, 109.
- (5) Wittig, G.; Fuhrmann, G. *Chem. Ber.* **1940**, *73*, 1197.
- (6) Herbert, S. A. Oxazoline Directed Lithiation of Calix[4]arene and Ferrocene, PhD, Stellenbosch University, 2011.
- (7) Herbert, S. A. Oxazoline directed lithiation of calix[4]arene and ferrocene, Stellenbosch University, 2011.
- (8) Herbert, S. A.; Castell, D. C.; Clayden, J.; Arnott, G. E. *Org. Lett.* **2013**, *15*, 3334.
- (9) Gilman, H.; Zoellner, E. A.; Selby, W. M. *J. Am. Chem. Soc.* **1932**, *54*, 1957.
- (10) Fraenkel, G.; Henrichs, I. M.; Hewitt, I. J. M.; Biing, I.; Su, M.; Gecklela, M. J. *J. Am. Chem. Soc.* **1980**, *102*, 3345.
- (11) Bartlett, P. D.; Swain, C. D.; Woodward, R. B. *J. Am. Chem. Soc.* **1941**, *63*, 3229.
- (12) Bartlett, P. D.; Tauber, S. J.; Weber, W. P. *J. Am. Chem. Soc.* **1969**, *91*, 6362.
- (13) Kühnel, M. F.; Lentz, D. *Dalton Trans.* **2009**, 4747.
- (14) Meyers, A. I.; Barner, B. A. *J. Am. Chem. Soc.* **1984**, *106*, 1865.
- (15) Clayton, J.; Clayden, J. *Tetrahedron Lett.* **2011**, *52*, 2436.
- (16) Williard, P. G.; Sun, C. *J. Am. Chem. Soc.* **1997**, *119*, 11693.
- (17) Kwon, O.; Sevin, F.; Mckee, M. L. *J. Phys. Chem. A* **2001**, *105*, 913.
- (18) Hoffmann, D.; Collum, D. B. *J. Am. Chem. Soc.* **1998**, *120*, 5810.
- (19) Pratt, L. M.; Truhlar, D. G.; Cramer, C. J.; Kass, S. R.; Thompson, J. D.; Xidos, J. D. *J. Org. Chem.* **2007**, *72*, 2962.
- (20) Reich, H. J. *Chem. Rev.* **2013**, *113*, 7130.
- (21) Waldmuller, D.; Kotsatos, B. J.; Nichols, M. A.; Williard, P. G. *J. Am. Chem. Soc.* **1997**, *119*, 5479.
- (22) Sammakia, T.; Latham, H. A. *J. Org. Chem.* **1995**, *60*, 6002.

Chapter 3: Ortholithiation of oxazoline calixarenes

- (23) Collum, B. *Acc. Chem. Res.* **1992**, *25*, 448.
- (24) van Eikeman Hommes, N. J. R.; von Rague Schleyer, P. *Tetrahedron Lett.* **1994**, *50*, 5903.
- (25) DeLong, G. T.; Pannell, D. K.; Clarke, M. T.; Thomas, R. D. *J. Am. Chem. Soc.* **1993**, *115*, 7013.
- (26) Snieckus, V. *Chem. Rev.* **1990**, *90*, 879.
- (27) Roberts, J. D.; Curtin, D. Y. *J. Am. Chem. Soc.* **1946**, *68*, 1658.
- (28) van Eikeman Hommes, N. J. R.; von Rague Schleyer, P. *Angew. Chem., Int. Ed.* **1992**, *31*, 755.
- (29) Meyers, A. I. *Acc. Chem. Res.* **1978**, *11*, 375.
- (30) Beak, P.; Snieckus, V. *Acc. Chem. Res.* **1982**, *15*, 306.
- (31) Anderson, D. R.; Faibish, N. C.; Beak, P. *J. Am. Chem. Soc.* **1999**, *121*, 7553.
- (32) Saá, J. M. *Helv. Chim. Acta* **2002**, *85*, 814.
- (33) Chadwick, S. T.; Rennels, R. A.; Rutherford, J. L.; Collum, D. B. *J. Am. Chem. Soc.* **2000**, *122*, 8640.
- (34) Shimano, M.; Meyers, A. I. *J. Am. Chem. Soc.* **1994**, *116*, 10815.
- (35) Maggi, R.; Schlosser, M. *J. Org. Chem.* **1996**, *61*, 5430.
- (36) Chadwick, S. T.; Ramirez, A.; Gupta, L.; Collum, D. B.; *J. Am. Chem. Soc.* **2007**, *129*, 2259.
- (37) Rennels, R. A.; Maliakal, A. J.; Collum, D. B. *J. Am. Chem. Soc.* **1998**, *120*, 421.
- (38) Clayden, J. *Organolithiums: Selectivity for Synthesis*; Pergamon Oxford, 2002.
- (39) Gessner, V. H.; Däschlein, C.; Strohmann, C. *Chem.-Eur. J.* **2009**, *15*, 3320.
- (40) West, P.; Waack, R. *J. Am. Chem. Soc.* **1966**, *89*, 4395.
- (41) Hoffmann, R. W.; Kemper, B. *Tetrahedron Lett.* **1981**, *22*, 5263.
- (42) Harper, K. C.; Bess, E. N.; Sigman, M. S. *Nat. Chem.* **2012**, *4*, 366.
- (43) Taft, R. W. *J. Am. Chem. Soc.* **1950**, *74*, 3120.
- (44) Charton, M. *J. Org. Chem.* **1976**, *41*, 2217.
- (45) Perna, F. M.; Salomone, A.; Dammacco, M.; Florio, S.; Capriati, V. *Chemistry* **2011**, *17*, 8216.

4 Chapter 4 - Ortholithiation of sulfoxide calixarene*

4.1 Introduction.

It was not until the first reports of chiral sulfoxide auxiliaries in the early 1980s, that the interest in the stereochemical behavior, as well as potential synthetic applications of these compounds grew rapidly.¹ Since this initial discovery, many different asymmetric synthetic strategies based around sulfoxides have been reported. In addition to this, they have been incorporated in a wide range of ligands to further stereochemical application studies.²⁻⁶ A general overview and summary of both the synthesis and application of chiral sulfoxides can be found in the following review articles.⁷⁻¹¹

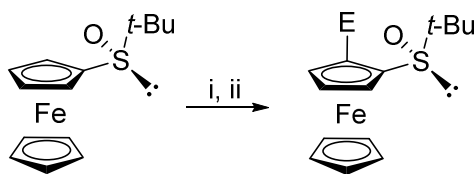
The popularity and widespread use of the sulfoxide functional group can be attributed to its numerous favourable properties including reasonable to high levels of optical stability. The rate of thermal racemization of aryl, diaryl, alkyl and dialkyl sulfoxides was investigated by Rayner and co-workers.¹² Their study incorporated a series of structural variables with the aim of establishing a range of temperatures required to induce racemization. It was found that racemization only begun upwards of 190 °C. Standard homogenous asymmetric reactions rarely exceed 120 °C, making the sulfoxide functional group suitable for use in most asymmetric catalytic studies. Thermal stability was less of a concern for this investigation, as lithiation studies are almost exclusively performed at lower temperatures. Any increase in popularity in the synthetic world is naturally coupled with an influx of newly developed synthetic methods. Therefore the literature contains many examples of chiral sulfoxide syntheses, as well as options to access both of the chiral configurations.⁷ Sulfoxides have also been established as efficient carriers of chiral information.^{13,14} A sulfoxide usually contains a central sulfur atom with the following four general components; an oxygen atom, a lone pair of electrons and two remaining alkyl or aryl R-groups. The large stereoelectronic differences between these groups creates a distinct and well-defined chiral environment around the sulfur atom. Furthermore, the polarizable sulfur-oxygen bond aids in coordination of the sulfur and oxygen atoms to Lewis acids and transition metals. Lastly, having an efficient desulfurization method gives sulfoxides an edge in versatility when compared to other auxiliaries such as the oxazolines. Raney Nickel is a well-known desulfurization reagent and has been widely reported as an efficient means of cleaving the sulfur-carbon bond since the early 1940s.^{15,16}

Ferrocenes have been extensively used to synthesize planar chiral ligands. As mentioned in **Chapter 3**, the development of asymmetric synthetic methods toward these compounds has been comprehensive, and many strategies have been centered on this directed metalation chemistry.⁷⁻¹¹

*This work was initially undertaken by Mr N. Lesotho during his research towards a PhD. Due to unfortunate circumstances he was unable to complete this work. This chapter seeks to confirm and conclude that initial pilot study.

Chapter 4: Ortholithiation of sulfoxide calixarene

The chiral sulfoxide auxiliary is one of many directing groups that has proven itself to be more than capable in this area of chemistry and one of the earliest examples of this was reported in 1993 by Kagan and co-workers (**Scheme 4.1**).¹⁷



Scheme 4.1: The diastereoselective ortholithiation of ferrocene. Reagents and conditions: i) LDA, THF, $-78\text{ }^{\circ}\text{C}$; ii) E.¹⁷

The above strategy was both efficient and versatile. The major diastereomer product was synthesized in diastereomeric ratios of up to 99:1. On top of being extremely selective, the method was relatively flexible as it tolerated a variety of electrophiles. The yields ranged from moderate to high and were generally electrophile dependent. This reaction can be regarded as one of the first steps taken toward what has amounted to an impressive collection of work today. Currently there are hundreds of publications based on this idea. The following are only a few examples of reactions that used ligands containing the chiral sulfoxide motif: Michael addition,¹⁸ Diels-Alder reaction,¹⁹⁻²¹ radical addition²² as well as many transition metal catalytic C-C bond forming reactions.^{9,23,24} By using various directing groups, chemists have been able to synthesize many possible variations of ligands that have seen use in transition metal catalysis. A common problem associated with the introduction of chirality into organic frameworks, is what to do with the remaining directing group after the functionalization. They can be difficult to remove or modify, which can become problematic as the chiral information on the auxiliary can interfere when one is only interested in investigating a separate steric property all together. Although the removal of the sulfoxide directing group was not reported in this specific publication, subsequent related studies have reported this for the synthesis of purely planar chiral ligands.²⁵ This approach has enabled chemists to understand how the planar chiral information of these ligands is imparted during an asymmetric process.

Owing to the similarity of planar and inherent chirality, the incorporation of a chiral sulfoxide on the upper rim of the calixarene presented an exciting alternative directing group for the selective ortholithiation reaction. The targeted sulfoxide calixarene compound was based on the structure of the ferrocene sulfoxides first reported by Kagan and co-workers (**Figure 4.1**).¹⁷

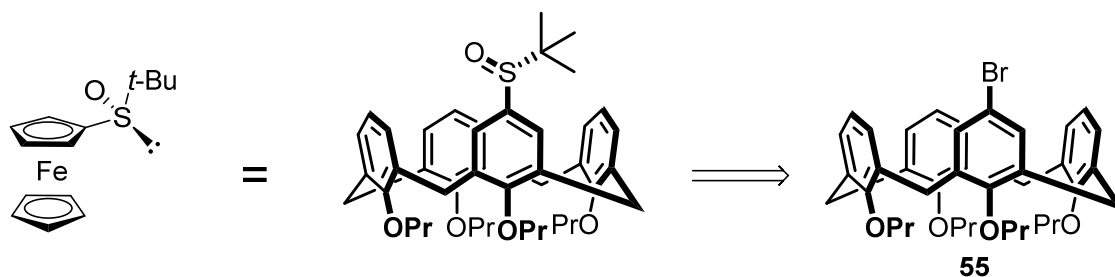
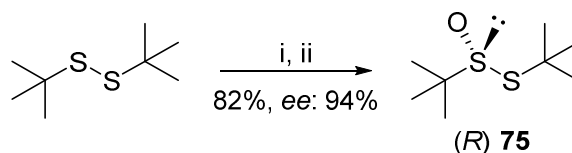


Figure 4.1: Target chiral sulfoxide calixarene.

The sulfoxide calixarene could theoretically be obtained in one step from calixarene **55**. The lithium halogen exchange chemistry was an efficient method of generating a strong nucleophilic intermediate. A procedure reported by Ellman and co-workers reported the highly selective preparation of a chiral thiosulfinate ester, which functioned as an electrophilic source of the chiral sulfoxide functional group.²⁶ Alternatively, the reaction could be quenched with di-*tert*-butyldisulfide, which would form the *tert*-butyl thioether calixarene. This could then be asymmetrically oxidized to the chiral *tert*-butylsulfoxide. It was found that the preparation of the chiral thiosulfinate ester before introduction onto the calixarene was the preferable approach. This highly selective preparation would guarantee the incorporation of sulfoxide onto the calixarene in a high enantiomeric ratio. It was possible that if the same asymmetric oxidation was performed directly on the calixarene, that both the selectivities and/or yields of the oxidation could be significantly different, thereby creating unnecessary problems and the potential need to enrich the sulfoxide calixarene product at a later stage.

4.2 Synthesis of the chiral thiosulfinate ester.

Using a vanadium catalyzed asymmetric oxidation, the chiral thiosulfinate ester was prepared according to the procedure reported by Ellman and co-workers (**Scheme 4.2**).²⁶



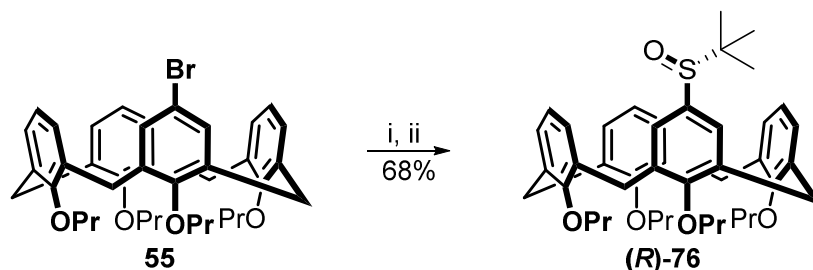
Scheme 4.2: Asymmetric oxidation of di-*tert*-butyl disulfide. Reagents and conditions: i) Vanadyl acetoacetate (0.5 mol%), ligand, (0.52 mol%), H₂O₂ (30% aq) (1.25 equiv), acetone, 0 °C; ii) Recrystallization from petroleum ether –20 °C.

The product mixture was optically enriched via low temperature recrystallization from petroleum ether (–20 °C). Subsequent storage and use of the electrophile required constant low temperatures of at least 0 °C.[†]

[†] A low temperature had to be maintained throughout the synthesis, work up and purification steps. The reason being poor thermal stability of the sulfinate ester product, as temperatures above 30 °C would result in rapid racemization of the product.

4.3 Synthesis of chiral sulfoxide calix[4]arene.

Using a lithium halogen exchange reaction with **55** and *n*-BuLi, the chiral *tert*-butyl sulfoxide was next introduced to the upper rim of the calixarene (**Scheme 4.3**).



Scheme 4.3: Synthesis of calixarene (**R**)-**76**. Reagents and conditions: i) *n*-BuLi (1.5 equiv), THF, $-78\text{ }^{\circ}\text{C}$, 10 - 20 min; ii) **75** (4.0 equiv), $-78\text{ }^{\circ}\text{C}$ to rt. 12 h.

Initial attempts at the lithium halogen exchange reaction afforded (**R**)-**76** in quite low yields (25 – 35%). Unlike simpler electrophiles, **75** proved to be more capricious in nature. After multiple attempts, the conditions of the reaction were optimized until the highest yield of 68% was reproducibly obtained. There were two primary factors that were found to influence the yield. The solid electrophile could not be added directly to the reaction lithiated intermediate, but instead had to be dissolved in cooled ($0\text{ }^{\circ}\text{C}$) and freshly distilled THF. This solution then had to be added drop-wise to the reaction as rapid addition also resulted in lower yields. Secondly, after addition of the electrophile, the reaction mixture had to be warmed to room temperature very slowly and then stirred for at least 8 hours. As discussed in **Chapter 2**, the fully protonated calixarene **54** formed as a by-product. The product mixture was separated via column chromatography, and for each reaction **54** was collected and later recycled to synthesize more of the **55** starting material. The introduction of the sulfoxide groups adds one crucial signal to the ^1H NMR spectrum of the product, a singlet with a chemical shift of δ 0.61 ppm that integrated for 9 protons, corresponding to the *tert*-butyl group of the sulfoxide (**Figure 4.2**).

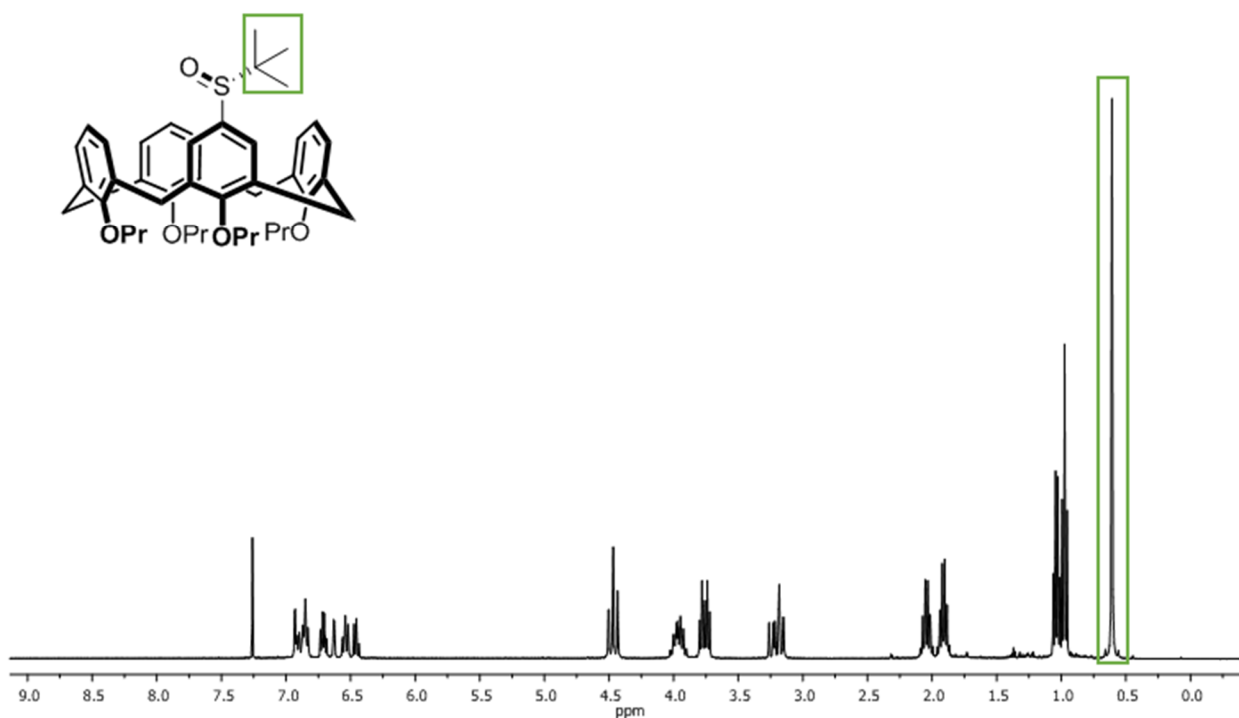
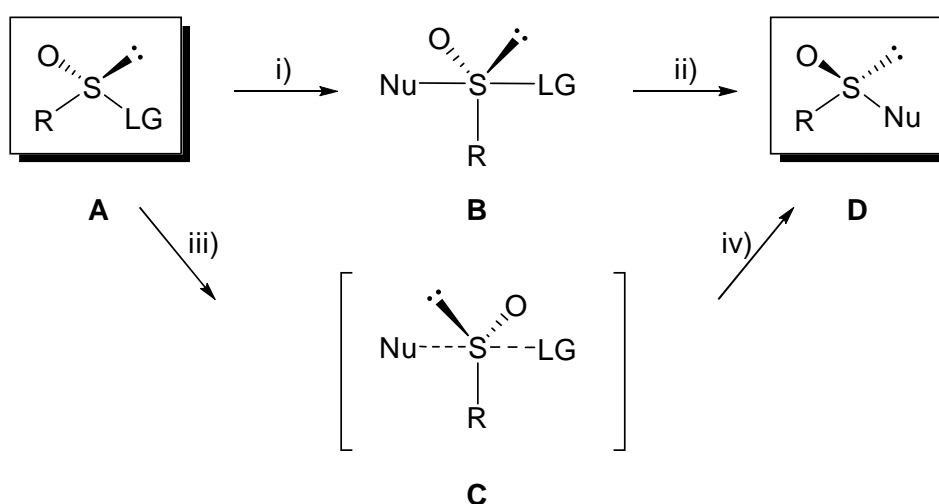


Figure 4.2: ^1H Spectrum of (*R*)-**76**. The sulfoxide *tert*-butyl signal is outlined in green.

The change in chemical shift of this signal was used to determine the conversions of the subsequent ortholithiation reactions, the details of which will be provided in the following section. Chiral HPLC was used to calculate the *ee* of (*R*)-**76** as 94%. A subtle but important consideration was the configuration of the chiral thiosulfinate ester and how it carried over to the sulfoxide on the calixarene. Unlike carbonyl functional groups, the sulfoxide is tetrahedral and adopts a mechanism in which the stereochemistry of the sulfur is inverted. The nucleophilic addition of the lithiated intermediate to the thiosulfinate ester is more complicated, and takes place via one of two proposed pathways (**Scheme 4.4**).²⁷



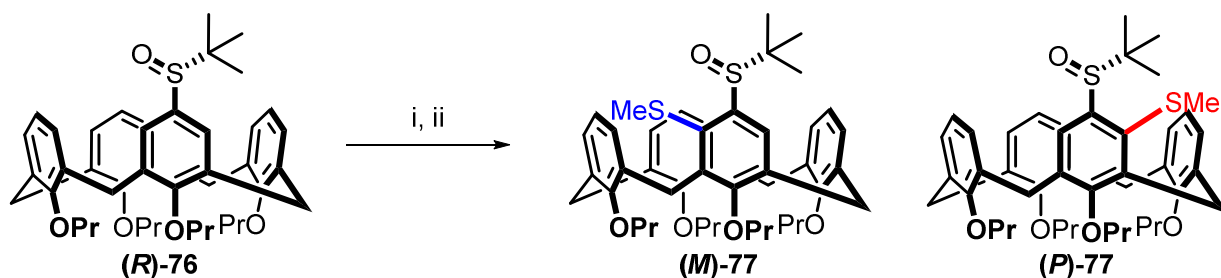
Scheme 4.4: The potential addition/elimination (i, ii) and $\text{S}_{\text{N}}2$ (iii, iv) mechanisms for the nucleophilic addition of the lithiated intermediate to the chiral sulfoxide ester.

Chapter 4: Ortholithiation of sulfoxide calixarene

The above scheme was proposed by Ellman and co-workers, but the idea of an addition-elimination mechanism was previously put forth by Mikolajczyk in 1986.²⁸ The first step in the addition-elimination pathway (i, ii) from **A** to **D**, is the addition of the nucleophile to **A**, resulting in the trigonal bipyramidal sulfurane intermediate, with both the approaching and leaving groups in the apical positions of the intermediate. Subsequent elimination of the leaving group affords the final product **D** with the inverted stereochemistry. Alternatively, the simultaneous bond forming and breaking of the conserved S_N2 substitution (iii, iv) depicted by intermediate **C** also accounts for the inversion of stereochemistry seen on the sulfur atom. It is important to note, that although inversion is taking place, due to the priority rules the thiosulfonate ester and calixarene sulfoxide both end up with the same stereochemical descriptor, namely (*R*).

4.4 Ortholithiation of mono-sulfoxide calixarene – 76.*4.4.1 Previously reported results.*

The experimental protocol for the ortholithiation of the sulfoxide calixarene was similar to the oxazoline calixarenes. An excess of the alkyllithium/TMEDA mixtures, low temperature as well as lengthy reaction times (24-48 h) were required to ensure the selective formation of the product in good yields (**Scheme 4.5**).



Scheme 4.5: Ortholithiation of calixarene (**R**)-76. Reagents and conditions: i) RLi (6.0 equiv), TMEDA (12.0 equiv), solvent, $-78\text{ }^{\circ}\text{C}$, 24 h; ii) E, $-78\text{ }^{\circ}\text{C}$ to rt, 24 h.

The initial optimization of the reaction conditions had previously been carried out by Mr Ntlama Lesotho. Several different alkyllithium reagents, solvents and additives were evaluated. The results of his study have been summarized in **Table 4.1**.

Chapter 4: Ortholithiation of sulfoxide calixarene

Table 4.1: Summary of the ortholithiation study initially carried out by Mr. Ntlama Lesotho.

Entry	RLi	Additive	Solvent	Electrophile	Time (h)	Conv (%) ^a	de (%) ^a
1	<i>n</i> -BuLi	-	THF	S ₂ Me ₂	8	71	0
2	<i>s</i> -BuLi	-	THF	S ₂ Me ₂	8	54	34
3	<i>t</i> -BuLi	-	THF	S ₂ Me ₂	8	10	0
4	<i>n</i> -BuLi	-	Et ₂ O	S ₂ Me ₂	8	-	-
5	<i>s</i> -BuLi	-	Et ₂ O	S ₂ Me ₂	8	-	-
6	<i>t</i> -BuLi	-	Et ₂ O	S ₂ Me ₂	8	-	-
7	<i>n</i> -BuLi	TMEDA	Et ₂ O	S ₂ Me ₂	8	67	66
8	<i>s</i> -BuLi	TMEDA	Et ₂ O	S ₂ Me ₂	8	33	0
9	<i>t</i> -BuLi	TMEDA	Et ₂ O	S ₂ Me ₂	8	59	88
10	<i>i</i> -PrLi	TMEDA	Et ₂ O	S ₂ Me ₂	8	22	70
11	<i>c</i> -PentLi	TMEDA	Et ₂ O	S ₂ Me ₂	8	15	78
12	<i>t</i> -BuLi	TMEDA	Pentane	S ₂ Me ₂	8	65	80
13	<i>n</i> -BuLi	diglyme	Et ₂ O	S ₂ Me ₂	8	-	-
14	<i>s</i> -BuLi	diglyme	Et ₂ O	S ₂ Me ₂	8	-	-
15	<i>t</i> -BuLi	Diglyme	Et ₂ O	S ₂ Me ₂	8	-	-

Reagents and conditions reported by Mr Lesotho[‡]: i) RLi (6.0 equiv), additive (12.0 equiv), -78 °C, 8 h; ii) S₂Me₂ (exs), -78 °C to rt 24 h. ^aConversion and *de* were determined using ¹H NMR spectroscopy.

The above collection of data was used as a foundation to further expand the study. Several of these results, such as entries 8 and 12 proved unreliable. For entry 8, there was no selectivity and the product was isolated in a low yield, while in entry 12, the selectivity for *t*-BuLi in pentane was lower than that in Et₂O, which was unexpected considering that the opposite was seen for the oxazoline calixarenes. Past experiments carried out by Mr. Lesotho has shown that the ortholithiation reaction is under kinetic control, and the lower reaction rates commonly seen for pentane would suggest an improved selectivity, as was generally the case for the oxazoline calixarenes. Unfortunately, only one of the diastereomers formed as the major product for all of these reactions. When attempting to reverse the selectivity of the reaction (entries 13-15) using a diglyme-based ligand, no product formed. Taking the generally poor performances of *i*-PrLi and *c*-PentLi into account, the most promising reactions of *n*, *s* and *t*-BuLi in Et₂O were revisited, with the aim of verifying these results and characterizing the ortholithiation products (**Table 4.2**).

Table 4.2: Verification of the previously reported ortholithiation study.

Entry	RLi	Additive	Solvent	Electrophile	t (h)	Conv (%) ^a	de (%) ^a
1	<i>n</i> -BuLi	TMEDA	Et ₂ O	S ₂ Me ₂	24	52	54
2	<i>s</i> -BuLi	TMEDA	Et ₂ O	S ₂ Me ₂	24	80	70
3	<i>t</i> -BuLi	TMEDA	Et ₂ O	S ₂ Me ₂	24	53-70	90

Reagents and conditions used in this study: i) RLi (6.0 equiv), additive (12.0 equiv), -78 °C, 8 h; ii) S₂Me₂ (exs), -78 °C to rt 24 h.

^aConversion and *de* were determined using ¹H NMR spectroscopy.

[‡] The reactions performed in Et₂O were actually a mixture of Et₂O and hexane/pentane as the solvent of the alkyllithium was not removed before addition.

Chapter 4: Ortholithiation of sulfoxide calixarene

Each of the reported selectivities and conversions presented above is an average value from at least three reactions, with minimal variations between them. The only considerable variation was for the conversions of entry 3, when *t*-BuLi was used as the alkyllithium, so a range of 53-70% is reported instead.

The conversions and selectivities of these reactions were calculated using the ^1H NMR spectra of the crude product mixtures (**Figure 4.3**).

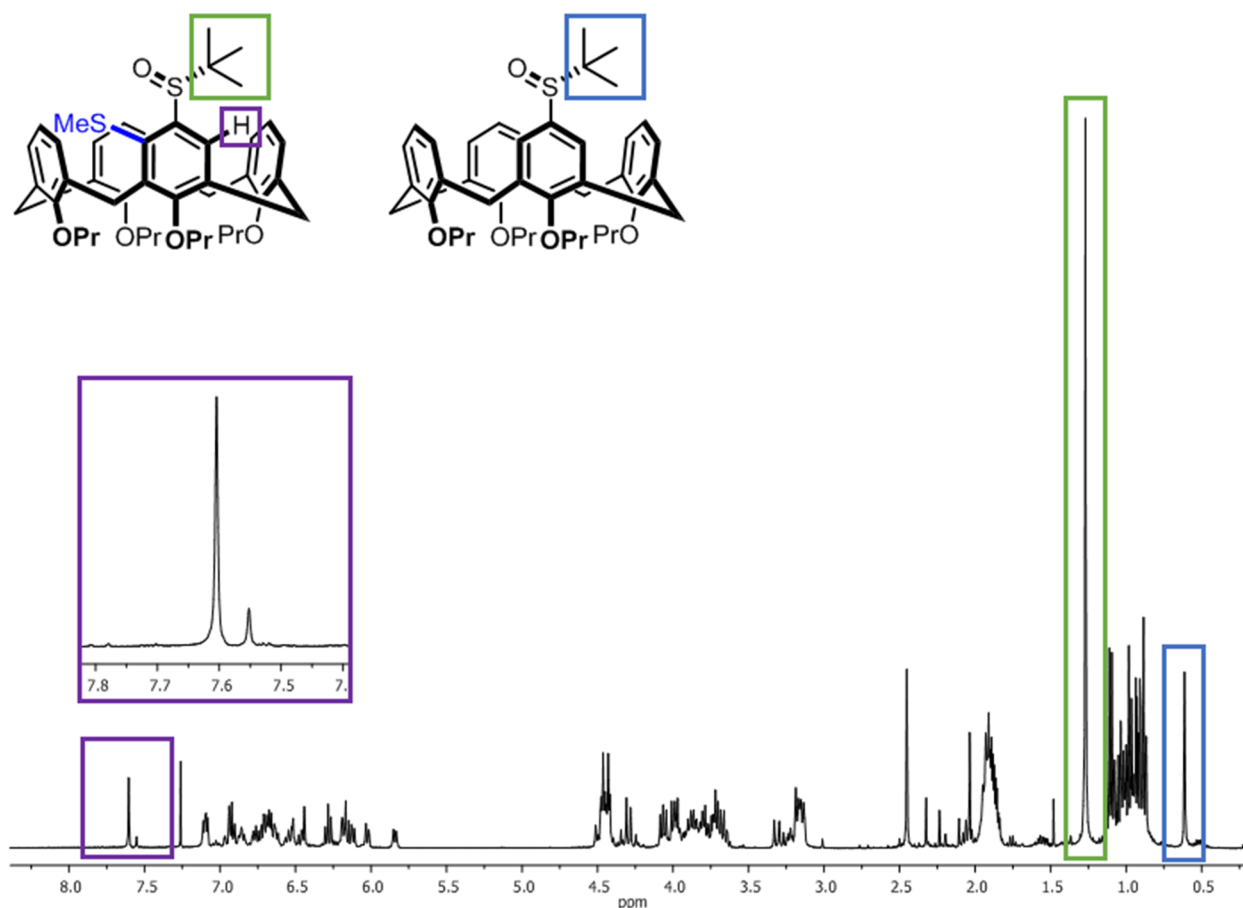


Figure 4.3: ^1H NMR spectrum of a crude mixture of (*M*)-77 and (*P*)-77. The tert-butyl groups of the sulfoxide of the product and starting material have been outlined in green and blue respectively. The aromatic signals of the *ortho*-proton for (*M*)-77 and (*P*)-77 have been outlined in purple.

The figure above depicts the typical ^1H NMR spectrum that was obtained for the crude product mixtures of these ortholithiation reactions. The conversions of each reaction were calculated by comparing the areas of the sulfoxide *tert*-butyl signal of the starting material (δ 0.61 ppm, outlined in blue) to that of the product (δ 1.27 ppm, outlined in green). As seen previously for the inherently chiral oxazoline diastereomers, the selectivity of these reactions were determined by comparing the areas of the single *ortho*-proton for the major (δ 7.60 ppm) and minor (δ 7.55 ppm) diastereomers, outlined in purple. The results obtained when repeating the study differed significantly from the values that were reported previously.

Chapter 4: Ortholithiation of sulfoxide calixarene

These reactions were repeated a minimum of three times and it is with confidence that these newly obtained results are presented as accurate.[§]

4.4.1 The nature of the solvent mixture.

During the ortholithiation of the oxazolines, the reactivity of the alkyllithiums in pure Et₂O and pentane was at times completely different. In **Table 4.1**, a reduced selectivity was reported for the ortholithiation reaction carried out in pentane (entry 8). With the purpose of accurately representing the experimental conditions of the previous study, the solvents of the alkyllithiums were not removed and so all of the reactions repeated in **Table 4.2** were carried out in a hydrocarbon/Et₂O mixture. Past results suggested that the selectivity for the ortholithiation of **(R)-76** was higher in Et₂O. The conversions for the reactions using *t*-BuLi fluctuated considerably when using a mixture of solvents. For the oxazolines, the general trend for ortholithiations performed in pure Et₂O was a higher conversion but a reduced selectivity, suggesting a higher reaction rate relative to the improved selectivities of the slower reactions performed in pentane.

It was hypothesized that because the selectivity of *t*-BuLi appeared to be higher in Et₂O for the sulfoxide, while the reactivity of alkyllithiums was generally higher in pure Et₂O, performing the reaction in pure Et₂O would give both the optimal conversion and selectivity for the ortholithiation of **(R)-76**. When this was first attempted it produced an unexpected, but interesting result. The conversion for the reaction was slightly improved, but the expected *de* value of 90% had instead plummeted to 26%. Almost all of the selectivity had been lost and so this result prompted a small solvent dependent study. After the reaction was carried out in pure Et₂O, it was repeated in solvent mixtures with increasing concentrations of pentane, until the last reaction was carried out in pure pentane. The results of this inquiry are summarized below (**Table 4.3**).

Table 4.3: The effect of Et₂O compositions on the ortholithiation of calixarene **(R)-76**

Entry	RLi	Additive	Solvent ^a	E	t (h)	Conv (%) ^b	<i>de</i> ^b
1	<i>t</i> -BuLi	TMEDA	Et ₂ O	S ₂ Me ₂	24	73	26
2	<i>t</i> -BuLi	TMEDA	Et ₂ O/Pentane (0.75/0.25)	S ₂ Me ₂	24	62	90
3	<i>t</i> -BuLi	TMEDA	Et ₂ O/Pentane (0.50/0.50)	S ₂ Me ₂	24	50	90
4	<i>t</i> -BuLi	TMEDA	Et ₂ O/Pentane (0.25/0.75)	S ₂ Me ₂	24	53	90
5	<i>t</i> -BuLi	TMEDA	Pentane	S ₂ Me ₂	24	70	90

Reagents and conditions: i) *t*-BuLi (6.0 equiv), TMEDA (12.0 equiv), solvent, -78 °C, 24 h; ii) S₂Me₂ (exs), -78 °C to rt, 12 h. ^aAlkyllithium solvents were removed under reduced pressure, after which they were added to the appropriate solvent mixtures. ^bConversions and selectivities were determined using ¹H NMR spectroscopy.

The concentrations of pentane were increased in 25% increments, until the reaction was carried out in pure pentane (entry 5). The varied conversions over entries 2 – 5 further demonstrate the fickle nature of this reaction and it was extremely difficult to reproducibly acquire the product in high yields.

[§] Once all of the synthesis results have been reported, the implications of this conformational change will be covered in detail in **Section 4.5**.

Chapter 4: Ortholithiation of sulfoxide calixarene

What was most interesting was the fact that the selectivity was essentially the same for all of the reactions regardless of the pentane concentration. Without a detailed mechanistic study, we were hesitant to draw too many conclusions from the above data.

There are two principal arguments that could be made accounting for the unique role played by the solvent in ortholithiation reactions. ** Either it significantly affects the rate of the reaction, by potentially increasing or decreasing the rate of lithiation, or it determines the structural properties of the reactive *t*-BuLi aggregate. In this case the outcome of the reaction had to be rationalized by comparing what we know about pentane and Et₂O, and how they individually affect these two factors.

Considering the fact that generally poorer selectivities for the oxazolines were obtained when the reactions were performed in pure Et₂O, it can be hypothesized that the rate of these ortholithiation reactions was potentially higher, which led to the poorer kinetic control. This could also be the case here, where in entry 1, the poor selectivity resulted from a much higher reaction rate. Instead of seeing a gradual increase in the selectivity as the concentration of pentane increased, there appeared to be an almost immediate switch. From a 25% pentane concentration and upwards, the maximum selectivity for the reaction was always obtained. This could be regarded as evidence that something else is at play, and that the overall rate of the reaction is not strongly dependent on the pentane concentration. However, this might be incorrect and it could have a significant influence on the rate, but only between concentrations of 0 and 25%.

The alternative, and also more complicated explanation, requires knowledge of the alkyllithium aggregate structures in solution. The different aggregation states of alkyllithium reagents are known to play an instrumental role, with regards to both reactivity and selectivity, in the outcome of ortholithiation reactions.^{29,30} In pure Et₂O, *t*BuLi exists as a dimer,³¹ but when complexed to TMEDA it forms a monomer.³⁰ As was previously suggested for the oxazolines, without the presence of a hydrocarbon solvent, the Et₂O outcompetes the TMEDA for coordination to the *t*-BuLi, and the structural differences between the *t*-BuLi/Et₂O dimer and *t*-BuLi/TMEDA monomer (in pentane) are responsible for varied stereocontrol.

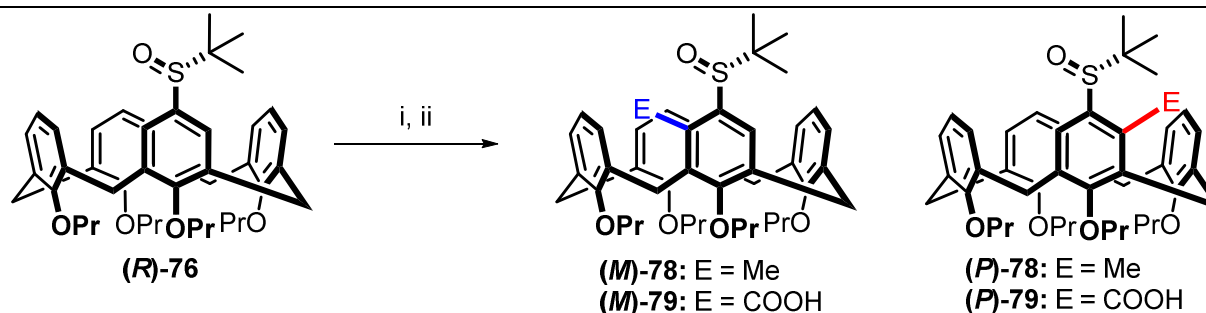
** The different structures and reactivity's of the alkyllithium aggregates were discussed in **Chapter 3**.

Chapter 4: Ortholithiation of sulfoxide calixarene

4.4.2 Quenching with different electrophiles – an investigation of versatility.

The S_2Me_2 electrophile had been used almost exclusively throughout the study. In terms of applicability and functionality, the thioether functional group offers limited use for further synthesis, both as a ligand or a building block for new inherently chiral compounds. In an effort to improve this, the scope of the method was evaluated by using numerous different electrophiles (Table 4.4).

Table 4.4: A summary of the different electrophiles tested for the ortholithiation of (*R*)-76.



Entry	RLi	Additive	Solvent	Electrophile	t (h)	Conv (%) ^a	de (%) ^a
1	<i>t</i> -BuLi	TMEDA	Et ₂ O/Pentane	S ₂ Me ₂	24	73	90
2	<i>t</i> -BuLi	TMEDA	Et ₂ O/Pentane	MeI	24	68	90
3	<i>t</i> -BuLi	TMEDA	Et ₂ O/Pentane	CO ₂	24	90	90
4	<i>t</i> -BuLi	TMEDA	Et ₂ O/Pentane	PPh ₂ Cl	24	-	-
5	<i>t</i> -BuLi	TMEDA	Et ₂ O/Pentane	DBE	24	-	-
6	<i>t</i> -BuLi	TMEDA	Et ₂ O/Pentane	B(OBn) ₃	24	-	-
7	<i>t</i> -BuLi	TMEDA	Et ₂ O/Pentane	B(OBu) ₃	24	-	-
8	<i>t</i> -BuLi	TMEDA	Et ₂ O/Pentane	Selectfluor	24	-	-
9	<i>t</i> -BuLi	TMEDA	Et ₂ O/Pentane	NFSI	24	-	-
10	<i>t</i> -BuLi	TMEDA	Et ₂ O/Pentane	DMF	24	-	-

Reagents and conditions: i) *t*-BuLi (6.0 equiv), TMEDA (12.0 equiv), Et₂O/Pentane, -78 °C, 24 h; ii) Electrophile (exs), -78 °C to rt, 12 h.

^aDetermined using ¹H NMR spectroscopy.

Of all the tested RLi electrophiles only CO₂, MeI and S₂Me₂ were able to successfully quench the ortholithiation reaction (entries 1-3). Even after multiple attempts of entries 4-10, only the starting material was ever recovered. To aid the quench, the method was adapted by heating the reaction mixture to 40 °C for 12 h after the addition of the electrophile. The experimental method was kept constant for each of the reactions (barring the later attempts of warming the reaction mixture). It is difficult to explain why these electrophiles yielded no product, especially because the ferrocene sulfoxides have been shown to tolerate many different reagents with little limitation. In fact, many classes of chiral sulfoxide ligand have been synthesized that incorporate a ferrocene core.^{7,8,10,32} On top of this, there are no literature examples of sulfoxide-based lithiation studies limited by electrophile choice. The only general differences between the successful and unsuccessful electrophiles might be their steric properties. The three electrophiles that formed the product were quite small, with minimal steric bulk, however the fact that dibromoethane is also a non-bulky electrophile and failed to yield the product works against a steric based argument.

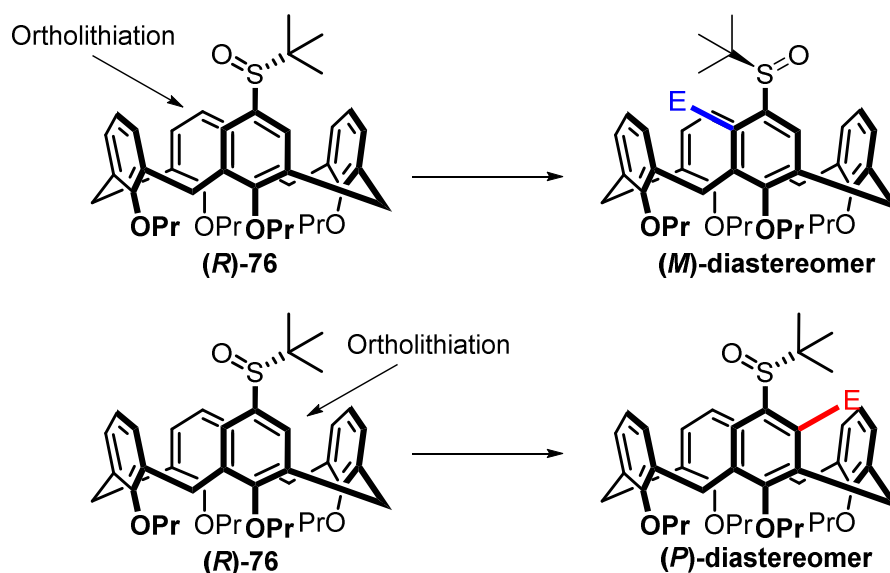
Chapter 4: Ortholithiation of sulfoxide calixarene

These results were unfortunate, as we had hoped to expand the scope of the reaction by incorporating numerous functional groups. This would have opened up new opportunities toward creating some of the first examples of inherently chiral sulfoxide ligands.

4.5 Determining the absolute configuration of inherently chiral calixarene products.

4.5.1 Configurations of the major and minor product diastereomers.

A subtle but important consideration was how the conformation of the sulfoxide, with respect to the inside of the calixarene bowl, changed upon formation of the product. Even though the same major diastereomer was forming for all of the alkyllithiums, at this point the absolute configuration of these two products was unknown. The chemical shift change of the sulfoxide *tert*-butyl group (δ 0.61 \rightarrow 1.27 ppm) indicated that the conformation of sulfoxide changed over the course of the reaction. For the starting material (**R**)-**76**, the *tert*-butyl group was positioned over the bowl of the calixarene, and was shielded by the calixarene's magnetic anisotropic effect. However, for the lithiated products the chemical shift of this functional group always changed to δ 1.27 ppm, suggesting that the *tert*-butyl functional group was no longer effected by the shielding inside the ring. At first it was assumed that that absolute configuration of the products could be determined using this information, since dipole interactions might determine the final conformation of the sulfoxide in the product diastereomers as depicted in (**Scheme 4.6**).



Scheme 4.6: Potential conformational changes of the sulfoxide induced by ortholithiation.

If ortholithiation were to take place on the left of the sulfoxide (top), it was rationalized that the oxygen atom would rotate towards the inside of the bowl, to avoid any dipole interactions, which would result in the *tert*-butyl functional group now being positioned on the outside of the calixarene. This would account for the downfield shift observed in the product. However, using this same argument, the formation of the opposite diastereomer would be unlikely to cause any changes in the sulfoxide's conformation.

Chapter 4: Ortholithiation of sulfoxide calixarene

If this were the case, then logically the chemical shift of the *tert*-butyl functional group for the (*P*)-diastereomer product would either be equal, or close to that of the starting material. This was however not observed, since reactions with low diastereoselectivity also gave good yields, using this signal as the marker (see entry 1, **Table 4.3**). The other possibility was that the chemical shift of the *tert*-butyl group for the (*P*)-diastereomer product was unique, but careful review of these ^1H NMR spectra showed no sign of the signal, and it was concluded that the *tert*-butyl group of both diastereomers occurred at the same chemical shift. Not only did this pose a problem for assigning the absolute configuration of the diastereomer products, it introduced inconsistencies when trying to rationalize the sulfoxide group's conformational change. These ^1H proton NMR spectra indicated that the sulfoxide in both (*P*) and (*M*) diastereomers had the same conformation. In order to explain why this shift was equal for the (*P*) and (*M*) diastereomers, the thio-methyl products required good quality characterization data, as there were too many contaminant signals in the crude ^1H NMR spectra to be certain of the assignments.

As discussed for the oxazolines in **Chapter 3**, the starting sulfoxide material and product compounds had almost identical R_f values and any attempts at chromatographic separation resulted in co-elution. Unfortunately, the ortholithiation of (**R**)-**76** was never as efficient as the oxazolines, and a substantial amount of starting material was always present in the crude reaction mixtures. Using an extremely slow separation on an auto column, enabled the partial separation of the product diastereomers and starting material. The fractions that contained only the major diastereomer were collected, and **77** was fully characterized for the first time. The ^1H NMR spectrum for this compound is depicted below (**Figure 4.4**).

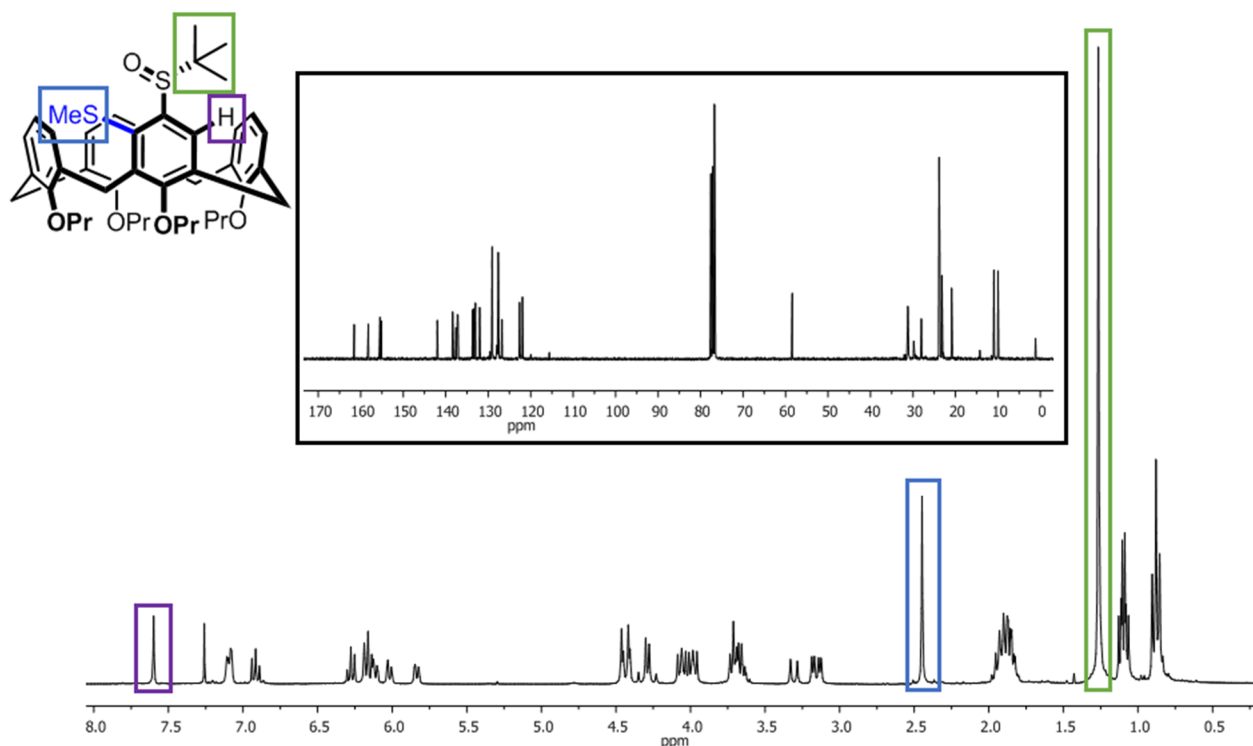


Figure 4.4: The ^1H (below) and ^{13}C (above, outlined in black) NMR spectra of the major thioether diastereomer **77**. Sulfoxide *tert*-butyl signal outlined in green. Thio-methyl signal outlined in blue. *Ortho*-proton outlined in purple.

Both 1D and 2D NMR spectra were collected for this compound, which have been fully assigned in **Section 4.9**. Combination of the 1D and 2D NMR spectroscopic data collected for **77** revealed some less obvious conformational differences between the calixarene structures of this compound and (**R**)-**76**. The ^1H NMR spectrum contained the three characteristic signals expected for the sulfoxide thio-ether **77**. After ortholithiation the singlet for the sulfoxide *tert*-butyl group shifted more down-field, with a chemical shift of δ 1.27 ppm that integrated for 9 protons (outlined in green). The thio-methyl singlet had a chemical shift of δ 2.45 ppm and integrated for three protons (outlined in blue). The remaining *ortho*-proton of the major diastereomer had a chemical shift of δ 7.60 ppm (outlined in purple). After careful comparison (**Figure 4.5**), the NMR spectra of **76** and **77** revealed several significant differences, and these were essential to understanding more about the conformational differences of the product. One of the most notable of these changes were the signals for the axial and equatorial protons. (**R**)-**76** had the expected 4/4 signal distribution (the de-shielded signals corresponding to the four axial protons and the shielded signals corresponding to the four equatorial protons). At first glance both sets seemed to be a complex multiplet, but closer investigation revealed four separate groups of doublets that overlapped with each other. Two of these were almost identical, and represented the equatorial protons on the methylene bridges on either side of the sulfoxide group. The other two separate doublets corresponded to the two remaining equatorial bridging protons. The doublets for the four axial protons appeared to be more uniform, suggesting a shared electronic environment.

Chapter 4: Ortholithiation of sulfoxide calixarene

What was interesting was the comparison of these signals to the same two signal-groups in **77**. The expected 4/4 integration pattern was replaced by a 5/3 grouping instead. This unusual arrangement of signals is further supported by a change in the ^{13}C NMR spectra, where a shift in one of the methylene carbon signals was observed ($\pm \delta 30.00 \rightarrow 28.03$ ppm). This carbon shift corresponded to the unusual shift in $\text{ArCH}_2^{\text{eq}}\text{Ar}$ proton signal and was confirmed by a correlation seen in the 2D hsqc NMR data ($\delta 4.30 / 28.03$ ($\text{ArCH}_2^{\text{ax}}\text{Ar}$ / C-7) and $\delta 4.31 / 28.03$ ($\text{ArCH}_2\text{Ar}^{\text{eq}}$ / C-7) (see **Experimental section** for the fully assigned spectral data)). The 5/3 distribution of the axial and equatorial protons in **77** is depicted below (**Scheme 4.5**).

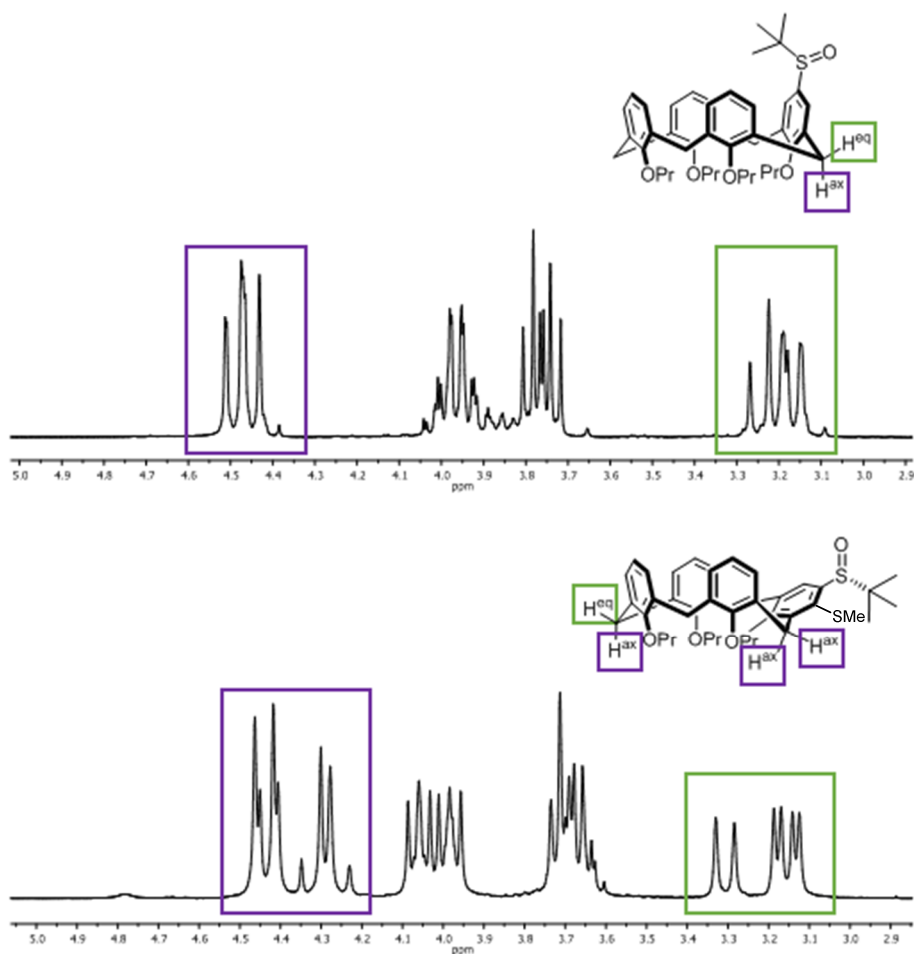


Figure 4.5: 4/4 (top) and 5/3 (bottom) distribution of the axial (outlined in purple) and equatorial (outlined in green) protons in **76** and **77**.

It could be that the presence of the thioether group significantly changes the electronic environment of the H^{ax} and H^{eq} bridging protons, but one would have expected to see a change for both of the protons and not just the one. Rather, it is proposed that the addition of the thioether distorts the conformation of the molecule slightly, pushing one of the methylene bridges down, and in so doing moving the equatorial proton out of the anisotropic shielding environment. This departure from the pinch cone conformation of the starting material was more apparent when comparing the aromatic regions of (*R*)-**76** and **77** (**Figure 4.6**).

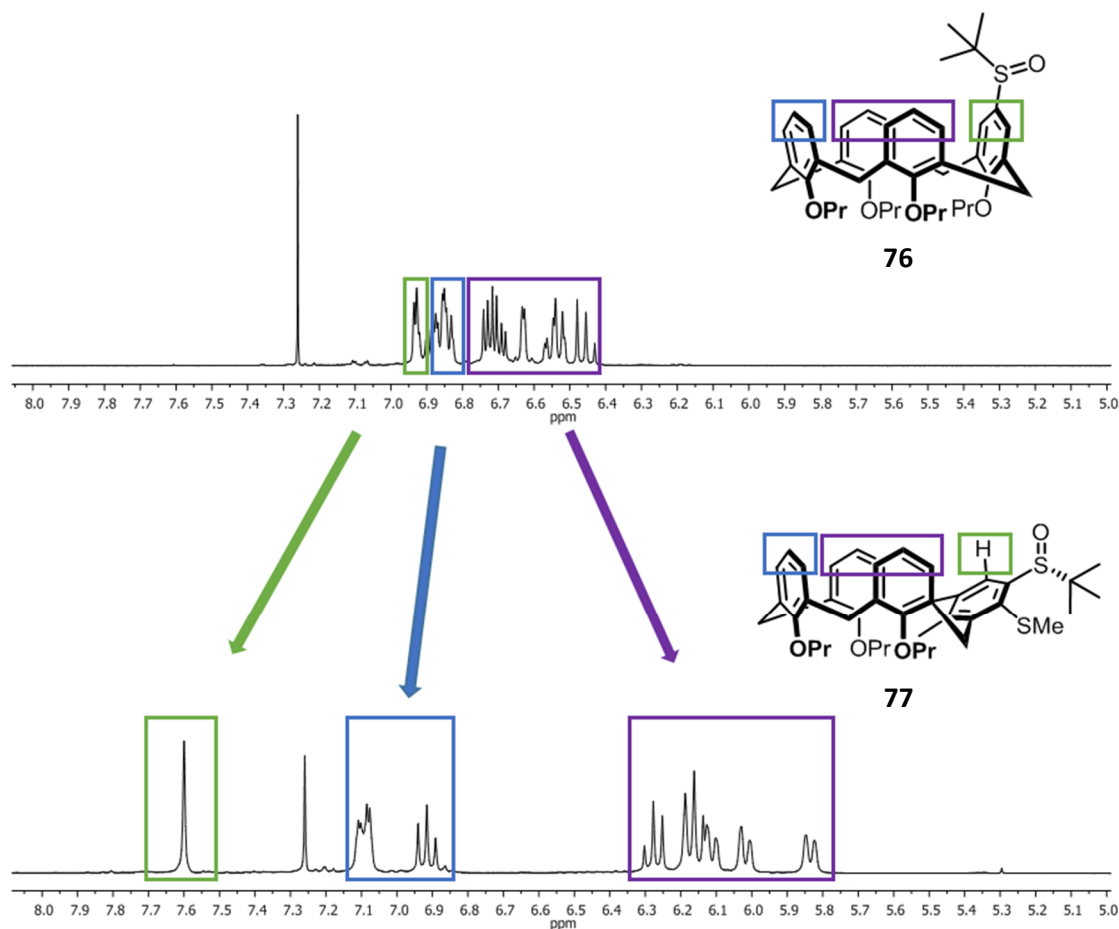


Figure 4.6: Comparison of the ^1H NMR spectroscopy aromatic regions for compounds **76** and **77**. The proton signals have been outlined in green for the functionalized aryl ring, and in blue on the aromatic ring opposite it. The signals on the remaining two rings have been outlined in purple.

In the pinched cone conformation for **76**, the signals for all of the aromatic protons are spaced relatively close together, and lie within a chemical shift range of δ 6.43-6.94 ppm. After lithiation, the conformation of the product changes considerably. This is represented by a significant chemical shift (δ 6.43-6.74 \rightarrow 5.82-6.30 ppm, outlined in purple) of the proton signals for the aromatic rings on either side of the functionalized aryl ring. The up-field shift can be explained by the position of these aromatic rings bending inwards, closer to the center of the calixarene, into the magnetic anisotropic environment. The signals for the protons on the aromatic ring opposite the sulfoxide, have shifted slightly downfield in the product (δ 6.83-6.90 \rightarrow 6.89-7.11 ppm, outlined in blue) suggesting that the position of this aromatic ring has shifted further away from the calixarene center. Lastly, the signals for the protons on the sulfoxide aryl ring have also undergone a significant downfield shift (δ 6.92 \rightarrow 7.60 ppm, outlined in green). The changes in the chemical shifts for these signals suggest that the pinched cone conformation of **77** is severely distorted, to the point where the sulfoxide aryl ring is positioned entirely away from the center of the calixarene (as it has been depicted in **Figure 4.6**).

Chapter 4: Ortholithiation of sulfoxide calixarene

It is proposed that when in this acutely distorted pinched cone conformation, the sulfoxide functional group is situated far enough from the centre of the calixarene, so that it is no longer affected by the magnetic anisotropic environment. This would explain why the changes in the sulfoxide conformation, if any, during the formation of the (*M*) and (*P*) products were undetectable spectroscopically. This made it impossible to assign the absolute configuration of these products from their spectral data, and an alternative strategy was required.

4.5.2 Assigning the absolute configuration of the diastereomer products.

When confronted with the problem of determining the absolute stereochemistry of the major and minor diastereomers in the ortholithiation reaction, three possible solutions were envisioned. The most convenient method would have been to obtain a crystal structure of the product. Alternatively, the theoretical CD spectra of the major and minor diastereomers could have been determined, and then compared to the actual CD spectrum of the product.^{33–36} Lastly, **76** could be used to synthesize an inherently chiral calixarene, previously synthesized by Dr Simon Herbert, with a known absolute configuration (**Figure 4.7**).³⁷ Comparison of their specific rotation $[\alpha_D]$ values would confirm the identities of the major and minor sulfoxide diastereomers (*M*)-**77** and (*P*)-**77**.

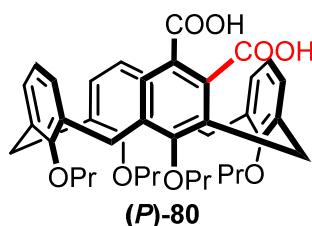
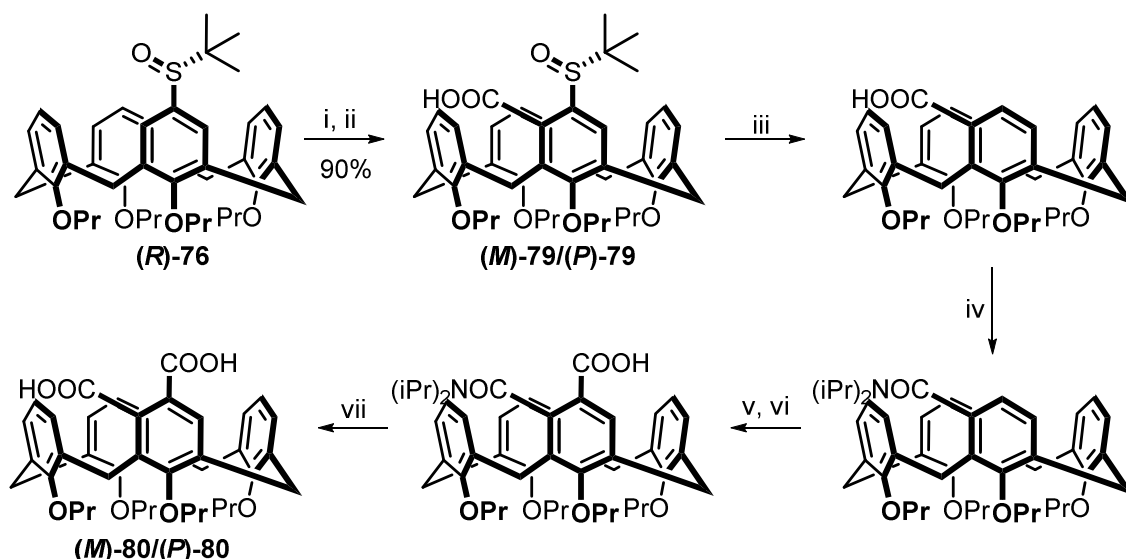


Figure 4.7: Inherently chiral di-carboxyl calixarene (**(P)-80**).³⁷

4.5.2.1 The synthetic approach.

Mr. Lesotho had previously attempted the crystallization of the thiomethyl sulfoxides (*M*)-**77** and (*P*)-**77**, but was unsuccessful. Therefore, we decided to approach the problem synthetically and planned the synthesis of **80** with the chiral sulfoxide calixarene (**(R)-76**) as the starting point (**Scheme 4.7**).



Scheme 4.7: The proposed synthetic strategy for the synthesis of inherently chiral **80** for comparison with the optical rotation of a known sample. Reagents and conditions: i) *t*-BuLi (6.0 equiv), TMEDA (12.0 equiv), pentane/Et₂O, -78 °C, 24 h; ii) CO₂ (gas, exs); iii) Raney nickel; iv) SOCl₂, di-isopropyl amine; v) *n*-BuLi (2.0 equiv), TMEDA (4.0 equiv); vi) CO₂ (gas, exs); vii) KOH (exs), EtOH, Δ, 24 h.

Unlike the oxazoline that hydrolyzed directly to the carboxylic acid, the sulfoxide would be completely removed upon desulfurization. The aim of the above strategy was focused on re-introducing the carboxylic acid functional group *para* to the propoxy group on the functionalized aryl ring. After the ortholithiation of **(R)-76** (i, ii), the following step was going to be a desulfurization reaction using Raney nickel. The carboxylic acid was then going to be used to synthesis di-isopropyl amide, a known directing group for metalation chemistry.³⁸ Another ortholithiation reaction was planned for the second last step, which would have added the second carboxylic acid group. Finally, hydrolysis of the amide would have yielded the targeted inherently chiral di-acid **80** whose optical rotation could be compared with a known sample. Fortunately, the crystallization of the diastereomers was successfully revisited after the carboxylic acid sulfoxide diastereomer mixture **79** was synthesized, thus avoiding the need to continue with this synthetic plan.

4.5.3 The crystallographic approach.

After isolating the carboxyl sulfoxide acid mixture **79**, a new series of crystallization experiments were attempted. The previous failed attempts at crystallization could be rationalized by the lack of symmetry in thioether calixarenes **77**. In addition to this, the thio-methyl functional group added little to aid the crystallization process. When the carboxylic acid **79** was first isolated, the ¹H NMR spectrum was filled with broad signals. It is likely that hydrogen bonding was causing an intermolecular interaction in the sample, which would have been slow on the NMR spectroscopy timescale and caused the line broadening. Fortunately, deuterated methanol improved the resolution of the broad peaks confirming this hypothesis.

Chapter 4: Ortholithiation of sulfoxide calixarene

A 20 mg sample of the inseparable mixture of diastereomers (**M**)/(**P**)-**79** ($de = 90\%$) was dissolved in chloroform (1.0 ml) in a small glass sample vial. This was then placed inside a larger vial containing ethanol and the system was closed to the atmosphere. After several days of slow diffusion under ambient conditions, a few colourless, block shaped crystals were obtained. A crystal was selected, mounted and a data set was collected.

The (**M**)/(**P**)-**79** calixarene mixture crystallized in the triclinic space group $P-1$, with one calixarene molecule and one ethanol solvent molecule located in the ASU (**Figure 4.8**). The molecule as depicted in **Figure 4.8** contains two complex structural elements that merit further discussion. These relate to the space group in which the calixarene has crystallized, as well as the distribution of the major and minor carboxylic acid components in the asymmetric unit (ASU). It is surprising to note that the chiral calixarene was found to crystallize in a centrosymmetric space group. The configuration of the sulfoxide group may appear to be fixed, but due to the inversion center, the molecule depicted in **Figure 4.8** represents only one half of the overall structural content, and it would be equally accurate to represent a mirrored version of this ASU. Since the major configuration of the sulfoxide auxiliary is known to be (*R*) (**Section 4.3**), it is depicted as such in the figure, but both (*R*) and (*S*) occur in equal amounts in the crystal structure.

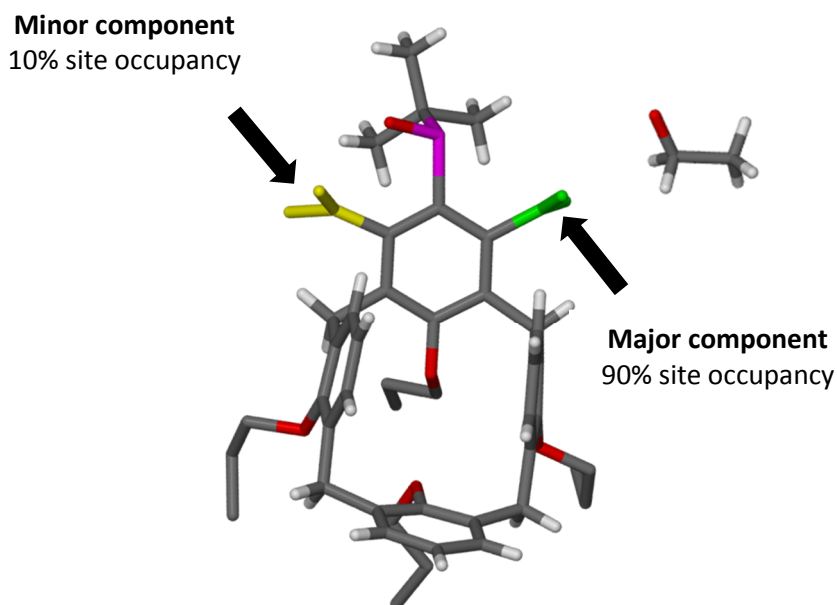
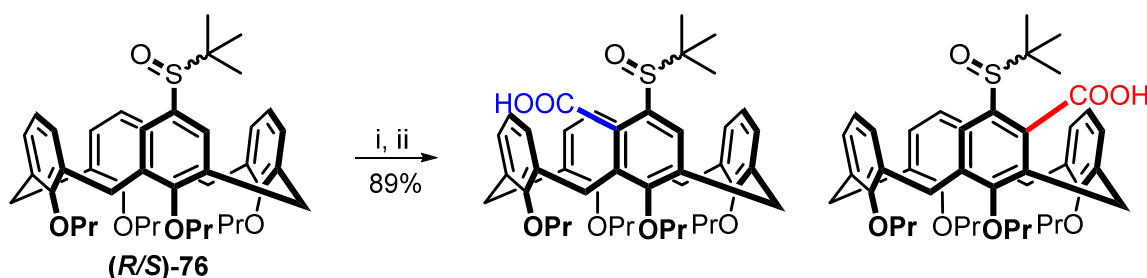


Figure 4.8: The asymmetric unit (ASU) of the (**M**)/(**P**)-**79** crystal structure showing one calixarene molecule (major carboxylic acid component shown in green, and minor in yellow) and one ethanol solvent molecule. The hydrogen atoms located on the propyl chains have been excluded for clarity.

Chapter 4: Ortholithiation of sulfoxide calixarene

Despite multiple crystallization attempts, employing various solvents, with several data collections (using both copper and molybdenum sources), the situation remained unchanged with all collected crystals exhibiting racemic behavior. The *ee* of **(R)**-76 was 94%, meaning that 97% of the sulfoxide group in the sample had the (*R*) configuration, and the remaining 3% the (*S*). To explain the formation of a racemic crystal, we propose that for crystallization to occur, both configurations of the sulfoxide auxiliary need to be present in order to facilitate efficient packing in the solid-state. Our hypothesis was that either configuration of the sulfoxide could act as a seed, enabling bulk nucleation. Once all of the (*S*)-sulfoxide crystallized, the remaining calixarene with the (*R*)-sulfoxide could no longer crystallize, and remained in solution. This could be due to unfavorable packing limitations associated with the presence of a single sulfoxide conformation. In support of this, it was observed that only a small number of crystals (<1 mg) were obtained from a 20 mg sample.

In an attempt to verify this hypothesis the afore mentioned crystallization experiment was repeated, but in place of **(M)/(P)**-79, a new version of the compound containing a racemic mixture of sulfoxide configurations was used. The racemic chiral *tert*-butyl thiosulfinate was synthesized by an achiral oxidation of di-*tert*-butyl disulfide. This was then used in the previously discussed lithium halogen exchange reaction to synthesize a racemic version of the chiral sulfoxide calixarene **(R/S)**-76. Finally, an ortholithiation reaction was used to synthesise the carboxylic acid sulfoxides (**Scheme 4.8**).



Scheme 4.8: Synthesis of the carboxylic sulfoxides. Reagents and conditions: i) *t*-BuLi (6.0 equiv), TMEDA (12.0 equiv), pentane, $-78\text{ }^{\circ}\text{C}$, 24 h; ii) CO_2 (gas, exs) $-78\text{ }^{\circ}\text{C}$ to rt, 12 h.

If the hypothesis that both configurations of the sulfoxide are necessary for crystallization to take place is correct, then a sample containing a 1:1 mixture of the two, should be much easier to crystallize. The same crystallization method was performed using 10 mg of the racemic mixture. After several days, small clusters had crystallized on the bottom of the vial, supporting our hypothesis (**Figure 4.9**).



Figure 4.9: Photomicrograph showing the pin-cushion clusters of the carboxylic sulfoxide crystals.

The crystals were isolated and dried, yielding a total mass of approximately 10 mg. TLC analysis of the mother liquor showed that minimal amounts of the calixarene material still remained in solution. ^1H NMR spectroscopic analysis of the crystals matched that of the bulk material used in the experiment and this result further supports the hypothesis that the presence of both configurations was necessary for crystallization to occur. Due to the morphological nature of the crystalline material (thin plates), a single crystal x-ray diffraction data set could unfortunately not be obtained.

The second aspect of the structure of **(M)/(P)-79** that requires further discussion involved the distribution of carboxylic acid functional group. The crystal structure depicted above shows an average, where one calixarene core is located superimposed on top of another, while the carboxylic acid is present in two positions of varying ratios on either side of the sulfoxide group (**Figure 4.8**). The major diastereomer has the carboxyl group (green) located opposite the oxygen atom with 90% site occupancy, while the carboxyl group (yellow) for the minor diastereomers occupies the opposite *ortho*-position with 10% site occupancy. Therefore, the *de* of diastereomers in the solid-state is 80%, which was considerably less than the bulk material with 90%. Closer examination of the structure showed hydrogen bonding between the minor diastereomer's carboxylic acid and the sulfoxide functional groups (**Figure 4.10**). This weakly stabilizing interaction was thought to be responsible for the increased inclusion of the carboxylic acid minor diastereomer during the crystallization process, thus effectively lowering the *de* of the product mixture in the solid-state.

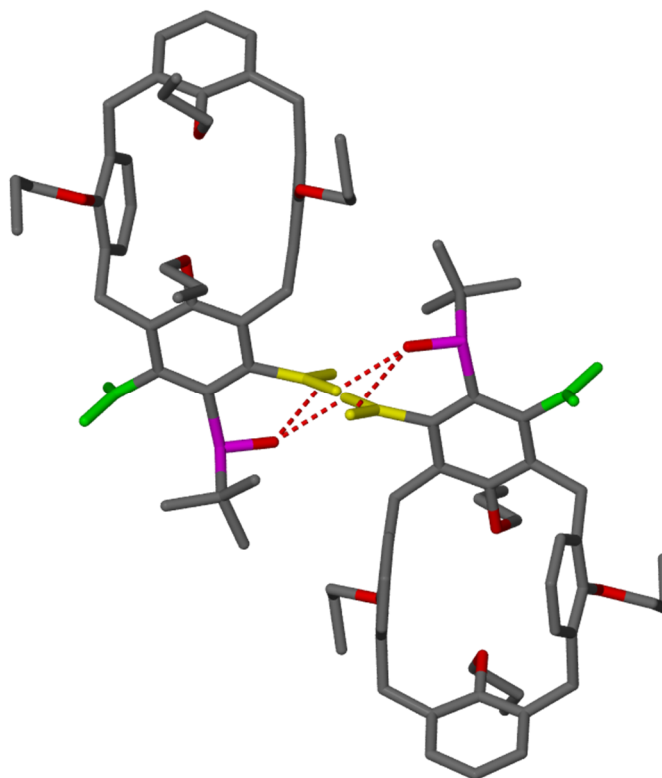


Figure 4.10: Hydrogen bonding (red dotted lines) between the carboxylic acid (yellow) and the neighboring sulfoxide oxygen atoms. This strong intermolecular interaction facilitates packing in the solid-state. Hydrogen atoms have been hidden for clarity.

When the asymmetric unit is extended, the structure adopts a brick like packing motif wherein neighboring calixarene molecules assemble with the propyl groups (lower-rim) alternating in an AB type arrangement (up-green/down-yellow). The two *tert*-butyl groups face in opposite directions, most likely to alleviate steric strain and enable π - π stacking interactions to occur between neighboring aryl rings (**Figure 4.11**).

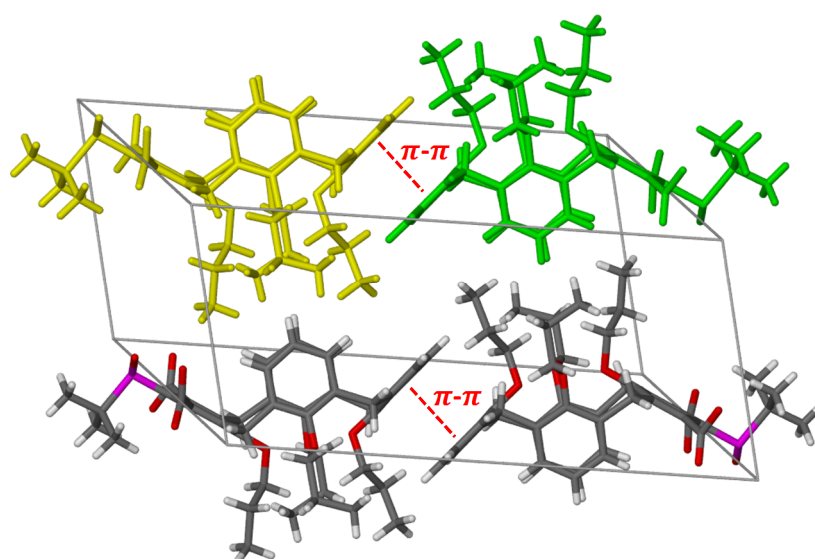


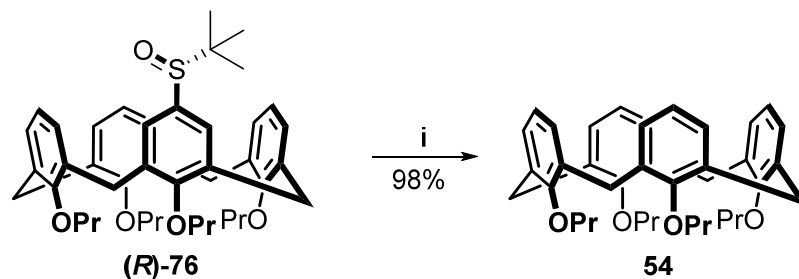
Figure 4.11: Alternating AB packing arrangement of molecules in the *(M)/(P)*-79 crystal structure.

Chapter 4: Ortholithiation of sulfoxide calixarene

This was the first definitive crystallographic example of an inherently chiral sulfoxide calixarene. In summary, this crystal structure definitely showed that the sulfoxide ortholithiation products have the (*M*) major and (*P*) minor inherently chiral configurations.

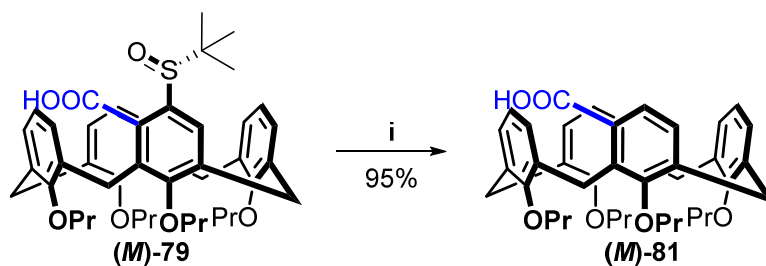
4.6 Removal of the sulfoxide group – the desulfurization reaction.

The removal of the sulfoxide group after the ortholithiation would yield a purely inherent chiral calixarene. Raney nickel is well known for its use as a desulfurization reagent.^{15,16} Our most commonly used electrophile, dimethyl disulfide, was an obvious problem when considering the removal of the sulfoxide group after lithiation. Fortunately the (*M*)-**78** and carboxylic acid sulfoxides (*M*)-**79** were suited for the Raney nickel reaction. Synthetically speaking, a methyl functional group is less interesting than a carboxylic acid, as it offers little option for further functionalization. Therefore we focused on (*M*)-**79** instead. At first, a test reaction was attempted with (*R*)-**76**, using the reaction conditions most often reported for desulfurization reactions (Scheme 4.9).



Scheme 4.9: Raney nickel test reaction. Reagent and conditions: i) Raney nickel (exs), EtOH, reflux, 12 h.

Even though excess Raney nickel under reflux conditions were the most commonly reported conditions, the reaction was first attempted at room temperature in the hopes of avoiding higher reaction temperatures. Unfortunately, after 12 hours there was no product formation. The same reaction mixture was then heated to reflux, checked again after an additional twelve hours, and none of **76** remained. In addition to the convenient experimental conditions, the work up for the reaction was a simple filtration. Due to the significant change in polarity after the removal of the sulfoxide, purification was readily achieved using column chromatography, which yielded **54** in an extremely high yield of 98%. The same reaction conditions were then attempted using calixarene (*M*)-**79** (Scheme 4.10).



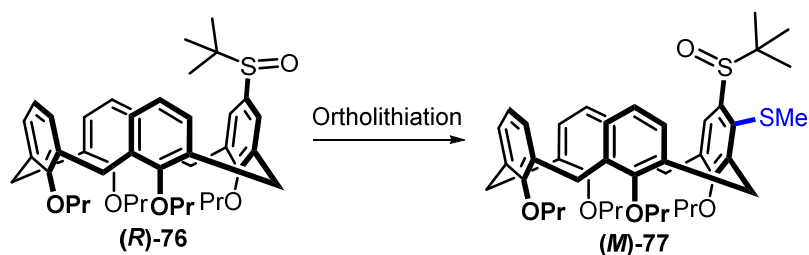
Scheme 4.10: Desulfurization of **(M)-79**. Reagents and conditions: i) Raney nickel (exs), EtOH, reflux, 12 h.

Raney nickel proved to be not only experimentally convenient, but also extremely efficient as the conversions for these reactions were consistently near quantitative. In this manner, the inherently chiral **(M)-81** was isolated in a 95% yield using column chromatography. The aromatic region of the ^1H NMR spectrum no longer had the characteristic singlet generally seen for the ortholithiation products, and instead had two new doublet signals, for the *ortho* and *ipso* protons, with chemical shifts of δ 7.01 ppm and δ 7.49 ppm ($J = 7.9$ Hz). The data for this compound was recently published and the ^1H NMR spectrum compares well with the reported data.³⁹

4.7 Discussion – unravelling the ortholithiation of sulfoxide calixarene 76.

The complexities associated with the mechanistic detail of directed metalation reactions were discussed in detail in **Chapter 3**. The aim of this section is not to repeat what has already been said, but rather to suggest a few of the simpler mechanistic details that could be applicable to chemistry reported here.

In **Section 4.4.1**, the stark difference in the outcome of the reactions performed in Et_2O and pentane already point to complexities associated with the reactivities of the different alkyllithium aggregation states. Despite this, careful review of the ^1H NMR spectra for the sulfoxide **(R)-76** and thioether **(M)-77** suggested that the conformation of the compound changed significantly over the course of the reaction. After *ortho*-functionalization of **(R)-76** a downfield shift in the *tert*-butyl signal of the sulfoxide always occurred. This implied that before lithiation, the preferred orientation of the *tert*-butyl group was toward the centre of the calixarene, and after lithiation it faced towards the outside of the bowl (**Scheme 4.11**). This is most likely due to the oxygen atom rotating to avoid dipole interactions or the steric clash it would experience with the newly introduced functional group in the *ortho*-position.



Scheme 4.11: Rotation of the sulfoxide group after ortholithiation to avoid steric clash.

In addition to the conformational differences between the starting material and product, the results from the ortholithiation using *n*, *s* and *t*-BuLi point to an increase in the stereocontrol as the bulk of the base increased. In an attempt to keep this explanation simple the general three step reaction sequence of 1) coordination, 2) proton abstraction and finally 3) electrophilic quench will be used.

The configuration of the starting material in solution is potentially one of the most important factors when trying to rationalize the stereochemical outcome of the reaction. Considering the (*R*) configuration of the sulfoxide functional group, the following two structures could be potential lithium-sulfoxide coordination intermediates (**Figure 4.12**).

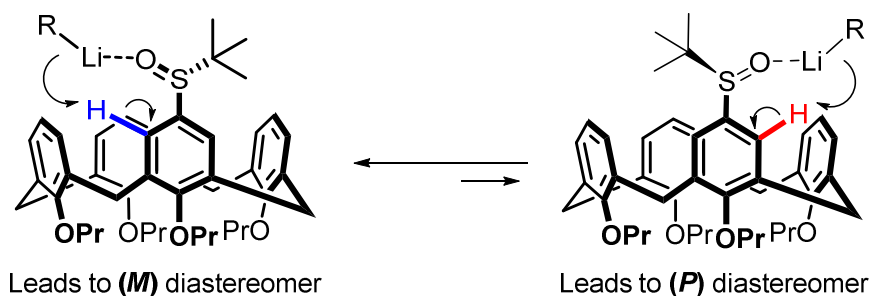


Figure 4.12: Two potential lithium-sulfoxide coordination intermediate structures.

The orientation of the sulfoxide would determine the position of the oxygen atom, which in turn would preferentially direct the coordination of the alkyllithium and subsequent selective deprotonation. Similar intermediate structures suggesting this oxygen-directed coordination and deprotonation have been previously suggested for the ferrocene sulfoxides.⁴⁰ Considering that the *tert*-butyl group prefers to be orientated over the calixarene bowl, the intermediate structure on the left would explain why deprotonation is directed to the *ortho*-position on the left of the aryl ring, forming the major diastereomer product. With the oxygen orientated to the other side, depicted by the intermediate on the right, deprotonation would lead to the minor diastereomer of the reaction.

The different selectivities seen for the reaction could be explained by the following consideration. Two of the proposed steps in the general mechanism are the coordination of the alkyllithium to the directing group, which is then followed by a proton abstraction, forming the anionic lithiated intermediate. If the deprotonation of the *ortho*-proton occurred at a much higher rate, relative to the formation of the lithium-directing group complex, then in the case of the sulfoxide we would expect a similar selectivity for all

Chapter 4: Ortholithiation of sulfoxide calixarene

of the alkyllithium bases. If the deprotonation was essentially taking place just as, or right after the coordination, then the preferred conformation of the sulfoxide before coordination would dominate the selectivity and not the base. However, this is not what is suggested by the results, as each of the alkyllithium bases gave a unique selectivity.

Alternatively, if the coordination was much faster, and the deprotonation the much slower rate limiting step, then the structural properties of the coordination complex would potentially have a significant effect on the stereochemical outcome of the reaction. Given that the structures of the different alkyllithium aggregates differ, it could be that coordination effects the conformation of the sulfoxide, and in so doing the position of the oxygen group. After coordination, the conformation and position of the sulfoxide would adjust to accommodate any newly introduced steric strain and this adjusted structural conformation could shift the position of the oxygen and affect the preferred site of deprotonation.

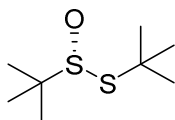
Even though we are again only able to theorize and suggest explanations, the mechanistic study of the sulfoxide presents an interesting opportunity. With only one coordinating group (the oxygen) coupled with the ease of its synthesis and introduction to the calixarene, it presents far less of a challenge compared to the oxazoline calixarenes.

4.8 Conclusion.

We have reported the successful ortholithiation of a chiral sulfoxide calixarene. We have shown that the chiral *tert*-butyl sulfoxide can be used to selectively synthesize inherently chiral calixarenes in *de* up to 90%. Additionally, an efficient desulfurization method has been used to synthesize a new inherently chiral calixarene. Despite the method's limitation, with respect to electrophile choice, the carboxyl functional group does provide some degree of versatility and opens up the possibility of synthesizing new inherently chiral materials. Unlike the oxazoline calixarenes, the use of sulfoxide directing group in the ortholithiation reaction was only able to selectively yield one of the diastereomers. In spite of this, both configurations of the sulfinate ester are easily accessible and the opposite diastereomer of the ortholithiation reaction could be obtained by simply inverting the configuration of the sulfoxide directing group. Lastly, the absolute stereochemistry of the inherently chiral diastereomers was determined using a crystallographic approach.

4.9 Experimental section.

4.9.1 (*R*)-*tert*-butyl *tert*-butanethiosulfinate – 75.²⁷

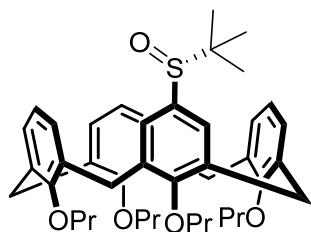


VO(acac)₂ (55.7 mg, 0.25 mol%) and ligand (73.0 mg, 0.26 mol%) were added to freshly distilled chloroform under argon and stirred at room temperature for 15 min. Di-*tert*-butyl-disulfide (15.0 g, 84.1 mmol) was then added and the reaction mixture was cooled (–18 °C). 30% aq. H₂O₂ (11.0 ml, 1.15 equiv) was then added drop-wise and after addition the low temperature was maintained while stirring the reaction mixture for 24 h. The contents of the flask was transferred to a separating funnel, after which the organic layer was washed with brine (2 × 100 ml), dried over MgSO₄ and the excess solvent was removed under reduced pressure. The colourless oil was purified by a low temperature recrystallization in pentane (–18 °C), affording the chiral sulfinate ester as white crystals (7.83 g, 40.36 mmol, 48%).

The characterisation data collected for this compound compared well with the reported literature values.²⁷

¹H NMR (300 MHz, CHLOROFORM-*d*) δ 1.38 (s, 9H, C(CH₃)₃), 1.55 (s, 9H, C(CH₃)₃) ppm.

4.9.2 (*R*)-5-*tert*-butylsulfinyl-25,26,27,28-tetrapropoxycalix[4]arene – 76.



Calixarene **55** (1.30 g, 1.94 mmol) was added to dry THF (8 ml), and cooled to –78 °C. *n*-BuLi (2.12 ml, 2.98 mmol, 2.0 equiv) was carefully added, turning the colourless mixture a clear pale yellow. After stirring for 20 minutes at –78 °C, (*R*)-*tert*-butyl *tert*-butanethiosulfinate (867 mg, 4.47 mmol, 3.0 equiv) was added to dry THF (4.0 ml) and slowly added dropwise to the cool mixture. The mixture was then stirred for 3 h at –78 °C, after which, it was given time to slowly warm to room temperature. The reaction was quenched with water (5 ml) and EtOAc (30 ml) was added to the flask. The contents of the flask was transferred to a separating funnel and the organic layer was washed once with both 1 M HCl (50 ml) and Brine (50 ml). The organic layer was dried over MgSO₄ and the excess solvent was removed under reduced pressure. After drying over MgSO₄, the excess solvent was removed under reduced pressure, yielding a pale yellow semi-solid as the crude product. Purification was achieved via silica gel column chromatography (EtOAc:PET, 20:80) yielding a white foam (0.92 g, 68 %) as the final product.

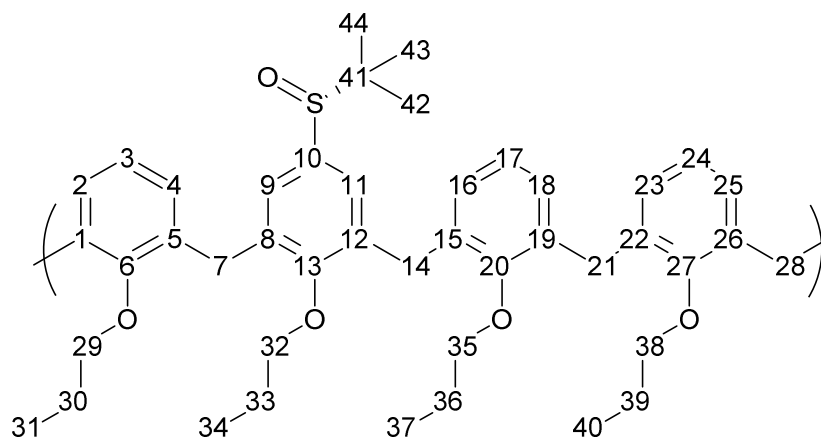


Figure 4.13: Numbering of **76** used to assign the 1D and 2D NMR spectroscopic data.

^1H NMR (300 MHz, CHLOROFORM-*d*) δ 0.61 (s, 9H, $\text{SC}(\text{CH}_3)_3$), 0.96 (t, $J = 7.5$ Hz, 6H, $\text{OCH}_2\text{CH}_2\text{CH}_3$), 1.04 (t, $J = 7.5$ Hz, 3H, $\text{OCH}_2\text{CH}_2\text{CH}_3$), 1.05 (t, $J = 7.5$ Hz, 3H, $\text{OCH}_2\text{CH}_2\text{CH}_3$), 1.87-1.96 (m, 4H, $\text{OCH}_2\text{CH}_2\text{CH}_3$), 2.00-2.11 (m, 4H, $\text{OCH}_2\text{CH}_2\text{CH}_3$), 3.16 (d, $J = 12.9$ Hz, 1H, $\text{ArCH}_2^{\text{ax}}\text{Ar}$), 3.17 (d, $J = 12.9$ Hz, 1H, $\text{ArCH}_2^{\text{ax}}\text{Ar}$), 3.20 (d, $J = 12.9$ Hz, $\text{ArCH}_2^{\text{ax}}\text{Ar}$), 3.34 (d, $J = 12.9$ Hz, 1H, $\text{ArCH}_2^{\text{ax}}\text{Ar}$), 3.74 (t, $J = 7.3$ Hz, 2H, $\text{OCH}_2\text{CH}_2\text{CH}_3$), 3.79 (t, $J = 7.3$ Hz, 2H, OCH_2CH_2), 3.90-4.03 (m, 4H, $\text{OCH}_2\text{CH}_2\text{CH}_3$), 4.45 (d, $J = 12.9$ Hz, 2H, $\text{ArCH}_2^{\text{eq}}\text{Ar}$), 4.48 (d, $J = 12.9$ Hz, 1H, $\text{ArCH}_2^{\text{eq}}\text{Ar}$), 6.44-6.47 (m, 1H, ArH), 6.52-5.56 (m, 2H, ArH), 6.63 (d, $J = 1.8$ Hz, 1H, ArH), 6.69-6.73 (m, 2H, ArH), 6.83-6.93 (m, 5H, ArH) ppm.

Owing to minimal variations in the chemical shifts for certain signals in the ^{13}C NMR spectrum, the values have been reported with two decimal places instead of one.

^{13}C NMR (75 MHz, CHLOROFORM-*d*) δ 10.21 (2 \times C-31|34|37|40), 10.64 (C-31|34|37|40), 10.65 (C-31|34|37|40), 22.62 (C-42, 43 and 44), 23.24 (2 \times C-30|33|36|39), 23.46 (C-30|33|36|39), 23.50 (C-30|33|36|39), 30.93 (C-7|14), 30.96 (C-7|14), 31.00 (C-21|28), 31.10 (C-21|28), 55.11 (C-41), 76.78 (2 \times C-29|32|35|38), 77.47 (C-29|32|35|38), 77.66 (C-29|32|35|38), 122.50 (C-3|17), 122.64 (C-3|17), 122.75 (C-24), 125.79 (C-9|11), 126.70 (C-9|11), 128.06 (C-4|16), 128.18 (C-4|16), 128.37 (C-2|18), 128.67 (C-2|18), 128.88 (C-23|25), 128.89 (C-23|25), 131.92 (C-10), 134.11 (C-8|12), 134.18 (C-8|12), 134.43 (C-1|5|15|19), 135.18 (C-1|5|15|19), 135.24 (C-22|26), 135.42 (C-22|26), 135.86 (C-1|5|15|19), 136.04 (C-1|5|15|19), 155.72 (C-27), 156.74 (C-6|20), 156.80 (C-6|20), 158.18 (C-13) ppm.

^1H , ^1H COSY (300/300 MHz 278 K, CHLOROFORM-*d*): $\delta^1\text{H} / \delta^1\text{H}$ 1.88 / 1.05 ($\text{OCH}_2\text{CH}_2\text{CH}_3$ / $\text{OCH}_2\text{CH}_2\text{CH}_3$), 3.88 / 2.04 ($\text{OCH}_2\text{CH}_2\text{CH}_3$ / $\text{OCH}_2\text{CH}_2\text{CH}_3$), 4.43 / 3.18 ($\text{ArCH}_2^{\text{ax}}\text{Ar}$ / $\text{ArCH}_2^{\text{eq}}\text{Ar}$), 4.51 / 3.19 ($\text{ArCH}_2^{\text{ax}}\text{Ar}$ / $\text{ArCH}_2^{\text{eq}}\text{Ar}$), 6.54 / 6.48 (ArH / ArH), 6.85-6.69 (ArH / ArH), 6.92 / 6.75 (ArH / ArH) ppm.

Chapter 4: Ortholithiation of sulfoxide calixarene

^1H , ^{13}C HSQC (300/75 MHz, 278 K, CHLOROFORM-*d*) δ ^1H / δ ^{13}C : 0.62 / 22.62 ($\text{C}(\text{CH}_3)_3$ / C-42,43 and C-44, 0.97 / 10.21 ($\text{OCH}_2\text{CH}_2\text{CH}_3$ / C-31|34|37|40), 1.03 / 10.64 ($\text{OCH}_2\text{CH}_2\text{CH}_3$ / C-31|34|37|40), 1.05 / 10.65 ($\text{OCH}_2\text{CH}_2\text{CH}_3$ / C-31|34|37|40), 1.85-1.98 / 23.24 ($\text{OCH}_2\text{CH}_2\text{CH}_3$ / C-30|33|36|39), 1.99-2.10 / 23.46 ($\text{OCH}_2\text{CH}_2\text{CH}_3$ / C-30|33|36|39), 1.99-2.10 / 23.50 ($\text{OCH}_2\text{CH}_2\text{CH}_3$ / C-30|33|36|39), 3.16 / 30.93 ($\text{ArCH}_2^{\text{eq}}\text{Ar}$ / C-7|14), 3.17 / 30.96 ($\text{ArCH}_2^{\text{eq}}\text{Ar}$ / C-7|14), 3.19 / 31.00 ($\text{ArCH}_2^{\text{eq}}\text{Ar}$ / C-21|28), 3.25 / 31.10 ($\text{ArCH}_2^{\text{eq}}\text{Ar}$ / C-21|28), 3.74 / 76.78 ($\text{OCH}_2\text{CH}_2\text{CH}_3$ / C-29|32|35|38), 3.78 / 76.78 ($\text{OCH}_2\text{CH}_2\text{CH}_3$ / C-29|32|35|38), 3.88-4.04 / 77.47, 77.66 ($\text{OCH}_2\text{CH}_2\text{CH}_3$ / C-29|32|35|38, C-29|32|35|38), 4.45 / 30.93, 30.96 ($\text{ArCH}_2^{\text{eq}}\text{Ar}$ / C-7 and C-14), 4.49 / 31.00 ($\text{ArCH}_2^{\text{ax}}\text{Ar}$ / C-21|28), 4.53 / 31.10 ($\text{ArCH}_2^{\text{ax}}\text{Ar}$ / C-21|28), 6.46 / 128.18, 128.37 (ArH / C-4|16, C-2|18), 6.54 / 128.06, 128.67 (ArH / C-4|16, C-2|18), 6.63 / 128.06 (ArH / C-4|16), 6.65 / 128.37 (ArH / C-2|18), 6.71 / 122.50 (ArH / C-3|17), 6.87-6.84 / 122.75, 128.88, 128.89 (ArH / C-24 and C-23|35), 6.93 / 125.79, 127.70 (ArH / C-9|11, C-9|11) ppm.

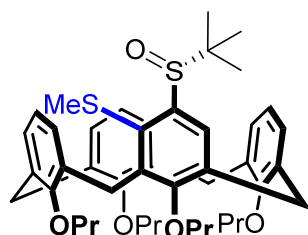
^1H , ^{13}C HMBC (300/75 MHz, 278 K, CHLOROFORM-*d*) δ ^1H / δ ^{13}C : 0.61 / 55.11 ($\text{C}(\text{CH}_3)_3$ / C-41), 0.93 / 23.24, 76.78 ($\text{OCH}_2\text{CH}_2\text{CH}_3$ / C-30|33|36|39, C-29|32|35|38), 1.03 / 23.46, 77.47 ($\text{OCH}_2\text{CH}_2\text{CH}_3$ / C-30|33|36|39, C-29|32|35|38), 1.05 / 23.50, 77.66 ($\text{OCH}_2\text{CH}_2\text{CH}_3$ / C-30|33|36|39, C-29|32|35|38), 1.85-2.10 / 10.21, 10.64, 10.65, 76.78, 77.47, 77.66 ($\text{OCH}_2\text{CH}_2\text{CH}_3$ / C-31|34|37|40, C-31|34|37|40, C-31|34|37|40, C-29|32|35|38, C-29|32|35|38, C-29|32|35|38), 3.16 / 128.37, 128.67, 135.86, 136.04, 156.80, 158.18 ($\text{ArCH}_2^{\text{eq}}\text{Ar}$ / C-2|18, C-2|18, C-1|5|15|19, C-6|20, C-13), 3.23 / 128.06, 128.18, 135.24, 135.42, 155.72, 156.74 ($\text{ArCH}_2^{\text{eq}}\text{Ar}$ / C-4|16, C-4|16, C-22|26, C-22|26, C-27, C-6|20), 3.74 / 10.64, 23.46, 155.72 ($\text{OCH}_2\text{CH}_2\text{CH}_3$ / C-31|34|37|40, C-30|33|36|39, C-27), 3.78 / 10.65, 23.24, 156.74 ($\text{OCH}_2\text{CH}_2\text{CH}_3$ / C-31|34|37|40, C-30|33|36|39, C-6|20), 3.88-4.04 / 10.21, 23.24, 156.80, 158.18 ($\text{OCH}_2\text{CH}_2\text{CH}_3$, C-31|34|37|40, C-6|20, C-13), 4.44 / 128.67, 128.88, 134.11, 135.86, 155.72 ($\text{ArCH}_2^{\text{ax}}\text{Ar}$, C-2|18, C2-18, C-8|12, C1|5|15|19, C-27), 4.53 / 128.88, 135.20, 158.18 ($\text{ArCH}_2^{\text{eq}}\text{Ar}$, C-23|25, C-22|26, C-13), 6.43-6.57 / 30.93, 30.96, 31.00, 31.10 122.50, 122.64, 135.86, 136.04, 156.74, 156.80 (C-16|18 and C2|4-*H* / C-7|14, C-7|14, C-21|28, C-21|28, C-3|17, C-3|17, C-1|5|15|19, C-1|5|15|19, C-6|20, C-6|20), 6.62-6.74 / 125.75, 128.08, 128.16, 135.86, 136.04, 156.72, 156.74 (C-3 and C-17 / C-9|11, C-4|16, C-2|18, C-1|5|15|19, C-1|5|15|19, C-6|20, C-6|20), 6.83-6.90 / 31.00, 31.10, 122.75, 128.68, 128.89, 135.24, 135.42, 155.72 (C23,24 and C-25-*H* / C-21|28, C21|28, C-24, C23|25, C23|25, C-22|26, C22|26, C-27), 6.94 / 30.96, 126.70, 134.11, 134.18, 158.18 (C9-*H* or C11-*H*) / C-7|14, C9|11, C-8|12, C-8|12, C-13) ppm.

IR (ATR) cm^{-1} : 2873 (s, -CH stretch), 1450 (s, C=C stretch), 1049 (s, S=O stretch), 959 (m, C-H oop bend), 758 (s, C-H oop bend).

HRMS-TOF MS ESI+: m/z [$\text{M}+\text{H}$] $^+$ calculated for $\text{C}_{45}\text{H}_{58}\text{O}_5\text{S}$: 697.3926; Found: 697.3929.

Chapter 4: Ortholithiation of sulfoxide calixarene

4.9.3 (M)-((R)-5-tert-butylsulfinyl)-4-methylthio-25,26,27,28-tetrapropoxycalix[4]arene – 77.



Thioether calixarene (**M**)-77 was synthesized according to the general ortholithiation procedure outlined in **Chapter 3**, however the alkyllithium solvent was not removed. (**R**)-76 (100 mg, 0.143 mmol), *t*-BuLi (0.659 mmol, 6.0 equiv), TMEDA (0.264 ml, 1.72 mmol, 12 equiv) and dimethyl disulfide (0.254 ml, 2.86 mmol, 20.0 equiv) were combined with a reaction time of 24 h. Purification was achieved via silica gel column chromatography (auto column) using 24 g of silica, EtOAc/PET (15:85) with a flow rate of 18 ml/min, affording a white semi-solid (51.0 mg, 48%).

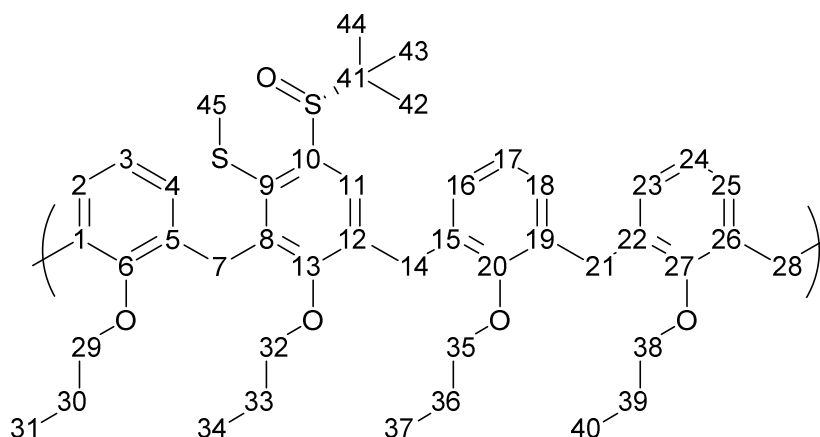


Figure 4.14: Numbering of (**M**)-77 used to assign the 1D and 2D NMR data.

^1H NMR (300 MHz, CDCl_3) δ 0.90 (t, 6H, $J = 7.4$ Hz, $\text{CH}_2\text{CH}_2\text{CH}_3$), 1.11 (t, 3H, $J = 7.4$ Hz, $\text{CH}_2\text{CH}_2\text{CH}_3$), 1.13 (t, 6H, $J = 7.4$ Hz, $\text{CH}_2\text{CH}_2\text{CH}_3$), 1.29 (s, 9H, $\text{C}(\text{CH}_3)_3$), 1.82-2.00 (m, 8H, $\text{CH}_2\text{CH}_2\text{CH}_3$), 2.47 (s, 3H, SCH_3), 3.15 (d, $J = 13.5$ Hz, 1H, $\text{ArCH}_2^{\text{eq}}\text{Ar}$), 3.17 (d, $J = 13.5$ Hz, 1H, $\text{ArCH}_2^{\text{eq}}\text{Ar}$), 3.33 (d, $J = 13.5$ Hz, 1H, $\text{ArCH}_2^{\text{eq}}\text{Ar}$), 3.63-3.74 (m, 4H, $\text{CH}_2\text{CH}_2\text{CH}_3$), 3.96-4.09 (m, 4H, $\text{CH}_2\text{CH}_2\text{CH}_3$), 4.23-4.35 (m, 2H, $\text{ArCH}_2^{\text{ax}}\text{Ar}$, $\text{ArCH}_2^{\text{eq}}\text{Ar}$), 4.42 (d, $J = 13.5$ Hz, 1H, $\text{ArCH}_2\text{Ar}^{\text{ax}}$), 4.44 (d, $J = 13.5$ Hz, 2H, $\text{ArCH}_2\text{Ar}^{\text{ax}}$), 5.84 (d, $J = 7.1$ Hz, 1H, ArH), 6.02 (d, $J = 7.1$ Hz, 1H, ArH), 6.12 (d, $J = 7.1$ Hz, ArH), 6.14-6.19 (m, 2H, ArH), 6.28 (t, $J = 7.5$ Hz, 1H, ArH), 6.92 (t, $J = 7.5$ Hz, 1H, ArH), 7.08-7.11 (m, 2H, ArH), 7.60 (s, 1H, ArH) ppm.

Owing to minimal variations in the chemical shifts for certain signals in the ^{13}C NMR spectrum, the values have been reported with two decimal places instead of one.

Chapter 4: Ortholithiation of sulfoxide calixarene

^{13}C NMR (300 MHz, CDCl_3) δ 9.98 (C-31|34|37|40), 10.00 (C-31|34|37|40), 10.95 (C-31|34|37|40), 10.97 (C-31|34|37|40), 20.89 (C-45), 23.15 (C-30|33|36|39), 23.17 (C-30|33|36|39), 23.61 (C30|33|36|39), 23.66 (C-30|33|36|39), 23.84 (C-42, 43 and 44), 28.03 (C-7), 31.07 (C-14), 31.20 (C-21), 31.24 (C-28), 58.42 (C-41), 76.55 (C-29|32|35|38), 76.73 (C-29|32|35|38), 77.02 (C-29|32|35|38), 121.93 (C-24), 122.57 (C-3), 122.63 (C-17), 126.77 (C-4), 127.65 (C-2 and C-18), 127.68 (C-16), 127.90 (C-11), 129.07 (C-23 and 25), 132.01 (C-5), 133.00 (C-1), 133.44 (C-15), 133.69 (C-8), 133.83 (C-12), 137.11 (C-26|22), 137.24 (C-22|26), 137.59 (C-9), 138.37 (C-19), 141.98 (C-10), 155.14 (C-20), 155.48 (C-6), 158.22 (C-27), 161.56 (C-13) ppm.

^1H , ^1H COSY (300/300 MHz 278 K, CDCl_3): $\delta^1\text{H}/\delta^1\text{H}$ 1.88 / 1.08 ($\text{OCH}_2\text{CH}_2\text{CH}_3$ / $\text{OCH}_2\text{CH}_2\text{CH}_3$), 1.92 / 0.90 ($\text{OCH}_2\text{CH}_2\text{CH}_3$ / $\text{OCH}_2\text{CH}_2\text{CH}_3$), 1.91 / 0.89 ($\text{OCH}_2\text{CH}_2\text{CH}_3$ / $\text{OCH}_2\text{CH}_2\text{CH}_3$), 3.72 / 1.85 ($\text{OCH}_2\text{CH}_2\text{CH}_3$ / $\text{OCH}_2\text{CH}_2\text{CH}_3$), 4.04 / 1.92 ($\text{OCH}_2\text{CH}_2\text{CH}_3$ / $\text{OCH}_2\text{CH}_2\text{CH}_3$), 4.45 / 3.14 ($\text{ArCH}_2\text{Ar}^{\text{ax}}$ / $\text{ArCH}_2^{\text{eq}}\text{Ar}$), 4.46 / 3.19 ($\text{ArCH}_2^{\text{ax}}\text{Ar}$ / $\text{ArCH}_2^{\text{eq}}\text{Ar}$), 4.46 / 3.28 ($\text{ArCH}_2^{\text{ax}}\text{Ar}$ / $\text{ArCH}_2^{\text{eq}}\text{Ar}$), 4.46 / 3.33 ($\text{ArCH}_2^{\text{ax}}\text{Ar}$ / $\text{ArCH}_2^{\text{eq}}\text{Ar}$), 6.18 / 5.85 (ArH / ArH), 6.17 / 5.82 (ArH / ArH), 6.18 / 6.03 (ArH / ArH), 6.19 / 6.01 (ArH / ArH), 6.29 / 6.10 (ArH / ArH), 6.31 / 6.16 (ArH / ArH), 6.29 / 6.26 (ArH / ArH) ppm.

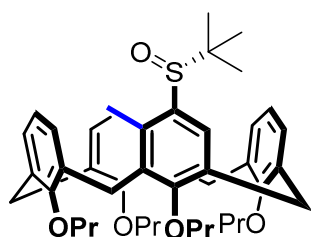
^1H , ^{13}C HSQC (300/75 MHz, 278 K, CDCl_3) $\delta^1\text{H} / \delta^{13}\text{C}$: 0.90 / 9.98 ($\text{OCH}_2\text{CH}_2\text{CH}_3$ / C-31|34|37|40), 0.90 / 10.00 ($\text{OCH}_2\text{CH}_2\text{CH}_3$ / C-31|34|37|40), 1.11 / 10.95 ($\text{OCH}_2\text{CH}_2\text{CH}_3$ / C-31|34|37|40), 1.13 / 10.97 ($\text{OCH}_2\text{CH}_2\text{CH}_3$ / C-31|34|37|40), 1.29 / 23.84 ($\text{CH}(\text{CH}_3)_3$ / C-42, 43 and 44), 1.82 / 23.61 ($\text{OCH}_2\text{CH}_2\text{CH}_3$ / C-30|33|36|39), 1.84 / 23.66 ($\text{OCH}_2\text{CH}_2\text{CH}_3$ / C-30|33|36|39), 1.91 / 23.15 ($\text{OCH}_2\text{CH}_2\text{CH}_3$ / C-30|33|36|39), 1.89 / 23.17 ($\text{OCH}_2\text{CH}_2\text{CH}_3$ / C-30|33|36|39), 2.46 / 20.89 (SCH_3 / C-45), 3.15 / 31.07 ($\text{ArCH}_2^{\text{eq}}\text{Ar}$ / C-14), 3.17 / 31.20 ($\text{ArCH}_2^{\text{eq}}\text{Ar}$ / C-21), 3.33 / 31.24, ($\text{ArCH}_2^{\text{eq}}\text{Ar}$ / C-24), 4.30 / 28.03 ($\text{ArCH}_2^{\text{ax}}\text{Ar}$ / C-7), 4.31 / 28.03 ($\text{ArCH}_2^{\text{ax}}\text{Ar}$ / C-7), 4.45 / 31.07 ($\text{ArCH}_2^{\text{ax}}\text{Ar}$ / C-14), 4.46 / 31.20 and 31.24 ($\text{ArCH}_2^{\text{ax}}\text{Ar}$ / C-21 and C-24), 3.70 / 77.02 ($\text{OCH}_2\text{CH}_2\text{CH}_3$ / C-29|32|35|38), 3.73 / 76.73 ($\text{OCH}_2\text{CH}_2\text{CH}_3$ / C-29|32|35|38), 4.04 / 76.55 ($\text{OCH}_2\text{CH}_2\text{CH}_3$ / C-29|32|35|38), 5.86 / 126.77 (ArH / C-4), 6.04 / 127.65 (ArH / C-2|18), 6.17 / 122.57, 127.65, 127.68 (ArH / C-2|18, C-3 and C-16), 6.28 / 122.63 (ArH / C-17), 6.94 / 121.93 (ArH / C-24), 7.15 / 129.07 (ArH / C-23 and C-25), 7.62 / 127.90 (ArH / C-11) ppm.

Chapter 4: Ortholithiation of sulfoxide calixarene

^1H , ^{13}C HMBC (300/75 MHz, 278 K, CDCl_3) δ ^1H / δ ^{13}C : 0.90 / 23.15, 76.55 ($\text{OCH}_2\text{CH}_2\text{CH}_3$ / C-30|33|36|39, C-29|32|35|38), 1.11 / 23.61 / 76.73 ($\text{OCH}_2\text{CH}_2\text{CH}_3$ / C-30|33|36|39, C-29|32|35|38), 1.29 / 58.42 ($\text{C}(\text{CH}_3)_3$ / C-41), 1.92 / 9.98, 10.00, 10.95, 76.55, 76.73, 77.02 ($\text{OCH}_2\text{CH}_2\text{CH}_3$ / C-31|34|37|40, C-30|33|36|39, C-29|32|35|38, C-30|33|36|39, C-29|32|35|38, C-29|32|35|38, C-29|32|35|38, C-29|32|35|38), 3.15 / 122.57, 127.65, 133.44, 137.11, 155.14, 158.22 ($\text{ArCH}_2^{\text{eq}}\text{Ar}$ / C-3, C-18, C-14, C-26 or 22, C-20, C-22), 3.20 / 122.57, 126.77, 133.69, 137.14, 155.48, ($\text{ArCH}_2^{\text{eq}}\text{Ar}$ / C-3, C-4, C-8, C-5, C-6), 3.33 / 122.63, 127.91, 138.37, 155.14, ($\text{ArCH}_2^{\text{eq}}\text{Ar}$ / C-17, C-11, C-19, C-20), 3.72 / 10.00, 10.95, 23.61, 23.66, 155.14, 155.48 ($\text{OCH}_2\text{CH}_2\text{CH}_3$ / C-31|34|37|40, C-31|34|37|40, C-30|33|36|39, C-30|33|36|39, C-20, C-6), 4.04 / 9.98, 10.97, 23.15, 23.17, 158.22, 161.56 ($\text{OCH}_2\text{CH}_2\text{CH}_3$ / C-31|34|37|40, C-31|34|37|40, C-30|33|36|39, C-30|33|36|39, C-27, C-13), 4.24-4.35 / 127.90, 133.44, 133.69, 141.98, 155.48, 161.56 ($\text{ArCH}_2^{\text{eq+ax}}\text{Ar}$ / C-11, C-15, C-8, C-10, C-20, C-20), 4.47 ($\text{ArCH}_2^{\text{ax}}\text{Ar}$ / C-3, C-2 and C-18, C-11, C-2, C-8, C-12, C-22|16, C-19, C-20, C-6, C-27, C-13), 5.84 / 28.03, 122.57, 127.65, 133.69, 155.48 (C4-H / C-7, C-3, C-2, C-8, C-6), 6.04 / 122.63, 126.77, 133.0, 155.48, 158.22 (C2|18-H / C-17, C-4, C-1, C-20, C-6) 6.12 – 6.23 / 31.07, 127.68, 133.44, 155.14 (C16|18-H / C-14, C-16, C-15, C-20), 6.30 / 127.68, 133.44, 155.14 (C17-H / C-16, C-15, C-20), 6.94 / 129.07, 137.24, 158.22 (C24-H / C-23 and 25, C-22|26, C-27), 7.15 / 31.20, 137.11, 158.22 (C23 and C25-H / C-21, C-22 or 26, C-27), 7.60 / 31.07, 133.83, 137.59, 141.98, 161.56 (C11-H / C-14, C-12, C-9, C-10, C-13) ppm.

IR (ATR) cm^{-1} : 2880 (s, -CH stretch), 1450 (s, C=C stretch), 1055 (s, S=O stretch), 990 (m, C-H oop bend), 763 (s, C-H oop bend).

HRMS–TOF MS ESI+: m/z $[\text{M}+\text{H}]^+$ calculated for $\text{C}_{45}\text{H}_{58}\text{O}_5\text{S}_2$: 743.3803; Found: 743.3806.

4.9.1 (*M*)-((*R*)-5-*tert*-butylsulfinyl)-4-methyl-25,26,27,28-tetrapropoxycalix[4]arene – 78.

Thioether calixarene (**M**)-78 was synthesized according to the general ortholithiation procedure outlined in **Chapter 3**, however the alkyllithium solvent was not removed. (**R**)-76 (100 mg, 0.143 mmol), *t*-BuLi (0.659 mmol, 6.0 equiv), TMEDA (0.264 ml, 1.72 mmol, 12 equiv) and MeI (0.130 ml, 2.15 mmol, 15.0 equiv) were combined with a reaction time of 24 h. Purification was achieved via silica gel column chromatography (auto column) using 24 g of silica, EtOAc/PET (12.5:87.5) with a flow rate of 18 ml/min, affording a white semi-solid (35 mg, 35%).

Chapter 4: Ortholithiation of sulfoxide calixarene

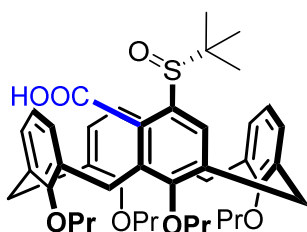
^1H NMR (300 MHz, CDCl_3) δ 0.88 (t, 3H, $J = 7.5$ Hz, $\text{CH}_2\text{CH}_2\text{CH}_3$), 0.91 (t, 3H, $J = 7.5$ Hz, $\text{CH}_2\text{CH}_2\text{CH}_3$), 1.11 (t, 6H, $J = 7.5$ Hz, $\text{CH}_2\text{CH}_2\text{CH}_3$), 1.20 (s, 9H, $\text{C}(\text{CH}_3)_3$), 1.83-1.98 (m, 8H, $\text{CH}_2\text{CH}_2\text{CH}_3$), 2.52 (s, 3H, ArCH_3), 3.14 (d, 1H, $J = 13.5$ Hz, $\text{ArCH}_2^{\text{eq}}\text{Ar}$), 3.16 (d, 2H, $J = 13.5$ Hz, $\text{ArCH}_2^{\text{eq}}\text{Ar}$), 3.60-3.78 (m, 4H, $\text{CH}_2\text{CH}_2\text{CH}_3$), 3.91-4.03 (m, 4H, $\text{CH}_2\text{CH}_2\text{CH}_3$), 4.14-4.17 (m, 1H, $\text{ArCH}_2^{\text{eq}}\text{Ar}$), 4.31 (d, 1H, $J = 13.5$ Hz, $\text{ArCH}_2^{\text{ax}}\text{Ar}$), 4.43 (d, 3H, $J = 13.5$ Hz, $\text{ArCH}_2\text{Ar}^{\text{ax}}$), 5.85 (d, $J = 7.4$ Hz, ArH), 6.05-6.33 (m, 5H, ArH), 6.82-6.98 (m, 2H, ArH), 7.11 (d, $J = 7.4$ Hz, ArH), 7.62 (s, 1H, ArH) ppm.

^{13}C NMR (300 MHz, CDCl_3) δ 9.96 ($\text{OCH}_3\text{CH}_3\text{CH}_3$), 10.02 ($\text{OCH}_3\text{CH}_3\text{CH}_3$), 11.00 ($2 \times \text{OCH}_3\text{CH}_3\text{CH}_3$), 16.83 (ArCH_3), 23.09 ($\text{OCH}_3\text{CH}_2\text{CH}_3$), 23.28 ($\text{OCH}_3\text{CH}_2\text{CH}_3$), 23.31 ($\text{OCH}_3\text{CH}_2\text{CH}_3$), 23.69 ($\text{OCH}_3\text{CH}_2\text{CH}_3$), 25.35 ($\text{CH}(\text{CH}_3)_3$), 27.64 (ArCH_2Ar), 31.03 (ArCH_2Ar), 31.13 (ArCH_2Ar), 31.20 (ArCH_2Ar), 57.43 ($\text{CH}(\text{CH}_3)_3$), 76.59 ($\text{OCH}_2\text{CH}_2\text{CH}_3$), 76.62 ($\text{OCH}_2\text{CH}_2\text{CH}_3$), 76.78 ($\text{OCH}_2\text{CH}_2\text{CH}_3$), 77.01 ($\text{OCH}_2\text{CH}_2\text{CH}_3$), 121.92 ($\text{C}_{\text{Ar}}\text{H}$), 122.47 ($\text{C}_{\text{Ar}}\text{H}$), 122.50 ($\text{C}_{\text{Ar}}\text{H}$), 126.36 ($\text{C}_{\text{Ar}}\text{H}$), 126.39 ($\text{C}_{\text{Ar}}\text{H}$), 127.64 ($\text{C}_{\text{Ar}}\text{H}$), 127.71 ($\text{C}_{\text{Ar}}\text{H}$), 127.84 ($\text{C}_{\text{Ar}}\text{H}$), 128.98 ($\text{C}_{\text{Ar}}\text{H}$), 129.11 ($\text{C}_{\text{Ar}}\text{H}$), 131.74 (C_{Ar}), 132.37 ($\text{C}_{\text{Ar}}\text{C}$), 132.55 ($\text{C}_{\text{Ar}}\text{C}$), 133.20 ($\text{C}_{\text{Ar}}\text{C}$), 133.42 ($\text{C}_{\text{Ar}}\text{C}$), 134.62 ($\text{C}_{\text{Ar}}\text{C}$), 134.91 ($\text{C}_{\text{Ar}}\text{C}$), 136.59 ($\text{C}_{\text{Ar}}\text{C}$), 137.22 ($\text{C}_{\text{Ar}}\text{C}$), 137.29 ($\text{C}_{\text{Ar}}\text{C}$), 155.00 ($\text{C}_{\text{Ar}}\text{O}$), 155.32 ($\text{C}_{\text{Ar}}\text{O}$), 158.17 ($\text{C}_{\text{Ar}}\text{O}$), 161.09 ($\text{C}_{\text{Ar}}\text{O}$) ppm.

IR (ATR) cm^{-1} : 2870 (s, -CH stretch), 1455 (s, C=C stretch), 1048 (s, S=O stretch), 988 (m, C-H oop bend), 766 (s, C-H oop bend).

HRMS–TOF MS ES+: m/z $[\text{M}+\text{H}]^+$ calculated for $\text{C}_{45}\text{H}_{58}\text{O}_5\text{S}$: 711.4084; Found: 711.4079.

4.9.2 (*M*)-((*R*)-5-*tert*-butylsulfinyl)-4-carboxyl-25,26,27,28-tetrapropoxycalix[4]arene – 79.



Thioether calixarene (**M**)-79 was synthesized according to the general ortholithiation procedure outlined in **Chapter 3**, however the alkyllithium solvent was not removed. (**R**)-76 (500 mg, 0.719 mmol), *t*-BuLi (4.272 mmol, 6.0 equiv), TMEDA (1.30 ml, 8.54 mmol, 12 equiv) and CO_2 (gas exs) were combined with a reaction time of 24 h. Purification was achieved via silica gel column chromatography with a gradient elution DCM (100) to EtOAc/DCM (20:80) affording a white solid (480 mg, 90%).

^1H NMR (300 MHz, $\text{METHANOL-}d$) δ 0.81-0.89 (m, 6H, $\text{OCH}_2\text{CH}_2\text{CH}_3$), 0.98-1.07 (m, 6H, $\text{OCH}_2\text{CH}_2\text{CH}_3$), 1.16 (s, 9H, $\text{C}(\text{CH}_3)_3$), 1.91-1.99 (m, 8H, $\text{OCH}_2\text{CH}_2\text{CH}_3$), 3.10 (d, $J = 13.0$ Hz, 2H, ArCH_2Ar), 3.30 (d, $J = 13.1$ Hz, 1H, ArCH_2Ar), 3.45 (d, $J = 13.1$ Hz, 1H, ArCH_2Ar), 3.53-3.73 (m, 4H, $\text{OCH}_2\text{CH}_2\text{CH}_3$), 3.88-4.09 (m, 4H, $\text{OCH}_2\text{CH}_2\text{CH}_3$), 4.32-4.48 (m, 4H, ArCH_2Ar), 6.00-6.34 (m, 6H, ArH), 6.88 (t, $J = 7.32$ Hz, 1H, ArH), 7.04-7.10 (m, 2H, ArH), 7.56 (s, 1H, ArH) ppm.

Chapter 4: Ortholithiation of sulfoxide calixarene

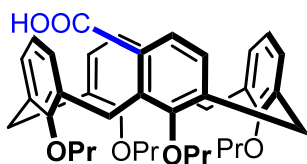
^{13}C NMR (75 MHz, METHANOL-*d*) δ 9.9, 10.0, 10.9, 11.0, 23.1, 23.2, 23.4, 23.5, 23.6, 27.8, 29.8, 31.1, 31.3, 50.9, 57.7, 76.7, 76.8, 77.0, 77.2, 122.0, 122.6, 122.7, 126.7, 127.6, 127.9, 128.0, 128.4, 129.0, 129.1, 131.8, 132.0, 133.3, 133.5, 134.8, 135.0, 137.0, 137.1, 138.7, 155.2, 155.4, 158.1, 162.0, 169.8 ppm.

HRMS–TOF MS ES+: m/z [M+H] $^+$ calculated for $\text{C}_{45}\text{H}_{57}\text{O}_7\text{S}$: 741.3825; found: 741.3830.

IR (ATR) cm^{-1} : 3200 (br, -OH stretch), 2880 (s, -CH stretch), 1715 (br, C=O stretch), 1450 (s, C=C stretch), 1055 (s, S=O stretch), 990 (m, C-H oop bend), 763 (s, C-H oop bend).

(M)/(P)-79 crystal structure data	
Empirical formula	$\text{C}_{47}\text{H}_{54}\text{SO}_8$
Formula weight (g mol $^{-1}$)	777.17
Temperature (K)	100 (2)
Wavelength (Å)	0.71073
Crystal system	Triclinic
$a/\text{Å}$	9.335(6)
$b/\text{Å}$	12.118(7)
$c/\text{Å}$	20.805(3)
$\alpha/^\circ$	77.56(3)
$\beta/^\circ$	77.82(3)
$\gamma/^\circ$	68.13(8)
Volume (Å 3)	2110.9(6)
Space group	$P-1$
Z	2
Calculated density (g cm $^{-3}$)	1.212
Refinement method	Full-matrix least-squares on F^2
Final R indices [$I > 2\sigma(I)$]	$R1 = 0.0858$

Chapter 4: Ortholithiation of sulfoxide calixarene

4.9.3 (M)-4-carboxy-25,26,27,28-tetrapropoxycalix[4]arene – **81**.³⁹

Calixarene (**M**)-**79** (60 mg, 0.081 mmol) was added to EtOH (3 ml). Excess amounts of Raney nickel was added and the mixture was heated to reflux, which was maintained for 24 h. The reaction mixture was cooled to room temperature, filtered through a celite plug. After removing the excess solvent under reduced pressure, the product was purified using silica column chromatography EtOAc/PET (40:60) yielding a white solid (48 mg, 95%).

The characterisation data collected for this compound compared well with the reported literature values.³⁹

¹H NMR (300 MHz, CDCl₃)³⁹ δ 0.88-0.97 (m, 6H, OCH₂CH₂CH₃), 1.02-1.10 (m, 6H, OCH₂CH₂CH₃), 1.79-2.05 (m, 8H, OCH₂CH₂CH₃), 3.10-3.24 (m, 3H, ArCH₂Ar), 3.63-3.80 (m, 4H, OCH₂CH₂CH₃), 3.89-4.06 (m, 4H, OCH₂CH₂CH₃), 4.33-4.53 (m, 5H, ArCH₂Ar), 6.17-6.37 (m, 6H, ArH), 6.78-6.86 (m, 1H, ArH), 6.92-6.99 (m, 2H, ArH), 7.01 (d, $J = 7.9$ Hz, 1H, ArH), 7.52 (d, $J = 7.9$ Hz, 1H, ArH) ppm.

4.10 References.

- (1) Solladie, G. *Synthesis*, **1981**, *1*, 185.
- (2) Chen, J.; Chen, J.; Lang, F.; Zhang, X.; Cun, L.; Zhu, J.; Deng, J.; Liao, J. *J. Am. Chem. Soc.* **2010**, *132*, 4552.
- (3) Chen, Q.-A.; Dong, X.; Chen, M.-W.; Wang, D.-S.; Zhou, Y.-G.; Li, Y. X. *Org. Lett.* **2010**, *12*, 1928.
- (4) Qi, W.-Y.; Zhu, T.-S.; Xu, M.-H. *Org. Lett.* **2011**, *13*, 3410
- (5) Chen, G.; Gui, J.; Li, L.; Liao, J. *Angew. Chem., Int. Ed.* **2011**, *50*, 7681.
- (6) Evans, D. A.; Campos, K. R.; Tedrow, J. S.; Michael, F. E.; Gagne, M. R. *J. Am. Chem. Soc.* **2000**, *122*, 7905.
- (7) Fernández, I.; Khiar, N. *Chem. Rev.* **2003**, *103*, 3651.
- (8) Trost, B. M.; Rao, M. *Angew. Chem., Int. Ed.* **2015**, *54*, 5026.
- (9) Pellissier, H. *Tetrahedron* **2007**, *63*, 1297.
- (10) Lagneau, N. M.; Chen, Y.; Robben, P. M.; Sin, H.-S.; Takasu, K.; Chen, J.-S.; Robinson, P. D.; Hua, D. H. *Tetrahedron* **1998**, *54*, 7301.
- (11) Walker, A. J. *Tetrahedron: Asymmetry* **1992**, *3*, 961.
- (12) Rayner, D.; Gordon, A.; Mislow, K. *J. Am. Chem. Soc.* **1968**, *90*, 4854.
- (13) Carreño, M. C.; Ruano, J. L. G.; Martin, A. M.; Pedregal, C.; Rodriguez, J. H.; Rubio, A.; Sanchez, J.; Solladie, G. *J. Mol. Biol.* **1990**, *55*, 2120.
- (14) Kosugi, H.; Uda, H.; Konta, H. *J. Chem. Soc., Chem. Commun.* **1985**, 211.
- (15) Mazingo, R.; Wolf, D. E.; Harris, S. A.; Folkers, K. *J. Am. Chem. Soc.* **1943**, *65*, 1013.
- (16) Hauptmann, H.; Walter, W. *Chem. Rev.* **1962**, *62*, 347.
- (17) Riant, O.; Samuel, O.; Kagan, H. B. *J. Am. Chem. Soc.* **1993**, *115*, 5835.
- (18) Posner, G. *Acc. Chem. Res.* **1987**, *20*, 72.
- (19) Chan, H.; Albert, W. M.; Lee, W. *Top. Curr. Chem.* **1997**, *190*, 103.
- (20) Garcia Ruana, J. *Pure Appl. Chem.* **1996**, *68*, 925.
- (21) Garcia Ruana, J.; De La Plata, C. B. *Top. Curr. Chem.* **1999**, *204*, 1.
- (22) Renaud, P.; Gerster, M. *Angew. Chem., Int. Ed.* **1998**, *37*, 2562.

Chapter 4: Ortholithiation of sulfoxide calixarene

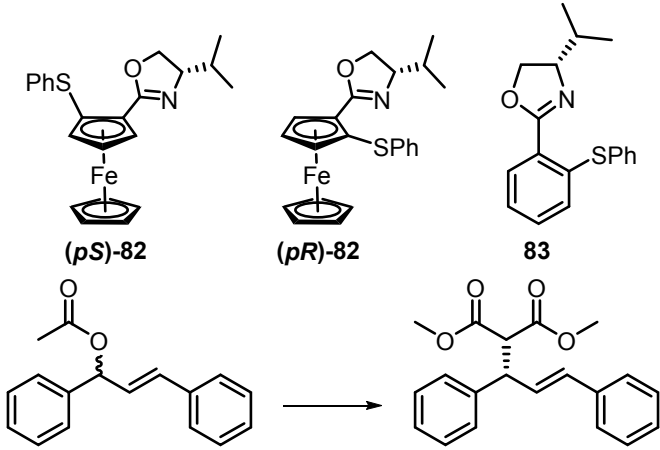
- (23) Olefins, E.; Mariz, R.; Luan, X.; Gatti, M.; Linden, A.; Dorta, R. *J. Am. Chem. Soc.* **2008**, *130*, 2172.
- (24) Morrison, J. D.; Scott, J. W. *Asymmetric Synthesis, Volume 5*, **1983**, Academic Press.
- (25) D'Antona, N.; Lambusta, D.; Morrone, R.; Nicolosi, G.; Secundo, F. *Tetrahedron: Asymmetry* **2004**, *15*, 3835.
- (26) Liu, G.; Cogan, D. A.; Ellman, J. A. *J. Am. Chem. Soc.* **1997**, *119*, 9913.
- (27) Cogan, D. A.; Liu, G.; Kim, K.; Backes, B. J.; Ellman, J. A. *J. Am. Chem. Soc.* **1998**, *120*, 8011.
- (28) Mikołajczyk, M. *Phosphorous Sulfur Relat. Elem.* **1986**, *27*, 31.
- (29) Gessner, V. H.; Däschlein, C.; Strohmann, C. *Chem.-Eur. J.* **2009**, *15*, 3320.
- (30) Reich, H. J. *Chem. Rev.* **2013**, *113*, 7130.
- (31) Hoffmann, R. W.; Kemper, B. *Tetrahedron Lett.* **1981**, *22*, 5263.
- (32) Gomez, R. A.; Adrio, A.; Carretero, C. *Angew. Chem. Int. Ed.* **2006**, *45*, 7674.
- (33) Freedman, T. B.; Cao, X.; Dukor, R. K.; Nafie, L. A. *Chirality* **2003**, *15*, 743.
- (34) Slade, D.; Ferreira, D.; Marais, J. P. J. *Phytochemistry* **2005**, *66*, 2177.
- (35) Berova, N.; Di Bari, L.; Pescitelli, G. *Chem. Soc. Rev.* **2007**, *36*, 914.
- (36) Gaffield, W. *Tetrahedron* **1970**, *26*, 4093.
- (37) Herbert, S. A. Oxazoline Directed Lithiation of Calix[4]arene and Ferrocene, Stellenbosch University, **2011**.
- (38) Chen, C.; Beak, P. *J. Org. Chem.* **1986**, *51*, 3325.
- (39) Slavík, P.; Eigner, V.; Lhoták, P. *Org. Lett.* **2015**, *17*, 2788.
- (40) Rebiere, B. F.; Riant, O.; Ricard, L. *Angew. Chem., Int. Ed.* **1993**, *32*, 568.

5 Chapter 5 – Synthesis of phosphine oxazoline calixarene ligands

5.1 Introduction.

Thus far, all of the focus in the project had been on the synthesis of inherently chiral calixarenes. Using two different classes of chiral functional groups, the oxazoline and sulfoxide, a directed *ortho*-metalation strategy had been used to successfully synthesize several inherently chiral calixarene compounds. Originally a report by Dai and co-workers had shown that bidentate S/N planar chiral ferrocene oxazoline ligands were able to asymmetrically catalyze the Tsuji-Trost allylation coupling reaction (**Table 5.1**).¹ What was interesting about this was the role played by the planar chirality in the asymmetric induction process.

Table 5.1: Asymmetric catalysis of the Tsuji-Trost allylation reaction by planar chiral S/N ligands.¹



Entry	Ligand	Yield (%)	ee (%) (S)
1	(<i>pS</i>)- 82	98	91
2	(<i>pR</i>)- 82	98	89
3	83	96	90

The results presented above show that performing the reaction with planar chiral ligands, (*pS*)-**82** and (*pR*)-**82**, gave slightly higher and lower *ee* values, 91% and 89% respectively. The model ligand **83** had a selectivity of 90%, which fell in between these values. This suggested a slight matched and mismatched correlation between the planar and point chirality of the ligands. Despite the planar chirality only playing a minor role, this result had an interesting implication for inherent chirality. From a structural viewpoint, planar chirality can be considered closely related to inherent chirality and these findings posed an interesting question. Would it be possible for inherent chirality to function as source of chiral induction in an asymmetric reaction?

This initiated a pilot study on the application of bidentate S/N inherently chiral ligands on the asymmetric Tsuji-Trost allylation reaction.² The results were previously discussed in **Chapter 1**, but just to reiterate, the same matched/mismatched relationship between the inherent and point chirality of these ligands was noted.

Chapter 5: The synthesis of phosphine oxazoline ligands

The contribution made by inherent chirality towards chiral induction during an asymmetric reaction is not a novel concept.

Despite this, only a handful of attempts aimed at exploiting inherent chirality as a source of chiral information have been made, most of which have had limited success.²⁻⁶ The encouraging preliminary results of the pilot study, as well as the fact this area of research is still largely unexplored, provided an opportunity to contribute to this field of calixarene chemistry.

To improve upon the S/N based ligands, the literature covering the application of planar chiral ferrocene ligands had to be revisited. When compared to calixarene based ligands, the application of planar chiral ferrocenes has received far more attention and is a popular topic in asymmetric catalysis. Another important consideration was the incorporation of the oxazoline functionality into the overall structure of the target ligands, as it was already an integral part of these compounds. The so-called Phox ligands were originally reported concurrently by Pfaltz, Helmchen and Williams in 1993.⁷⁻⁹ This functionality was later successfully incorporated into the ferrocene framework by Dai and co-workers (**Figure 5.1**).¹⁰ The structure of Dai's ferrocenes, (*pS*)-**84** and (*pR*)-**84**, served as the foundation for the four targeted inherently chiral calixarene Phox ligands.

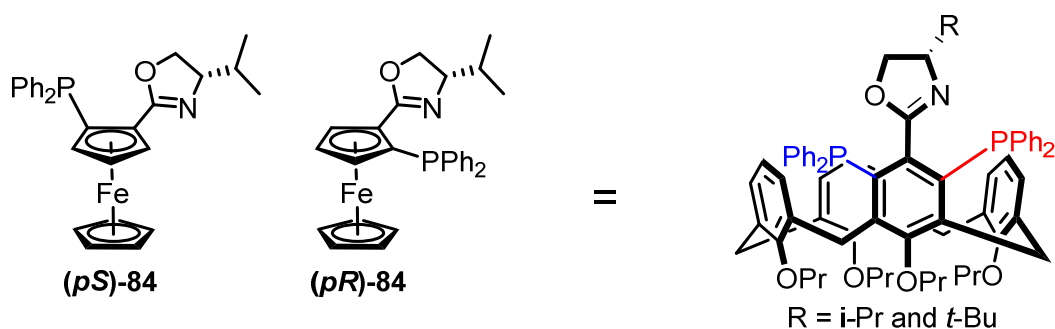


Figure 5.1: The proposed inherently chiral calixarene Phox ligand targets based on the ferrocenes reported by Dai.¹⁰

The calixarene Phox ligands were an attractive choice for a number of reasons. The directed ortholithiation strategy was ideally suited to synthesize either of the inherently chiral diastereomers for each of the oxazolines. In addition to this, the chemistry was familiar and well understood. The application of planar chiral ferrocene Phox ligands, as well as others containing the structurally similar P/N bidentate motif have covered a broad scope of asymmetric catalysis.¹¹⁻¹³ Furthermore, there are a number of asymmetric reactions that have not been explored with Phox ligands that have an incorporated stereoplane, the effect of which has potential. A few examples include the following; hydrogenations,¹⁴⁻¹⁶ allylic substitutions,¹⁷⁻¹⁹ Suzuki²⁰⁻²³ and Heck cross-couplings,²⁴⁻²⁶ and asymmetric electrocyclizations.^{27,28} As mentioned in **Chapter 1**, the synthesis of inherently chiral calixarenes alone has posed a number experimental challenges and difficulties in the past.

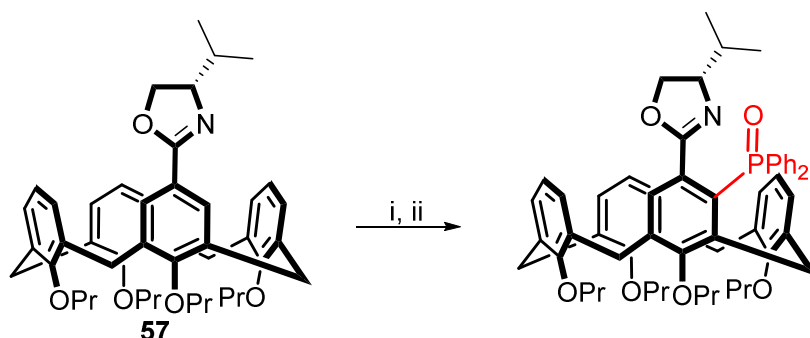
Chapter 5: The synthesis of phosphine oxazoline ligands

This has had the consequence of deterring further investigation into potential asymmetric catalytic applications. A crucial element of the chemistry was that it provided access to both forms of inherent chirality. This has created a unique opportunity to make a significant contribution toward the study of inherent chirality.

The synthesis of these Phox calixarene ligands could potentially introduce inherent chirality to a well-established class of ligands. The successful application of these compounds may provide a fresh perspective and a renewed interest in the nature of this structural property.

5.2 First attempts at phosphine oxazoline calixarene synthesis.

Theoretically, simply replacing the S_2Me_2 electrophile with chlorodiphenylphosphine should have yielded the targeted phosphine calixarene. Instead, after attempting the synthesis several times, the calixarene phosphine oxide was obtained as the only calixarene product (**Scheme 5.1**).



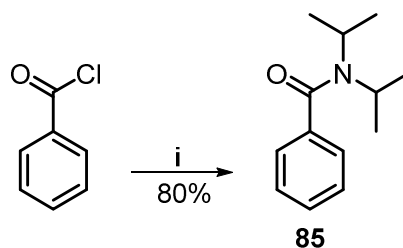
Scheme 5.1: Attempted synthesis of a calixarene Phox ligand. Reagents and conditions: i) *s*-BuLi (5.0 equiv), TMEDA (10.0 equiv), pentane, $-78\text{ }^{\circ}\text{C}$, 12 h; ii) PPh_2Cl (15.0 equiv), $-78\text{ }^{\circ}\text{C}$ to rt, 24 h.

Exposure of the phosphine to oxygen in the aqueous work up, or during column chromatography were the most probable explanations for the oxidation. The oxidation state of the phosphine atom could be verified by ^{31}P NMR spectroscopy. The chemical shift ranges are notably different for the phosphines and their corresponding oxides. When phosphorus is bonded to three alkyl groups, the signal falls between a chemical shift range of $\delta -55.0$ and -5.0 ppm, while the corresponding oxide lies in a range of $\delta 10.0$ and 60.0 ppm. After experiencing these initial problems, an alternative approach to gaining the necessary experience for this chemistry was considered. The chiral amino acids used to build the oxazoline functional groups were expensive. Before continuing with the synthesis of any phosphine ligands, the techniques required for phosphine synthesis under similar reaction conditions had to be established. In order to minimize the waste of any more precious starting material, a lithiation type reaction using a cheap and easily prepared starting material was deemed necessary.

5.3 “Taming the beast” that was phosphorus.

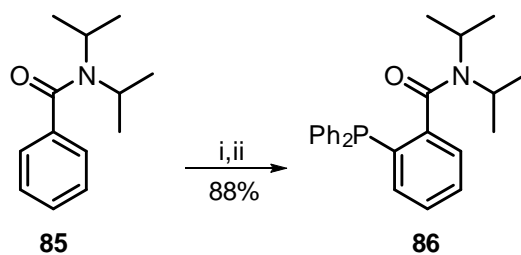
5.3.1 Synthesis and ortholithiation of *N,N*-di-isopropyl benzamide.

Returning to early metalation literature showed that *N,N*-di-isopropyl benzamide was a structurally simple and widely used amide in *ortho*-directed metalation chemistry. In this work, the first synthesis of diphenyl phosphines was reported by Beak.²⁹ An addition-elimination reaction between di-isopropyl amine and benzoyl chloride afforded the desired amide starting material **85** in multi-gram quantities (**Scheme 5.2**).



Scheme 5.2: Synthesis of *N,N*-di-isopropyl benzamide **85**. Reagents and conditions: i) di-isopropyl amine (1.5 equiv), Et₃N (2.0 equiv), Et₂O, 0 °C, 20 h.²⁹

With a suitable replacement for the valuable oxazoline compounds in hand, the issue of preventing the oxidation of the phosphine, as well as its purification could now be addressed. After consulting a number of supplementary information documents for papers that reported the synthesis and purification of numerous different phosphine compounds, it was evident that the problem of oxidation was a universal one. Frustratingly, there didn't seem to be a universal or general experimental method that covered all phosphine synthesis. The sensitivity of these compounds towards oxidation varied extensively. Some tolerated an aqueous work-up, while for others, inert filtration followed by vacuum distillation was the only way to prevent oxidation. With regards to chromatographic purification techniques, the majority seemed to tolerate the use of silica, but the more sensitive ligands required the use of neutral alumina. After previously only isolating the phosphine oxide from the reaction mixture, it was safe to assume that calixarene phosphine compounds were of the sensitive variety. In a publication by Bunt and co-workers, an aqueous work-up was avoided and oven-dried silica was added directly to the flask to quench the reaction.³⁰ After removing the excess solvent under reduced pressure, the crude product/silica mixture was dry-loaded directly onto a silica column, which successfully isolated the phosphine from the reaction mixture and prevented oxidation. Making use of this method, the synthesis and purification of a phosphine compound was revisited (**Scheme 5.3**).



Scheme 5.3: Synthesis of phosphine di-isopropyl benzamide **86**. Reagents and conditions: i) *n*-BuLi (1.5 equiv), THF, $-78\text{ }^{\circ}\text{C}$, 4 h; ii) PPh_2Cl (1.6 equiv), $-78\text{ }^{\circ}\text{C}$ to rt, 12 h.

After cooling the amide/THF mixture to $-78\text{ }^{\circ}\text{C}$, *n*-BuLi was carefully added to the reaction. After 4 h, freshly distilled diphenyl phosphine chloride was injected dropwise, and the reaction was slowly warmed to room temperature overnight. TLC analysis indicated the formation of two new products. After the silica quench, an EtOAc/PET mixture was used to isolate the two products as colourless oils. A combination of ^1H and ^{31}P NMR spectroscopy confirmed that the more polar of the two compounds was indeed the phosphine product. The newly added phenyl groups appeared as a set of overlapping multiplet signals that integrated for 10 protons in the ^1H NMR spectrum. Furthermore, the ^{31}P NMR spectrum ascertained that no oxidation took place (**Figure 5.2**). A singlet, with a chemical shift of $\delta -13.96$ ppm confirmed the presence of the phosphine and almost none of the phosphine oxide was present. Closer examination of the spectrum revealed an extremely small signal at $\delta 30.38$ ppm, indicating that oxidation was starting to take place. To prevent this, all phosphine ligands were stored in degassed DCM, under argon, and at low temperatures ($-18\text{ }^{\circ}\text{C}$).

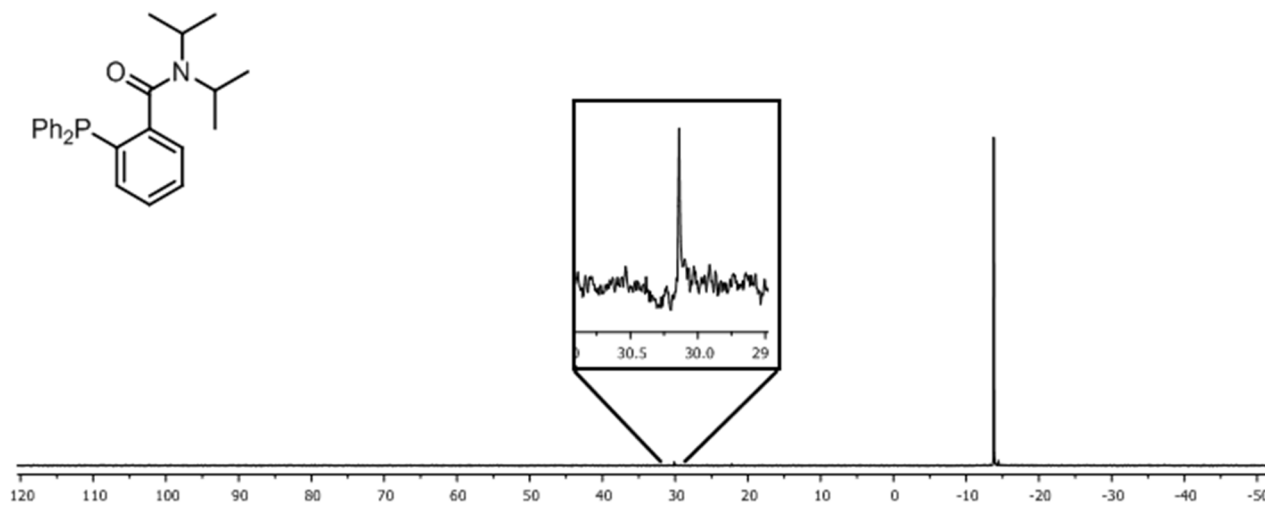


Figure 5.2: ^{31}P NMR spectrum of compound **86**. The outlined and expanded region shows the early stages of phosphine oxidation.

^1H and ^{31}P NMR spectroscopic analysis of the less polar compound suggest that diphenyl(*n*-butyl)phosphine had formed as a secondary product in the reaction. This can be rationalized by nucleophilic attack of the excess *n*-BuLi during the addition of chlorodiphenylphosphine.

Chapter 5: The synthesis of phosphine oxazoline ligands

The ^1H NMR spectrum only contained aromatic signals for the two phenyl rings, as well as several different groups of multiplet signals in the alkane region that integrated for a total of 9 protons.* The synthesis of diphenyl(*n*-butyl)phosphine has previously been reported under similar experimental conditions and their spectroscopic analysis correlated well with the data collected for this compound.³¹ *N,N*-di-isopropyl benzamide proved to be an appropriate oxazoline replacement, and had served its purpose of outlining the subtle experimental requirements of phosphine synthesis.

5.4 Synthesis of the model phosphine oxazoline ligands.

5.4.1 Selecting a suitable model compound.

After gaining an improved understanding of phosphine chemistry, the next goal was the synthesis of a model Phox ligand. Even though the overall aim was to investigate inherent chirality, the synthesis of two simpler model ligands was also a necessity. The calixarene Phox ligands would contain two varieties of chirality, the classic sp^3 , or central chirality on the oxazoline, and the inherent chirality of the calixarene backbone. In the related investigations of planar chirality, it was common practice to always compare the outcomes of the planar chiral ligands to simpler model compounds.^{1,17,32} This would help isolate and establish individual contributions made by the different classes of chirality on an asymmetric chemical process. Using the targeted Phox calixarenes as a source, the proposed structures for the simplified phosphine oxazoline models were constructed, using only the front of the calixarene ligand (**Figure 5.3**). The simplified versions of these Phox ligands would serve as a representation for the central chirality of the oxazolines.

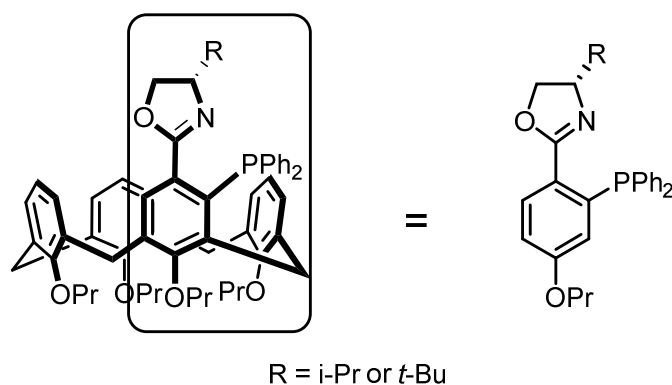


Figure 5.3: The proposed model ligands based on the functionalized aryl ring of the calixarene.

R = *i*-Pr or *t*-Bu.

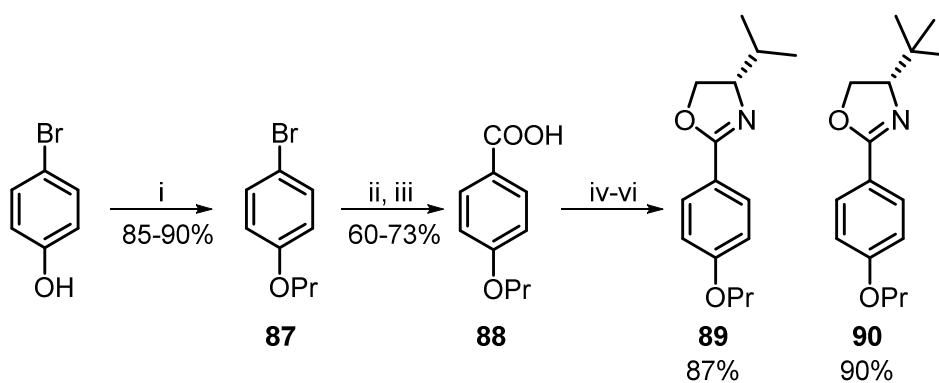
* It was found that similar by-products formed during the synthesis of all phosphine ligands. Their chemical structures varied depending on the alkyl group of the alkyllithium used. Fortunately they were always far less polar than the ligands and were separated from the reaction mixtures using either alumina or silica chromatography.

Chapter 5: The synthesis of phosphine oxazoline ligands

If the catalysis of an asymmetric reaction with both the calixarene and model Phox ligands was successful, comparative analysis of the findings would hopefully aid in identifying the individual influences of these discrete structural properties on the overall stereochemical outcome.

5.4.2 Synthesis of isopropyl and tert-butyl model oxazolines – **89** and **90**.

The synthesis of a structurally related thio-ether oxazoline model compound was reported during the former evaluation of the inherently chiral S/N calixarene ligands.² Consequently, the majority of the chemistry required for the synthesis of these new model compounds had previously been described. From 4-bromo-phenol as the starting material, the thio-ether model compounds were obtained in 4 steps. The synthesis of the new models shared three of these, with the only difference being the final ortholithiation step. The three-step synthesis of the oxazoline models is presented below (**Scheme 5.4**).



Scheme 5.4: The three-step synthesis of the model oxazolines **89** and **90**. Reagents and conditions: i) K_2CO_3 (2.5 equiv), iodo-propane (5.0 equiv), DMF, reflux 24 h; ii) *n*-BuLi (1.5 equiv), THF, $-78\text{ }^\circ\text{C}$ 10 min; iii) CO_2 (gas, exs), $-78\text{ }^\circ\text{C}$ to rt, 12 h; iv) oxalyl chloride (5.0 equiv), DCM, rt, 12 h; v) L-valinol/L-tert-leucinol (1.15 equiv), Et_3N (3.0 equiv), DCM, $0\text{ }^\circ\text{C}$ to rt, 12 h; vi) MsCl (3.0 equiv), Et_3N (5.0 equiv), DCM, $0\text{ }^\circ\text{C}$, 12 h.

This chemistry was closely related to the synthesis of calixarenes **57** and **58**, which was covered in **Chapter 2**. Having previously presented the details of these reactions, only a brief discussion will be presented here. In the first reaction, propylation of the phenol was accomplished using an $\text{S}_{\text{N}}2$ substitution reaction with iodo-propane and K_2CO_3 (i). The crude product was purified using column chromatography, yielding compound **87** as a colourless oil in high yields (85-90%). Introduction of the carboxylic acid group required a lithium halogen exchange reaction (ii and iii). The same conditions used for the synthesis of the mono-carboxylic acid calixarene **56** were employed. The formation of a protonated by-product was noted again. After purification, **88** was isolated as a white solid in moderately good yields (60-73%).[†]

[†] The method used to quench the reaction affected the yield. Once again, it was found that bubbling CO_2 through the mixture gave the best results.

Chapter 5: The synthesis of phosphine oxazoline ligands

The standard conditions for the three step synthesis of the oxazoline calixarene were employed to synthesize the new oxazoline compounds (iv, v and vi). Both of the model oxazolines, **89** and **90**, were isolated in high yields of 87% and 90%, respectively. A comparison between the ^1H NMR spectra of the starting material and final compound **90** is presented below (Figure 5.4).

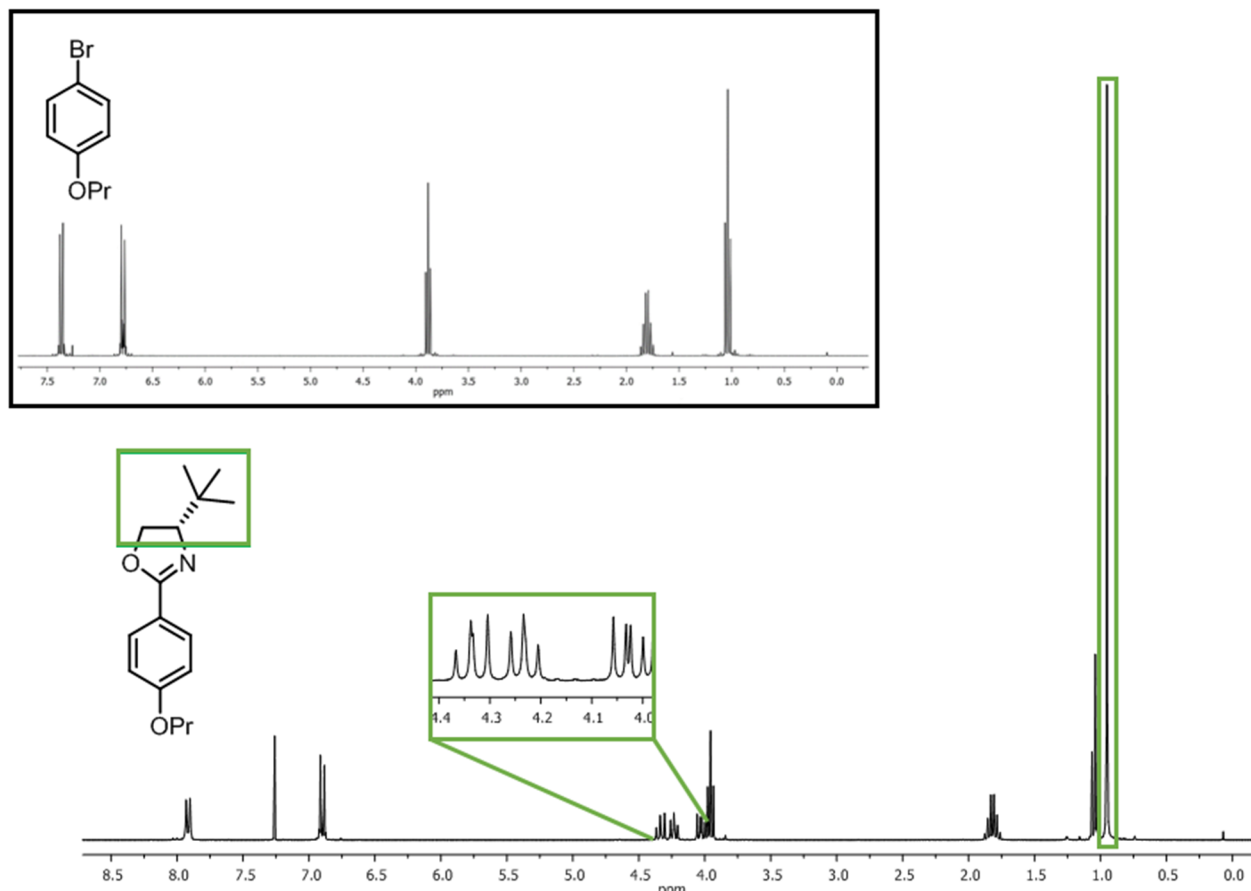
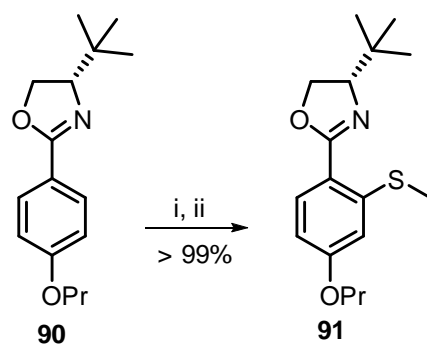


Figure 5.4: ^1H NMR spectra of the model bromo **87** (above, outlined in black), and *tert*-butyl oxazoline **90** (below). The signals corresponding to the oxazoline have been outlined in green.

The ^1H NMR spectra for the propylated bromo **87**, and acid **88** model compounds were very similar and compared well with data reported in the literature.^{33,34} The ^1H NMR spectra for oxazolines **89** and **90** were also comparatively alike and the signals for the newly introduced oxazoline can be seen outlined in green. The structures for these compounds had not been published so both were fully characterized.

5.4.3 Ortholithiation of the model oxazoline – an optimization study.

In the past, all of the ortholithiation chemistry had been optimized for the oxazoline calixarenes, which required large excesses of the ligand/alkyllithium mixtures to ensure both reasonable reaction times and high conversions. Before the synthesis of the model phosphine oxazolines was attempted on a larger scale, the reaction conditions required optimization. **Scheme 5.5** shows several small scale test reactions which were first carried out to attain improved reaction conditions.



Scheme 5.5: Optimal reaction conditions for the ortholithiation of **90**. Reagents and conditions:

i) *n*-BuLi (2.0 equiv), TMEDA (4.0 equiv), THF, $-78\text{ }^{\circ}\text{C}$, 20 h; ii) S_2Me_2 (exs), $-78\text{ }^{\circ}\text{C}$ to rt, 12 h.

Two equivalents of the *n*-BuLi/TMEDA mixture as a 1:2 ratio in THF at $-78\text{ }^{\circ}\text{C}$ followed by the addition of the disulfide was found to form **91** in almost quantitative yields.[‡] The ^1H NMR spectrum of the crude product confirmed an almost complete conversion to the thio-ether product (**Figure 5.5**).

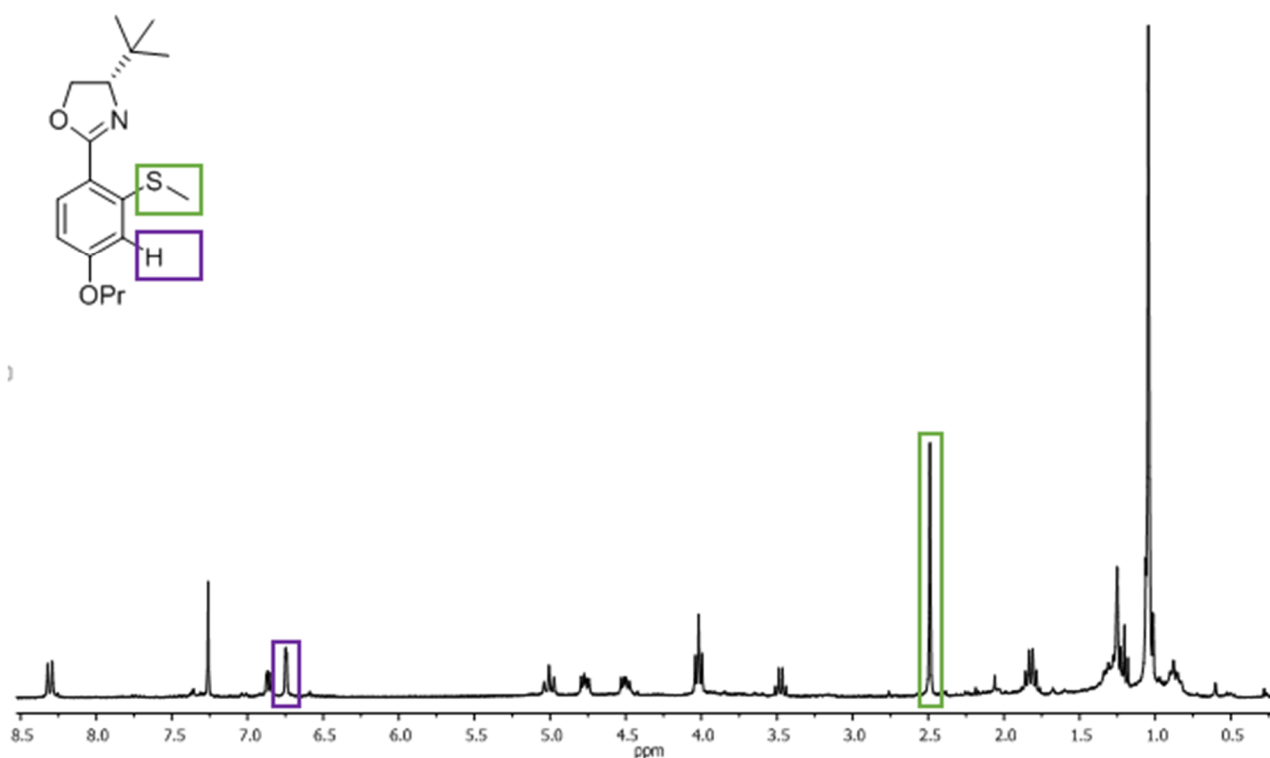


Figure 5.5: ^1H NMR spectrum of the crude *tert*-butyl oxazoline thio-ether **91**. The thio-methyl signal has been outlined in green. The *meta*-proton below the thio-methyl group has been outlined in purple.

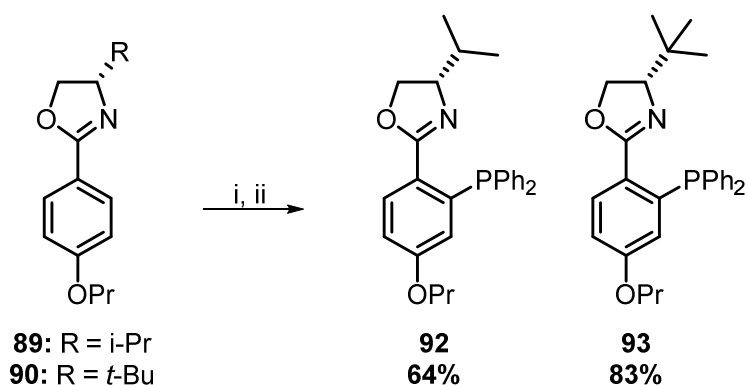
[‡] The observations with regards to color changes and precipitate formation were similar to that of the ortholithiation of the calixarene and model compounds.

Chapter 5: The synthesis of phosphine oxazoline ligands

The spectrum contained a new singlet, corresponding to the thio-methyl functional group, with a chemical shift of δ 2.49 ppm (outlined in green). The singlet (outlined in purple) with a chemical shift of δ 6.75 ppm, represents the proton in the *meta*-position, between the propyl and thio-methyl functional groups. For the sake of confirmation, the same conditions were attempted with the isopropyl oxazoline model **89**, yielding much the same result. With an optimal means to successfully ortholithiate both **89** and **90** in high yields, the synthesis of the model phosphine ligand could now be attempted.

5.4.4 Synthesis of the model phosphine oxazoline ligands – **92** and **93**.

Proceeding with caution, all targeted phosphines were assumed to be unstable in air and prone towards oxidation. Therefore, a combination of the experimental conditions for the synthesis of **86** and **91** were used to prepare the model phosphine ligands **92** and **93** (Scheme 5.6).



Scheme 5.6: The synthesis of model phosphine ligands **92** and **93**. Reagents and conditions: i) *n*-BuLi (2.0 equiv), TMEDA (4.0 equiv), THF, -78 °C, 24 h; ii) PPh_2Cl (6.0 equiv), -78 °C to rt, 12 h.

TLC analysis after quenching the reaction with silica confirmed that none of the phosphine oxide had formed. Both ligands **92** and **93** were isolated as white solids, using a silica column and a mixture of EtOAc/hexane (7:93), in yields of 64% and 83% respectively. The lower yield of **92** could be explained by the fact that it was synthesized earlier on in the study. Over time, the yields for these reactions gradually improved as the synthetic techniques were refined. Careful inert sample preparation allowed for good quality ^1H and ^{31}P NMR spectra of these compounds to be collected before any oxidation took place. To demonstrate this, both spectra for **93** are presented below (Figure 5.6).

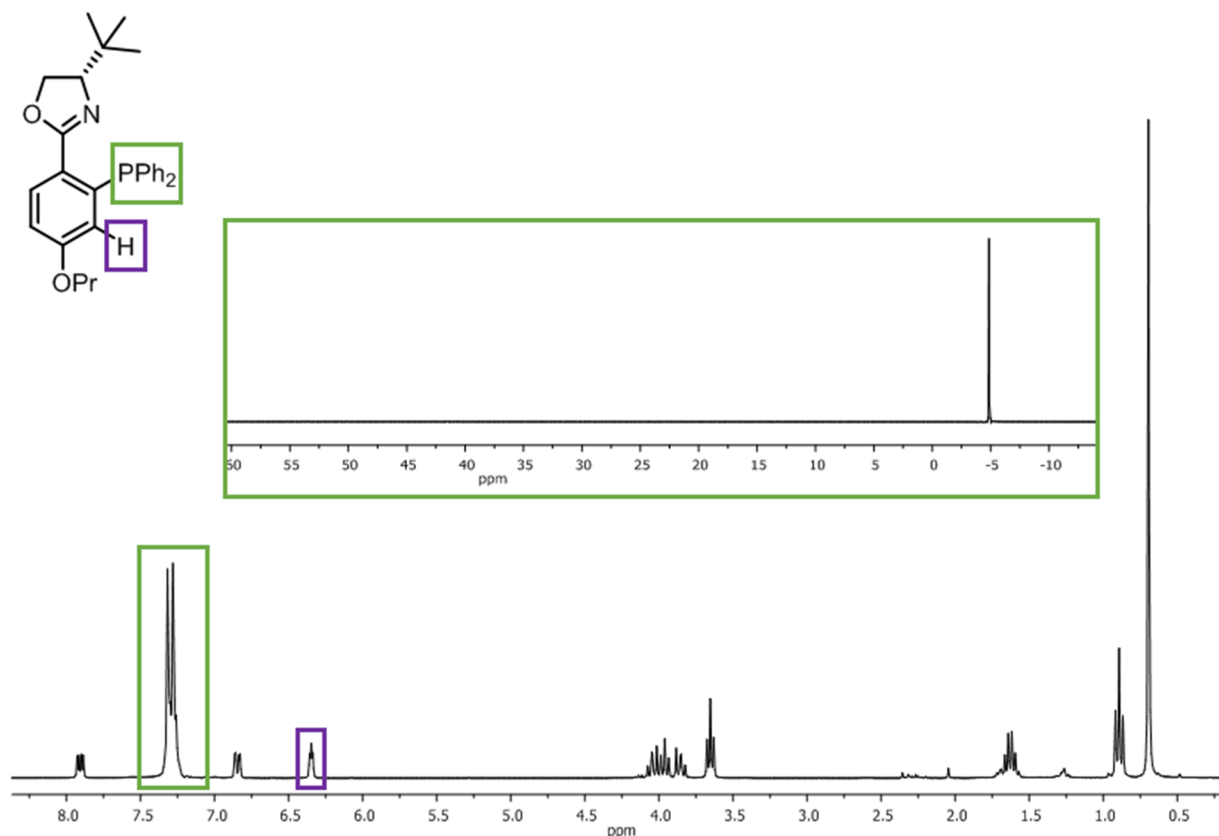


Figure 5.6: ^1H (below) and ^{31}P (above) NMR spectra of **93**. Characteristic aromatic signals outlined in green and purple.

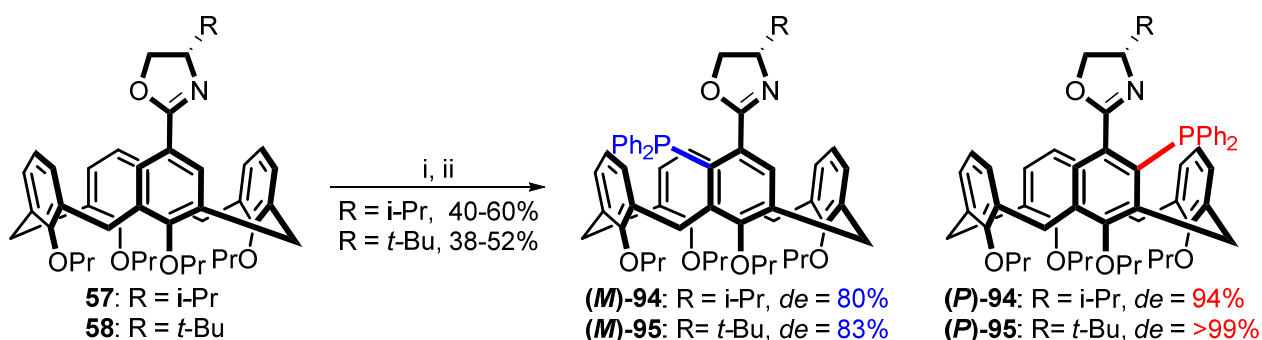
The splitting pattern of the three aromatic signals for **93** matched that seen in **91**. The chemical shift for the proton in the *meta*-position below the diphenyl phosphine group (outlined in purple) was the most downfield of the three, with a chemical shift of δ 6.35 ppm. The proton signals for the two new phenyl groups appeared as a large multiplet over δ 7.16–7.24 ppm. The ^{31}P spectrum, also outlined in green above the ^1H NMR spectrum, contained a single signal with the chemical shift of δ -4.86 ppm. The lack of any other signals confirmed that no oxidation took place. This was the most important piece of analytical data for these compounds. Even though high quality spectral data was collected for the model phosphine oxazoline ligands, the model ligands oxidized to the corresponding phosphine oxides during MS and IR analysis.

Finally, having a method to synthesize and purify a phosphine compound was a big step forward. We were now confident to test these methods on the calixarenes, and in so doing, synthesize the first small library of inherently chiral phosphine oxazoline calixarene ligands.

5.5 Synthesis of calixarene Phox ligands.

5.5.1 Preventing phosphine oxidation.

Once again, the first attempts to synthesize the calixarene ligands using the reworked experimental procedure for the model ligands only yielded the calixarene phosphine oxide. This indicated that the calixarene phosphines were even more air sensitive than the model ligands **92** and **93**. It was speculated that the mildly acidic nature of the silicon dioxide was promoting the oxidation process. To verify this, the silica was replaced with neutral alumina for the quench and subsequent purification steps in the reaction. This proved to be successful and enabled the synthesis of the four targeted calixarene Phox ligands (**M**)/(**P**)-**94** and (**M**)/(**P**)-**95** (Scheme 5.7).



Scheme 5.7: Synthesis of the four inherently chiral calixarene Phox ligands. Reagents and conditions:

i) RLi (5.0 equiv), additive (10.0 equiv), solvent, $-78\text{ }^{\circ}\text{C}$, 24 h; ii) PPh_2Cl (15 equiv), $-78\text{ }^{\circ}\text{C}$ to rt, 12 h.

The biggest practical challenge associated with this chemistry was avoiding exposure to atmospheric oxygen at all times, as it led to rapid oxidation of the ligands. Due to the sensitive nature of the calixarene Phox ligands and their enthusiasm toward oxidation, collecting the necessary characterization data for these ligands proved to be a major problem. All of the ^1H and ^{31}P NMR spectra collected consisted of a mixture of the phosphine and phosphine oxide. A typical example of this problem is clearly seen in the ^{31}P NMR spectrum of (**P**)-**95** (Figure 5.7).

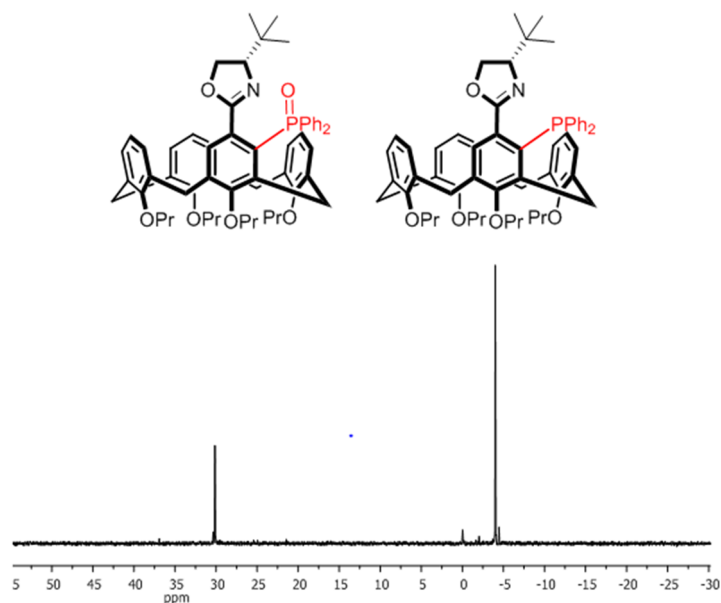
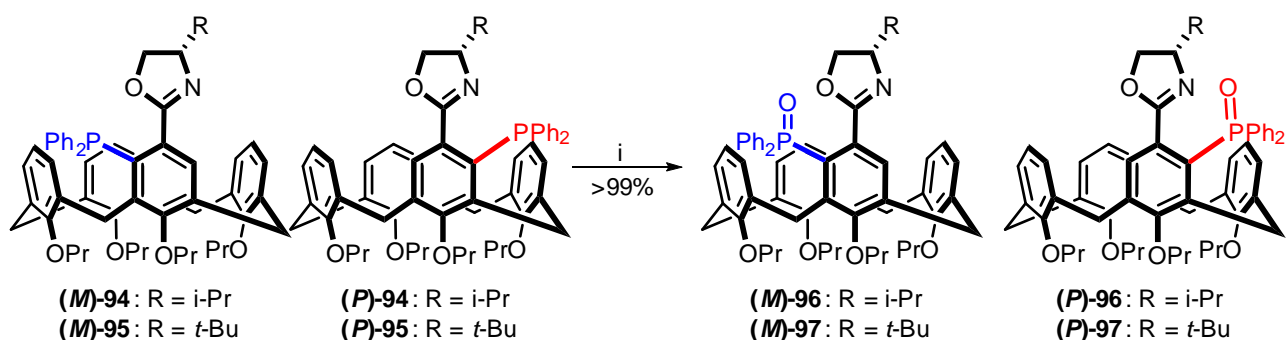


Figure 5.7: Typical ^{31}P NMR spectrum of the phosphine and phosphine oxide mixture.

Even employing the preparative techniques used for the NMR spectroscopic characterization of **92** and **93** was not sufficient. Despite these difficulties, the techniques to synthesize, purify, store and handle these ligands without oxidation had been established. However, the characterization of these ligands required a different approach altogether.

5.6 Indirect characterisation of the calixarene Phox ligands.

It was unfortunate, but to fully characterize these compounds, the corresponding phosphine oxides had to be used instead. Despite this not being the ideal solution, the accurate analysis of the related oxides would serve as an indirect means of characterization for these compounds. In spite of their rapid rate of oxidation when exposed to oxygen, small amounts of the phosphine still remained after exposure of the solid product material to the atmosphere for 24 h. To ensure quantitative conversion, the ligands were treated with an excess of aqueous H_2O_2 in THF at room temperature (**Scheme 5.8**).



Scheme 5.8: Oxidation of the calixarene Phox ligands **(P)/(M)-94** and **(P)/(M)-95**. Reagents and conditions: i) 30% H₂O₂ (exs), THF, rt, 0-30 min.

The conversions to phosphine oxides **(P)/(M)-96** and **(P)/(M)-97** were almost instantaneous and quantitative in the presence of excess amounts of peroxide at room temperature. They were all purified using silica column chromatography and fully characterized with a combination of ¹H NMR, ¹³C NMR, MS and IR spectroscopy. The ¹H and ³¹P NMR spectra of **(P)-97** are a representation of what the spectra for these phosphine oxides generally looked like (**Figure 5.8**).

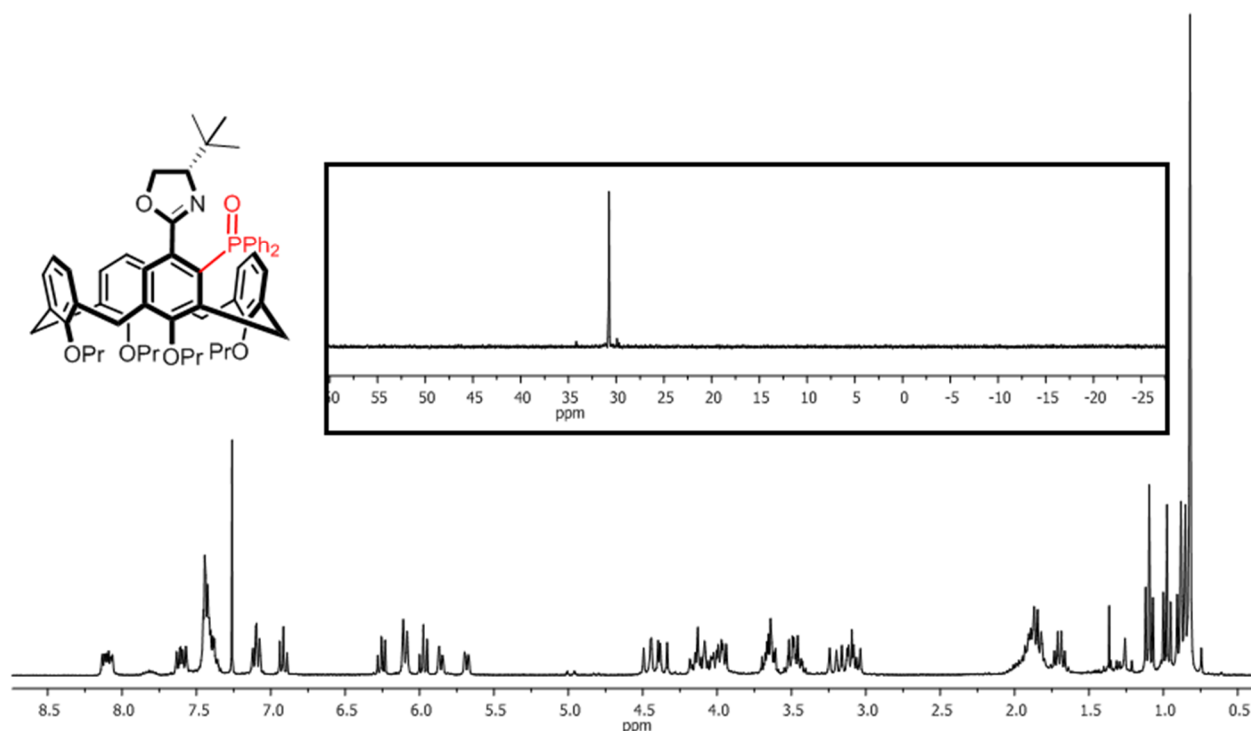


Figure 5.8: ¹H (below) and ³¹P (outlined above) NMR spectra of **(P)-97**.

The ¹H and ³¹P NMR spectra of the two phosphine oxide diastereomer pairs were almost identical. The diphenyl phosphine aromatic signals overlapped with characteristic singlets of each diastereomer, which prevented *dr* calculations.

Chapter 5: Synthesis of phosphine oxazoline calixarene ligands

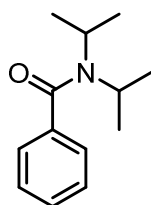
An important question that could not be answered with the sensitive phosphine ligands, or the NMR spectral data collected for the phosphine oxides, was whether or not the selectivities of the ortholithiation reactions were consistent when using the diphenyl phosphine chloride electrophile. However, HPLC analysis of the stable phosphine oxides confirmed *dr* values that were equal to their thio-ether counterparts.

5.7 Conclusion.

To conclude, two new model, **92** and **93**, and four inherently chiral calixarene, (*P*)/(*M*)-**94** and (*P*)/(*M*)-**95**, ligands were successfully synthesized and fully characterized. The careful use of inert experimental techniques and neutral aluminum oxide proved to be key for the synthesis and purification of the more sensitive calixarene ligands. These results meant that the application of a new class of phosphine oxazoline ligand could finally be investigated.

5.8 Experimental section.

5.8.1 *N,N*-diisopropylbenzamide – **85**.³⁵

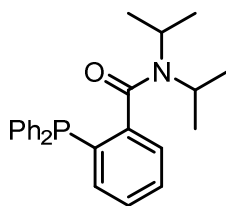


Benzoyl chloride (7.00 ml, 60.3 mmol) was added to dry Et₂O (150 ml) and cooled (0 °C). Diisopropylamine (12.7 ml, 90.4 mmol, 1.5 equiv) was added and the salt immediately formed. Et₃N (15.7 ml, 120 mmol, 2.0 equiv) was added and the mixture was stirred overnight. The organic phase was washed with 1M HCl, dried over MgSO₄ and the excess solvent was removed under reduced pressure, yielding an off white solid as the crude product. Purification was achieved via crystallization from PET, yielding a white solid (11.2 g, 91%).

The characterisation data collected for this compound compared well with the reported literature values.³⁵

¹H NMR (300 MHz, CHLOROFORM-*d*) δ 1.20 (br. s, 6H CH(CH₃)₂), 1.49 (br. s, 6H (CH(CH₃)₂), 3.58 (br. s, 1H, CH(CH₃)₂), 3.77 (s (broad), 1H, CH(CH₃)₂), 7.29-7.31 (m, 2H, ArH), 7.34-7.38 (m, 3H, ArH) ppm.

Chapter 5: Synthesis of phosphine oxazoline calixarene ligands

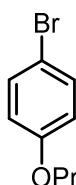
5.8.2 2-(diphenylphosphanyl)-N,N-diisopropylbenzamide – **86**.³⁶

85 (200 mg, 0.970 mmol) and TMEDA (0.310 ml, 2.00 mmol 2.0 equiv) were added to dry THF (4 ml) and the mixture was cooled ($-78\text{ }^{\circ}\text{C}$). *n*-BuLi (1.95 mmol, 2.0 equiv) was then slowly added, turning the colourless mixture a dark clear yellow/orange. After stirring at $-78\text{ }^{\circ}\text{C}$ for approximately an hour the mixture had changed to a cloudy yellow. The reaction was stirred for 5 h before diphenylphosphine chloride (0.700 ml, 3.90 mmol, 4.0 equiv) was added dropwise. The mixture was then given time to slowly warm to room temperature, after which it was quenched with oven dried silica. The excess solvent was then removed under reduced pressure and the crude product was dry-loaded onto a silica column. Separation was achieved using (EtOAc:PET, 10:90), yielding **86** as a clear oil (332 mg, 88%) that solidified upon standing at room temperature.

The characterisation data collected for this compound compared well with the reported literature values.³⁶

^1H NMR (300 MHz, CHLOROFORM-*d*) δ 0.86-0.92 (m, 6H, $\text{CH}(\text{CH}_3)_2$), 1.37-1.48 (m, 6H, $\text{CH}(\text{CH}_3)_2$), 2.04-2.10 (m, 2H, $\text{CH}(\text{CH}_3)_2$), 7.30-7.43 (m, 8H, ArH), 7.40-7.49 (m, 6H, ArH) ppm.

^{31}P NMR (120 MHz, CHLOROFORM-*d*) $\delta = -14.80$ ppm.

5.8.3 1-bromo-4-propoxybenzene – **87**.³⁴

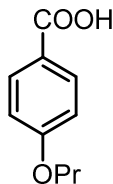
4-bromo phenol (10.0 g, 57.8 mmol) and K_2CO_3 (19.7 g, 145 mmol, 2.5 equiv) were added to dry DMF (250 ml). The clear yellow/orange mixture was heated to reflux and after 1 h, the iodopropane (20.2 ml, 202 mmol, 5.0 equiv) was added all at once. Reflux was maintained for 24 h. Once the flask had cooled to room temperature, and the reaction was carefully quenched with 1M HCl, the mixture was transferred to a separating funnel. EtOAc (100 ml) was added and the organic layer was washed with 1M HCl (2 x 100 ml) and dist. H_2O (1 x 150 ml), yielding a brown liquid as the crude product. Purification was achieved using column chromatography (EtOAc:PET, 5:95), affording the product as a clear oil (11.6 g, 93 %).

The characterisation data collected for this compound compared well with the reported literature values.³⁴

Chapter 5: Synthesis of phosphine oxazoline calixarene ligands

^1H NMR (300 MHz, CHLOROFORM-*d*) δ 1.04 (t, $J = 7.4$ Hz, 3H, $\text{OCH}_2\text{CH}_2\text{CH}_3$), 1.75-.86 (m, 2H, $\text{OCH}_2\text{CH}_2\text{CH}_3$), 3.88 (t, $J = 6.6$ Hz, 2H, $\text{OCH}_2\text{CH}_2\text{CH}_3$), 6.78 (d, $J = 9.0$ Hz, 2H, ArH), 7.36 (d, $J = 9.0$ Hz, 2H, ArH) ppm.

5.8.4 4-propoxybenzoic acid – **88**.³³



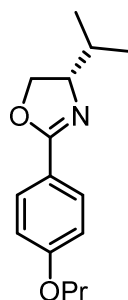
Compound **87** (13.8 g, 64.1 mmol) was added to dry THF (500 ml), and the solution was cooled (-78 °C). *n*-BuLi (74.0 ml, 96.2 mmol, 2.5 equiv) was carefully added turning the reaction mixture a pale yellow colour. The mixture was stirred for 30 minutes, after which CO_2 gas was bubbled through the mixture for 15 minutes. The reaction was allowed to warm to room temperature, after which it was carefully quenched with 1M HCl. DCM (250 ml) was added to the flask and the content was transferred to a separating funnel. The organic layer was washed with 1M HCl (1 x 150 ml), dried over MgSO_4 and the excess solvent was removed under reduced pressure, yielding an orange solid as the crude product. The product was purified using column chromatography, the protonated product was washed off using a (EtOAc:PET, 10:90) mixture, after which, the propoxybenzoic acid was flushed off with (EtOAc, 100), yielding a white solid (8.36 g, 72%).

Further purification was achieved via trituration from EtOH. The mixture was cooled to -15 °C overnight and the white crystals were filtered from the mixture. This procedure had to be repeated several times until the bulk of the product was isolated (8.15 g, 70%).

The characterisation data collected for this compound compared well with the reported literature values.³³

^1H NMR (300 MHz, CHLOROFORM-*d*)³³ δ 1.06 (t, $J = 7.4$ Hz, 3H, $\text{OCH}_2\text{CH}_2\text{CH}_3$), 1.91-1.78 (m, 2H, $\text{OCH}_2\text{CH}_2\text{CH}_3$), 4.00 (t, $J = 6.6$ Hz, 2H), 6.94 (d, $J = 9.0$ Hz, 2H, ArH), 8.06 (d, $J = 9.0$ Hz, 2H, ArH) ppm.

5.8.5 (S)-4-isopropyl-2-(4-propoxyphenyl)-4,5-dihydrooxazole – 89.



SOCl₂ (10 ml, exs) was added to **88** (2.00 g, 1.67 mmol) at room temperature under argon, immediately resulting in the formation of a purple reaction mixture. The reaction was stirred at room temperature for 20 h, after which the excess thionyl chloride was removed under reduced pressure, affording a purple liquid as the acid chloride product. The acid chloride was then dried for 5 h under high vacuum. L-valinol (1.48 g, 14.4 mmol, 1.1 equiv) and Et₃N (7.75 ml, 55.6 mmol, 5.0 equiv) were added to dry DCM (50 ml) and cooled (0 °C). The acid chloride was dissolved in dry DCM (10 ml) which was then added dropwise to the cooled mixture, resulting in a pale yellow solution. The mixture was given time to warm to room temperature and stirred for 12 h. Once TLC showed that no starting material remained, mesyl chloride (4.34 ml, 55.6 mmol, 5.0 equiv) was added to the flask at room temperature, turning the pale yellow solution a darker yellow/orange. After 20 h, TLC showed that none of the amide product remained. 1M HCl was carefully added to quench the mixture and the content of the flask was added to a separating funnel. The organic layer was washed with 2M NaOH (2 x 50 ml) and dist. H₂O (1 x 100 ml). The excess solvent was removed under reduced pressure affording a dark orange/brown oil as the crude product. Purification was achieved via column chromatography (EtOAc:PET, 5:95), yielding a white solid (2.48 g, 90%).

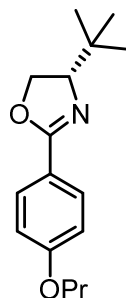
¹H NMR (300 MHz, CHLOROFORM-*d*) δ 0.91 (d, *J* = 6.8 Hz, 3H, CH(CH₃)₂), 1.03 (d, *J* = 6.8 Hz, 3H, CH(CH₃)₂), 1.05 (t, *J* = 7.5 Hz, 3H, OCH₂CH₂CH₃), 1.69-1.84 (m, 3H, OCH₂CH₂CH₃, CH(CH₃)₂), 3.88 (t, *J* = 6.6 Hz, 2H, OCH₂CH₂CH₃), 4.03-4.14 (m, 2H, OCH₂CHN), 4.32-4.42 (m, 1H, OCH₂CHN), 6.87-6.91 (m, 2H, ArH), 7.86-7.90 (m, 2H, ArH) ppm.

¹³C NMR (75 MHz, CHLOROFORM-*d*) δ 10.6 (OCH₂CH₂CH₃), 19.1 (CH(CH₃)₂), 22.6 (OCH₂CH₂CH₃), 33.0 (CH(CH₃)₂), 69.7 (OCH₂CH₂CH₃), 70.1 (OCH₂CH), 72.6 (NCH), 114.3 (C_{Ar}H), 120.2 (C_{Ar}H), 130.1 (C_{Ar}H), 161.7 (C_{Ar}O), 163.4 (C_{Ar}C=N) ppm.

IR (film) cm⁻¹: 2950 (s, CH), 1665 (s, C=N), 1450 (s, C=C), 1140 (m, C-O stretch), 980 (m, C-H oop bend), 760 (s, C-H oop bend).

HRMS-TOF MS ESI+: *m/z* [M+H]⁺: calculated for C₁₅H₂₁NO₂: 248.1651; Found: 248.1653.

5.8.6 (S)-4-(tert-butyl)-2-(4-propoxyphenyl)-4,5-dihydrooxazole – 90.



88 (610 mg, 2.80 mmol) was added to freshly distilled DCM (20 ml). Oxazyl chloride (1.10 ml, 13.9 mmol, 5.0 equiv) was added at room temperature, turning the reaction mixture a pale yellow. The reaction was stirred at room temperature for 20 h, after which the excess solvent and oxalyl chloride were removed under reduced pressure, affording an orange liquid as the acid chloride product. The acid chloride was then dried for 5 h under high vacuum. L-*tert*-leucinol (390 mg, 3.33 mmol, 1.2 equiv) and Et₃N (1.93 ml, 13.9 mmol, 5.0 equiv) were added to dry DCM (20 ml) and cooled (0 °C). The acid chloride was dissolved in dry DCM (10 ml) which was then added dropwise to the cooled mixture, resulting in a pale yellow solution. The mixture was given time to warm to room temperature and stirred for an additional 12 h. Once TLC showed that no starting material remained, the reaction was quenched with 1M HCl. The amide was extracted with DCM (50 ml). The organic layer was washed with an additional portion of 1M HCl (50 ml), dried over MgSO₄ and the excess solvent was then removed under reduced pressure. The amide was purified with column chromatography, with gradient elution from (PET, 100) to (EtOAc:PET, 60:40) mixture yielding the amide as a white solid. Mesyl chloride (1.05 ml, 13.9 mmol, 5.0 equiv) and Et₃N (1.93 ml, 13.9 mol, 5.0 equiv) were added to freshly distilled DCM (20.0 ml) and cooled (0 °C). The amide was dissolved in DCM (10 ml) which was added dropwise to the cooled mixture. The reaction was allowed to warm to room temperature and stirred overnight. TLC confirmed that no starting material remained and 1M HCl was carefully added to quench the reaction. The content of the flask was added to a separating funnel and the organic layer was washed with 2M NaOH (2 x 50 ml) and dist. H₂O (1 x 100 ml). The excess solvent was removed under reduced pressure, affording a dark orange/brown oil as the crude product. Purification was achieved via column chromatography (EtOAc:PET, 10:90) yielding the oxazoline as a white solid (662 mg, 87%).

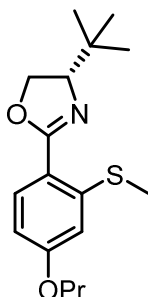
¹H NMR (300 MHz, CHLOROFORM-*d*) δ 0.94 (s, 9H, C(CH₃)₃), 1.04 (t, *J* = 7.4 Hz, 3H, OCH₂CH₂CH₃), 1.76-1.88 (m, 2H, OCH₂CH₂CH₃), 3.95 (t, *J* = 6.6 Hz, 2H OCH₂CH₂CH₃), 4.01 (dd, *J* = 10.1, 7.5 Hz, 1H, CH₂CHN), 4.20 (dd, *J* = 8.5, 7.5 Hz, 1H, OCH₂CHN), 4.31 (dd, *J* = 10.1, 8.6 Hz, 1H, OCH₂CH), 6.89 (d, *J* = 8.9 Hz, 2H, ArH), 7.88 (d, *J* = 8.9 Hz, ArH, 2H) ppm

¹³C NMR (75 MHz, CHLOROFORM-*d*) δ 10.7 (OCH₂CH₂CH₃), 22.8 (OCH₂CH₂CH₃), 26.0 (C(CH₃)₃), 34.1 (C(CH₃)₃), 68.7 (NCH), 70.1 (OCH₂CH₂CH₃), 70.1 (OCH₂CH), 114.3 (C_{Ar}H), 120.2 (C_{Ar}H), 130.2 (C_{Ar}H), 161.7 (C_{Ar}H), 163.4 (OC(Ar)=N) ppm.

Chapter 5: Synthesis of phosphine oxazoline calixarene ligands

IR (film) cm^{-1} : 2970 (s, CH), 1670 (s, C=N), 1460 (s, C=C), 1150 (m, C-O stretch), 975 (m, C-H oop bend), 755 (s, C-H oop bend).

HRMS-TOF MS ESI+: m/z $[\text{M}+\text{H}]^+$ calculated for $\text{C}_{16}\text{H}_{21}\text{NO}_2$: 260.1650; Found: 260.1658.

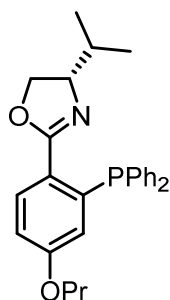
5.8.7 (*S*)-4-(*tert*-butyl)-2-(2-(methylthio)-4-propoxyphenyl)-4,5-dihydrooxazoline – **91**.

The aim of synthesizing this was to confirm the ortholithiation procedure, in order to make the phosphine model compounds. Pre-drying of the starting material: Solvation/desolvation in THF followed by drying under high vacuum for 4 h. *n*-BuLi (0.17 ml, 0.12 mmol, 2.0 equiv) was added to an oven dried Schlenk flask under argon. The excess hexane was removed under reduced pressure yielding a white solid that was then cooled ($-78\text{ }^\circ\text{C}$). THF (0.45 ml) and TMEDA (0.035 ml, 0.23 mmol, 4.0 equiv) were then added resulting in a pale yellow mixture. Oxazoline **90** (15 mg, 0.057 mmol) was added to dry THF (0.2 ml) and added drop wise to the cooled mixture quickly turning it a dark clear yellow. The mixture was stirred at $-78\text{ }^\circ\text{C}$ for 4 h, after which, S_2Me_2 (0.05 ml, 0.57 mmol, exs) was added dropwise, lightening the dark yellow colour significantly. After approximately 20 minutes a precipitate started to form. The mixture was given time to warm to room temperature overnight. The reaction was quenched using 1M HCl. The product was extracted using EtOAc (15 ml), which was washed with additional 1M HCl (1 x 40 ml). The organic layer was dried over MgSO_4 and the excess solvent was removed under reduced pressure yielding a brown/orange semi solid as the crude product. No further purification was done. Analysis of the crude ^1H NMR spectrum showed a near quantitative conversion, confirming the success of the method.

^1H NMR (300 MHz, CHLOROFORM-*d*) δ 1.05 (s, 9H, $\text{C}(\text{CH}_3)_3$), 1.20 (t, $J = 6.9$ Hz, 3H, $\text{OCH}_2\text{CH}_2\text{CH}_3$), 1.79-1.86 (m, 2H, $\text{OCH}_2\text{CH}_2\text{CH}_3$), 2.40 (s, 3H, SCH_3), 4.02 (t, $J = 6.5$ Hz, 2H $\text{OCH}_2\text{CH}_2\text{CH}_3$), 4.50 (dd, $J = 10.2, 5.8$ Hz, 1H, OCH_2CHN), 4.77 (dd, $J = 10.2, 5.8$ Hz, 1H, OCH_2CH), 5.01 (t, $J = 9.8$ Hz, 1H, NCHC), 6.74 (d, $J = 2.1$ Hz, 1H, ArH), 6.86 (dd, $J = 8.9, 2.1$ Hz, 1H, ArH), 8.31 (d, $J = 8.9$ Hz, 1H, ArH) ppm.

Chapter 5: Synthesis of phosphine oxazoline calixarene ligands

5.8.8 (S)-2-(2-(diphenylphosphanyl)-4-propoxyphenyl)-4-isopropyl-4,5-dihydrooxazole – 92.

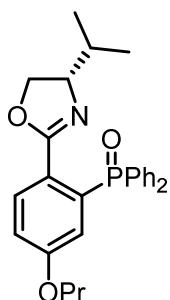


Pre-drying of the starting material: Solvation/desolvation in Et₂O followed by drying under high vacuum for 4 h. Oxazoline **89** (100 mg, 0.406 mmol) and TMEDA (0.130 ml, 0.812 mmol, 2.0 equiv) were added to dry Et₂O (1 ml) and cooled (−78 °C). After stirring for 10 minutes, *n*-BuLi (0.650 mmol, 1.5 equiv) was carefully added. Approximately 40 minutes after addition a yellow/white precipitate had formed. The reaction mixture was stirred for a further 4 h before diphenylphosphine chloride (0.300 ml, 1.62 mmol, 4.0 equiv) was added. The mixture was then stirred for a further 2 h at −78 °C, after which it was given time to slowly warm to room temperature and stirred overnight. The reaction was finally quenched by the addition of oven dried silica. The excess solvent was removed under reduced pressure and the resulting solid was dry-loaded onto a silica column. Separation was achieved using silica column chromatography (EtOAc:PET, 7:93) which yielded the phosphine oxazoline ligand as a clear oil (77 mg, 44% yield).

¹H NMR (300 MHz, CHLOROFORM-*d*) δ 0.67 (d, *J* = 6.7 Hz, 3H, CH(CH₃)₂), 0.79 (d, *J* = 6.7 Hz, 3H, CH(CH₃)₂), 0.90 (t, *J* = 7.4 Hz, 3H, OCH₂CH₂CH₃), 1.41-1.52 (m, 1H, CH(CH₃)₂), 1.58-1.69 (m, OCH₂CH₂CH₃), 3.66 (t, *J* = 6.7 Hz, 2H, OCH₂CH₂CH₃), 3.77-3.89 (m, 2H, OCH₂CH, CHN), 4.06-4.16 (m, 1H, OCH₂CHN), 6.35 (dd, *J* = 4.1, 2.6 Hz, 1H, ArH), 6.84 (dd, *J* = 8.6, 2.6 Hz, 1H, ArH), 7.29-7.33 (m, 10H, P-ArH), 7.89 (dd, *J* = 8.6, 4.1 Hz, 1H, ArH) ppm.

¹³C NMR (75 MHz, CHLOROFORM-*d*) δ 10.4, 18.4, 19.0, 22.3, 32.9, 69.3, 66.9, 73.0, 113.9, 112.0, 120.0 (d, ³*J* = 1.9 Hz), 124.0 (d, ²*J* = 18.4 Hz), 128.3 (d, ³*J* = 3.2 Hz), 128.4 (d, ³*J* = 3.2 Hz), 128.5, 128.7, 131.7 (d, ²*J* = 3.1 Hz), 133.8 (d, ²*J* = 20.4 Hz), 134.5 (d, ²*J* = 21.2 Hz), 138.3 (d, ¹*J* = 23.1 Hz), 138.4 (d, ¹*J* = 25.8 Hz), 141.1 (d, ¹*J* = 27.2 Hz), 160.5, 162.8 (d, ³*J* = 3.4 Hz) ppm.

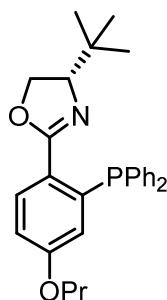
³¹P NMR (300 MHz, CHLOROFORM-*d*) δ −3.49 ppm.



IR (ATR) cm^{−1}: 2960 (s, C-H stretch), 1660 (s, C=N stretch), 1598 (m, C=C stretch), 1460 (s, C=C stretch), 1198 (s, P=O stretch), 1010 (s, C-O stretch), 768 (s, C-H oop bend).

HRMS-TOF MS ESI+: *m/z* [M+H]⁺ calculated for C₂₇H₃₁NO₃P: 448.2042; Found: 448.2046.

Chapter 5: Synthesis of phosphine oxazoline calixarene ligands

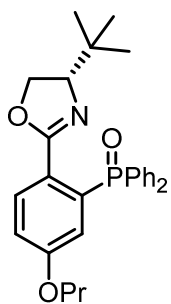
5.8.9 (S)-4-(tert-butyl)-2-(2-(diphenylphosphinanyl)-4-propoxyphenyl)-4,5-dihydrooxazole – **93**.

Pre-drying of the starting material: Solvation/desolvation in Et₂O followed by drying under high vacuum for 4 h. **90** (100 mg, 0.382 mmol) was added to dry Et₂O (3 ml) and cooled (–78 °C). TMEDA (0.240 ml, 1.52 mmol, 4.0 equiv) was then added, shortly followed by *n*-BuLi (0.415 ml, 0.760 mmol, 2.0 equiv), immediately forming a light pink precipitate. The mixture was stirred for 24 h at –78 °C. Diphenylphosphine chloride (0.360 ml, 2.00 mmol, 6.0 equiv) was then added drop wise, turning the mixture white. The Schlenk was flushed with Ar, sealed and given time to warm to room temperature overnight. Alumina was added to the flask and the excess solvent was removed under reduced pressure. The product was purified using alumina column chromatography (EtOAc:PET, 3:97) yielding both the product (70 mg, 45%) and the starting material (65 mg).

¹H NMR (300 MHz, CHLOROFORM-*d*) δ 0.70 (s, 9H, C(CH₃)₃), 0.89 (t, *J* = 7.4 Hz, 3H, OCH₂CH₂CH₃), 1.57-1.70 (m, 2H, OCH₂CH₂CH₃), 3.65 (t, *J* = 6.7 Hz, 3H, OCH₂CH₂CH₃), 3.85 (dd, *J* = 9.9, 8.1 Hz, 1H, OCH₂CHN), 3.96 (t, *J* = 8.1 Hz, NCHC(CH₃)), 4.05 (dd, *J* = 9.9, 8.1 Hz, 1H, OCH₂CHN), 6.53 (m, 1H, ArH), 6.85 (dd, *J* = 8.6, 2.3 Hz, 1H, ArH), 7.26-7.32 (m, 10H, P-ArH), 7.91 (dd, *J* = 8.6, 4.0 Hz, 1H, ArH) ppm.

¹³C NMR (75 MHz, CHLOROFORM-*d*) δ 10.4, 22.3, 25.8, 33.7, 68.1, 69.3, 76.7, 114.1, 120.2 (d, ³*J* = 1.4 Hz), 124.5 (d, ²*J* = 18.4 Hz), 128.2 (d, ³*J* = 3.3 Hz), 128.3 (d, ³*J* = 3.3 Hz), 128.4, 128.6, 131.6 (d, ²*J* = 3.3 Hz), 133.5 (d, ²*J* = 20.2 Hz), 134.5 (d, ²*J* = 21.1 Hz), 138.4 (d, ¹*J* = 29.7 Hz) 138.6 (d, ¹*J* = 31.6 Hz), 140.9 (d, ¹*J* = 27.3 Hz), 160.5, 162.4 (d, ³*J* = 3.3 Hz) ppm.

³¹P NMR (300 MHz, CHLOROFORM-*d*) δ –4.86 ppm.

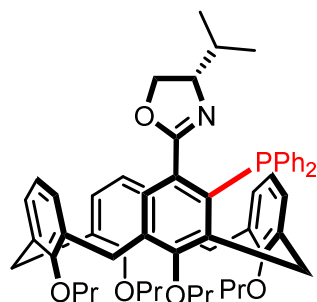


IR (ATR) cm⁻¹: 2968 (s, C-H stretch), 1658 (s, C=N stretch), 1598 (m, C=C stretch), 1460 (s, C=C stretch), 1200 (s, P=O stretch), 1010 (s, C-O stretch), 764 (s, C-H oop bend).

HRMS-TOF MS ESI+: *m/z* [M+H]⁺ calculated for C₂₈H₃₃NO₃P: 462.2198; Found: 462.2194.

Chapter 5: Synthesis of phosphine oxazoline calixarene ligands

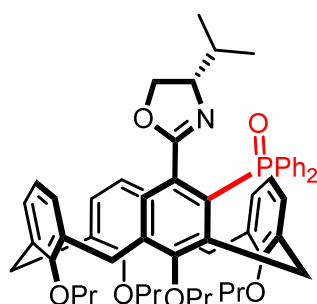
5.8.10 (P)-5-((S)-4-Isopropyl-4,5-dihydrooxazol-2-yl)-4-diphenylphosphine-25,26,27,28-tetrapropoxycalix[4]arene – 94.



Calixarene (**P**)-**94** was synthesized according to the general ortholithiation procedure (**Chapter 3**), but was quenched by the addition of oven dried alumina. Oxazoline calixarene **57** (100 mg, 0.141 mmol), *c*-PentLi (0.706 mmol, 5.0 equiv), TMEDA (0.220 ml, 1.41 mmol, 10.0 equiv), pentane (4 ml) and diphenylphosphine chloride (0.200 ml, excess) with a reaction time of 24 h. The product was purified using alumina column chromatography gradient elution (EtOAc:PET, 0:100 to 5:95) yielding a white solid (50 mg, 40%).

Due to the sensitive nature of these compounds, characterization of the phosphine was not possible. Techniques were developed so that the compound could be isolated, handled, stored and used for asymmetric catalytic reactions. NMR spectroscopy was attempted but due to the rapid oxidation of the compound, as well as its size and complexity, the spectra were cluttered and difficult to interpret. Instead, the ligands were fully oxidized and the corresponding phosphine oxides were properly purified and fully characterized instead.

5.8.11 (P)-5-((S)-4-Isopropyl-4,5-dihydrooxazol-2-yl)-4-diphenylphosphineoxide-25,26,27,28-tetrapropoxycalix[4]arene – 96.



(**P**)-**94** (70.0 mg, 0.116 mmol) was added to THF (3 ml) at room temperature. H₂O₂ (2.00 ml, 30% aq, exs) was added all at once. The reaction mixture was stirred at room temperature for 30 minutes. Alumina TLC confirmed full conversion to the phosphine oxide. The reaction was quenched by the addition of 1M HCl. The crude product was extracted using DCM. The organic layer was then washed with additional 1M HCl, dried over MgSO₄ and the excess solvent was removed under reduced pressure, yielding a white solid.

Chapter 5: Synthesis of phosphine oxazoline calixarene ligands

Purification was achieved using alumina column chromatography, (EtOAc:PET, 30:70), yielding the phosphine oxide (**P**)-**96** as a white solid (99.6 mg, 95%). Mp: > 330 °C.

^1H NMR (300 MHz, CHLOROFORM-*d*) 0.73 (d, $J = 6.7$ Hz, 3H, $\text{CH}(\text{CH}_3)_2$), 0.82-1.00 (m, 12H, $\text{CH}(\text{CH}_3)_2$, $\text{OCH}_2\text{CH}_2\text{CH}_3$), 1.12 (t, $J = 7.4$ Hz, 3H, $\text{OCH}_2\text{CH}_2\text{CH}_3$), 1.24-1.39 (m, 1H, $\text{CH}(\text{CH}_3)_2$), 1.59-1.71 (m, 2H, $\text{OCH}_2\text{CH}_2\text{CH}_3$), 1.82-2.04 (m, 6H, $\text{OCH}_2\text{CH}_2\text{CH}_3$), 3.06 (d, $J = 13.4$ Hz, 1H, $\text{ArCH}_2^{\text{eq}}\text{Ar}$), 3.15 (d, $J = 13.4$ Hz, 1H, $\text{ArCH}_2^{\text{eq}}\text{Ar}$), 3.19-3.26 (m, 2H, $\text{ArCH}_2^{\text{eq}}\text{Ar}$), 3.60-3.70 (m, 2H, $\text{OCH}_2\text{CH}_2\text{CH}_3$), 3.77-4.05 (m, 6H, $\text{OCH}_2\text{CH}_2\text{CH}_3$, OCH_2CHN), 4.16 (m, 1H, OCH_2CHN), 4.34 (d, $J = 13.4$ Hz, 1H, $\text{ArCH}_2^{\text{ax}}\text{Ar}$), 4.43 (d, $J = 13.4$ Hz, 1H, $\text{ArCH}_2^{\text{ax}}\text{Ar}$), 4.47 (d, $J = 13.4$ Hz, 2H, $\text{ArCH}_2^{\text{ax}}\text{Ar}$), 5.76 (d, $J = 6.7$ Hz, 1H, ArH), 5.86 (d, $J = 7.4$ Hz, 1H, ArH), 6.02 (t, $J = 7.4$ Hz, 1H, ArH), 6.10 (t, $J = 7.9$ Hz, 2H, ArH), 6.27 (t, $J = 7.6$ Hz, 1H, ArH), 6.93 (t, $J = 7$ Hz, 1H, ArH), 7.08-7.13 (m, 2H, ArH), 7.96-8.07 (m, 6H, ArH), 7.55 (d, $J = 4.7$ Hz, 1H, ArH), 7.60-7.68 (m, 2H, ArH), 7.96-8.05 (m, 2H, ArH) ppm.

Owing to the complexity of the aromatic region in the ^{13}C NMR spectrum, the P-C coupling could not be accurately determined. Instead, all of the ^{13}C signals have been reported which explains why there are more signals than expected.

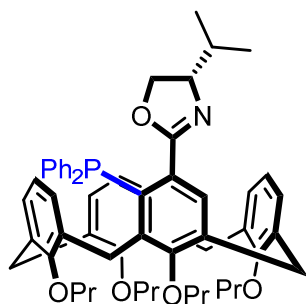
^{13}C NMR (75 MHz, CHLOROFORM-*d*) δ 9.7, 9.8, 10.7, 10.8, 18.7, 20.0, 22.9, 23.3, 23.5, 30.5, 30.6, 30.8, 30.9, 31.0, 32.6, 70.5, 73.1, 76.4, 76.5, 76.6, 76.9, 77.2, 121.7, 122.2, 122.4, 126.8, 126.9, 127.0, 127.1, 127.8, 128.0, 128.1, 128.2, 128.7, 129.0, 130.3, 130.4, 130.5, 130.6, 130.7, 130.9, 131.0, 131.3, 131.4, 131.5, 131.7, 131.8, 132.6, 132.7, 133.4, 133.9, 135.0, 137.1, 137.3, 137.4, 138.4, 141.1, 145.3, 145.4, 155.0, 158.2, 161.3, 161.4, 164.0, 164.1 ppm.

^{31}P NMR (300 MHz, CHLOROFORM-*d*) δ 29.05 ppm.

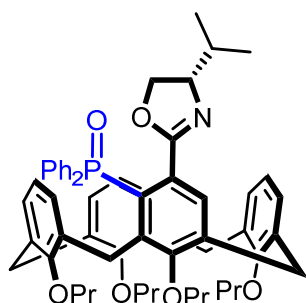
IR (ATR) cm^{-1} : 2965 (s, C-H stretch), 1660 (s, C=N stretch), 1595 (m, C=C stretch), 1455 (s, C=C stretch), 1195 (s, P=O stretch), 1010 (s, C-O stretch), 760 (s, C-H oop bend).

HRMS-TOF MS ESI+: m/z $[\text{M}+\text{H}]^+$ calculated for $\text{C}_{58}\text{H}_{67}\text{NO}_6\text{P}$: 904.4705; found: 904:4709.

Chapter 5: Synthesis of phosphine oxazoline calixarene ligands

5.8.12 (M)-5-((S)-4-Isopropyl-4,5-dihydrooxazol-2-yl)-4-diphenylphosphine-25,26,27,28-tetrapropoxycalix[4]arene – **94**.

Calixarene (**M**)-**94** was synthesized according to the general ortholithiation procedure, but was quenched by the addition of oven dried alumina. Oxazoline calixarene **57** (100 mg, 0.141 mmol), *c*-PentLi (0.706 mmol, 5.0 equiv), di-*t*Bu-diglyme (370 mg, 1.41 mmol, 10.0 equiv), pentane (3 ml) and diphenylphosphine chloride (0.200 ml, exs) were combined with a reaction time of 24 h. The product was purified using alumina column chromatography, (EtOAc:PET, 0:100 to 5:95), yielding a white semi-solid. Owing to the persistence of the diglyme ligand, the yield for this reaction could not be accurately determined. Heating the product to 60 °C under high vacuum resulted in product degradation.

5.8.13 (M)-5-((S)-4-Isopropyl-4,5-dihydrooxazol-2-yl)-4-diphenylphosphineoxide-25,26,27,28-tetrapropoxycalix[4]arene – **96**.

(**M**)-**94** (30 mg, 0.033 mmol) was added to THF (2 ml) at rt. H₂O₂ (1.0 ml, 30% aq, exs) was added all at once. The reaction mixture was stirred at room temperature for 30 minutes. Alumina TLC confirmed full conversion to the phosphine oxide. The reaction was quenched by the addition of 1M HCl. The crude product was extracted using DCM. The organic layer was then washed with additional 1M HCl, dried over MgSO₄ and the excess solvent was removed under reduced pressure yielding a white solid.

Purification was achieved using alumina column chromatography (EtOAc:PET, 30:70), yielding the phosphine oxide (**M**)-**96** as a white solid (27 mg). Mp: > 330 °C.

Chapter 5: Synthesis of phosphine oxazoline calixarene ligands

^1H NMR (300 MHz, CHLOROFORM-*d*) 0.73 (d, $J = 6.7$ Hz, 3H, $\text{CH}(\text{CH}_2)$), 0.82-1.00 (m, 12H, $\text{CH}(\text{CH}_3)_2$, $\text{OCH}_2\text{CH}_2\text{CH}_3$), 1.12 (t, $J = 7.4$ Hz, 3H, $\text{OCH}_2\text{CH}_2\text{CH}_3$), 1.24-1.39 (m, 1H, $\text{CH}(\text{CH}_3)_2$), 1.59-1.71 (m, 2H, $\text{OCH}_2\text{CH}_2\text{CH}_3$), 1.82-2.04 (m, 6H, $\text{CH}_2\text{CH}_2\text{CH}_3$), 3.05 (d, $J = 13.4$ Hz, 1H, $\text{ArCH}_2^{\text{eq}}\text{Ar}$), 3.15 (d, $J = 13.4$ Hz, 1H, $\text{ArCH}_2^{\text{eq}}\text{Ar}$), 3.19-3.26 (m, 2H, $\text{ArCH}_2^{\text{eq}}\text{Ar}$), 3.60-3.70 (m, 2H, $\text{OCH}_2\text{CH}_2\text{CH}_3$), 3.77-4.05 (m, 6H, $\text{OCH}_2\text{CH}_2\text{CH}_3$, OCH_2CH , OCH_2CHN), 4.15-4.17 (m, 1H, $\text{ArCH}_2^{\text{ax}}\text{Ar}$), 4.33 (d, $J = 13.4$ Hz, 1H, $\text{ArCH}_2^{\text{ax}}\text{Ar}$), 4.43 (d, $J = 13.4$ Hz, 1H, $\text{ArCH}_2^{\text{ax}}\text{Ar}$), 4.47 (d, $J = 13.4$ Hz, 1H, $\text{ArCH}_2^{\text{ax}}\text{Ar}$), 5.77 (d, $J = 6.7$ Hz, 1H, ArH), 5.86 (d, $J = 7.4$ Hz, 1H, ArH), 6.02 (t, $J = 7.5$ Hz, 1H, ArH), 6.10 (t, $J = 7.9$ Hz, 2H, ArH), 6.27 (t, $J = 7.6$ Hz, 1H, ArH), 6.94 (t, $J = 7.4$ Hz, 1H, ArH), 7.09-7.13 (m, 2H, ArH), 7.96-8.07 (m, 6H, ArH), 7.53 (d, $J = 4.7$ Hz, 1H, ArH), 7.60-7.68 (m, 2H, ArH), 7.96-8.05 (m, 2H, ArH) ppm.

Owing to the complexity of the aromatic region in the ^{13}C NMR spectrum, the P-C coupling could not be accurately determined. Instead, all of the ^{13}C signals have been reported which explains why there are more signals than expected.

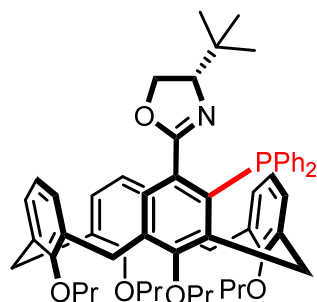
^{13}C NMR (75 MHz, CHLOROFORM-*d*) δ 9.7, 9.8, 10.7, 10.8, 18.7, 20.0, 22.9, 23.3, 23.5, 30.5, 30.6, 30.8, 30.9, 31.0, 32.6, 70.5, 73.1, 76.4, 76.5, 76.6, 76.9, 77.2, 121.7, 122.2, 122.4, 126.8, 126.9, 127.0, 127.1, 127.8, 128.0, 128.1, 128.3, 128.7, 129.0, 130.3, 130.4, 130.5, 130.6, 130.8, 130.9, 131.1, 131.3, 131.4, 131.6, 131.7, 131.8, 132.6, 132.7, 133.4, 133.9, 135.0, 137.1, 137.3, 137.4, 138.4, 141.1, 145.3, 145.4, 155.0, 158.2, 161.3, 161.4, 164.0, 164.1 ppm.

^{31}P NMR (300 MHz, CHLOROFORM-*d*) δ 29.04 ppm.

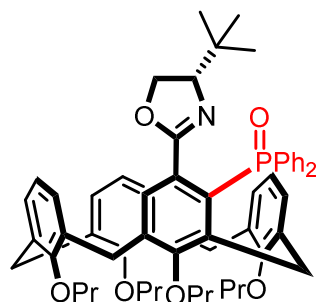
IR (ATR) cm^{-1} : 2960 (s, C-H stretch), 1670 (s, C=N stretch), 1600 (m, C=C stretch), 1455 (s, C=C stretch), 1198 (s, P=O stretch), 1010 (s, C-O stretch), 760 (s, C-H oop bend).

HRMS-TOF MS ES+: m/z $[\text{M}+\text{H}]^+$ calculated for $\text{C}_{58}\text{H}_{67}\text{NO}_6\text{P}$: 904.4706; found: 904:4692.

Chapter 5: Synthesis of phosphine oxazoline calixarene ligands

5.8.14 (*P*)-5-((*S*)-4-(*tert*-butyl)-4,5-dihydrooxazol-2-yl)-4-diphenylphosphine-25,26,27,28-tetrapropoxycalix[4]arene – **95**.

Calixarene (**P**)-**95** was synthesized according to the general ortholithiation procedure, but was quenched by the addition of oven dried alumina. Oxazoline calixarene **58** (100 mg, 0.140 mmol), *s*-BuLi (0.700 mmol, 5.0 equiv), TMEDA (0.220 ml, 1.40 mmol, 10.0 equiv), pentane (3 ml) and diphenyl phosphine chloride (0.3 ml, excess) with a reaction time of 24 h. The product was purified using alumina gel column chromatography (EtOAc:PET, 0:100 to 10:90) yielding a white solid (77 mg, 60%).

5.8.15 (*P*)-5-((*S*)-4-Isopropyl-4,5-dihydrooxazol-2-yl)-4-diphenylphosphineoxide-25,26,27,28-tetrapropoxycalix[4]arene – **97**.

Calixarene (**P**)-**95** (105 mg, 0.120 mmol) was added to THF (3 ml) at room temperature. H₂O₂ (2.0 ml, 30% aq, exs) was added all at once. The reaction mixture was stirred at room temperature for 30 minutes. Alumina TLC confirmed full conversion to the phosphine oxide. The reaction was quenched by the addition of 1M HCl. The crude product was extracted using DCM. The organic layer was then washed with additional 1M HCl, dried over MgSO₄, and the excess solvent was removed under reduced pressure yielding a white solid. Purification was achieved using alumina column chromatography (EtOAc:PET, 30:70), yielding the phosphine oxide (**P**)-**97** as a white solid (100 mg, 90%). Mp: > 330 °C

Chapter 5: Synthesis of phosphine oxazoline calixarene ligands

^1H NMR (300 MHz, CHLOROFORM-*d*) δ 0.82 (s, 9H, C(CH₃)₃), 0.85-0.91 (m, 6H, OCH₂CH₂CH₃), 0.98 (t, *J* = 7.4 Hz, 3H, OCH₂CH₂CH₃), 1.09 (t, *J* = 7.4 Hz, 3H, OCH₂CH₂CH₃), 1.64-1.76 (m, 2H, OCH₂CH₂CH₃), 1.80-1.97 (m, 6H, OCH₂CH₂CH₃), 3.04-3.24 (m, 4H, ArCH₂^{eq}Ar), 3.41-3.55 (m, 3H, OCH₂CH₂CH₃), 3.59-3.70 (m, 3H, OCH₂CH₂CH₃), 3.94-4.18 (m, 6H, OCH₂CH₂CH₃, OCH₂CHN, OCH₂CHN, ArCH₂^{ax}Ar), 4.34-4.49 (m, 3H, ArCH₂^{ax}Ar), 5.68 (d, *J* = 7.3 Hz, 1H, ArH), 5.86 (d, *J* = 7.6 Hz, 1H, ArH), 5.97 (t, *J* = 7.6 Hz, 1H, ArH), 6.10 (d, *J* = 7.7 Hz, 2H, ArH), 3.26 (t, *J* = 7.6 Hz, 1H, ArH), 6.91 (t, *J* = 7.4 Hz, 1H, ArH), 7.36-7.45 (m, 8H, ArH), 7.57-7.64 (m, 2H, ArH), 7.77-7.86 (m, 1H, ArH), 8.06-8.14 (m, 2H, ArH) ppm.

Owing to the complexity of the aromatic region in the ^{13}C NMR spectrum, the P-C coupling could not be accurately determined. Instead, all of the ^{13}C signals have been reported which explains why there are more signals than expected.

^{13}C NMR (75 Hz, CHLOROFORM-*d*) δ 9.8, 9.9, 10.9, 11.0, 23.0, 23.1, 23.5, 23.6, 23.70, 30.0, 30.1, 31.0, 31.2, 33.4, 68.4, 76.2, 76.6, 77.1, 77.4, 121.8, 122.2, 122.6, 126.9, 127.0, 127.2, 128.0, 128.1, 128.2, 128.3, 128.4, 128.8, 129.2, 130.6, 130.7, 130.8, 131.0, 131.1, 131.3, 131.4, 131.6, 131.7, 132.6, 132.7, 132.9, 133.1, 133.3, 133.6, 134.7, 136.3, 137.3, 137.5, 137.7, 140.9, 141.0, 145.6, 145.7, 155.2, 155.3, 158.4, 161.2, 161.4, 163.7, 163.8 ppm.

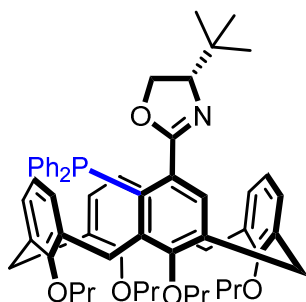
^{31}P NMR (300 MHz, CHLOROFORM-*d*) δ 30.29 ppm.

IR (ATR) cm^{-1} : 2950 (s, C-H stretch), 1660 (s, C=N stretch), 1590 (m, C=C stretch), 1460 (s, C=C stretch), 1196 (s, P=O stretch), 1050 (s, C-O stretch), 760 (s, C-H oop bend).

HRMS-TOF MS ESI+: *m/z* [M+H]⁺ calculated for C₅₉H₆₉NO₆P: 918.4863; found: 918:4873.

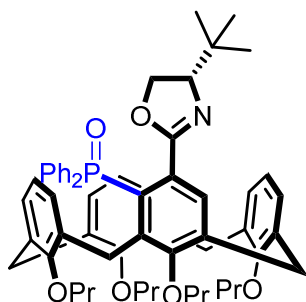
Chapter 5: Synthesis of phosphine oxazoline calixarene ligands

5.8.16 (M)-5-((S)-4-(tert-butyl)-4,5-dihydrooxazol-2-yl)-4-diphenylphosphine-25,26,27,28-tetrapropoxycalix[4]arene – 95.



Calixarene (**M**)-**95** was synthesized according to the general ortholithiation procedure, but was quenched by the addition of oven dried alumina. Oxazoline calixarene **58** (100 mg, 0.140 mmol), *t*-BuLi (0.700 mmol, 5.0 equiv), TMEDA (0.220 ml, 1.40 mmol, 10.0 equiv), pentane (3 ml) and diphenylphosphine chloride (0.30 ml, excess) were combined with a reaction time of 24 h. The product was purified using alumina gel column chromatography gradient elution (EtOAc:PET, 0:100 to 10:90) yielding a white solid (64 mg, 51%).

5.8.17 (M)-5-((S)-4-Isopropyl-4,5-dihydrooxazol-2-yl)-4-diphenylphosphineoxide-25,26,27,28-tetrapropoxycalix[4]arene – 97.



Calixarene (**M**)-**95** (106 mg, 0.120 mmol) was added to THF (3 ml) at room temperature. H₂O₂ (2.00 ml, 30% aq, exs) was added all at once. The reaction mixture was stirred at room temperature for 30 minutes. Alumina TLC confirmed full conversion to the phosphine oxide. The reaction was quenched by the addition of 1M HCl. The crude product was extracted using DCM. The organic layer was then washed with additional 1M HCl, dried over MgSO₄ and the excess solvent was removed under reduced pressure yielding a white solid. Purification was achieved using alumina column chromatography (EtOAc:PET, 30:70), yielding the phosphine oxide (**P**)-**97** as a white solid (105 mg, 95%). Mp: > 330 °C.

Chapter 5: Synthesis of phosphine oxazoline calixarene ligands

^1H NMR (300 MHz, CHLOROFORM-*d*) δ 0.82 (s, 9H, C(CH₃)₃), 0.85-0.91 (m, 6H, OCH₂CH₂CH₃), 0.98 (t, *J* = 7.4 Hz, 3H, OCH₂CH₂CH₃), 1.10 (t, *J* = 7.4 Hz, 3H, OCH₂CH₂CH₃), 1.63-1.74 (m, 2H, OCH₂CH₂CH₃), 1.81-1.97 (m, 6H, OCH₂CH₂CH₃), 3.04-3.24 (m, 4H, ArCH₂^{eq}Ar), 3.41-3.55 (m, 3H, OCH₂CH₂CH₃), 3.59-3.70 (m, 3H, OCH₂CH₂CH₃), 3.94-4.18 (m, 6H, OCH₂CH₂CH₃, OCH₂CH, OCH₂CH, ArCH₂^{ax}Ar), 4.34-4.49 (m, 3H, ArCH₂^{ax}Ar), 5.68 (d, *J* = 7.3 Hz, 1H, ArH), 5.86 (d, *J* = 7.6 Hz, 1H, ArH), 5.96 (t, *J* = 7.6 Hz, 1H, ArH), 6.10 (d, *J* = 7.7 Hz, 2H, ArH), 3.26 (t, *J* = 7.6 Hz, 1H, ArH), 6.90 (t, *J* = 7.4 Hz, 1H, ArH), 7.36-7.45 (m, 8H, ArH), 7.56-7.65 (m, 2H, ArH), 7.77-7.86 (m, 1H, ArH), 8.06-8.14 (m, 2H, ArH) ppm.

Owing to the complexity of the aromatic region in the ^{13}C NMR spectrum, the P-C coupling could not be accurately determined. Instead, all of the ^{13}C signals have been reported which explains why there are more signals than expected.

^{13}C NMR (75 Hz, CHLOROFORM-*d*) δ 9.8, 9.9, 10.9, 11.0, 23.0, 23.1, 23.5, 23.6, 23.7, 30.0, 30.1, 31.0, 31.2, 33.4, 68.4, 76.2, 76.6, 77.1, 77.4, 121.8, 122.3, 122.6, 126.9, 127.0, 127.2, 128.0, 128.1, 128.2, 128.3, 128.4, 128.8, 129.2, 130.6, 130.7, 130.8, 131.0, 131.2, 131.3, 131.5, 131.6, 131.8, 132.6, 132.8, 132.9, 133.2, 133.3, 133.6, 134.7, 136.3, 137.3, 137.5, 137.7, 140.9, 141.0, 145.6, 145.7, 155.2, 155.3, 158.4, 161.2, 161.4, 163.7, 163.8 ppm.

^{31}P NMR (300 MHz, CHLOROFORM-*d*) δ 30.19 ppm.

IR (ATR) cm⁻¹: 2961 (s, C-H stretch), 1658 (s, C=N stretch), 1590 (m, C=C stretch), 1455 (s, C=C stretch), 1198 (s, P=O stretch), 1087 (s, C-O stretch), 759 (s, C-H oop bend).

HRMS-TOF MS ESI+: *m/z* [M+H]⁺ calculated for C₅₉H₆₉NO₆P: 918.4863; found: 918:4862.

5.9 References.

- (1) You, S-L.; Zhou, Y-G.; Hou, X-L.; Dai, L-X. *Chem. Commun.* **1998**, *2*, 2765.
- (2) Herbert, S. A.; van Laeren, L. J.; Castell, D. C.; Arnott, G. E. *Beilstein J. Org. Chem.* **2014**, *10*, 2751.
- (3) Shirakawa, S.; Moriyama, A.; Shimizu, S. *Org. Lett.* **2007**, *9*, 3117.
- (4) Dieleman, C.; Steyer, S.; Jeunesse, C.; Matt, D. *J. Chem. Soc., Dalton Trans.* **2001**, *3*, 2508.
- (5) Amato, M. E.; Ballistreri, F. P.; Pappalardo, A.; Tomaselli, G. A.; Toscano, R. M.; Williams, D. J. *Eur. J. Org. Chem.* **2005**, 3562.
- (6) Xu, Z-X.; Li, G-K.; Chen, C-F.; Huang, Z-T. *Tetrahedron* **2008**, *64*, 8668.
- (7) von Matt, P.; Pfaltz, A. *Angew. Chem., Int. Ed.* **1993**, *32*, 566.
- (8) Sprinz, J.; Helmchen, G. *Tetrahedron Lett.* **1993**, *34*, 1769.
- (9) Dawson, G. J.; Coote, S. J.; Frost, C. G.; Williams, M. J. *Tetrahedron Lett.* **1993**, *34*, 3149.
- (10) Wang, L.; Kwok, W. H.; Chan, A. S. C.; Tu, T.; Hou, X.; Dai, L. *Tetrahedron: Asymmetry* **2003**, *14*, 2291.
- (11) Gómez, R. A.; Adrio, J.; Carretero, J. C. *Angew. Chem., Int. Ed.* **2006**, *45*, 7674.
- (12) Hargaden, G. C.; Guiry, P. J. *Chem. Rev.* **2009**, *109*, 2505.
- (13) Dai, L. X.; Hou, X. L. *Chiral Ferrocenes in Asymmetric Catalysis: Synthesis and Applications*; Dai, L.; Hou, X.-L., Eds.; 1st ed.; Wiley-VCH, 2010.
- (14) Lu, S. M.; Han, X. W.; Zhou, Y. G. *Adv. Synth. Catal.* **2004**, *346*, 909.
- (15) Sammakia, T.; Stangeland, E. *J. Org. Chem.* **1997**, *62*, 6104.
- (16) Tellers, D. M.; Bio, M.; Song, Z. J.; McWilliams, J. C.; Sun, Y. *Tetrahedron Asymmetry* **2006**, *17*, 550.
- (17) Geisler, F. M.; Helmchen, G. *J. Org. Chem.* **2006**, *71*, 7498.
- (18) Jin, M. J.; Takale, V. B.; Sarkar, M. S.; Kim, Y. M. *Chem. Commun.* **2006**, *4*, 663.
- (19) Dai, L-X.; Tu, T.; You, S-L.; Deng, W-P.; Hou, X-L. *Acc. Chem. Res.* **2003**, *36*, 659.
- (20) Jensen, J. F.; Sjøtofte, I.; Sørensen, H. O.; Johannsen, M. *J. Org. Chem.* **2003**, *68*, 1258.
- (21) Jensen, J. F.; Johannsen, M. *Org. Lett.* **2003**, *5*, 3025.
- (22) Bringmann, G.; Hamm, A.; Schraut, M. *Org. Lett.* **2003**, *5*, 2805.
- (23) Cammidge, A. N.; Crépy, K. V. L. *Tetrahedron* **2004**, *60*, 4377.

Chapter 5: Synthesis of phosphine oxazoline calixarene ligands

- (24) Tu, T.; Deng, W-P.; Hou, X-L.; Dai, L-X.; Dong, X-C. *Chem.-Eur. J.* **2003**, *9*, 3073.
- (25) Kilroy, T. G.; Hennessy, A. J.; Connolly, D. J.; Malone, Y. M.; Farrell, A.; Guiry, P. J. *J. Mol. Catal. A Chem.* **2003**, *196*, 65.
- (26) Tu, T.; Hou, X-L.; Dai, L-X. *Org. Lett.* **2003**, *5*, 3651.
- (27) Yan, X-X.; Peng, Q.; Zhang, Y.; Zhang, K.; Hong, W.; Hou, X-L.; Wu, Y-D. *Angew. Chem., Int. Ed.* **2006**, *45*, 1979.
- (28) Gao, W.; Zhang, X.; Raghunath, M. *Org. Lett.* **2005**, *7*, 4241.
- (29) Chen, C.; Beak, P. *J. Org. Chem.* **1986**, *51*, 3325.
- (30) Constantine, R. N.; Kim, N.; Bunt, R. C. *Org. Lett.* **2003**, *5*, 2279.
- (31) Kermagoret, A.; Braunstein, P. *Dalton Trans.* **2008**, *33*, 822.
- (32) Deng, W-P.; Hou, X-L.; Dai, L-X.; Dong, X-W. *Chem. Commun.* **2000**, 1483.
- (33) Gruzdev, M. S.; Akopova, O. B.; Frolova, T. V. *Russ. J. Gen. Chem.* **2013**, *83*, 652.
- (34) Bang, J. S.; Kim, Y. J.; Song, J.; Yoo, J. S.; Lee, S.; Lee, M. J.; Min, H.; Hwang, K. W.; Min, K. H. *Bioorg. Med. Chem.* **2012**, *20*, 5262.
- (35) Barbe, G.; Charette, B. *J. Am. Chem. Soc.* **2008**, *130*, 18.
- (36) Bai, X-F.; Song, T.; Xu, Z.; Xia, C-G.; Huang, W-S.; Xu, L-W. *Angew. Chem., Int. Ed.* **2015**, *54*, 5255.

6 Chapter 6 - The application of inherently chiral phosphine oxazoline ligands

6.1 Introduction.

Oxazoline- and ferrocene-based ligands have both received widespread attention and have been applied to many different asymmetric catalytic reactions.¹⁻³ Catalytic systems well suited for the study of our new calixarene ligands were chosen by merging the relevant findings of these two fields. Two primary criteria dictated which of these reactions were deemed fit for the task. Examples where the planar chirality of the ferrocene back-bone was found to have a specific and/or unique impact on the stereochemical outcome were considered, especially where the planar chirality was able to accomplish greater steric induction when compared to an inferior performance of simpler ligands lacking this structural property. Furthermore, uninvestigated reactions in which ligands incorporated a stereoplane, were looked at. In addition to this, cases that presented an opportunity for improving the general performance or stereocontrol were considered for evaluation. The motivation for deciding on specific reactions will be outlined in the sections that follow.

6.2 Asymmetric Tsuji-Trost allylation.

6.2.1 Introduction.

The findings for the previously reported *S/N* inherently chiral ligands offered an ideal starting point for this study. They provided an opportunity to verify whether or not the matched/mismatched relationship between the opposing forms of inherent chirality would be seen for another class of inherently chiral ligand. In addition to this, the Tsuji-Trost reaction has been extensively studied and is routinely used for the evaluation of new chiral Phox ligands.⁴

6.2.2 Results.

The reaction conditions for the successful asymmetric allylic alkylation of 1,2-diphenylallyl acetate in high yields, were initially determined using a combination of the model **93** and the achiral ethylene bis-diphenyl phosphine as ligands (**Table 6.1**, entries 2 and 3). Following this, each of the calixarene ligands (**(P)/(M)-94** and **(P)/(M)-95**) were assessed (entries 4, 5, 7 and 8). The results of the study are summarized below.

Table 6.1: Asymmetric Tsuji-Trost allylation reaction.

Entry	Ligand	Conversion (%) ^a	ee (%) (<i>S</i>) ^b
1	-	-	-
2	Et ₂ (PPh ₂) ₂	>99	0
3	92	>99	96
4	(M)-94	>99	0
5	(P)-94	>99	60
6	93	>99	97
7	(M)-95	>99	95
8	(P)-95	>99	32
9	(P)-96	-	-
10	(P)-97	-	-

Reagents and conditions: i) [Pd(allyl)Cl]₂ (5.0 mol%), ligand (10.0 mol%), Cs₂CO₃ (3.0 equiv), dimethylmalonate (3.0 equiv), DCM, rt, 24 h. ^aDetermined by ¹H NMR spectroscopy. ^bDetermined by chiral HPLC (Chiralpak IC column).*

The entire study was carried out using the experimental procedure reported by Li and co-workers, which consistently yielded the alkylated product in near quantitative yields.⁵ A racemic mixture of the product was obtained when the non-chiral ethylene bis-diphenylphosphine was used (entry 2). This mixture was used to determine the *R_f* values for the (*R*) and (*S*) enantiomers.

* All reactions were performed in triplicate and the reported conversions and selectivities are averaged values.

Chapter 6: The application of inherently chiral phosphine oxazoline ligands

To confirm that the calixarene Phox ligands were indeed responsible for the catalysis, reactions with no ligand (entry 1) and two phosphine oxides (entries 9 and 10) were carried out. None of the allylated product formed for any of these examples. The two models **92** and **93** (entries 3 and 5) yielded the product in high *ee* values of 96% and 97% respectively, which compared well with reports on structurally analogous Phox ligands.⁶

By comparison, the results for the calixarene ligands were far more interesting. The reactions using the *tert*-butyl oxazoline calixarene ligands, **(M)-95** and **(P)-95** (entries 7 and 8), afforded the product in vastly different enantioselectivities of 95% and 32% respectively. This suggested that the match/mismatch relationship for the calixarene Phox ligands was significantly more pronounced than selectivities for the thio-oxazoline ligands reported previously (90% and 75%).⁷ The selectivity for **(M)-95** (95%) with the matched chiral configurations, might seem a little low compared to the model **93** (96%). If both the inherent and point chirality of **(M)-95** are selective for the same product, why does a combination of the two give an *ee* lower than the model **93** (96%) by itself?

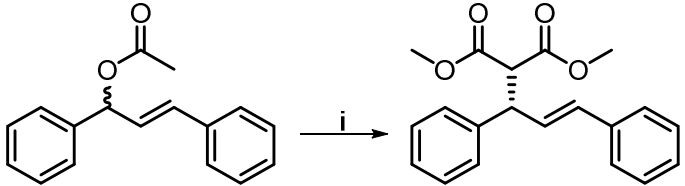
This outcome can be attributed to one of, or a combination of two factors. Firstly, the *de* obtained for the synthesis of ligand **(M)-95** (80%), was an important consideration. Each of the allylation reactions performed with the calixarenes is in actual fact a mixture of ligands; a combination of both configurations of inherent chirality. With **(M)-95** (entry 7), the opposite diastereomer **(P)-95** makes up 10% of the ligand mixture. For the *ee* of 32% (entry 8), **(P)-95** makes up over 99% of the ligand mixture, which suggests that the mismatched configuration of the inherent chirality strongly competes with the point chirality for the formation of the (*R*) enantiomer. Taking this into consideration, a ligand mixture where 10% heavily favours the opposite diastereomer would explain why the selectivity was lower than expected. Secondly, even if the configuration of the inherent chirality for **(M)-95** was selective for the (*S*) product, it could be a significantly weaker source of chiral induction. This would effectively cripple the performance of the point chirality.

The same trend was expected for the isopropyl oxazoline ligands **(M)-94** and **(P)-94** (entries 4 and 5). This was true for **(P)-94** where a selectivity of 60% was obtained, a value much lower than the *ee* of 96% for **92**, and similar to the *ee* of 32% for calixarene **(P)-95**. Both of these calixarenes have the suspected mismatched chiral relationship. When attempting the reaction with **(M)-94**, a racemic product mixture was obtained. At first it was speculated that some of the diphenyl(*s*-butyl)phosphine by-product, that formed during the synthesis of the ligand was present in the reaction, as this achiral phosphine would have been able to catalyse the reaction. However, this was not the case and a problem associated with the purification of **(M)-94** turned out to be responsible. Once again, it was not possible to separate the di-*t*Bu-diglyme ligand from **(P)-94** chromatographically, and heating the mixture to 60 °C under vacuum for 48 h resulted in the degradation of the phosphine ligand. Therefore **(M)-94** had to be used with an excess of the diglyme additive present. Even though large amounts of the diglyme ligand were present in the reaction, the literature presented no examples of oxygen based donor ligands and it was assumed that the di-*t*Bu-diglyme would not interfere.

Chapter 6: The application of inherently chiral phosphine oxazoline ligands

This assumption was supported by the fact that both phosphine oxides (**P**)-96 and (**P**)-97 (Table 6.1, entries 9 and 10) yielded none of the allylated product. To test the assumption, a small study was carried out to determine if oxygen donor ligands were capable of catalyzing the allylation reaction (Table 6.2).

Table 6.2: Evaluation of oxygen donor ligands.



Entry	Ligand (mol%)	Conversion (%) ^a	ee (%) (S) ^b
1	di- <i>t</i> Bu-diglyme (10%)	-	-
2	di- <i>t</i> Bu-diglyme (50%)	>99	0
3	diglyme (50%)	-	-
4	glyme (50%)	-	-

Reagents and conditions: i) [Pd(allyl)Cl]₂ (5.0 mol%), ligand (10-50 mol%), Cs₂CO₃ (3.0 equiv), dimethylmalonate (3.0 equiv), DCM, rt, 24 h. ^aDetermined by ¹H NMR spectroscopy. ^bDetermined by chiral HPLC (Chiralpak IC column).[†]

The reaction was first carried out with 10 mol% of the diglyme ligand (entry 1) and none of the allylated product formed in the reaction time. With 50 mol% of the ligand (entry 2), a complete conversion of the starting material occurred within 24 h. Interested by this observation, the reaction was tested with di-glyme (50%) and glyme (50%), both of which failed to yield any of the allylated product. However, this did provide an explanation for the 0% ee seen for (**M**)-94 (Table 6.1, entry 8). The reaction was likely catalyzed by the vast excess (>10:1) of the di-*t*Bu-diglyme relative to calixarene (**M**)-94 in the reaction mixture. This study was not taken any further, and no other oxygen-based ligands were evaluated. These results could create an opportunity to further explore bulky oxygen-based ligand systems for this reaction.

6.2.3 Discussion.

The findings for the calixarene ligands propose a substantial match/mismatch relationship between their chiral configurations. An alternative perspective on this is that the inherent chirality of these ligands is acting as a prominent source of chiral induction for these reactions. The asymmetric allylic alkylation reaction has been well documented, becoming a benchmark test reaction in the field of asymmetric catalysis. For the last 30 years, the mechanism behind the stereo-control has been an active area of research. At first, purely steric based models were proposed, which were a good fit for the earlier simpler ligand systems.^{8,9} Over time, the development of analytical and computational techniques enabled the study of both the solid state and *in situ* behavior of these active catalytic intermediates.¹⁰⁻¹³ This gradual addition of new information has improved on the earlier models, simultaneously introducing an element of uncertainty to complex systems.

[†] All reactions were run in triplicate and the reported conversion and selectivities are average values.

Chapter 6: The application of inherently chiral phosphine oxazoline ligands

A review by Trost and Crawley provided an introduction to the mechanistic detail behind the origin of the enantiocontrol in this reaction.⁴ The earliest model proposed in 1985 by Trost suggested that once the catalyst had complexed to the symmetric allyl substrate in solution, it formed an intermediate *meso* π -allyl component bound to a chiral template (**2**) (Figure 6.1).⁹

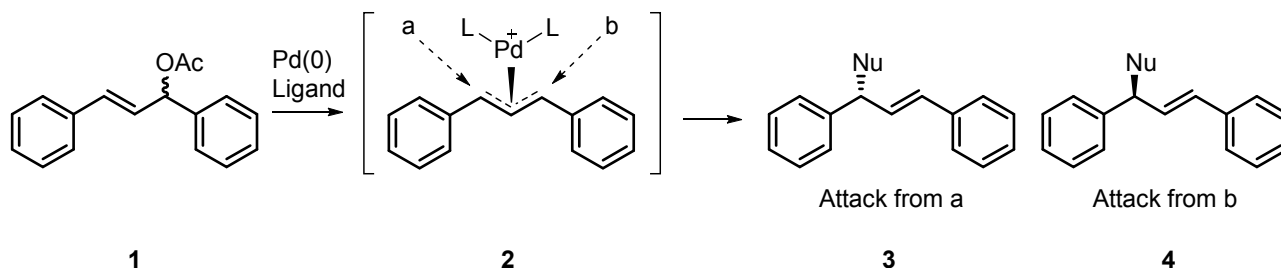


Figure 6.1: Stereocontrol directed by nucleophilic attack on either side of the *meso*-allyl palladium complex.

The axiom behind the model is the formation of a chiral pocket by the ligands present in the active catalyst. This would then direct the approach of the incoming nucleophile to either side of palladium-allyl complex. At this point in time, the behavior of the allyl-palladium complex in solution was unknown. As more became understood about this chemistry, it was discovered that phosphine oxazoline ligands have a unique and interesting mode of function, which was more mechanistically complex than the earlier steric-based models. As a result, they have been meticulously studied and a number of detailed substrate and ligand dependent models have been proposed.^{14–22} In an attempt to better understand the results for the calixarene ligands, the relevant components of these mechanistic explanations will be combined with the structural properties of our ligands, in order to propose a catalytic model which is applicable to the calixarenes.

The overall catalytic cycle has the following steps; olefin complexation (**A**), followed by ionization of the leaving group (**B**), the equilibration between *endo* and *exo* intermediates (**C**), nucleophilic addition (**D**) and lastly decomplexation (**E**) (Figure 6.2).⁴

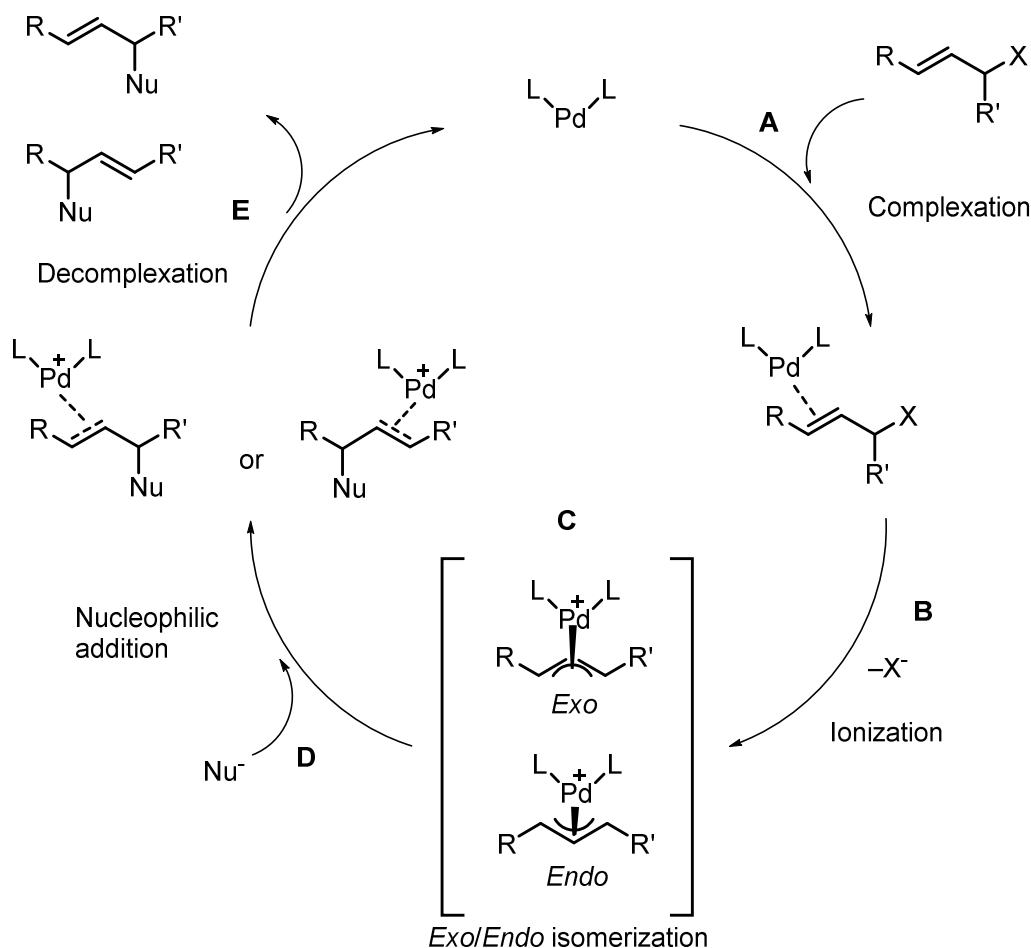


Figure 6.2: Catalytic cycle for the asymmetric allylic alkylation reaction.⁴

It is possible for the transfer of chiral information to take place at each of these steps, with the only exception being the decomplexation of the product from the palladium-ligand system, as the chirality of the product is already established at this point. Owing to the symmetrical nature of the starting material, enantioselection would only be able to take place either during *endo/exo* isomerization (C) of the active catalyst in solution, and the attack of the incoming nucleophile (D). These two factors (C and D), have been found to play integral roles in determining the stereochemical outcome of the Tsuji-Trost reaction catalyzed by a Phox ligand.^{10,23-25} As such, the detail behind these two critical stages in the cycle, and how it potentially relates to the behavior of the calixarene ligands, will form the core of this discussion.

After coordination of the bidentate Phox ligands to the palladium, it then undergoes a second coordination to the allyl fragment of the substrate, forming a square planar organo-palladium complex (Figure 6.3).[‡] The symmetric diphenyl allyl fragment has the option of bonding with its phenyl groups facing upwards, in the same direction as the oxazoline R-group (*exo*), or downwards with the opposite orientation (*endo*).

[‡] All of the π-allyl-palladium intermediates bonded to model Phox ligands in Figure 6.3, 6.4 and 6.5 were reproduced from their respective reported crystal structure data.^{22,31}

Chapter 6: The application of inherently chiral phosphine oxazoline ligands

The dynamic nature of these structures was first reported in 1994, where it was shown that these complexes exist as a rapid equilibrium between the two diastereomers.²⁶ A report on the computational study of this process suggests that the isomer interconversion occurs via an $\eta^3 \rightarrow \eta^1 \rightarrow \eta^3$ mechanism.²⁷ A simplified explanation of the process is the following. Two of the three carbon-palladium bonds are cleaved, which forms a T-shaped η^1 -palladium intermediate. This allows for rotation of the allyl moiety around the σ -bond to take place (flipping the orientation of the allyl fragment), after which the carbon-palladium bonds are reformed, yielding the η^3 -complex of the opposite isomer.

When 1,3-diphenylallyl acetate was complexed to a simple aryl Phox ligand, the calculated *exo:endo* ratio at room temperature was always in the region of 9:1 in favour of *exo*. There is strong evidence supporting the notion that the formation of the favoured intermediate was largely sterically driven.^{28–30} One of the most important features of all of these models was understanding the difference between the steric contribution of the two P-phenyl groups and the R-group of the oxazoline. The position of the P-phenyl groups, relative to the square planar complex, varied depending on the overall structures of different ligands. The preference for the *exo*-configuration depicted in **Figure 6.3** had little to do with the R-group of the oxazoline. Rather, it was a consequence of the repulsive interactions between the phenyl group of the 1,3-diphenyl acetate and the pseudo-equatorial P-phenyl group of the *endo*-isomer.²² The fact that the phenyl groups of the substrate always prefer an orientation which avoids steric interference from the pseudo-equatorial P-phenyl, makes the relative positions of these two functional groups in the π -allyl-palladium complex both an interesting and crucial factor.

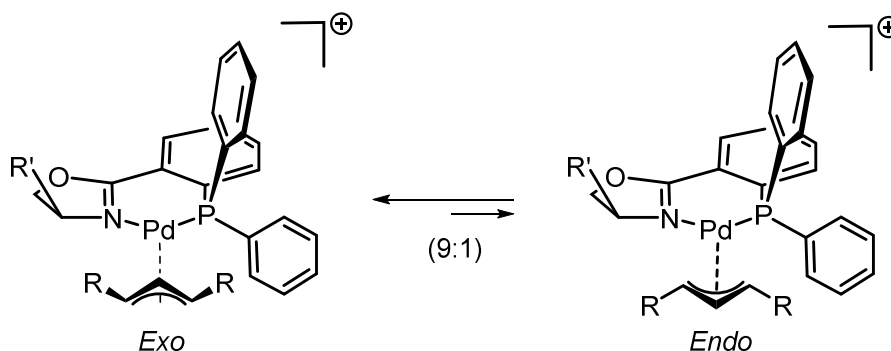


Figure 6.3: Dynamic *endo-exo* isomerism of the π -allyl palladium complex containing a Phox ligand.²²

From the above scheme, the role of the oxazoline's R-group is therefore not obvious, but it plays an important part in controlling the *exo:endo* ratio of these intermediates in solution (**Figure 6.4**). When the bulk of the oxazoline's R-group increases, it does not interact with the substrate, but rather increases the repulsion between the ligand and the palladium ion. This effectively pushes the P-phenyl rings closer to the π -allyl system, increasing that specific steric interaction, further destabilizing the *endo*-intermediate, favoring a higher *exo* to *endo* ratio.³¹ This scheme also makes the steric clash between the pseudo-equatorial P-phenyl and the allyl-phenyl groups in the *endo*-complex more obvious.

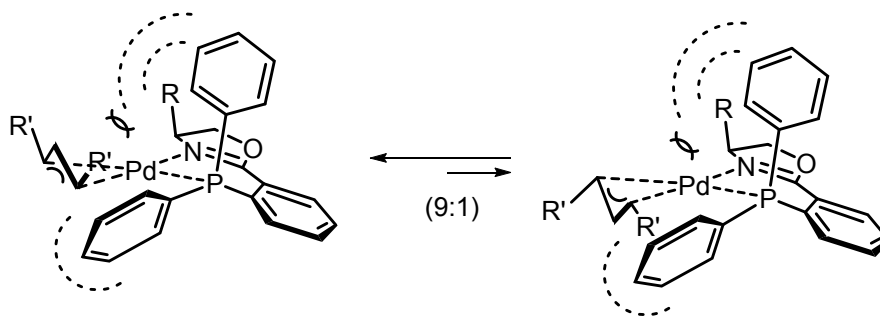


Figure 6.4: A representation of the steric influence of the P-Phenyl and oxazoline R-groups.³¹

The second crucial component of the reaction mechanism was how the addition of the nucleophile was specifically directed to one of the two seemingly equivalent carbons of the allyl fragment. The earlier models, based solely on the ligand's steric properties did not take this isomerization behavior into account. If the steric properties of the ligand alone directed the nucleophilic attack to the same carbon for both intermediates, the chirality of the products resulting from the attack on the *exo* and *endo* isomers would have the opposite configuration (**Figure 6.5**).

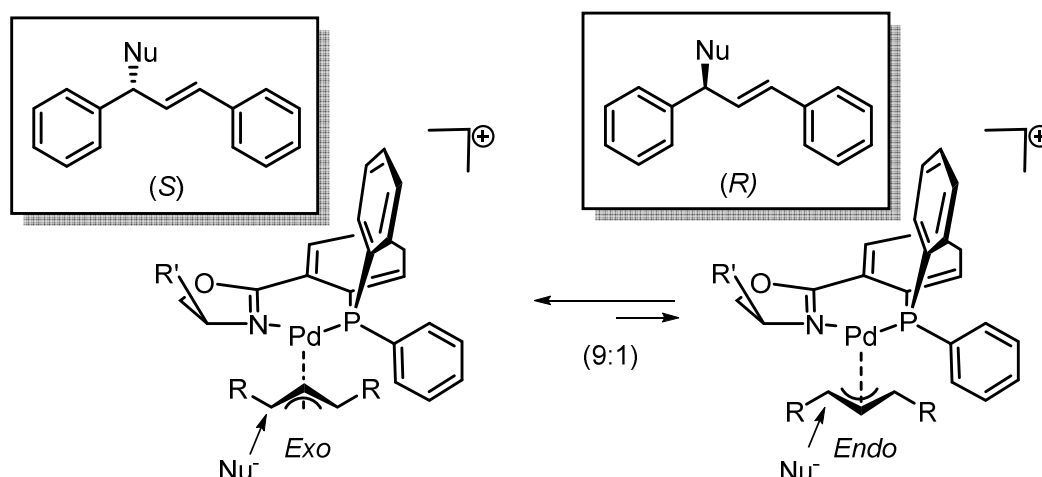


Figure 6.5: Attack of the nucleophile on the same side for the *exo* and *endo* intermediates yielding the (*S*) and (*R*) enantiomers respectively.²²

The combined results from subsequent computational, ¹H NMR spectroscopic, and X-ray diffraction studies have shown that the preferred site of addition is on the carbon *trans* to the phosphorus atom in these π -allyl intermediates. The π -accepting capability of the phosphorus atom has been found to make the carbon in the *trans*-position more electron deficient, and consequently more vulnerable to nucleophilic attack.^{21,32}

Chapter 6: The application of inherently chiral phosphine oxazoline ligands

A report by Togni and co-workers summarized that the stereocontrol during a Tsuji-Trost reaction, between a chiral catalyst and a symmetrically substituted allylic substrate, was determined by three main factors; a) the concentrations of the π -allyl-palladium isomers in solution, b) their relative reaction rates with the nucleophile, and lastly, c) the preferred position and rate of nucleophilic attack on the two non-equivalent allylic positions.³³ Even though a complete mechanistic model for the reaction was not proposed in this publication, one of their findings was especially relevant considering the unique structure of the calixarene ligands. The aim of their study was to determine whether or not the ratio between the two *endo* and *exo* intermediates could be influenced by the steric properties of the catalyst ligand. The observed trend for a series of ligands with the same chiral configuration, was a general increase in enantioselectivities as the bulk of the ligands increased. Nevertheless, one of the ligands completely inverted the selectivity, favoring the opposite diastereomer. The configuration for all of the ligands in the series was fixed, and the various R-groups presented no significant differences with regards to their electronic contributions. Therefore they deduced that the switch in the selectivity had to have a steric origin. Either by drastically changing the *endo:exo* equilibrium in solution, or altering the rate of nucleophilic addition with either intermediate. A number of other researchers have also found that the steric properties of Phox ligands were able to impact the relative ratios and equilibration rates between the *endo* and *exo* palladium-allyl intermediates.^{29,30,34}

The two publications that provided substantial as well as detailed insight into this catalytic mechanism were both reported by Bunt and co-workers.²² Their studies concluded and reiterated the two vital functions of the Phox ligands. Firstly, they control the ratio of the *endo:exo* π -allyl-palladium intermediates in solution, and secondly, they exclusively direct the addition of the nucleophile to the carbon *trans* to the phosphorus. Even though this preference to the point of addition, as well as the equilibrium of these intermediates has been shown before, little to no evidence exists explaining why the pathway to the minor enantiomer is not favoured. It was concluded that reactions proceeding with high enantioselectivities had to meet two general conditions. Firstly, that the ligand favoured a high *exo:endo* ratio in solution, and secondly, the nucleophilic attack on the *exo*-diastereomer had to be favoured, whilst attack on the minor *endo*-diastereomer was simultaneously suppressed.

The structural arrangement of the Phox ligand π -allyl-palladium intermediates has been crucial towards explaining the observed selectivity for different ligands. Even though we lacked the solid state data of an actual calixarene ligand intermediate, a crystal structure for (**P**)-**97** had been previously reported by the group (**Figure 6.6**).³⁵

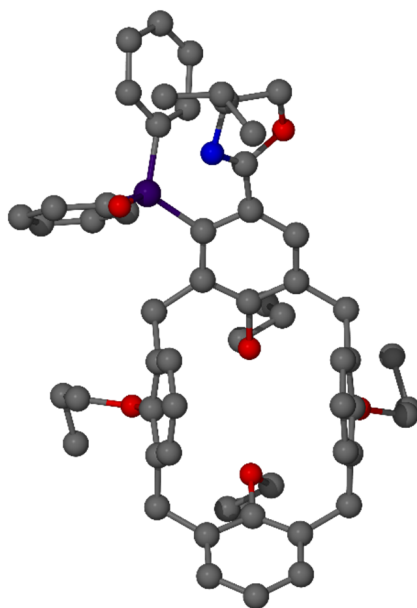


Figure 6.6: Crystal structure of calixarene (**(P)**-97).³⁵ Reproduced from reference.

This provided a good estimation of how the P-phenyl groups could potentially be positioned in the calixarene π -allyl-palladium intermediates. In combination with the solid state data of the simpler Phox systems, a potential model for these ligand intermediates was built (**Figure 6.7**).^{22,29}

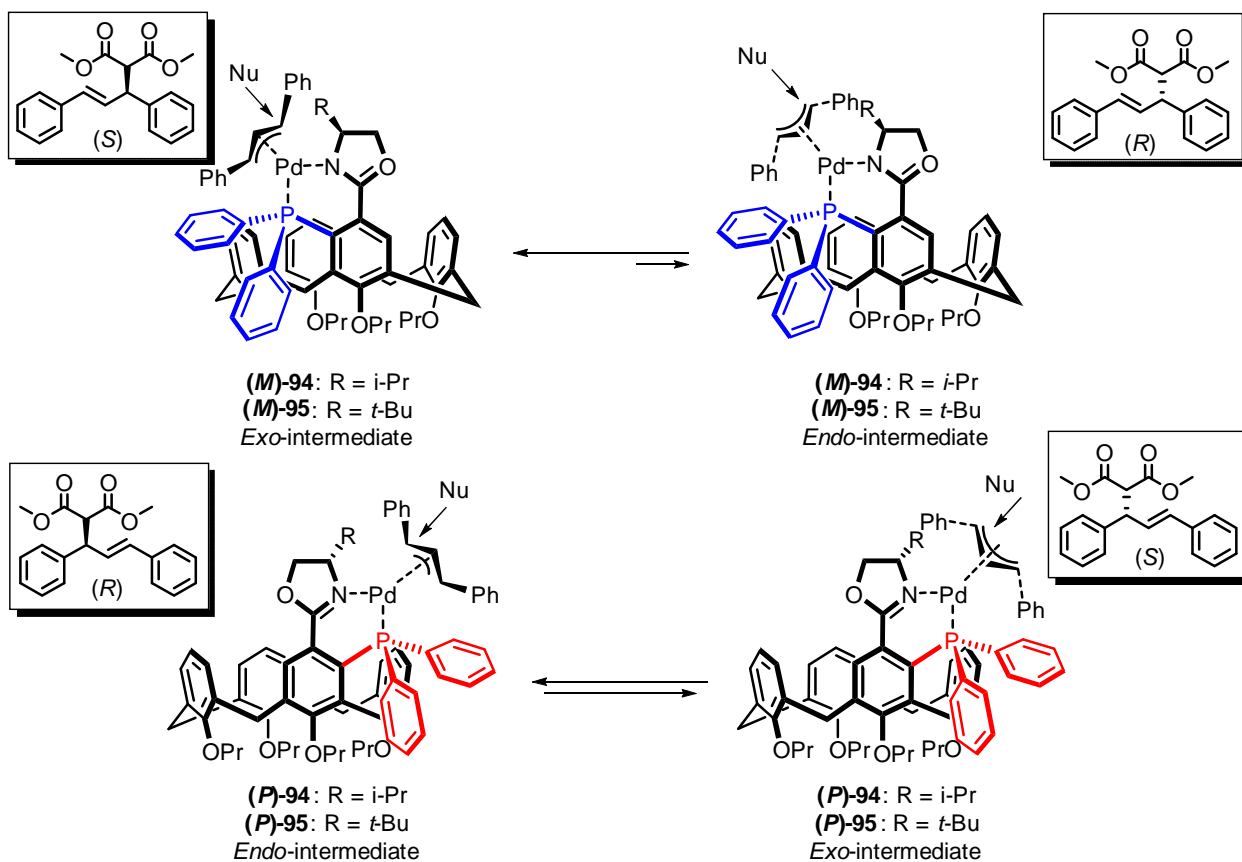


Figure 6.7: Models of *endo* and *exo* calixarene Phox π -allyl palladium intermediates.

Chapter 6: The application of inherently chiral phosphine oxazoline ligands

From an electronic perspective, the calixarene ligands have all of the same functional groups, and can be considered equivalent. Therefore, it was safe to assume that the variations in the enantioselectivities between the ligands primarily arose from their structural differences. The model structures above have been orientated with the square-planar palladium complexes in the plane of the page. The allyl component is situated perpendicularly, relative to the plane of the complex, so the substrate phenyl groups are positioned facing directly out of, or into the page.

Ligands **(M)-94** and **(M)-95** suggested a matched correlation between the two configurations of chirality. In order to form the P/N co-ordination bond with the palladium, the oxazoline functional group had to be rotated 180 °C with the R-group now facing upwards as well. The positions of the P-Phenyl groups are dominated by the steric influence of the calixarene bowl, and align themselves to minimize this clash. As seen in the simpler systems, the position of the more equatorial P-Phenyl ring introduces a repulsive interaction to the phenyl ring of the substrate. An additional steric contribution could also be made by the bowl structure of the calixarene. As the substrate phenyl rings are facing down in the *endo*-intermediate, the steric strain with the P-phenyl pointing backwards would be greater, so the *exo*-intermediate is proposed to be the more stabilized structure, with a potentially higher concentration in solution. The nucleophilic addition to the carbon *trans* to the phosphor on the *exo*-isomer yields the (*S*) enantiomer, which was the major product obtained in the reaction. The analogous nucleophilic addition to the less stable *endo*-intermediate forms the minor (*R*) enantiomer product.

The same reasoning can be used for the mismatched calixarene ligands **(P)-94** and **(P)-95**, both of which were significantly more selective for the product in the (*R*) configuration. The steric clash between the substrate phenyl groups with the P-phenyl and calixarene bowl now suggest that an *endo*-intermediate would be more stabilized. The *trans* nucleophilic addition on this isomer would yield the (*R*) product, and attack on the *exo*-intermediate the opposing (*S*) configuration. Without the solid state data, the positions of the P-phenyl groups can only be approximated. The opposite configurations of the oxazoline R-group could have a greater significance that cannot be accounted for using these crude models. Other important factors are the rate of nucleophilic addition to these intermediate structures, as well as their relative rates of inversion. Subtle differences in the overall structure could enhance or retard either of these processes and significantly impact the selectivity of the reaction. Even though we are unable to do so accurately, these models provide a potential explanation to why the formation of the different product configurations are favoured.

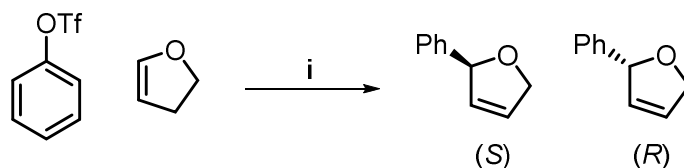
6.2.4 Conclusion.

The findings for the inherently chiral calixarenes used in the Tsuji-Trost allylation provided strong evidence that the inherent chirality was an important source of chiral information, capable of driving the asymmetric process. The proposed model and tentative explanations for the observations of this study have been based on the structural differences between the opposing configurations of the calixarene ligands. To the best of our knowledge, the difference in selectivity seen for ligands (**M**)-**95** and (**P**)-**95** is the largest seen for any calixarene ligands with opposite configurations of inherent chirality. Eager to see if the inherent chirality of these ligands would have the same effect on a different system, several other asymmetric reactions were also investigated.

6.3 Asymmetric Heck coupling.

6.3.1 Introduction.

The asymmetric Heck coupling reaction was chosen based on two separate publications by Dai and co-workers.^{36,37} They investigated the independent role of the central and planar chirality on both the regio- and stereo-selectivity in the palladium catalyzed coupling of phenyl triflate and 2,3-dihydrofuran (**Scheme 6.1**).

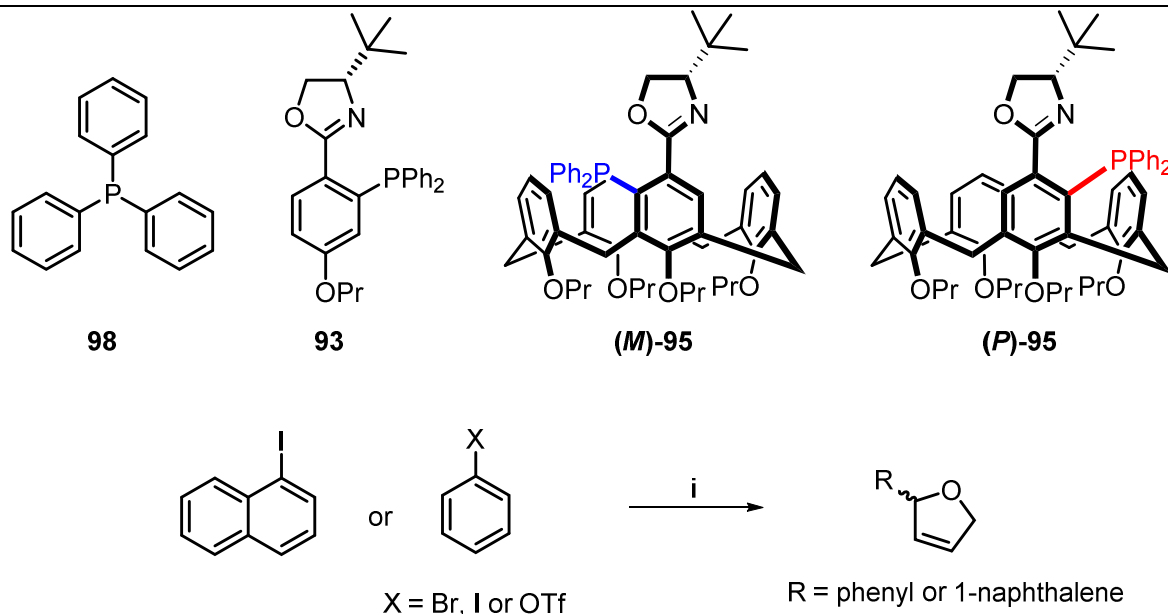


Scheme 6.1: Heck coupling of phenyl triflate and 2,3-dihydrofuran reported by Dai. Reagents and conditions: i) Pd(OAc)₂ (5 mol%), Ligand (10 mol%), base, benzene, 40 °C.³⁶

The asymmetric Heck coupling reaction thus seemed to be another promising opportunity. Dai had reported that the enantioselectivities could be controlled by varying the size of the planar chiral group, or by inverting the configuration of the planar chirality; an intriguing prospect for the calixarenes.

6.3.2 Results and discussion.

Initial attempts at the Heck coupling reaction using Dai's procedure were unsuccessful. After returning to the literature, several alternative Heck reaction conditions that made use of Phox ligands were found.^{38,39} Unwilling to admit defeat, an optimization study aimed at finding the necessary reaction conditions for the calixarene Phox ligands was carried out (**Table 6.3**).

Table 6.3: Asymmetric Heck coupling of aryl halides to 2,3-dihydrofuran.

Entry	Aryl halide	Ligand	Pd cat.	Solvent	Temp (°C)	Time (h)	Conv (%) ^a
1	OTf/Br/I-phenol	98	Pd(OAc) ₂	ACN	100	24/48	0
2	OTf/Br/I-phenol	93	Pd(OAc) ₂	ACN	100	24/48	0
3	OTf/Br/I-phenol	98	Pd ₂ (dba) ₃	THF	65	24/48	0
4	OTf/Br/I-phenol	93	Pd ₂ (dba) ₃	THF	65	24/48	0
5	OTf/Br/I-phenol	98	Pd(dba) ₂	THF	65	24/48	0
6	OTf/Br/I-phenol	93	Pd(dba) ₂	THF	65	24/48	0
7	OTf/Br/I-phenol	98	[Pd(allyl)Cl] ₂	THF	65	24/48	0
8	1-naphthalene	98	Pd(dba) ₂	THF	65	24	94
9	1-naphthalene	93	Pd(dba) ₂	THF	65	24/48	<5
10	1-naphthalene	93	Pd ₂ (dba) ₃	THF	65	24/48	<5
11	1-naphthalene	93	[Pd(allyl)Cl] ₂	THF	65	24/48	<5
12	1-naphthalene	93	Pd(OAc) ₂	THF	65	24/48	<5
13	1-naphthalene	93	[Pd(allyl)Cl] ₂	toluene	100	24/48	0
14	1-naphthalene	93	Pd(dba) ₂	dioxane	80	24/48	0
15	1-naphthalene	93	Pd(dba) ₂	DME	80	24/48	0
16	1-naphthalene	93	Pd(dba) ₂	EG	80	24/48	0
17	1-naphthalene	93	Pd(dba) ₂	toluene	80	24	96
18	1-naphthalene	(M)-95	Pd(dba) ₂	toluene	80	24/48	<5
19	1-naphthalene	(P)-95	Pd(dba) ₂	toluene	80	24/48	<5

Reagents and conditions: i) Pd cat. (5 mol%), ligand (5-10 mol%), *i*-Pr₂EtN, solvent, Δ, 24-48 h.^{38,39} ^aDetermined

by ¹H NMR spectroscopy.

The optimization process was largely performed using ligands **98** and **93**. The following list of potential parameters for this reaction were investigated: the nature of the substrate, ligand type, palladium source, solvent choice as well as reaction temperature and time. Three different phenyl-based starting materials, triflic, bromo and iodo phenol, were tested (entries 1-7). Each of these were submitted to several variations of the reaction conditions, none of which yielded any of the coupled product. The first positive result was obtained when changing the substrate to iodo-naphthalene (entry 8). Using Pd(dba)₂ in THF with **98** at 65 °C afforded the coupled product in a high yield after 24 h.

Chapter 6: The application of inherently chiral phosphine oxazoline ligands

Frustratingly, when the same conditions were attempted with **93**, the product only formed in negligible yields (<5%). Even though this performance was extremely poor, these reaction conditions served as the basis towards improving the results of the Phox ligand. Efforts toward this can be seen over entries 9-18, and after testing a range of different experimental conditions, the product was finally isolated in high yield (entry 17). This was the first successful reaction using a Phox ligand, but unfortunately the excitement was short lived. When the optimized conditions were attempted with the calixarene ligands (entries 19-20) the yields plummeted again. In addition to this, separation of the enantiomeric product mixtures (entries 8 and 17) were met with challenges of their own, as they were found to be inseparable, with the HPLC resources at our disposal.

6.3.3 Conclusion.

Even though a considerable amount of effort had been invested, we were unable to successfully apply a calixarene Phox ligand to the Heck reaction with a high conversion. The poor results from the catalytic study, combined with the limitations encountered during the analysis of these product mixtures were enough to conclude that the asymmetric Heck reaction was poorly suited for our requirements.

6.4 Asymmetric Suzuki-Miyaura coupling.

6.4.1 Introduction.

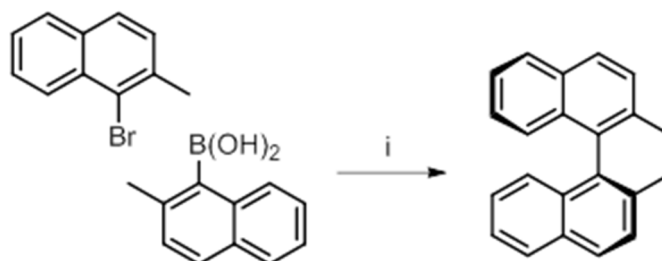
The first ever synthesis of axially chiral bi-naphthalenes via asymmetric Suzuki-Miyaura coupling was reported in 2000 by Cammidge and co-workers.⁴⁰ In the past, axially chiral bi-naphthalene ligands were usually prepared by the synthesis of racemic product mixtures, which would then be resolved either by a co-crystallization, or a derivitisation-crystallisation process. The procedures for the simpler versions of these compounds such as BINOL and BINAP have been established. Having an established chemical resolution process is one thing, but when new ligand systems are synthesized, new resolution techniques often have to be developed concurrently. The Suzuki cross-coupling reaction is a convenient method for the asymmetric preparation of chiral bi-naphthyl compounds, and has received limited attention using ligands with an incorporated stereoplane.^{1,2}

Chapter 6: The application of inherently chiral phosphine oxazoline ligands

6.4.2 Results.

Initially, the attempts toward asymmetric bi-naphthalene synthesis were made using the conditions reported by Johannsen and co-workers (**Table 6.4**).⁴¹

Table 6.4: First attempts of the Suzuki coupling toward the synthesis of bi-naphthalene.



Entry	Catalyst	Ligand	Solvent	Base	Temp (° C)	Time (h)	Conv.
1	Pd ₂ (dba) ₃	PPh ₃	Toluene/H ₂ O	K ₃ PO ₄	70	24	-
2	Pd ₂ (dba) ₃	Et(PPh ₂) ₂	Toluene/H ₂ O	K ₃ PO ₄	70	24	-
4	Pd ₂ (dba) ₃	PPh ₃	THF	KF	70	24	-
5	Pd(OAc) ₂	PPh ₃	Dioxane	Cs ₂ CO ₃	80	24/48	-

Reagents and conditions: i) Pd cat. (2.0 mol%), ligand (5.0-10.0 mol%), base (2.5 equiv), solvent, Δ, 24/48 h.

For all of the above reactions (entries 1-4) the consumption of the starting material and the formation of a new product was noted. Frustratingly, closer examination of the ¹H NMR spectra (**Figure 6.8**) of the crude product mixtures confirmed that it was not the coupled bi-naphthyl, but a mixture of the remaining aryl halide starting material and a de-boronated side product.

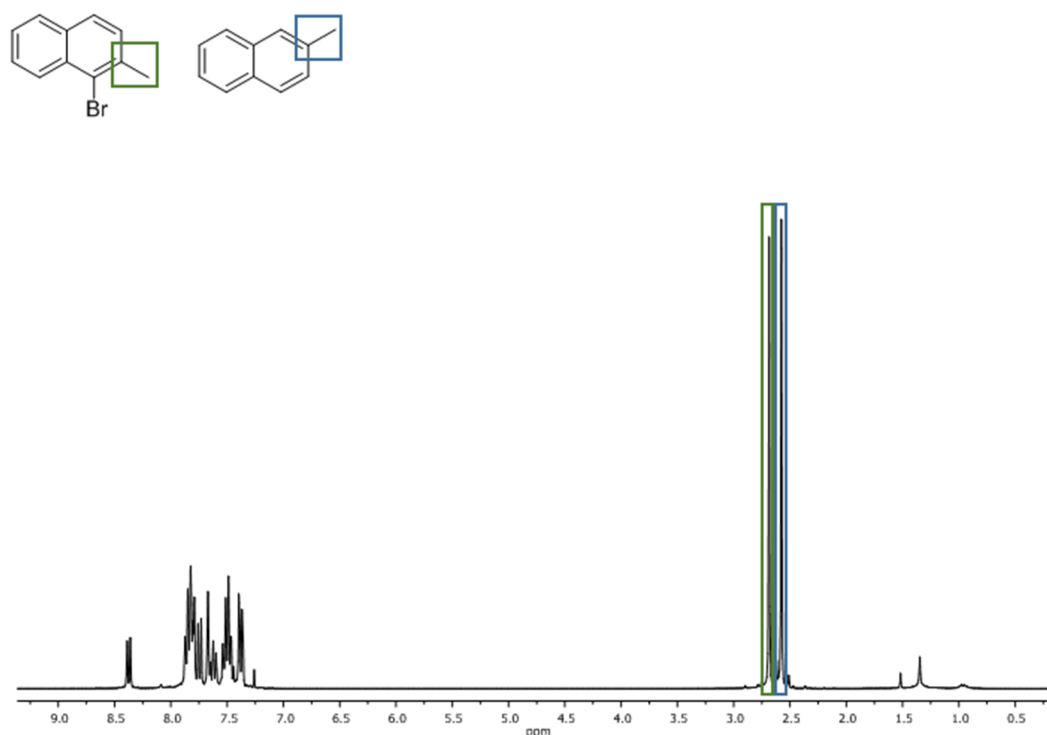
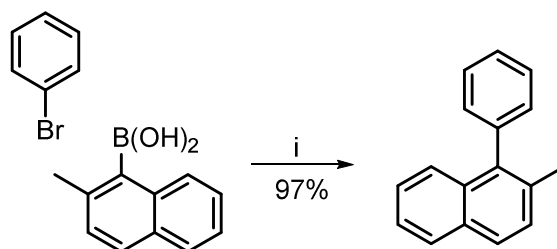


Figure 6.8: Typical crude ¹H NMR spectrum for entries 1-4, **Table 6.4**.

Chapter 6: The application of inherently chiral phosphine oxazoline ligands

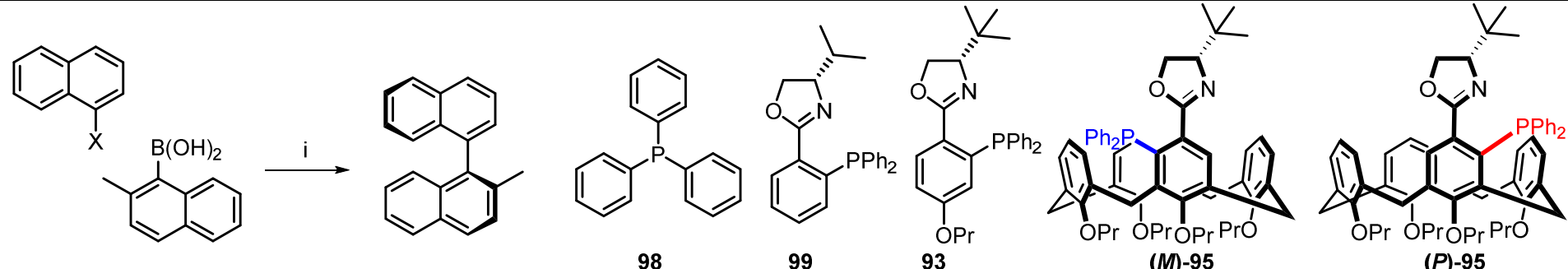
These ^1H NMR spectra contained two separate methyl signals with similar chemical shifts. The methyl group on the 1-bromo-2-methylnaphthyl starting material had a chemical shift of δ 2.65 ppm (outlined in green), and the de-boronated by-product had a shift of δ 2.54 ppm (outlined in blue). Returning to the literature showed that the presence of the methyl group on both the aryl-bromide and aryl-boronic acid posed a significant synthetic challenge, and only specific catalyst/ligand systems were able to successfully couple the two.^{42–44} Similar de-boronated by-products were reported by Cammidge and co-workers.^{45,46} This was a problem which persisted whenever the two components of the Suzuki reaction were sterically hindered. To verify that the formation of the by-product was due to the nature of the starting materials, rather than a flaw in the experimental conditions, a much simpler test reaction was attempted (**Scheme 6.2**).



Scheme 6.2: Suzuki coupling test reaction. Regents and conditions: i) $\text{Pd}(\text{OAc})_2$ (2.5 mol%), PPh_3 (10 mol%), Cs_2CO_3 (4.5 equiv), dioxane, 80 °C, 24 h.

To minimize the steric clash between the starting materials bromo-benzene was chosen as replacement for the naphthyl-bromide. The coupled product was formed in a 97% yield, with none of the de-boronated by-product forming. This result indicated that overcoming the obstacle of steric hindrance between the starting materials in **Table 6.4**, could potentially pose a new synthetic challenge altogether. Instead, an alternative test reaction for synthesis of axially chiral bi-aryls was considered. There were several examples which made use of bromo-naphthalene as the aryl halide with the same (2-methylnaphthalen-1-yl)-boronic acid.^{36,38,42,47} A number of different experimental conditions were reported over these publications. Given that the experimental procedure for the test reaction had shown success, these conditions were the first attempted for the asymmetric bi-naphthalene synthesis. The results have been summarized in (**Table 6.5**).

Chapter 6: The application of inherently chiral phosphine oxazoline ligands

Table 6.5: The asymmetric synthesis of chiral bi-naphthyl compounds via Suzuki coupling.


Entry	Catalyst/(mol%)	Ligand/(mol%)	Solvent	Halide (X)	Base	Temp (° C)	Time (h)	ee ^a (%) (<i>a.S</i>)	Conv ^b (%)
1	Pd(OAc) ₂ /(2.5%)	98 /(10.0%)	Dioxane	Bromine	Cs ₂ CO ₃	80	24	0	70
3	Pd(OAc) ₂ /(2.5%)	99 /(7.5%)	Dioxane	Bromine	Cs ₂ CO ₃	80	24	-	< 1%
4	[Pd(allyl)Cl] ₂ /(2.5%)	99 /(7.5%)	Dioxane	Bromine	Cs ₂ CO ₃	80	24	5	22
5	Pd ₂ (dba) ₃ /(2.5%)	99 /(7.5%)	Dioxane	Bromine	Cs ₂ CO ₃	80	24	5	5
6	[Pd(allyl)Cl] ₂ /(7.5%)	99 /(15.0%)	Dioxane	Bromine	Cs ₂ CO ₃	80	24	5	35
7	[Pd(allyl)Cl] ₂ /(2.5%)	99 /(7.5%)	DME	Bromine	Cs ₂ CO ₃	80	24	5	18
8	[Pd(allyl)Cl] ₂ /(2.5%)	99 /(7.5%)	Dioxane	Bromine	Cs ₂ CO ₃	80	24	5	4
9	[Pd(allyl)Cl] ₂ /(2.5%)	99 /(7.5%)	Dioxane	Bromine	Ba(OH) ₂ ·8H ₂ O	80	24	5	20
10	[Pd(allyl)Cl] ₂ /(2.5%)	99 /(7.5%)	Toluene	Bromine	Cs ₂ CO ₃	80	24	5	15
11	[Pd(allyl)Cl] ₂ /(7.5%)	99 /(15.0%)	Dioxane	Iodine	Cs ₂ CO ₃	80	24	5	38
12	[Pd(allyl)Cl] ₂ /(5.0%)	99 /(10.0%)	Dioxane	Iodine	Cs ₂ CO ₃	80	24	5	23
13	[Pd(allyl)Cl] ₂ /(5.0%)	99 /(10.0%)	Toluene	Iodine	Cs ₂ CO ₃	80	24	5	60
14	[Pd(allyl)Cl] ₂ /(7.5%)	99 /(15.0%)	Toluene	Iodine	Cs ₂ CO ₃	80	24	5	65
15	[Pd(allyl)Cl] ₂ /(7.5%)	93 /(15.0%)	Toluene	Iodine	Cs ₂ CO ₃	80	24	10	64
16	[Pd(allyl)Cl] ₂ /(7.5%)	(P)-95 /(15.0%)	Toluene	Iodine	Cs ₂ CO ₃	80	24	33	96
17	[Pd(allyl)Cl] ₂ /(7.5%)	(M)-95 /(15.0%)	Toluene	Iodine	Cs ₂ CO ₃	80	24	7	94
18	[Pd(allyl)Cl] ₂ /(7.5%)	-	Toluene	Iodine	Cs ₂ CO ₃	80	24	-	0
19	[Pd(allyl)Cl] ₂ /(7.5%)	93 - (oxide)	Toluene	Iodine	Cs ₂ CO ₃	80	24	-	0

^aDetermined using chiral HPLC (Chiralpak IC). ^bDetermined using ¹H NMR spectroscopy.

6.4.3 Discussion.

A large part of the study was focused on the gradual optimization of the reaction conditions (entries 1-16). Triphenylphosphine was used to synthesize a racemic mixture of the bi-naphthalene compounds (entry 1) which served as a reference for the two enantiomers during the HPLC analysis. When the same reaction conditions were attempted with ligand **99** (entry 2) barely any product formed and the yield dropped below 1%.[§] Two new sources of palladium were then tested (entries 4 and 5) with [Pd(allyl)Cl]₂ giving the highest conversion of 22% over all three. Increasing the catalyst load to 7.5% (entry 6) further improved the conversion to 35%. Next, the influence of different solvents (entries 7 and 10), base (entry 9) and increased equivalents of boronic acid (entry 8) were all evaluated, none of which gave a conversion of higher than 20%. In a review paper on the topic published by Suzuki himself, it was stated that the oxidative addition of the aryl halide is usually the rate-determining step in the catalytic cycle, with the relative reactivity decreasing in the order I>OTf>Br>>Cl.⁴⁸ With this in mind, bromo-naphthalene was replaced by iodo-naphthalene (entries 11 and 12) with little change to the conversions in dioxane. One final change was made by replacing the dioxane with toluene (entries 13-14) which significantly increased the conversions to 60% and 65% respectively. Even though these conversions were not remarkable, they compared well with results previously reported for this reaction. To confirm that the Phox ligands were responsible for product formation, ligand free (entry 18) and phosphine oxide (entry 19) reactions were attempted, neither of which yielded any of the coupled product. Ligand **99** gave a considerably poor, but constant enantioselectivity of 5% over all reactions. The use of model ligand **93** (entry 15) afforded the coupled product in a 64% yield with a slightly improved *ee* of 10%. Performing the reaction with (*P*)-**95** and (*M*)-**95** (entries 16 and 17) significantly improved the conversions to 96% and 94% respectively. More interestingly, their selectivities of 33% and 7% suggested that although slight, there was again the match/mismatched relationship between the configurations of the inherent and central chirality of the ligands.

[§] Ligand **99** was provided by Professor Jonathan Williams, and was used to optimize the Suzuki coupling reaction.

6.4.4 Conclusion.

In terms of efficiency, the calixarene ligands (*P*)/(*M*)-**95** significantly outperformed the simpler model ligands **93** and **99**, affording the bi-naphthalene product in much higher conversions of 94% and 96% respectively. Although slight, the matched/mismatch behavior seen for these calixarenes provides further evidence for the capability of this structural property to impart its chiral information in an asymmetric process. Unlike the Tsuji-Trost reaction, the additional control provided by the inherent chirality improved upon the performance of the central chirality on its own. This is the first example of the successful use of a calixarene based inherently chiral ligand for the synthesis of axially chiral bi-naphthalenes, via an asymmetric Suzuki-coupling reaction.

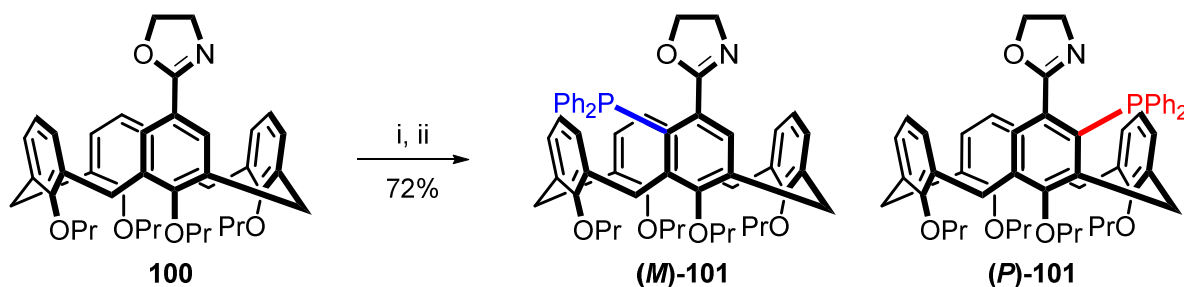
6.5 A phosphine oxazoline ligand with only inherent chirality.

6.5.1 Introduction.

The findings from the Tsuji-Trost and Suzuki coupling reactions point to a notable influence from the inherent chirality of the calixarene ligands. To isolate the effects of inherent chirality would require the synthesis of a purely inherently chiral calixarene ligand. Towards this goal, two purely inherently chiral calixarenes have been synthesized and have yielded tentative preliminary results after application to the Tsuji-Trost allylation reaction.

6.5.2 Synthesis of purely inherently chiral calixarene Phox ligands.

Before attempting the synthesis of the new targeted ligands, a racemic mixture of the purely inherently chiral ligands was investigated first (**Scheme 6.3**). This provided a means to establish both a purification method and the stability of these ligands.



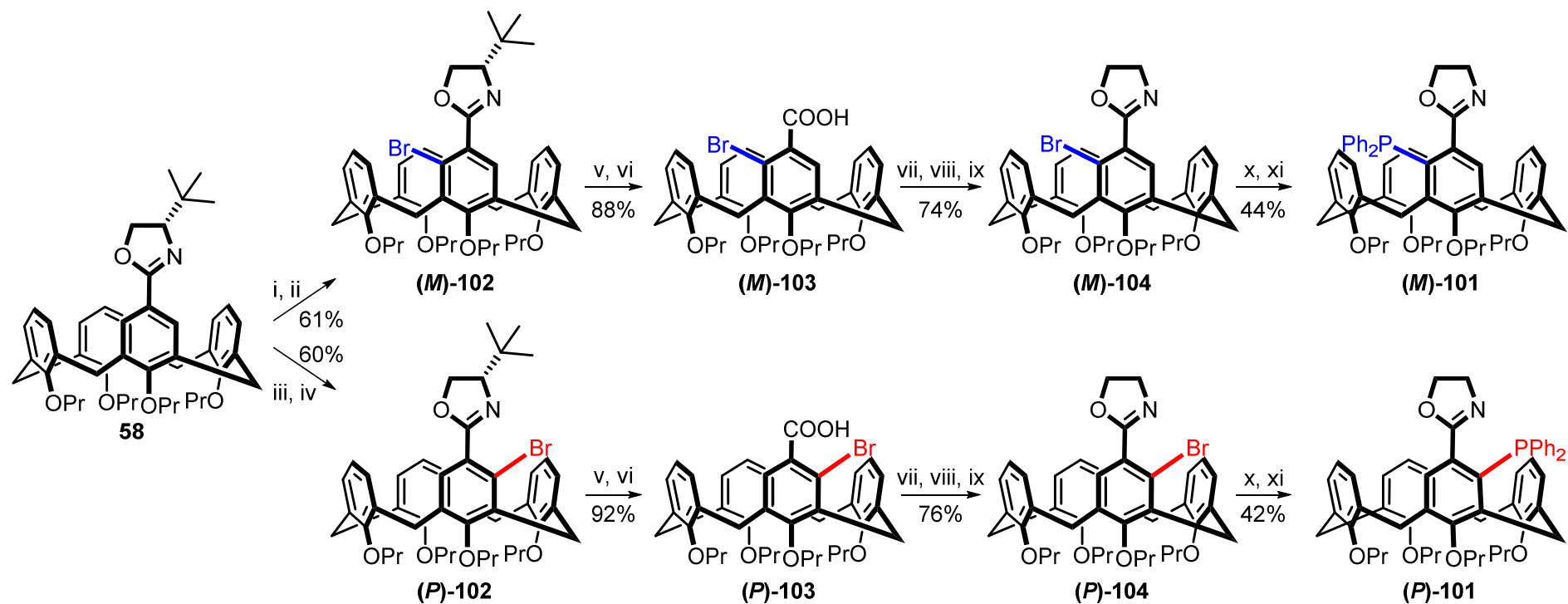
Scheme 6.3: Ortholithiation of **100** Reagents and conditions: i) *s*-BuLi (5.0 equiv), TMEDA (10.0 equiv), pentane, $-78\text{ }^{\circ}\text{C}$, 24 h. ii) PPh_2Cl (exs), $-78\text{ }^{\circ}\text{C}$ to rt 12 h.

Chapter 6: The application of inherently chiral phosphine oxazoline ligands

The ortholithiation of **100**, and subsequent purification of the product mixture was almost identical to that of ligands **(M)/(P)-94** and **(M)/(P)-95**. Despite this, **(M)-101** and **(P)-101** were found to be significantly more sensitive towards oxidation, as the formation of small amounts of phosphine oxide were noted even on the alumina TLC plate.

This was never seen during the synthesis of the other inherently chiral ligands and this increased sensitivity was an important factor to consider for the synthesis of enantiomerically enriched mixtures of **(M)-101** and **(P)-101**. With the ortholithiation of calixarene **58** as the starting point, the planned synthesis for the inherently chiral ligands would require four additional steps. The key idea behind the synthetic strategy was to first introduce the element of inherent chirality to the molecule. Following this, the chiral oxazoline was to be removed via hydrolysis. To retain the oxazoline component of the ligands, a new non-chiral oxazoline would then be reintroduced to the calixarene. The final step of the ligand synthesis would incorporate the diphenyl phosphine constituent using a lithium/halogen exchange reaction. The planned synthesis proved to be successful, and a summary of this process has been presented in **(Scheme 6.4)**.

Chapter 6: The application of inherently chiral phosphine oxazoline ligands



Scheme 6.4: Total synthesis of inherently chiral calixarene Phox ligands **(M)-101** and **(P)-101**. Reagents and conditions: i) *t*-BuLi (5.0 equiv), TMEDA (10.0 equiv), pentane, $-78\text{ }^{\circ}\text{C}$, 24 h; ii) 1,2-dibromoethane (exs), $-78\text{ }^{\circ}\text{C}$ to rt 24 h; iii) *s*-BuLi (5.0 equiv), TMEDA (10.0 equiv), pentane, $-78\text{ }^{\circ}\text{C}$, 24 h; iv) 1,2-dibromoethane, $-78\text{ }^{\circ}\text{C}$ to rt, 24 h; v) MeI (exs), ACN, $60\text{ }^{\circ}\text{C}$, 48 h; vi) KOH (exs), EtOH, $80\text{ }^{\circ}\text{C}$, 24 h; vii) oxalyl chloride (5.0 equiv), DCM, rt, 12 h; viii) ethanolamine (1.5 equiv), Et₃N (3.0 equiv), DCM, $0\text{ }^{\circ}\text{C}$ to rt 12 h; ix) MsCl (3.0 equiv), Et₃N (6.0 equiv), DCM, rt, 24 h; x) *n*-BuLi (1.5 equiv), THF, $-78\text{ }^{\circ}\text{C}$, 5 min; xi) PPh₂Cl (2.0 equiv), $-78\text{ }^{\circ}\text{C}$ to rt 30 min, alumina quench.

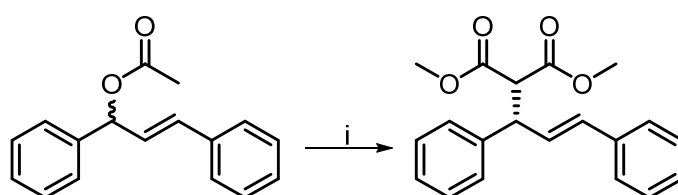
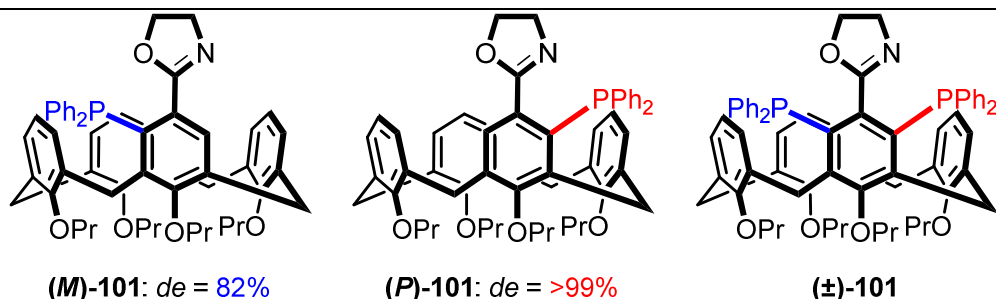
Chapter 6: The application of inherently chiral phosphine oxazoline ligands

The reaction conditions for the selective synthesis of either calixarene diastereomers were again used to yield both inherently chiral diastereomers (**M**)/(**P**)-**102**. Dibromoethane was used to introduce the bromine functionality in preparation for the final lithium halogen exchange step. The polarities of (**M**)-**102** and (**P**)-**102** appeared to be identical to the starting material when using an EtOAc/hexane solvent system. However, it was found that a 40% DCM/hexane mixture was able to separate the product from the starting material. Conveniently, this solvent system allowed for both (**M**)-**102** and (**P**)-**102** to be isolated from the reaction mixture in 61% and 60% yields, respectively. The hydrolysis of the oxazoline was the most challenging step in the overall synthesis. The microwave-assisted acid/base hydrolysis conditions, originally reported by Herbert, only tolerated small scale reactions and when attempted on a larger scale without the microwave, none of the hydrolyzed products would form.⁴⁹ Several other general basic hydrolysis methods were attempted, also with limited success. For most cases the starting material was recovered, but in others multiple side products would form or the hydrolysis would stop at the amide and go no further. The oxazoline functional group is known to be resistant to hydrolysis, and after returning to the literature, a promising two-step procedure reported by Hou and co-workers was used instead.⁵⁰ An excess of iodo-methane first methylated the nitrogen of the oxazoline ring. The methylated iodine salt was then submitted to basic hydrolysis conditions with KOH in EtOH, which yielded the bromo acids (**M**)-**103** and (**P**)-**103**, in high yields. Following this, the non-chiral oxazoline was synthesized using ethanolamine and same general reaction conditions for the synthesis of oxazolines discussed in **Chapter 2**. The final step was the use of standard lithium halogen exchange chemistry. Quenching the reaction with diphenylphosphine chloride yielded the purely inherently chiral phosphine oxide ligands (**M**)-**101** and (**P**)-**101**. Owing to their sensitivity towards oxidation these ligands were purified and used immediately.

6.6 The Tsuji-Trost allylation reaction revisited.

The reaction was successfully catalyzed using both a racemic and enriched enantiomeric mixtures of **(M)**-102 and **(P)**-102. The results have been summarized below (**Table 6.6**).

Table 6.6: Catalysis of the Tsuji-Trost reaction using purely inherently chiral ligands **(M)**-101 and **(P)**-101.



Entry	Ligand	Conversion ⁱ (%)	<i>ee</i> (<i>S</i>) ⁱⁱ
1	(M) -101	>99	80
2	(P) -101	>99	5
3	(±) -101	>99	0
4	(M) -95	>99	95
5	(P) -95	>99	32
6	93	>99	97

Reagents and conditions: i) [Pd(allyl)Cl]₂ (5 mol%), ligand (10 mol%), dimethylmalonate (3.0 equiv), Cs₂CO₃ (3.0 equiv), DCM, rt, 24 h.

ⁱDetermined using ¹H NMR. ⁱⁱDetermined using chiral HPLC (Chiralpak IC).

6.6.1 Discussion.

At first glance, the results seem to fit well with the apparent matched/mismatched relationship seen in ligands **(M)**/**(P)**-94 and **(M)**/**(P)**-95. Ligand **(M)**-101 gave a selectivity of 80% for the (*S*) enantiomer, so the selectivity of the matched calixarene **(M)**-95 (95%) can now be divided into its two contributory components and can be seen as a combination of the selectivities for the model **93** (97%) and inherently chiral **(M)**-101 (80%). The same can be seen for the mismatched calixarene **(P)**-95 (32%), where the two parts for this selectivity being **(P)**-101 (5%), and the model **93** (97%). However, what does not make sense is that **(M)**-101 and **(P)**-101 were both selective for the same product enantiomer (*S*). The selectivity for **(P)**-101 should not be selective for (*S*), but rather the opposite (*R*) enantiomer. It does not add up that the opposing configurations of inherent chirality were selective for the same product. ** This argument is supported by the previously proposed calixarene catalytic models (**Figure 6.9**).

** The reactions were tested three times each, but using the same batch of ligand.

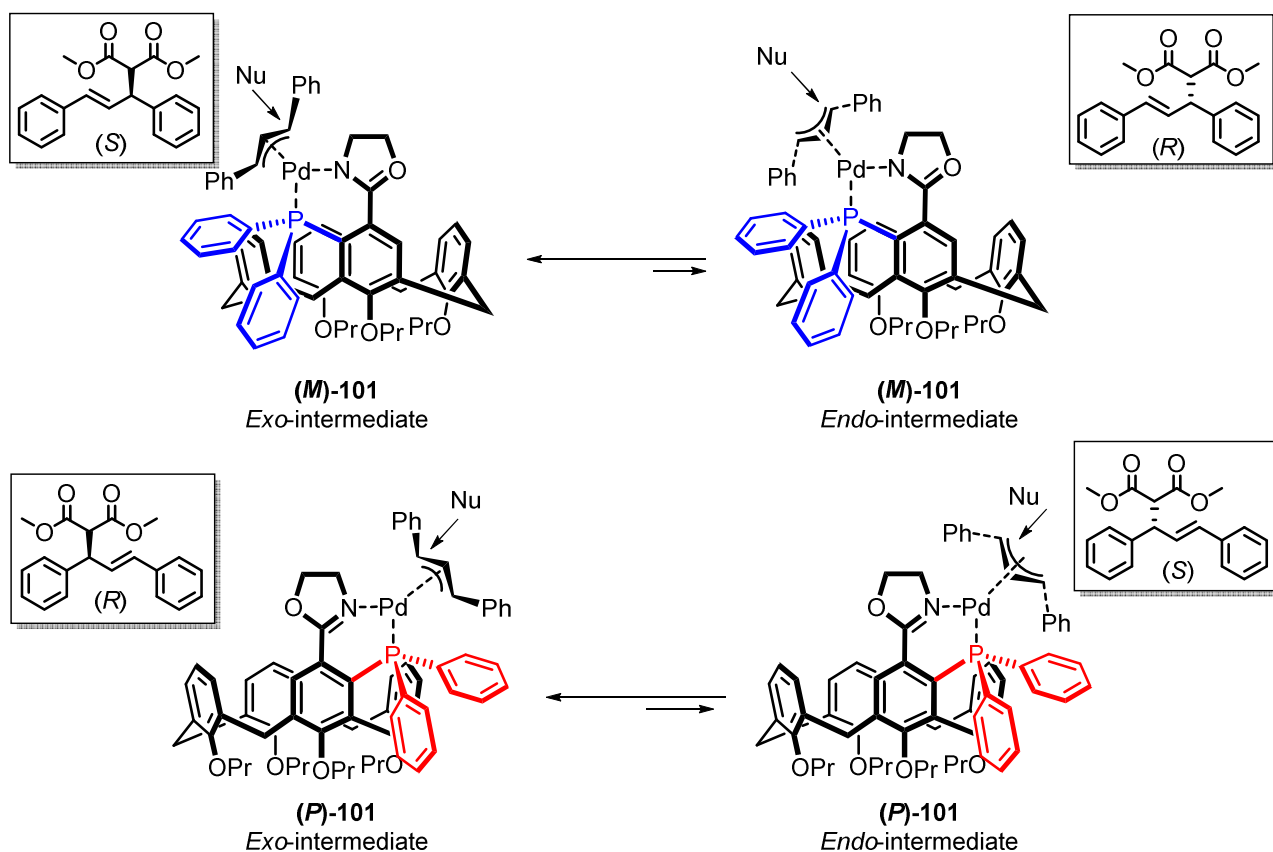


Figure 6.9: Application of the calixarene Phox model to ligands **(M)/(P)-101**.^{††}

Using the same steric arguments, an *exo*-intermediate would be the more stable isomer for both ligands **(M)-101** and **(P)-101**. The *trans* nucleophilic attack on the stabilized *exo*-intermediate for **(M)-101** would yield the product in the (*S*) configuration, which is in agreement with the findings. The addition to the *exo*-isomer for **(P)-101** should yield the product in the opposite (*R*) configuration. The only explanation is that the assumed *ee* for ligand **(P)-101** (*viz.* from the *de* after the asymmetric ortholithiation reaction) is not accurate. Unfortunately, this depleted the limited amount of available material. The total synthesis of both ligands is currently being repeated, as the confirmation of these findings is the last obstacle in the way of publishing these results. Despite the odd result seen for **(P)-101**, these are the first examples of *ortho*-functionalised purely inherently chiral calixarene ligands. In the past, inherent chirality has been shown to have little impact towards asymmetric induction, and the *ee* of 80% seen for **(M)-101**, is a significant improvement. To the best of our knowledge, it is the highest degree of stereocontrol seen for a purely inherently chiral ligand in the Tsuji-Trost allylation reaction between 1,3-diphenylallyl acetate and dimethyl malonate.

^{††} Without an R-group, the *endo/exo* designation was determined purely by the allyl-phenyl rings pointing out of (*exo*) or into (*endo*) the page.

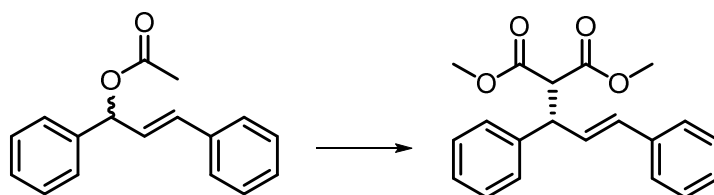
Chapter 6: The application of inherently chiral phosphine oxazoline ligands

6.6.2 Conclusion.

These results are encouraging with regards to furthering studies on the application of inherent chirality. In spite of the tentative findings, these results could serve as a good starting point towards expanding the study. There are many potential means in which the structures of both the phosphine and oxazoline components of these ligands could be manipulated towards fine tuning their performance.

6.7 Experimental section.

6.7.1 General procedure for the Tsuji-Trost allylation.



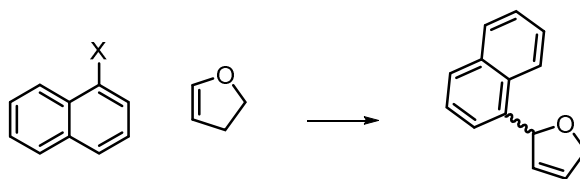
The DCM for all reactions was freshly distilled and degassed using the freeze/pump/thaw protocol. Afterwards it was stored over molecular sieves (4 Å) under argon. The $[\text{Pd}(\text{allyl})\text{Cl}]_2$ (5.0 mol %) and ligand (10.0 mol%) were added to DCM in a small Schlenk flask at room temperature under argon. Upon addition of the ligand, the pale yellow reaction mixture always darkened. After stirring for 30 min, the 1,3-diphenyl allyl acetate (1.0 equiv), dimethyl malonate (3.0 equiv) and Cs_2CO_3 (3.0 equiv) were sequentially added. The flask was flushed with argon, sealed and stirred at room temperature for 24 h. The reaction mixture was quenched by the addition of 1M HCl. Additional DCM (1.0 ml) was added to the flask and used to transfer the contents to a separating funnel. The organic layer was washed with additional portions of 1M HCl (2×25 ml) and brine (1×30 ml). The organic layer was then dried over MgSO_4 , after which the excess solvent was removed under reduced pressure affording a dark yellow/orange oil as the crude product.

^1H NMR (300 MHz, $\text{CHLOROFORM-}d^5$) δ 3.52 (s, 3H, OCH_3), 3.70 (s, 3H, OCH_3), 3.95 (d, $J = 11.0$ Hz, 1H, OCCHCO), 4.26 (dd, $J = 8.5, 10.8$ Hz, 1H, ArCHCH), 6.32 (dd, $J = 8.5, 15.7$ Hz, 1H, CHCHCH), 6.48 (d, $J = 15.7$ Hz, 1H, CHCHAR), 7.19-7.34 (m, 10H, ArH) ppm.

HPLC: Chiralpak IC, flow-rate 1.0 ml/min, IPA:Hexane, 5:95. R_t (R) = 9.01 min, (S) = 10.72 min.

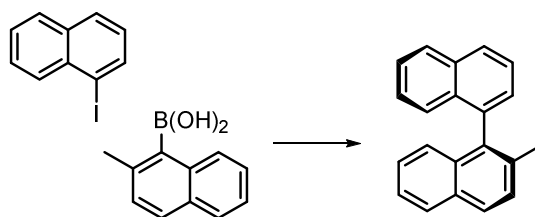
Chapter 6: The application of inherently chiral phosphine oxazoline ligands

6.7.2 General procedure for the asymmetric Heck coupling.



All solvents were freshly distilled and degassed using the freeze/pump/thaw protocol. Afterwards they were stored over molecular sieves (4 Å) under argon. The palladium catalyst and ligand were added to the solvent at room temperature in a microwave vial. This mixture was stirred at room temperature for 15 minutes, during which argon was very slowly bubbled through the reaction mixture, maintaining an inert atmosphere. Iodo-naphthalene (1.0 equiv), 2,3-dihydrofuran (5.0 equiv) and DIPEA (2.5 equiv) were sequentially added. The vial was flushed with argon, sealed and heated for 24 h. After cooling to room temperature, the reaction mixture was diluted with EtOAc and washed through a plug of silica gel. The excess solvent was removed under reduced pressure yielding a dark orange oil as the crude product. Purification was achieved using column chromatography, (PET, 100) affording a colourless oil as the product. After being unable to separate any of the product mixtures using HPLC, no further characterization was carried out.

6.7.3 General procedure for the Suzuki-Miyaura coupling – optimal conditions.

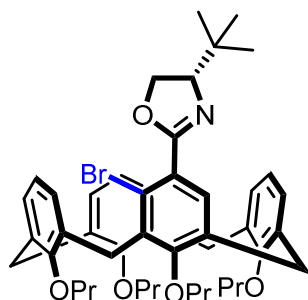


All solvents were freshly distilled and degassed using the freeze/pump/thaw protocol. Afterwards they were stored over molecular sieves (4 Å) under argon. $[\text{Pd}(\text{allyl})\text{Cl}]_2$ (7.5 mol%) and ligand (15.0 mol%) were added to toluene in a microwave vial at room temperature. The mixture was stirred for 15 min at room temperature, during which argon was very slowly bubbled through the reaction mixture, maintaining an inert atmosphere. 1-iodonaphthalene (1.0 equiv), boronic acid (2.0 equiv) and Cs_2CO_3 (3.5 equiv) were sequentially added. The flask was flushed with argon, sealed and heated to 80 °C. Soon after reaching 80 °C the reaction mixture always turned a dark brown. After stirring for 24 h the reaction was cooled to room temperature and the mixture was diluted with petroleum ether and washed through a plug of silica gel. The excess solvent was removed under reduced pressure yielding a colourless oil as the crude product.

^1H NMR (300 MHz, $\text{CHLOROFORM-}d$)⁴⁵ δ 2.11 (s, 3H, ArCH_3), 7.13-7.51 (m, 8H, ArH), 7.68 (dd, $J = 8.4, 7.0$ Hz, 1H, ArH), 7.88 (d, $J = 8.4$ Hz, 2H, ArH), 7.95 (d, $J = 8.4$ Hz, 2H, ArH) ppm.

HPLC: Chiralpak IC, flow-rate 1.0 ml/min, hexane, 100. R_t (S) = 4.35 min, (R) = 4.50 min.

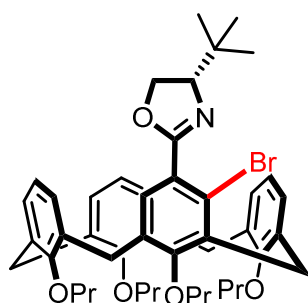
Chapter 6: The application of inherently chiral phosphine oxazoline ligands

6.7.1 (M)-5-((S)-4-tert-butyl-4,5-dihydrooxazol-2-yl)-4-bromo-25,26,27,28-tetrapropoxycalix[4]arene – **102**.

Calixarene (**M**)-**102** was synthesized according to the general ortholithiation procedure. Oxazoline calixarene **58** (300 mg, 0.420 mmol), *t*-BuLi (2.10 mmol, 5.0 equiv), TMEDA (0.620 ml, 4.20 mmol, 10.0 equiv), pentane (8 ml) and 1,2-dibromoethane (0.50 ml, exs) with a reaction time of 24 h. Purification was achieved via silica gel column chromatography (DCM:PET, 40:60 to 50:50) yielding a white solid (200 mg, 60%).

The characterisation data collected for this compound compared well with the reported literature values.⁴⁹

¹H NMR (300 MHz, CHLOROFORM-*d*) δ 0.90 (t, $J = 7.4$ Hz, 6H, OCH₂CH₂CH₃), 1.05 (s, 9H, (C(CH₃)₃), 1.09 (t, $J = 7.4$ Hz, 6H, OCH₂CH₂CH₃), 1.80-2.04 (m, 8H, OCH₂CH₂CH₃), 3.15 (d, $J = 13.2$ Hz, 3H, ArCH₂^{eq}Ar), 3.17 (d, $J = 13.2$ Hz, 1H, ArCH₂^{eq}Ar), 3.60-3.73 (m, 4H, OCH₂CH₂CH₃), 3.94-4.04 (m, 4H, OCH₂CH₂CH₃), 4.07-4.16 (m, 2H, OCH₂CHN), 4.31 (t, $J = 8.2$ Hz, 1H, OCH₂CHN), 4.35-4.47 (m, 4H, ArCH₂^{ax}Ar), 6.12-6.26 (m, 6H, ArH), 6.92 (t, $J = 7.4$ Hz, 1H, ArH), 7.11 (d, $J = 7.4$ Hz, 2H, ArH), 7.36 (s, 1H, ArH) ppm.

6.7.1 (P)-5-((S)-4-tert-butyl-4,5-dihydrooxazol-2-yl)-4-bromo-25,26,27,28-tetrapropoxycalix[4]arene – **102**.

Calixarene (**P**)-**102** was synthesized according to the general ortholithiation procedure. Oxazoline calixarene **58** (300 mg, 0.420 mmol), *s*-BuLi (2.10 mmol, 5.0 equiv), TMEDA (0.620 ml, 4.20 mmol, 10.0 equiv), pentane (8 ml) and 1,2-dibromoethane (0.50 ml, exs) with a reaction time of 24 h. Purification was achieved via silica gel column chromatography (DCM:PET, 40:60 to 50:50) yielding a white solid (205 mg, 61%).

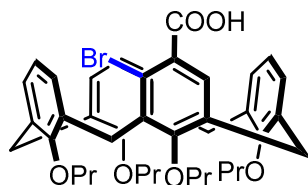
Chapter 6: The application of inherently chiral phosphine oxazoline ligands

^1H NMR (300 MHz, CHLOROFORM-*d*) δ 0.89 (t, $J = 7.4$ Hz, 6H, $\text{OCH}_2\text{CH}_2\text{CH}_3$), 1.05 (s, 9H, $(\text{C}(\text{CH}_3)_3)$), 1.09 (t, $J = 7.4$ Hz, 6H, $\text{OCH}_2\text{CH}_2\text{CH}_3$), 1.80-2.03 (m, 8H, $\text{OCH}_2\text{CH}_2\text{CH}_3$), 3.15 (d, $J = 13.2$ Hz, 3H, $\text{ArCH}_2^{\text{eq}}\text{Ar}$), 3.17 (d, $J = 13.2$ Hz, 1H, $\text{ArCH}_2^{\text{eq}}\text{Ar}$), 3.60-3.73 (m, 4H, $\text{OCH}_2\text{CH}_2\text{CH}_3$), 3.95-4.04 (m, 4H, $\text{OCH}_2\text{CH}_2\text{CH}_3$), 4.07-4.16 (m, 2H, OCH_2CHN), 4.31 (t, $J = 8.2$ Hz, 1H, OCH_2CHN), 4.35-4.47 (m, 4H, $\text{ArCH}_2^{\text{ax}}\text{Ar}$), 6.11-6.26 (m, 6H, *ArH*), 6.92 (t, $J = 7.4$ Hz, 1H, *ArH*), 7.11 (d, $J = 7.4$ Hz, 2H, *ArH*), 7.39 (s, 1H, *ArH*) ppm.

^{13}C NMR (300 MHz, CHLOROFORM-*d*) δ 9.9, 10.0, 10.9, 11.0, 23.1, 23.6, 23.7, 26.2, 29.8, 30.7, 31.1, 31.2, 34.2, 69.1, 76.6, 76.7, 77.0, 77.1, 77.2, 122.0, 122.42, 122.44, 125.1, 126.8, 127.7, 127.8, 127.9, 129.0, 129.1, 130.9, 131.2, 132.1, 133.25, 133.5, 136.1, 137.1, 137.3, 139.0, 155.1, 155.2, 158.1, 160.5, 164.3 ppm.

HRMS-TOF MS ESI+: m/z $[\text{M}+\text{H}]^+$ calculated for $\text{C}_{47}\text{H}_{59}\text{NO}_5\text{Br}$: 796.3572; found: 796.3560.

6.7.2 (*M*)-5-(carboxyl)-4-bromo-25,26,27,28-tetrapropoxycalix[4]arene – **103**.



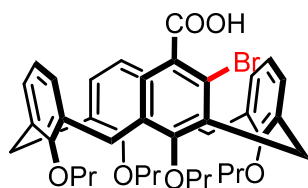
Calixarene (**M**)-**102** (200 mg, 0.250 mmol) was added to MeCN (10 ml). MeI (2.00 ml, exs) was added and the mixture was heated to 80 °C for 48 h. TLC analysis confirmed the complete formation of the methylated oxazoline product. The excess solvent was removed under reduced pressure yielding an orange semi-solid as the crude product. The crude product was added to EtOH (5.0 ml), KOH (0.3 g, exs) was added and the mixture was heated to reflux for 24 h. The reaction was quenched by the careful addition of 1M HCl. The product was extracted using DCM, and the organic later was washed with an additional portion of 1 M HCl (30 ml) and brine (30 ml). After drying over MgSO_4 the excess solvent was removed under reduced pressure yielding a yellow solid as the crude bromo-acid product. Purification was achieved using column chromatography (EtOAc:PET, 20:80), affording a white solid (158 mg, 88%).

The characterisation data collected for this compound compared well with the reported literature values.⁴⁹

^1H NMR (CHLOROFORM-*d*) δ 0.89 (t, $J = 7.4$ Hz, 3H, $\text{OCH}_2\text{CH}_2\text{CH}_3$), 0.92 (t, $J = 7.4$ Hz, 3H, $\text{OCH}_2\text{CH}_2\text{CH}_3$), 1.10 (t, $J = 7.4$ Hz, 6H, $\text{OCH}_2\text{CH}_2\text{CH}_3$), 1.81-2.01 (m, 8H, $\text{OCH}_2\text{CH}_2\text{CH}_3$), 3.16 (d, $J = 13.9$ Hz, 3H, $\text{ArCH}_2^{\text{eq}}\text{Ar}$), 3.22 (d, $J = 13.9$ Hz, 1H, $\text{ArCH}_2^{\text{eq}}\text{Ar}$), 3.63-3.73 (m, 4H, $\text{OCH}_2\text{CH}_2\text{CH}_3$), 3.96-4.09 (m, 4H, $\text{OCH}_2\text{CH}_2\text{CH}_3$), 4.40 (d, $J = 13.9$ Hz, 1H, $\text{ArCH}_2^{\text{ax}}\text{Ar}$), 4.44 (d, $J = 13.9$ Hz, 3H, $\text{ArCH}_2^{\text{ax}}\text{Ar}$), 6.10-6.29 (m, 6H, *ArH*), 6.91 (t, $J = 7.4$ Hz, 1H, *ArH*), 7.09 (d, $J = 7.4$ Hz, 2H, *ArH*), 7.77 (s, 1H, *ArH*) ppm.

HRMS-TOF MS ESI+: m/z $[\text{M}+\text{H}]^+$ calculated for $\text{C}_{41}\text{H}_{47}\text{BrO}_6$: 715.2634; found: 715.2651

Chapter 6: The application of inherently chiral phosphine oxazoline ligands

6.7.3 (P)-5-(carboxyl)-4-bromo-25,26,27,28-tetrapropoxycalix[4]arene – **103**.

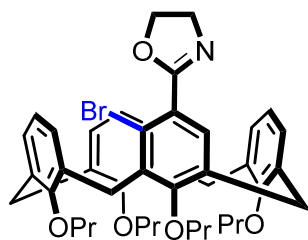
Calixarene (**P**)-**102** (205 mg, 0.260 mmol) was added to MeCN (10 ml). MeI (2.00 ml, exs) was added and the mixture was heated to 80 °C for 48 h. TLC analysis confirmed the complete formation of the methylated oxazoline product. The excess solvent was removed under reduced pressure yielding an orange semi-solid as the crude product. The crude product was added to EtOH (5.0 ml), KOH (0.3 g, exs) was added and the mixture was heated to reflux for 24 h. The reaction was quenched by the careful addition of 1M HCl. The product was extracted using DCM, and the organic later was washed with an additional portion of 1 M HCl (30 ml) and brine (30 ml). After drying over MgSO₄ the excess solvent was removed under reduced pressure yielding a yellow solid as the crude bromo-acid product. Purification was achieved using column chromatography (EtOAc:PET, 20:80), affording a white solid (188 mg, 92%).

The characterisation data collected for this compound compared well with the reported literature values.⁴⁹

¹H NMR (CHLOROFORM-*d*) δ 0.89 (t, *J* = 7.4 Hz, 3H, OCH₂CH₂CH₃), 0.92 (t, *J* = 7.4 Hz, 3H, OCH₂CH₂CH₃), 1.10 (t, *J* = 7.4 Hz, 6H, OCH₂CH₂CH₃), 1.81-2.01 (m, 8H, OCH₂CH₂CH₃), 3.16 (d, *J* = 13.9 Hz, 3H, ArCH₂^{eq}Ar), 3.22 (d, *J* = 7.4 Hz, 6H, OCH₂CH₂CH₃), 3.63-3.73 (m, 4H, OCH₂CH₂CH₃), 3.96-4.09 (m, 4H, OCH₂CH₂CH₃), 4.40 (d, *J* = 13.9 Hz, 1H, ArCH₂^{ax}Ar), 4.44 (d, *J* = 13.9 Hz, 3H, ArCH₂^{ax}Ar), 6.10-6.29 (m, 6H, ArH), 6.91 (t, *J* = 7.4 Hz, 1H, ArH), 7.09 (d, *J* = 7.4 Hz, 2H, ArH), 7.77 (s, 1H, ArH) ppm.

HRMS-TOF MS ESI+: *m/z* [M+H]⁺ calculated for C₄₁H₄₇BrO₆: 715.2634; found: 715.2640.

Chapter 6: The application of inherently chiral phosphine oxazoline ligands

6.7.1 (M)-5-(4,5-dihydrooxazole)-4-bromo-25,26,27,28-tetrapropoxycalix[4]arene – **104**.

The synthesis of calixarene **(M)-104** was achieved using the same three-step procedure for all oxazolines. Calixarene **(M)-103** (158 mg, 0.220 mmol), i) oxalyl chloride (exs), DCM (10 ml) rt. ii) ethanolamine (0.038 ml, 0.440 mmol, 2.0 equiv), Et₃N (0.170 ml, 1.10 mmol, 5.0 equiv), DCM (10 ml), room temperature, 12 h. iii) MsCl (0.050 ml, 0.660 mmol, 3.0 equiv), Et₃N (0.170 ml, 1.10 mmol, 5.0 equiv), DCM (15 ml), room temperature, 12 h. The ring closing reaction was finally quenched with 1M HCl.

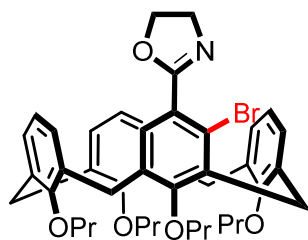
The product was extracted with DCM, which was washed with an additional portion of 1M HCl (30 ml) and brine (30 ml). The organic layer was dried over MgSO₄ and the excess solvent was removed under reduced pressure. Purification was achieved using column chromatography (EtOAc:PET, 20:80), affording a white solid (120 mg, 74%).

This intermediate compound was not fully characterized and only a ¹H NMR spectroscopy and MS data were collected.

¹H NMR (CHLOROFORM-*d*) δ 0.90 (t, *J* = 7.4 Hz, 3H, OCH₂CH₂CH₃), 0.92 (t, *J* = 7.4 Hz, 3H, OCH₂CH₂CH₃), 1.07 (t, *J* = 7.4 Hz, 6H, OCH₂CH₂CH₃), 1.81-2.00 (m, 8H, OCH₂CH₂CH₃), 3.15 (d, *J* = 13.2 Hz, 1H, ArCH₂^{eq}Ar), 3.16 (d, *J* = 13.2 Hz, 3H, ArCH₂^{eq}Ar), 3.64-3.74 (m, 4H, OCH₂CH₂CH₃), 3.77-3.87 (m, 4H, OCH₂CH₂CH₃), 3.94-4.09 (m, 4H, OCH₂CH₂N), 4.39 (d, *J* = 13.2 Hz, 1H, ArCH₂^{ax}Ar), 4.40 (d, *J* = 13.2 Hz, 1H, ArCH₂^{ax}Ar), 4.44 (d, *J* = 13.2 Hz, 2H, ArCH₂^{ax}Ar), 6.16-6.32 (m, 6H, ArH), 6.87 (t, *J* = 7.4 Hz, 1H, ArH), 7.05 (d, *J* = 7.4 Hz, 2H), 7.21 (s, 1H, ArH) ppm.

HRMS-TOF MS ESI+: *m/z* [M+H]⁺ calculated for C₄₃H₅₁NO₅Br : 740.2951; found: 740.2952.

Chapter 6: The application of inherently chiral phosphine oxazoline ligands

6.7.1 (P)-5-(4,5-dihydrooxazole)-4-bromo-25,26,27,28-tetrapropoxycalix[4]arene – **104**.

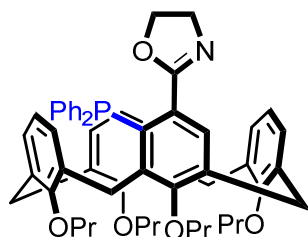
The synthesis of calixarene **(P)-104** was achieved using the same three-step procedure for all oxazolines. Calixarene **(P)-103** (188 mg, 0.260 mmol), i) oxalyl chloride (exs), DCM (10 ml) rt. ii) ethanolamine (0.031 ml, 0.520 mmol, 2.0 equiv), Et₃N (0.190 ml, 1.30 mmol, 5.0 equiv), DCM (10 ml), room temperature, 12 h. iii) MsCl (0.060 ml, 0.780 mmol, 3.0 equiv), Et₃N (0.190 ml, 1.30 mmol, 5.0 equiv), DCM (15 ml), room temperature, 12 h. The ring closing reaction was finally quenched with 1M HCl. The product was extracted with DCM, which was washed with an additional portion of 1M HCl (40 ml) and brine (40 ml). The organic layer was dried over MgSO₄ and the excess solvent was removed under reduced pressure. Purification was achieved using column chromatography (EtOAc:PET, 20:80), affording a white solid (146 mg, 76%).

This intermediate compound was not fully characterized and only a ¹H NMR spectroscopy and MS data were collected.

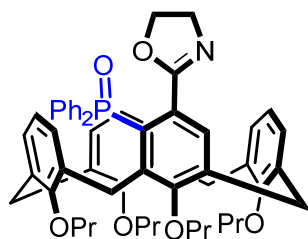
¹H NMR (CHLOROFORM-*d*) δ 0.90 (t, *J* = 7.4 Hz, 3H, OCH₂CH₂CH₃), 0.92 (t, *J* = 7.4 Hz, 3H, OCH₂CH₂CH₃), 1.07 (t, *J* = 7.4 Hz, 6H, OCH₂CH₂CH₃), 1.81-2.00 (m, 8H, OCH₂CH₂CH₃), 3.15 (d, *J* = 13.2 Hz, 1H, ArCH₂^{eq}Ar), 3.16 (d, *J* = 13.2 Hz, 3H, ArCH₂^{eq}Ar), 3.64-3.74 (m, 4H, OCH₂CH₂CH₃), 3.77-3.87 (m, 4H, OCH₂CH₂CH₃), 3.94-4.09 (m, 4H, OCH₂CH₂N), 4.39 (d, *J* = 13.2 Hz, 1H, ArCH₂^{ax}Ar), 4.40 (d, *J* = 13.2 Hz, 1H, ArCH₂^{ax}Ar), 4.44 (d, *J* = 13.2 Hz, 2H, ArCH₂^{ax}Ar), 6.16-6.32 (m, 6H, ArH), 6.87 (t, *J* = 7.4 Hz, 1H, ArH), 7.05 (d, *J* = 7.4 Hz, 2H), 7.21 (s, 1H, ArH) ppm.

HRMS-TOF MS ESI+: *m/z* [M+H]⁺ calculated for C₄₃H₅₁NO₅Br : 740.2951; found: 740.2960.

Chapter 6: The application of inherently chiral phosphine oxazoline ligands

6.7.1 (M)-5-(4,5-dihydrooxazole)-4-diphenylphosphine-25,26,27,28-tetrapropoxycalix[4]arene – **101**.

Calixarene (**M**)-**104** (100 mg, 0.130 mmol) was added to freshly distilled Et₂O (5 ml) and cooled (–78 °C). *n*-BuLi (0.198 mmol, 1.5 equiv) was added dropwise, turning the mixture a dark yellow colour. After stirring for 10 min, diphenylphosphine chloride (0.070 ml, 0.400 mmol, 3.0 equiv) was added to the reaction mixture and the yellow colour immediately faded. The reaction mixture was allowed to warm to room temperature, after which TLC analysis confirmed the formation of the product. The reaction was quenched with oven dried alumina, the excess solvent was removed under reduced pressure and the mixture was dry-loaded onto an alumina column. Separation was achieved using a (EtOAc:PET, 0:100 to 5:95) gradient elution, affording the product as a white solid (44 mg, 44%)



Calixarene (**M**)-**101** (15.0 mg, 0.0180 mmol) was added to THF (2 ml) at rt. H₂O₂ (1.00 ml, 30% aq, exs) was added all at once. The reaction mixture was stirred at room temperature overnight. Alumina TLC confirmed full conversion to the phosphine oxide. The reaction was quenched by the addition of 1M HCl. The crude product was extracted using DCM. The organic layer was then washed with additional 1M HCl, dried over MgSO₄, and the excess solvent was removed under reduced pressure yielding a white solid.

Purification was achieved using alumina column chromatography (EtOAc:PET, 30:70), yielding the phosphine oxide (**P**)-**97** as a white solid (14 mg, 92%).

Chapter 6: The application of inherently chiral phosphine oxazoline ligands

^1H NMR (CHLOROFORM-*d*) δ 0.84 (t, $J = 7.4$ Hz, 3H, $\text{OCH}_2\text{CH}_2\text{CH}_3$), 0.90 (t, $J = 7.4$ Hz, 3H, $\text{OCH}_2\text{CH}_2\text{CH}_3$), 0.93 (t, $J = 7.4$ Hz, 3H, $\text{OCH}_2\text{CH}_2\text{CH}_3$), 1.10 (t, $J = 7.4$ Hz, 3H, $\text{OCH}_2\text{CH}_2\text{CH}_3$), 1.56-1.68 (m, 4H, $\text{OCH}_2\text{CH}_2\text{CH}_3$), 1.80-1.94 (m, 4H, $\text{OCH}_2\text{CH}_2\text{CH}_3$), 3.01 (d, $J = 13.6$ Hz, 1H, $\text{ArCH}_2^{\text{eq}}\text{Ar}$), 3.10 (d, $J = 13.6$ Hz, 1H, $\text{ArCH}_2^{\text{eq}}\text{Ar}$), 3.15 (d, $J = 13.6$ Hz, 1H, $\text{ArCH}_2^{\text{eq}}\text{Ar}$), 3.22 (d, $J = 13.6$ Hz, 1H, $\text{ArCH}_2^{\text{eq}}\text{Ar}$), 3.39-3.53 (m, 5H, $\text{OCH}_2\text{CH}_2\text{CH}_3$), 3.60-3.68 (m, 3H, $\text{OCH}_2\text{CH}_2\text{CH}_3$), 3.96-4.03 (m, 2H, $\text{OCH}_2\text{CH}_2\text{N}$), 4.09-4.18 (m, 2H, OCH_2CH_2), 4.33 (d, $J = 13.6$ Hz, 2H, $\text{ArCH}_2^{\text{ax}}\text{Ar}$), 4.40 (d, $J = 13.6$ Hz, 2H, $\text{ArCH}_2^{\text{ax}}\text{Ar}$), 4.46 (d, $J = 13.6$ Hz, 2H, $\text{ArCH}_2^{\text{ax}}\text{Ar}$), 5.71 (d, $J = 7.6$ Hz, 1H, ArH), 5.86 (d, $J = 7.6$ Hz, 1H, ArH), 6.01 (t, $J = 7.6$ Hz, 1H, ArH), 6.08-6.11 (m, 2H, ArH), 6.26 (t, $J = 7.6$ Hz, 1H, ArH), 6.81 (m, 1H, ArH), 6.92 (t, $J = 7.6$ Hz, 1H, ArH), 7.08-7.14 (m, 2H, ArH), 7.37-7.47 (m, 6H, ArH), 7.64-7.71 (m, 2H, ArH), 7.91-7.98 (m, 2H, ArH) ppm.

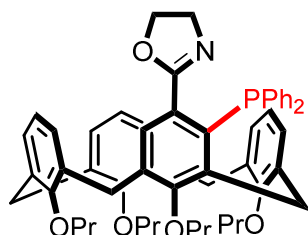
Owing to the complexity of the aromatic region in the ^{13}C NMR spectrum, the P-C coupling could not be accurately determined. Instead, all of the ^{13}C signals have been reported which explains why there are more signals than expected.

^{13}C NMR (75 Hz, CHLOROFORM-*d*) δ 9.9, 10.0, 10.9, 11.0, 23.1, 23.5, 23.7, 29.9, 31.0, 31.1, 31.2, 41.9, 43.2, 76.6, 76.8, 77.2, 77.4, 121.9, 122.4, 122.6, 126.6, 127.1, 127.3, 128.1, 128.2, 128.3, 128.4, 128.5, 129.0, 129.2, 130.0, 130.2, 131.1, 131.3, 131.4, 131.5, 131.6, 131.7, 131.8, 132.6, 133.1, 133.6, 134.6, 135.5, 135.6, 135.8, 137.2, 137.3, 137.4, 141.6, 141.7, 145.1, 145.2, 155.1, 155.2, 158.3, 161.0, 161.1, 169.4, 169.5 ppm.

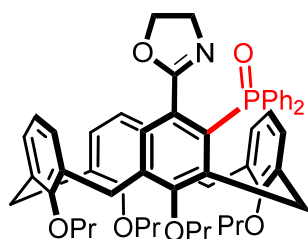
^{31}P NMR (300 MHz, CHLOROFORM-*d*) δ 30.58 ppm.

HRMS-TOF MS ESI+: m/z $[\text{M}+\text{H}]^+$ calculated for $\text{C}_{55}\text{H}_{60}\text{NO}_6\text{P}$: 862.4237; found: 862.4228.

Chapter 6: The application of inherently chiral phosphine oxazoline ligands

6.7.1 (P)-5-(4,5-dihydrooxazole)-4-diphenylphosphine-25,26,27,28-tetrapropoxycalix[4]arene – **101**.

Calixarene (**M**)-**104** (80 mg, 0.104 mmol) was added to freshly distilled Et₂O (5 ml) and cooled (–78 °C). *n*-BuLi (0.156 mmol, 1.5 equiv) was added dropwise, turning the mixture a dark yellow colour. After stirring for 10 min, diphenylphosphine chloride (0.056 ml, 0.312 mmol, 3.0 equiv) was added to the reaction mixture and the yellow colour immediately faded. The reaction mixture was allowed to warm to room temperature, after which TLC analysis confirmed the formation of the product. The reaction was quenched with oven dried alumina, the excess solvent was removed under reduced pressure and the mixture was dry-loaded onto an alumina column. Separation was achieved using a (EtOAc:PET, 0:100 to 5:95) gradient elution, affording the product as a white solid (36 mg, 42%).



Calixarene (**M**)-**101** (15 mg, 0.018 mmol) was added to THF (2 ml) at rt. H₂O₂ (1.0 ml, 30% aq, exs) was added all at once. The reaction mixture was stirred at room temperature overnight. Alumina TLC confirmed full conversion to the phosphine oxide. The reaction was quenched by the addition of 1M HCl. The crude product was extracted using DCM. The organic layer was then washed with additional 1M HCl, dried over MgSO₄, and the excess solvent was removed under reduced pressure yielding a white solid. Purification was achieved using alumina column chromatography (EtOAc:PET, 30:70), yielding the phosphine oxide (**P**)-**97** as a white solid (14 mg, 92%).

Chapter 6: The application of inherently chiral phosphine oxazoline ligands

^1H NMR (CHLOROFORM-*d*) δ 0.84 (t, $J = 7.4$ Hz, 3H, $\text{OCH}_2\text{CH}_2\text{CH}_3$), 0.90 (t, $J = 7.4$ Hz, 3H, $\text{OCH}_2\text{CH}_2\text{CH}_3$), 0.93 (t, $J = 7.4$ Hz, 3H, $\text{OCH}_2\text{CH}_2\text{CH}_3$), 1.10 (t, $J = 7.4$ Hz, 3H, $\text{OCH}_2\text{CH}_2\text{CH}_3$), 1.56-1.68 (m, 4H, $\text{OCH}_2\text{CH}_2\text{CH}_3$), 1.80-1.94 (m, 4H, $\text{OCH}_2\text{CH}_2\text{CH}_3$), 3.01 (d, $J = 13.6$ Hz, 1H, $\text{ArCH}_2^{\text{eq}}\text{Ar}$), 3.10 (d, $J = 13.6$ Hz, 1H, $\text{ArCH}_2^{\text{eq}}\text{Ar}$), 3.15 (d, $J = 13.6$ Hz, 1H, $\text{ArCH}_2^{\text{eq}}\text{Ar}$), 3.22 (d, $J = 13.6$ Hz, 1H, $\text{ArCH}_2^{\text{eq}}\text{Ar}$), 3.39-3.53 (m, 5H, $\text{OCH}_2\text{CH}_2\text{CH}_3$), 3.60-3.68 (m, 3H, $\text{OCH}_2\text{CH}_2\text{CH}_3$), 3.96-4.03 (m, 2H, $\text{OCH}_2\text{CH}_2\text{N}$), 4.09-4.18 (m, 2H, OCH_2CH_2), 4.33 (d, $J = 13.6$ Hz, 2H, $\text{ArCH}_2^{\text{ax}}\text{Ar}$), 4.40 (d, $J = 13.6$ Hz, 2H, $\text{ArCH}_2^{\text{ax}}\text{Ar}$), 4.46 (d, $J = 13.6$ Hz, 2H, $\text{ArCH}_2^{\text{ax}}\text{Ar}$), 5.71 (d, $J = 7.6$ Hz, 1H, ArH), 5.86 (d, $J = 7.6$ Hz, 1H, ArH), 6.01 (t, $J = 7.6$ Hz, 1H, ArH), 6.08-6.11 (m, 2H, ArH), 6.26 (t, $J = 7.6$ Hz, 1H, ArH), 6.81 (m, 1H, ArH), 6.92 (t, $J = 7.6$ Hz, 1H, ArH), 7.08-7.14 (m, 2H, ArH), 7.37-7.47 (m, 6H, ArH), 7.64-7.71 (m, 2H, ArH), 7.91-7.98 (m, 2H, ArH) ppm.

Owing to the complexity of the aromatic region in the ^{13}C NMR spectrum, the P-C coupling could not be accurately determined. Instead, all of the ^{13}C signals have been reported which explains why there are more signals than expected.

^{13}C NMR (75 Hz, CHLOROFORM-*d*) δ 9.9, 10.0, 10.9, 11.0, 23.1, 23.5, 23.7, 29.9, 31.0, 31.1, 31.2, 41.9, 43.2, 76.6, 76.8, 77.2, 77.4, 121.9, 122.4, 122.6, 126.6, 127.1, 127.3, 128.1, 128.2, 128.3, 128.4, 128.5, 129.0, 129.2, 130.0, 130.2, 131.1, 131.3, 131.4, 131.5, 131.6, 131.7, 131.8, 132.6, 133.1, 133.6, 134.6, 135.5, 135.6, 135.8, 137.2, 137.3, 137.4, 141.6, 141.7, 145.1, 145.2, 155.1, 155.2, 158.3, 161.0, 161.1, 169.4, 169.5 ppm.

^{31}P NMR (300 MHz, CHLOROFORM-*d*) δ 30.58 ppm.

HRMS-TOF MS ESI+: m/z $[\text{M}+\text{H}]^+$ calculated for $\text{C}_{55}\text{H}_{60}\text{NO}_6\text{P}$: 862.4237; found: 862.4229.

6.8 References.

- (1) McManus, H. A Guiry, P. J. *Chem. Rev.* **2004**, *104*, 4151.
- (2) Hargaden, G. C.; Guiry, P. J. *Chem. Rev.* **2009**, *109*, 2505.
- (3) Gómez, R. A.; Adrio, J.; Carretero, J. C. *Angew. Chem., Int. Ed.* **2006**, *45*, 7674.
- (4) Trost, B. M.; Crawley, M. L. *Chem. Rev.* **2003**, *103*, 2921.
- (5) Meng, X.; Li, X.; Xu, D. *Tetrahedron: Asymmetry* **2009**, *20*, 1402.
- (6) Dawson, G. J.; Coote, S. J.; Frost, C. G.; Williams, M. J. *Tetrahedron Lett.* **1993**, *34*, 3149.
- (7) Herbert, S. A.; van Laeren, L. J.; Castell, D. C.; Arnott, G. E. *Beilstein J. Org. Chem.* **2014**, *10*, 2751.
- (8) Auburn, P. R.; Mackenzie, P. B.; Bosnich, B. J. *Am. Chem. Soc.* **1985**, *107*, 2033.
- (9) Trost, B. M.; Murphy, D. J. *Organometallics* **1985**, *4*, 1143.
- (10) Kollmar, M.; Helmchen, G. *Organometallics* **2002**, *21*, 4771.
- (11) Van Haaren, R. J.; Goubitz, K.; Fraanje, J.; Van Strijdonck, G. P. F.; Oevering, H.; Coussens, B.; Reek, J. N. H.; Kamer, P. C. J.; Van Leeuwen, P. W. N. M. *Inorg. Chem.* **2001**, *40*, 3363.
- (12) Liu, S. Y.; Muller, J. F. K.; Neuburger, M.; Schaffner, S.; Zehnder, M. *Helv. Chim. Acta* **2000**, *83*, 1256.
- (13) Junker, J.; Reif, B.; Steinhagen, H.; Junker, B.; Felli, I. C.; Reggelin, M.; Griesinger, C. *Chem.-Eur. J.* **2000**, *6*, 3281.
- (14) Ayerbe Garcia, M.; Frey, W.; Peters, R. *Organometallics* **2014**, *33*, 1068.
- (15) Goldfuss, B. J. *Organomet. Chem.* **2006**, *691*, 4508.
- (16) Leca, F.; Fernández, F.; Muller, G.; Lescop, C.; Reau, R.; Gabbitas, N.; Gómez, M. *Eur. J. Inorg. Chem.* **2009**, 5583.
- (17) Cecilia Noguez, F. H. *Chirality* **2014**, *26*, 553.
- (18) Trost, B. M. *J. Org. Chem.* **2004**, *69*, 5813.
- (19) Carroll, M. P.; Guiry, P. J.; Brown, J. M. *Org. Biomol. Chem.* **2013**, *11*, 4591.
- (20) Chen, J.; Chen, J.; Lang, F.; Zhang, X.; Cun, L.; Zhu, J.; Deng, J.; Liao, J. *J. Am. Chem. Soc.* **2010**, *132*, 4552.
- (21) Armstrong, P. B.; Bennett, L. M.; Constantine, R. N.; Fields, J. L.; Jasinski, J. P.; Staples, R. J.; Bunt, R. C. *Tetrahedron Lett.* **2005**, *46*, 1441.

Chapter 6: The application of inherently chiral phosphine oxazoline ligands

- (22) Kollmar, M.; Steinhagen, H.; Janssen, J. P.; Goldfuss, B.; Malinovskaya, S. A.; Vazquez, J.; Rominger, F.; Helmchen, G. *Chem. -Eur. J.* **2002**, *8*, 3103.
- (23) Madrahimov, S. T.; Li, Q.; Sharma, A.; Hartwig, J. F. *J. Am. Chem. Soc.* **2015**, *137*, 14968.
- (24) Helmchen, G.; Pfaltz, A. *Acc. Chem. Res.* **2000**, *33*, 336.
- (25) Armstrong, P. B.; Dembicer, E. A.; Desbois, A. J.; Fitzgerald, J. T.; Gehrman, J. K.; Nelson, N. C.; Noble, A. L.; Bunt, R. C. *J. Am. Chem. Soc.* **2012**, *31*, 6933.
- (26) Sprinz, J.; Kiefer, M.; Helmchen, G. *Tetrahedron Lett.* **1994**, *35*, 1523.
- (27) Solin, N.; Szabo, K. J. *Organometallics* **2001**, *20*, 5464.
- (28) Togni, A.; Burckhardt, U.; Gramlich, V.; Pregosin, P. S.; Salzmann, R. *J. Am. Chem. Soc.* **1996**, *118*, 1031.
- (29) Constantine, R. N.; Kim, N.; Bunt, R. C. *Org. Lett.* **2003**, *5*, 2279.
- (30) Kleimark, J.; Johansson, C.; Olsson, S.; Hakansson, M.; Hansson, S.; Akermark, B.; Norrby, P. O. *Organometallics* **2011**, *30*, 230.
- (31) Wiese, B.; Helmchen, G. *Tetrahedron Lett.* **1998**, *39*, 5727.
- (32) Szabó, K. J. *Organometallics* **1996**, *15*, 1128.
- (33) Togni, A.; Burckhardt, U.; Gramlich, V.; Pregosin, P. S.; Salzmann, R. *J. Am. Chem. Soc.* **1996**, *118*, 1031.
- (34) Adams, H.; Anderson, J. C.; Cubbon, R.; James, D. S.; Mathias, J. P. *J. Org. Chem.* **1999**, *64*, 8256.
- (35) Herbert, S. A.; Arnott, G. E. *Org. Lett.* **2010**, *12*, 4600.
- (36) Tu, T.; Deng, W-P.; Hou, X-L.; Dai, L-X.; Dong, X-C. *Chem. -Eur. J.* **2003**, *9*, 3073.
- (37) Deng, W. P.; Hou, X. L.; Dai, L. X.; Dong, X. W. *Chem. Commun.* **2000**, 1483.
- (38) Yonehara, K.; Mori, K.; Hashizume, T.; Chung, K.; Ohe, K.; Uemura, S. *J. Organomet. Chem.* **2000**, *603*, 40.
- (39) Bélanger, É.; Pouliot, M. F.; Paquin, J. F. *Org. Lett.* **2009**, *11*, 2201.
- (40) Cammidge, A. N.; Crépy, K. V. L. *Chem. Commun.* **2000**, 1723.
- (41) Jensen, J. F.; Johannsen, M. *Org. Lett.* **2003**, *5*, 3025.
- (42) Bronger, R. P. J.; Guiry, P. J. *Tetrahedron: Asymmetry* **2007**, *18*, 1094.
- (43) Castanet, A. S.; Colobert, F.; Broutin, P. E.; Obringer, M. *Tetrahedron: Asymmetry* **2002**, *13*, 659.
- (44) Uozumi, Y.; Matsuura, Y.; Arakawa, T.; Yamada, Y. M. A. *Angew. Chem., Int. Ed.* **2009**, *48*, 2708.

Chapter 6: The application of inherently chiral phosphine oxazoline ligands

- (45) Cammidge, A. N.; Crépy, K. V. L. *Tetrahedron* **2004**, *60*, 4377.
- (46) Cammidge, A. N.; Crépy, K. V. L. *J. Org. Chem.* **2003**, *68*, 6832.
- (47) Bermejo, A.; Ros, A.; Fernández, R.; Lassaletta, J. M. *J. Am. Chem. Soc.* **2008**, *130*, 15798.
- (48) Miyaura, N.; Suzuki, A. *Chem. Rev.* **1995**, *95*, 2457.
- (49) Herbert, S. A. Oxazoline Directed Lithiation of Calix[4]arene and Ferrocene, PhD, Stellenbosch University, 2011.
- (50) Wu, X-W.; Zhang, T-Z.; Yuan, K.; Hou, X-L. *Tetrahedron: Asymmetry* **2004**, *15*, 2357.

7 Chapter 7 - Conclusions and future work

7.1 Conclusions.

In summary, herein we report our efforts towards further developing the methods required to synthesis inherently chiral calixarenes. Both oxazoline and sulfoxide chiral auxiliaries have been successfully used in a series of asymmetric ortholithiation reactions.

Despite the oxazoline-directed metalation having been previously optimized, the literature surrounding lithiation chemistry was reviewed with a view to elucidating the details of this complex process. The roles played by the solvent, additive and alkyllithium were all scrutinized and explanations for each of their functions have been proposed. During this research, several key calixarene compounds were resynthesized and fully characterized, enabling the publication of past results.

The chiral *tert*-butyl sulfoxide auxiliary was able to afford inherently chiral calixarenes in *de* values of up to 90%. The absolute configuration of the inherently chiral major (*M*) and minor (*P*) diastereomers were successfully determined crystallographically. Removal of the sulfoxide was achieved using an efficient desulfurization protocol, yielding a new inherently chiral calixarene. This has created an opportunity for future studies to examine the application of this new type of inherently chiral material.

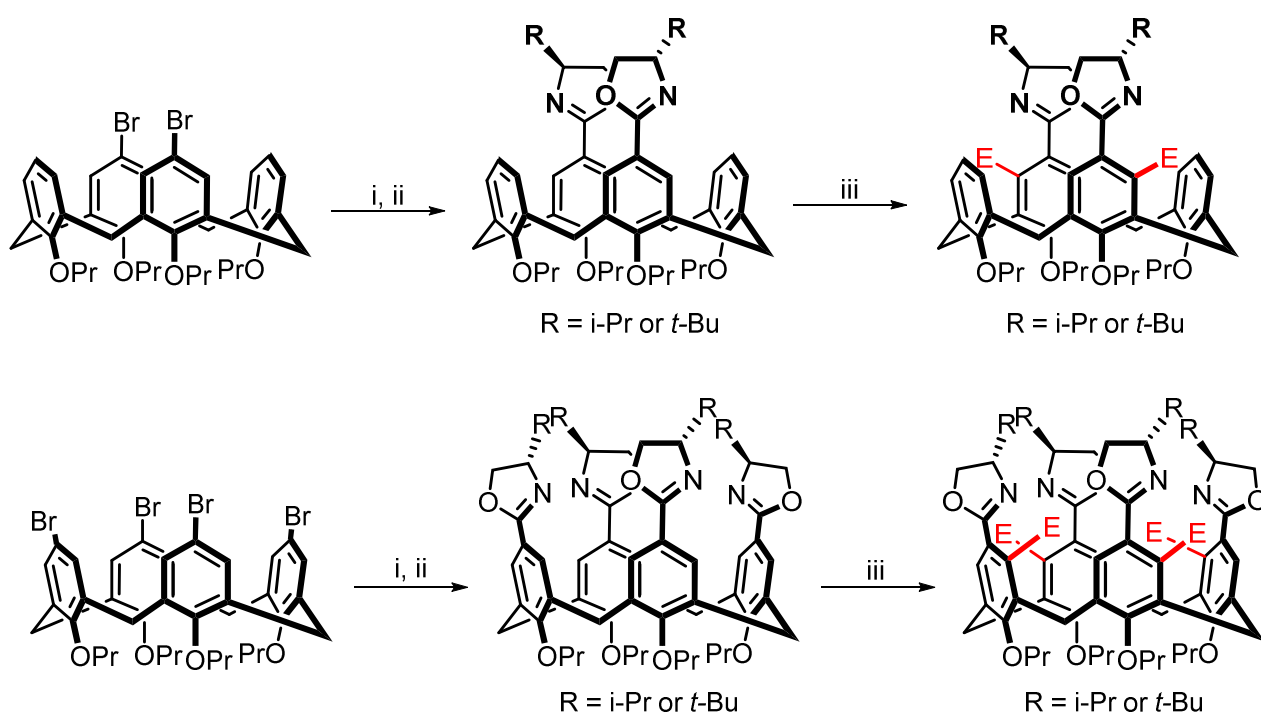
The oxazoline directed ortholithiation reaction was used to synthesize four new inherently chiral calixarenes, and two model Phox ligands, which formed the core of the application study. The Tsuji-Trost allylation and an asymmetric Suzuki-Miyaura coupling reaction were both evaluated with this library of ligands. In both cases, a matched/mismatched relationship between the configuration of the oxazoline and the inherent chirality of the calixarene was observed. The findings for the Tsuji-Trost allylation reaction were indicative of the fact that inherent chirality can function as a prominent source of chiral information. A model was proposed and used to correlate the structural properties of these ligands with the stereochemical outcome of these reactions. In spite of obtaining generally poor selectivities for the Suzuki-coupling reactions, the performance of the calixarene ligands surpassed that of the models. Furthermore, this was the first example of an asymmetric Suzuki-coupling reaction using calixarene Phox ligands, in the synthesis of axially chiral binaphthalenes.

The results from the Tsuji-Trost reactions suggested a considerable influence of the inherent chirality during the enantioselection process. In order to isolate the role played by inherent chirality, two new purely inherently chiral calixarene Phox ligands were synthesized, and the allylation reaction was revisited. These tentative results are indicative of the fact that the inherent chirality alone was able to function as a potentially useful source of chiral induction. To the best of our knowledge the selectivity's obtained within this study represent the highest values recorded to date for purely inherently chiral calixarene ligands.

7.2 Further developing asymmetric synthesis of inherently chiral calixarenes.

7.2.1 Oxazoline calixarenes.

The methods toward the synthesis of inherently chiral calixarenes are already efficient and well optimized. Currently all of the method development has focused on the asymmetric ortholithiation of a mono-oxazoline calixarene. The synthesis of new ligands with multiple components of inherent chirality still needs to be developed. The next step would be to advance the ortholithiation strategy by incorporating multiple oxazolines on the upper-rim of the calixarene. During the course of my honor's project, we accomplished the synthesis of a bis-oxazoline calixarene. With these earlier findings as the foundation, the synthesis of a new series of bis- and tetra-oxazolines could be developed (**Scheme 7.1**).



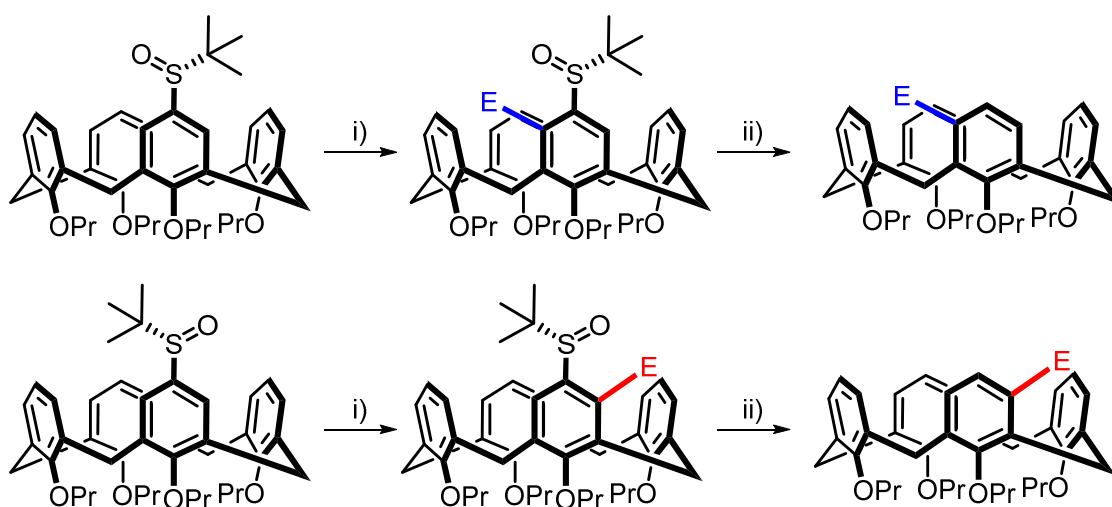
Scheme 7.1: Synthesis of di- and tetra-oxazoline calixarenes. Reactions: i) synthesis of di- and tetra-carboxylic acid calixarenes via lithium halogen exchange; ii) synthesis of di- and tetra-oxazolines; iii) ortholithiation of di- and tetra-oxazoline calixarenes.

The synthesis and subsequent ortholithiation of these new calixarenes would provide access to new types of inherently chiral compounds. The ortholithiation of these multi-oxazoline compounds would be a substantial synthetic and analytical challenge. However, if successful could have interesting implications not just for the synthesis of new ligands, but would allow for the development of new materials such as chiral stationary phases,^{1,2} selective storage materials,^{3,4} enzyme mimics^{5,6} and molecular receptors.^{7,8} All of which have incorporated calixarenes in the past.

Chapter 7: Conclusions and future work.

7.2.2 Sulfoxide calixarenes.

The progress of the ortholithiation of sulfoxide calixarenes has lagged behind oxazolines and there is still much room for improvement for the mono-sulfoxide **76** alone. Additional options need to be explored to overcome the limitations presented by electrophile choice. Without improving this aspect of the chemistry, the potential of the synthetic method will remain severely stunted. Furthermore, little effort has been made towards investigating the inversion of the stereochemistry in this reaction. However, a potential and simpler solution to this would be to invert the configuration of the sulfoxide, which should switch the selectivity of the ortholithiation reaction as well (**Scheme 7.2**).



Scheme 7.2: Inversion and ortholithiation of the sulfoxide. A route to both inherently chiral enantiomers. Reactions: i) ortholithiation; ii) desulfurization.

Strictly speaking, this would not be an inversion of the selectivity of the reaction reported in **Chapter 4**, but it would provide a route to obtaining both of the inherently chiral enantiomers after removal of the sulfoxide auxiliary. If the limitations associated with electrophile choice could be overcome, this would provide another route to developing new inherently chiral materials. In summary, the two biggest aspects of the ortholithiation of the mono-sulfoxide that require improvement are; overcoming the limited pool of usable electrophiles as well as establishing the route to the opposite configuration of the inherently chiral calixarene diastereomers and enantiomers. Both are required to evaluate the impact of inherent chirality during application studies. As mentioned above, a related synthesis of di- and tetra-sulfoxide calixarenes can also be undertaken.

Expanding the ortholithiation method to include di- and tetra-sulfoxides would again be a considerable synthetic challenge. The synthesis of the sulfoxides alone would be difficult. It was not reported in **Chapter 4**, but the synthesis of the di-sulfoxide calixarene was accomplished during this study. The mono-sulfoxide and protonated calixarene sulfoxide both formed as by-products in the reaction.

Chapter 7: Conclusions and future work.

Therefore the formation of mono-, di- and tri-sulfoxides, as well as the protonated calixarene **53**, would be by-products during the synthesis of the tetra-sulfoxide calixarene. In spite of this, if the synthesis and subsequent ortholithiation of these new sulfoxide calixarenes could be accomplished, it would open doors to new inherently chiral calixarene materials.

7.3 The application of inherently chiral calixarenes.

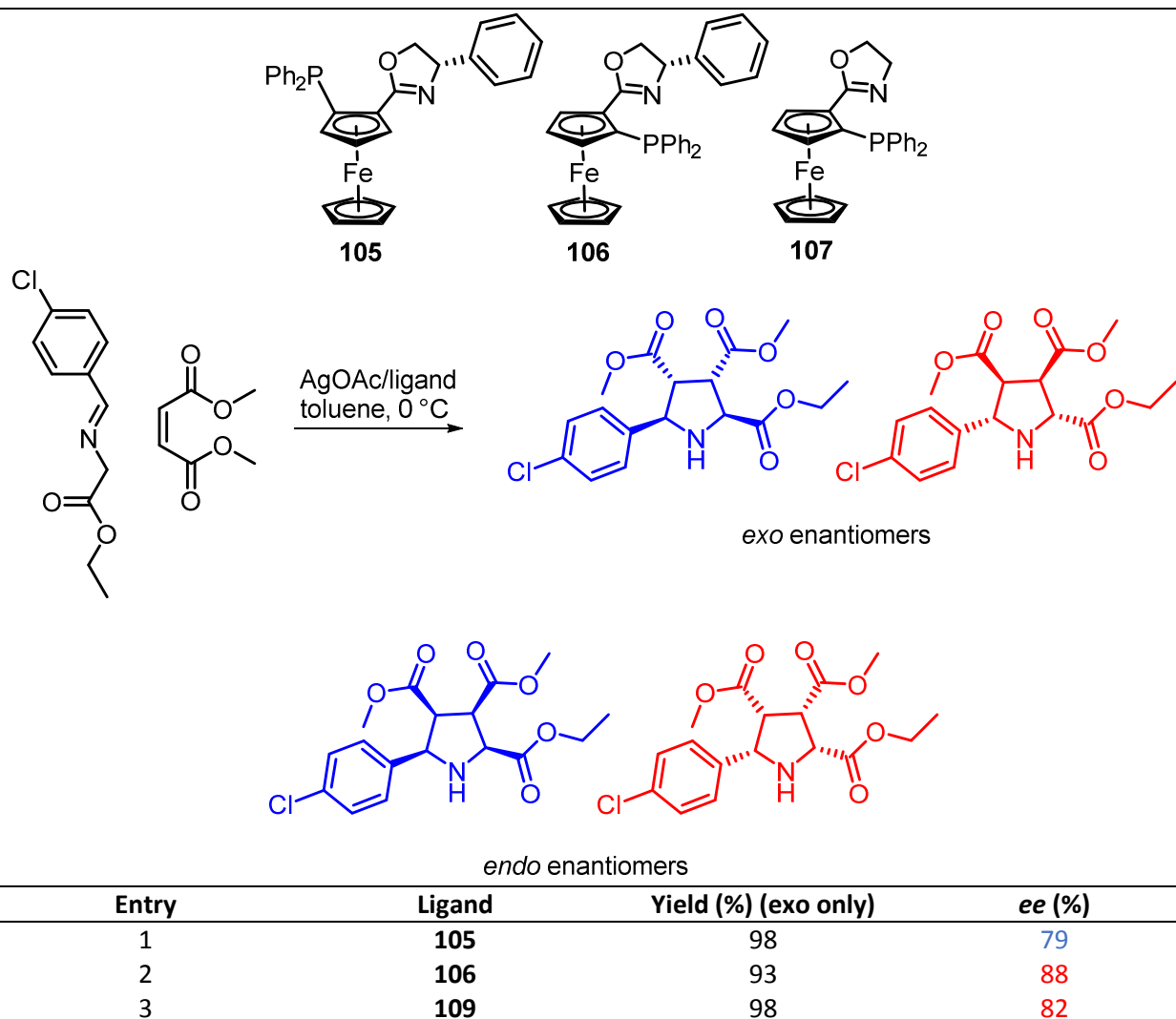
In this study the contribution of inherent chirality toward asymmetric induction was reported for two catalytic reactions. These results are only the very beginning of what has the potential to develop into an interesting and relatively unexplored area of chemistry. Up until now, only two ligand systems, the S/N and P/N bidentate oxazoline calixarenes have been investigated. There is still much room left for growth.

7.3.1 Calixarene Phox ligands.

Furthering the application of the calixarene Phox ligands has to be driven by two separate approaches. Firstly, the ligands need to be screened in many more catalytic reactions. Only a select few were reported in this study and there are still many options available. Toward this goal, two potential asymmetric reactions have been suggested below. In addition, there are still many different structural variations of the current calixarene ligands which could improve the results of the asymmetric Suzuki coupling and Tsuji-Trost allylation reactions.

7.3.1.1 Other asymmetric reactions.

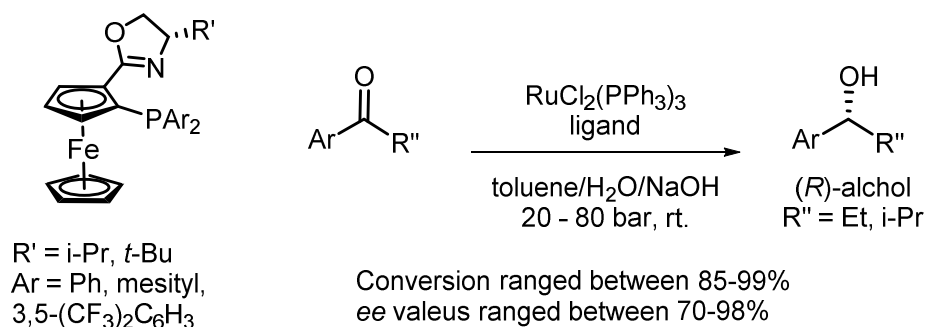
It wasn't reported in **Chapter 6**, but there was another asymmetric reaction that were briefly looked at, the outcomes of which were inconclusive. Even though these ligand systems weren't fully evaluated, they still have potential to yield interesting results. The asymmetric [3+2] cycloaddition of 1,3-dipole azomethine ylids with olefinic dipolarophiles to form highly substituted five-membered pyrrolidine rings, using planar chiral ligands was first reported by Zhou and co-workers in 2005 (**Table 7.1**).⁹ These nitrogen heterocycles are important components and motifs that are found in many biologically active molecules.¹⁰⁻¹³

Table 7.1: Planar chiral Phox ligands reported by Zhou in the [3+2] cycloaddition reaction.

The application of planar chiral ferrocene Phox ligands yielded remarkable results. Their method was exclusively selective for the synthesis of the endo diastereomer. By using the planar chiral ligand (*pS*) **107**, they were able to achieve a selectivity of **82%**. This selectivity was improved to **88%** when the central chirality of the oxazoline matched the planar chirality of the ferrocene (*S*, *pS*) in ligand **106**. Using a mismatched ligand (*S*, *pR*) **105**, yielded the opposite enantiomer with a slightly lower *ee* of **79%**. This result implied that the steric control in these reactions was largely governed by the planar chirality of the ferrocene and not the central chirality on the oxazolines. Based on this, we were hopeful that the inherently chiral calixarene Phox ligands would exhibit similar behavior. Unfortunately, when the reaction was attempted with our ligands, **93**, (*M*)-**95** and (*P*)-**95**, the cyclized product was formed in high yields, but in varied mixtures of the endo and exo enantiomers in racemic product mixtures. Even though we were initially discouraged, there are several other conditions for this reaction that need to be investigated further and could be used to fine-tune the reaction conditions and improve these preliminary results.^{14–17}

Chapter 7: Conclusions and future work.

Another field of catalysis that we were unable to investigate due to limited infrastructure, was the asymmetric reductive hydrogenation reactions.¹⁸⁻²⁰ In these reports, a variety of planar chiral ferrocene ligands were used in the ruthenium catalyzed asymmetric reductive hydrogenation of ketones, yielding the alcohol products in *ee* values of up to 98%. A few of these ligands and findings have been depicted below (**Scheme 7.3**).



Scheme 7.3: Asymmetric ruthenium catalyzed hydrogenation with planar chiral ferrocene Phox ligands.¹⁸⁻²⁰

The above is only a small representation of a sizable body of work. In these application studies the results of the ferrocene based ligands were often compared to those obtained with simpler model ligand compounds, and in many cases the planar chirality had a significant input in the asymmetric induction of the reaction.

The above mentioned are only two examples of catalytic reactions in which the inherent chirality of the calixarenes could play a significant role in the stereochemical outcome. There are many other potential asymmetric reactions that have been covered in several comprehensive reviews.²¹⁻²⁴ It's difficult to say for certain which of these would be well suited for the calixarene ligands, any example where the planar chirality was found to be important could have potential. All of these options would have to be assessed using a process of trial and error.

7.3.1.2 Structural variations of the calixarene Phox ligands.

Owing to the stereochemical outcome of the Tsuji-Trost reaction relying heavily on the steric and electronic input of the P-phenyl groups, modification of these functional groups would be the next logical step. Theoretically, this would be relatively easy to accomplish as all of the chemistry involved in the synthesis of the modified versions of the ligands would be almost identical. The only difference being the structure of the phosphine electrophile used in the ortholithiation reaction. Several potential variations of the P-phenyl group have been suggested below (**Figure 7.1**).

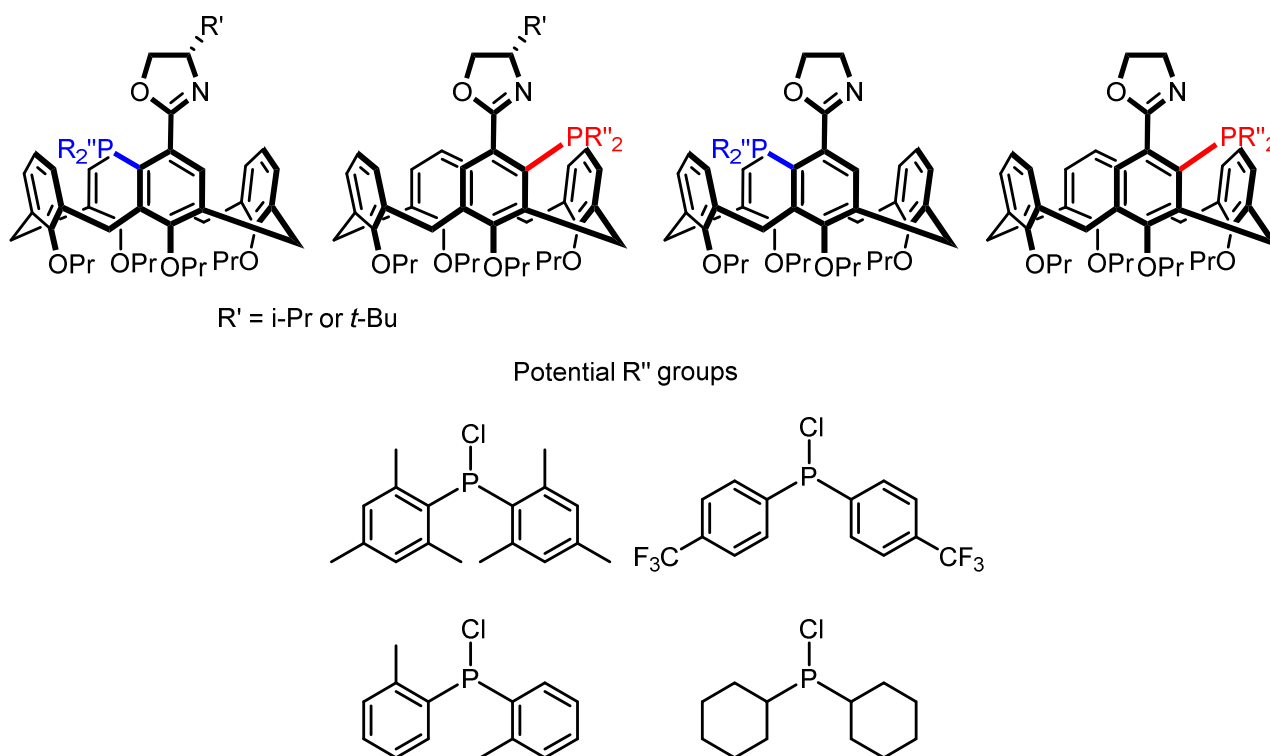


Figure 7.1: Introducing new diaryl and dialkyl phosphine functional groups to the calixarene ligands.

The potential R'' groups depicted above offer alternative steric and electronic variations to the phosphine component of the ligand, and have been previously reported on other systems. Introducing electron withdrawing groups could potentially increase the capability of the phosphorous atom to direct nucleophilic attack in the allyl palladium intermediate. Furthermore, changing the steric environment created by the diphenylphosphine would have interesting implications on the *endo:exo* ratio of these intermediates in solution, and therefore the overall selectivity. The following publications are examples of where the above four variations of the phosphine functional group have been included in chiral ligands.^{18–20,25–28}

Even though the synthesis and results using the purely inherently chiral calixarene ligands still need to be revisited, a publication by Dai and co-workers in 2001, reported an interesting and significant role played by structure of the achiral oxazoline backbone, in the outcome of the Tsuji-Trost allylation reaction. Examples of their findings using the planar chiral ferrocene ligands have been applied to the calixarene ligands as depicted below (**Figure 7.2**).

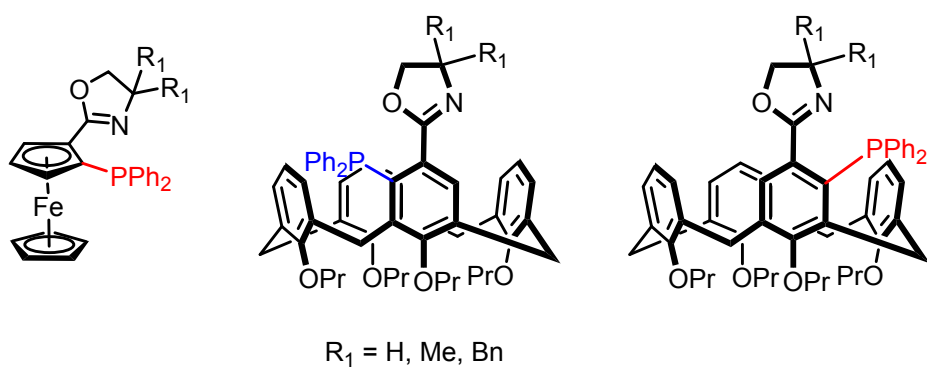


Figure 7.2: Variations on the achiral oxazoline backbone structure.

The ligands reported by Dai (left) where the planar chiral ferrocene equivalent of the calixarene ligands reported in this study. What they found was that the *ee* of the Tsuji-Trost reaction dropped from a 76% to 54% for (*S*), when the R_1 group was changed from a proton to a methyl functional group. What was even more interesting was the slight inversion of the selectivity to an *ee* of 6% for (*R*) when using two benzyl groups on the achiral oxazoline. These results suggested that the structure of the achiral oxazoline backbone made a significant stereochemical contribution to selectivity of the reaction. The new di-methyl and di-benzyl oxazolines could theoretically be incorporated into our ligand structures after the chiral oxazoline has been hydrolyzed, by simply using the appropriate aminoalcohol during the synthesis of the achiral oxazoline. The structure of achiral backbone could in itself have a matched and mismatched relationship with the configuration of the inherent chirality, which could create an interesting opportunity to fine-tune the performance of these ligands by selecting the optimal combination of achiral oxazoline backbone and inherently chiral configuration.

7.3.2 Synthesis of inherently chiral ligands using the sulfoxide chiral auxiliary.

We have not yet explored the potential of sulfoxide-based inherently chiral ligands. The literature contains numerous examples of chiral sulfoxide ligands that could be explored. The following are but a few examples of potential ligand systems that could be incorporated onto the calixarene framework if the chemistry outlined in **Chapter 4** can be improved (**Figure 7.3**).

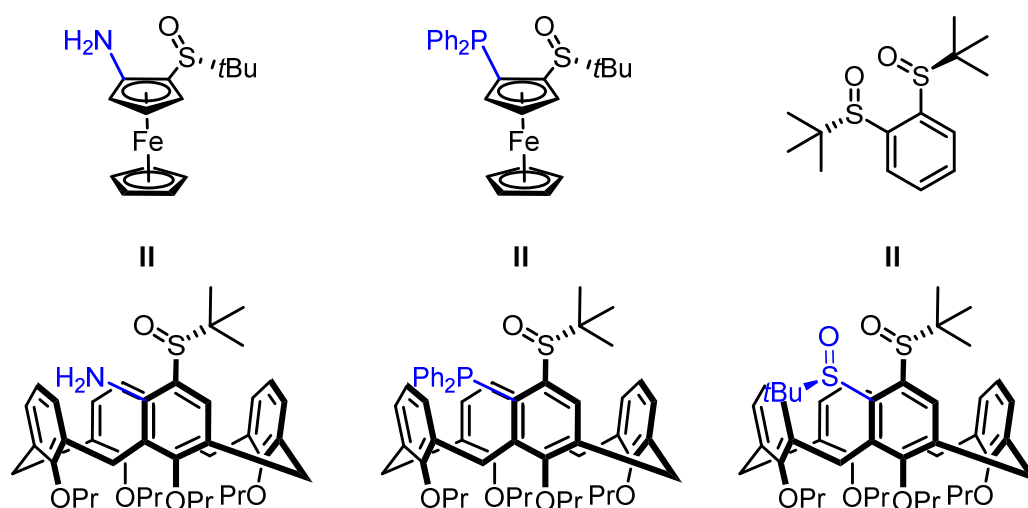


Figure 7.3: Three potential inherently chiral calixarenes including the chiral sulfoxide auxiliary.

The three examples above are based on previously reported amino sulfoxide (left),^{29,30} phosphine sulfoxide (middle)^{31,32} and disulfoxide ligands.³³

7.4 Final remarks.

We have only scratched the surface in the application of *meta*-functionalized inherently chiral ligands. There are many examples of asymmetric reactions which can be used to evaluate the calixarene Phox ligands. Besides this, there are still structural variations of the ligands reported here that can be investigated. The primary focus of this would be the incorporation of different dialkyl and diaryl phosphine groups, with a view to manipulating the electronic and steric contributions made by these functional groups on the transfer of chiral information seen in the Tsuji-Trost allylation reaction.

It has only been briefly discussed here, but there are still many potential mono- and bi-dentate ligand motifs that can be attained using the chemistry outlined in **Chapter 3** and **4**. This dissertation has focused exclusively on developing ligand based applications for these compounds, but there are still many other potential functions that can be explored. The previously mentioned selective storage, enzyme mimic, stationary phase and molecular recognition capabilities are only a few options.

7.5 References.

- (1) Sokolie, T.; Menyese, U.; Roth, U.; Jira, T. *J. Chromatogr. A* **2000**, *898*, 35.
- (2) Ding, C.; Qu, K.; Li, Y.; Hu, K.; Liu, H.; Ye, B.; Wu, Y.; Zhang, S. *J. Chromatogr. A* **2007**, *1170*, 73.
- (3) Enright, G. D.; Udachin, K. A.; Moudrakovski, I. L.; Ripmeester, J. A. *J. Am. Chem. Soc.* **2003**, *125*, 9896.
- (4) Dalgarno, S. J.; Thallapally, P. K.; Barbour, L. J.; Atwood, J. L. *Chem. Soc. Rev.* **2007**, *36*, 236.
- (5) Raynal, M.; Ballester, P.; Vidal-Ferran, A.; van Leeuwen, P. W. N. M. *Chem. Soc. Rev.* **2014**, *43*, 1734.
- (6) Dondoni, A.; Marra, A. *Chem. Rev.* **2010**, *110*, 4949.
- (7) Shirakawa, S.; Moriyama, A.; Shimizu, S. *Org. Lett.* **2007**, *9*, 3117.
- (8) Luo, J.; Zheng, Q-Y.; Chen, C-F.; Huang, Z-T. *Tetrahedron* **2005**, *61*, 8517.
- (9) Zeng, W.; Zhou, Y-G. *Org. Lett.* **2005**, *7*, 5055.
- (10) Bianco, A.; Maggini, M.; Scorrano, G.; Toniolo, C.; Marconi, G.; Villani, C.; Prato, M. *J. Am. Chem. Soc.* **1996**, *118*, 4072.
- (11) Sebahar, P. R.; Williams, R. M. *J. Am. Chem. Soc.* **2000**, *122*, 5666.
- (12) Garner, P.; Cox, P. B.; Anderson, J. T.; Protasiewicz, J.; Zaniewski, R. *J. Org. Chem.* **1997**, *62*, 493.
- (13) Denhart, D. J.; Griffith, D. A.; Heathcock, C. H. *J. Org. Chem.* **1998**, *63*, 9616.
- (14) Cabrera, S.; Arrayás, R. G.; Carretero, J. C. *J. Am. Chem. Soc.* **2005**, *127*, 16394.
- (15) Llamas, T.; Arrayás, R. G.; Carretero, J. C. *Synthesis*. **2007**, 0950.
- (16) Longmire, J. M.; Wang, B.; Zhang, X.; Park, U. V.; Pennsylv, V. *J. Am. Chem. Soc.* **2002**, 13400.
- (17) Gao, W.; Zhang, X.; Raghunath, M. *Org. Lett.* **2005**, 2003.
- (18) Nishibayashi, Y.; Yamauchi, A.; Onodera, G.; Uemura, S. *J. Org. Chem.* **2003**, *68*, 5875.
- (19) Onodera, G.; Nishibayashi, Y.; Uemura, S. *Angew. Chem., Int. Ed.* **2006**, *45*, 3819.
- (20) Naud, F.; Malan, C.; Spindler, F.; Rüggeberg, C.; Schmidt, A. T.; Blaser, H. U. *Adv. Synth. Catal.* **2006**, *348*, 47.
- (21) Trost, B. M.; Rao, M. *Angew. Chem., Int. Ed.* **2015**, *54*, 5026.
- (22) Gómez, R. A.; Adrio, J.; Carretero, J. C. *Angew. Chem., Int. Ed.* **2006**, *45*, 7674.
- (23) Hargaden, G. C.; Guiry, P. J. *Chem. Rev.* **2009**, *109*, 2505.

Chapter 7: Conclusions and future work.

- (24) McManus, H. A; Guiry, P. J. *Chem. Rev.* **2004**, *104*, 4151.
- (25) Xu, G.; Gilbertson, S. R. *Tetrahedron Lett.* **2003**, *44*, 953.
- (26) Franzke, A.; Pfaltz, A. *Chem. - A Eur. J.* **2011**, *17*, 4131.
- (27) Bolm, C.; Xiao, L.; Kesselgruber, M. *Org. Biomol. Chem.* **2003**, *1*, 145.
- (28) Gilbertson, S. R.; Fu, Z. *Org. Lett.* **2001**, *3*, 161.
- (29) Priego, J.; Mancheno, O. G.; Cabrera, S.; Carretero, J. C. *Chem. Commun.* **2001**, 2026.
- (30) Garcí, O.; Cabrera, S.; Carretero, J. C. *J. Org. Chem.* **2002**, 1346.
- (31) Lang, F.; Li, D.; Chen, J.; Chen, J.; Li, L.; Cun, L.; Zhu, J.; Deng, J.; Liao, J. *Adv. Synth. Catal.* **2010**, *352*, 843.
- (32) García Mancheño, O.; Priego, J.; Cabrera, S.; Gómez Arrayás, R.; Llamas, T.; Carretero, J. C. *J. Org. Chem.* **2003**, *68*, 3679.
- (33) Han, F.; Chen, J.; Zhang, X.; Liu, J.; Cun, L.; Zhu, J.; Deng, J.; Liao, J. *Tetrahedron Lett.* **2011**, *52*, 830.

8 Chapter 8 - Additional supporting information

8.1 General Practices.

8.1.1 *Solvents and reagents.*

Chemicals used in these experiments were purchased from Merck or Aldrich. Tetrahydrofuran, diethyl ether, toluene and pentane were distilled under nitrogen from sodium wire/sand using benzophenone as an indicator, alternatively they were dried for at least two days in a sealed Schlenk flask, under argon, with molecular sieves. Solvent was also collected under inert conditions from an Innovative Technologies PureSolve PS-MP-5 solvent purification system. Dichloromethane was distilled under nitrogen from calcium hydride. Other reagents requiring purification were purified according to standard procedures.¹

8.1.2 *Temperature control.*

Low temperature reactions were performed in a Dewar containing dry ice in acetone ($-78\text{ }^{\circ}\text{C}$), or a slurry of ethanol, sodium chloride and ice ($-20\text{ }^{\circ}\text{C}$). Reactions requiring precise, extended low temperature control, were performed in a Dewar regulated with a Thermo Scientific Haake EK90 Immersion Cooler.

8.1.3 *Inert conditions.*

Glassware was oven dried, thereafter it was placed under vacuum of $<0.5\text{ mm Hg}$ and cyclically flushed with nitrogen/argon and evacuated until it had reached room temperature. Standard Schlenk techniques were employed when necessary. All reactions were performed under a positive pressure of 2.8 kPa of 5.0 grade nitrogen or argon (Air Products).

8.1.4 *Chromatography.*

All column chromatography was performed on Merck silica gel 60 (particle size 0.040-0.063 mm) or neutral alumina, using one of or combinations of petroleum ether, diethyl ether, ethyl acetate, toluene, dichloromethane, ethanol and methanol as a solvent. Thin layer chromatography (TLC) was carried out on aluminum backed Merck silica gel or neutral alumina 60 F₂₅₄ plates. Visualization was performed with a UV lamp, using iodine on silica, or by spraying with a cerium ammonium molybdate (CAM) solution followed by heating

Chapter 8: Additional Supporting information

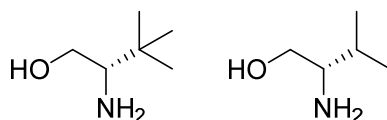
8.1.5 Characterization.

All nuclear magnetic resonance spectra were obtained using a 300 MHz Varian VNMRS (75 MHz for ^{13}C), 400 MHz Varian Unity Inova (100 MHz for ^{13}C), 600 MHz Varian Unity Inova (150 MHz for ^{13}C). Chemical shifts (δ) were recorded using the residual solvent peak or external reference. All chemical shifts are reported in ppm and all spectra were obtained at 25 °C unless otherwise reported. Data was processed using MestReNova version 6.0.2-5475.

Melting points were obtained using a Gallenkamp melting point apparatus or a Kofler microscope melting point machine and are uncorrected. Infrared spectra were obtained using the ATi Perkin Elmer Spectrum RX1 FTIR spectrometer using thin film (NaCl). High resolution mass spectrometry was performed by CAF (Central Analytical Facility) at Stellenbosch University using a Waters API Q-TOF Ultima.

8.2 Reagents required for starting material synthesis.

8.2.1 Reduction of chiral amino acids.²



L-*tert*-leucinol and L-valinol were prepared using the same experimental procedure. The amino acid (1.0 equiv) and NaBH₄ (2.5 equiv) were added all at once to dry THF under argon at room temperature. The resulting cloudy white reaction mixture was cooled (0 °C). Iodine (1.02 equiv) was then dissolved in dry THF and added dropwise to the cooled mixture, over a period of 30 min. Once the addition of iodine was complete, the reaction mixture was heated to reflux, which was maintained for 24 h. After cooling to room temperature, the reaction mixture was quenched by the careful addition of methanol. The excess solvent was then removed under reduced pressure affording a white viscous semi solid as the crude product. This was dissolved in a 4M solution of aqueous KOH and stirred at room temperature overnight. The product was extracted by washing the water layer numerous times with DCM. The organic layer was then washed with 1M HCl, brine and dried over MgSO₄. The excess solvent was removed under reduced pressure yielding an opaque oil as the crude product. Purification was achieved via Kugelrohr distillation, affording the L-*tert*-leucinol and L-valinol in yields of 80% and 72% respectively.

The characterisation data collected for this compound compared well with the reported literature values.²

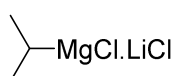
Chapter 8: Additional Supporting information

L-tert-leucinol

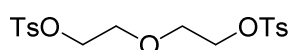
^1H NMR (300 MHz, CHLOROFORM-*d*) δ 0.89 (s, 9H, C(CH₃)₃), 2.00 (br. s, 3H, OH, NH₂), 2.50 (dd, *J* = 9.8, 3.7 Hz, 1H, NH₂NHCH₂), 3.20 (m, 1H, CHCH₂O), 3.70 (dd, *J* = 10.2, 3.8 Hz, 1H, CHCH₂O) ppm.

L-valinol

^1H NMR (300 MHz, CHLOROFORM-*d*) δ 0.92 (d, *J* = 4.2 Hz, 3H, CH(CH₃)₂), 0.93 (d, *J* = 4.2 Hz, 3H, CH(CH₃)₂), 1.49-1.66 (m, 1H, CH(CH₃)₂), 1.81 (br. s, 3H, OH, NH₂), 2.50-2.59 (m, 1H, CH₂CHN), 3.28 (dd, *J* = 10.5, 4.0 Hz, 1H, OCH₂CH), 3.64 (dd, *J* = 10.5, 4.0 Hz, 1H, OCH₂CH) ppm.

8.2.2 Synthesis of *i*PrMgCl·LiCl.

Magnesium metal turnings (4.00 g, 165 mmol, 1.65 equiv) were added to freshly distilled THF (100 ml) under argon at room temperature. Isopropyl chloride (9.20 ml, 100 mmol) was added dropwise and stirred at for 24 h at room temperature. During this time the reaction mixture had black. Oven dried LiCl (4.60 g, 110 mmol 1.1 equiv) was then added to the reaction mixture, which was stirred for a further 24 h at room temperature. The concentration of grey black solution was found to be 0.78 M after titration with *t*-BuOH and 2,2-bipyridine. The solution was stored at $-16\text{ }^\circ\text{C}$.

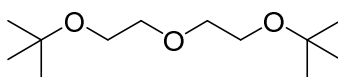
8.3 Reagents required for ortholithiation studies.8.3.1 Synthesis of di-tosyl-diethylene glycol.³

Diethylene glycol (9.0 ml, 93.1 mmol) and tosyl chloride (39.0 g, 205 mmol, 2.2 equiv) were added to freshly distilled DCM (150 ml) and cooled (0 °C). Et₃N (39.0 ml, 280.0 mmol, 3.0 equiv) and DMAP (cat.) were then added. The reaction mixture was then allowed to warm to room temperature and the reaction mixture was stirred overnight. Additional DCM was added to flask and the contents was transferred to a separating funnel. The organic layer was washed with H₂O (150 ml) and 1M HCl (150 ml). After drying over MgSO₄, the excess solvent was removed under reduced pressure yielding a white solid as the crude product. Purification was achieved by recrystallization from hot toluene, yielding a white solid (30.2 g, 79%).

The characterisation data collected for this compound compared well with the reported literature values.³

^1H NMR (300 MHz, CHLOROFORM-*d*) δ 2.43 (s, 6H, (SO₂)CH₃), 3.56-3.62 (m, CH₂O 4H), 4.06-4.10 (m, 4H, CH₂CH₂O), 7.31-7.36 (m, 4H, ArH), 7.76-7.78 (m, 4H, ArH) ppm.

Chapter 8: Additional Supporting information

8.3.2 Synthesis of di-tert-butyl-diethylene glycol.⁴

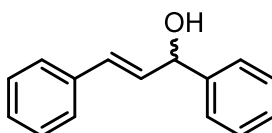
t-BuOH (60.0 ml, exs) was added to freshly distilled THF (40 ml) under argon. Sodium metal (5.00 g, 208 mmol, 5.8 equiv) was cut into small pieces and added to the mixture, which was then stirred at room temperature for 24 h. Once the sodium had dissolved, the reaction mixture had turned a cloudy white. Di-tosyl-diethylene glycol (15.0 g, 36.0 mmol) was then added, turning the white reaction mixture orange. After adding additional THF (50.0 ml), the reaction was heating to reflux, which was maintained for 24 h. The reaction mixture was then cooled to room temperature and stirred for an additional 24 h. The solid salts were filtered from the reaction and washed with portions of PET. The organic layers were then concentrated affording a yellow/brown oil as the crude product. Purification was achieved via Kugelrohr distillation, yielding a colourless oil (2.70 g, 34%).

The characterisation data collected for this compound compared well with the reported literature values.⁴

¹H NMR (300 MHz, CHLOROFORM-*d*) δ 1.17 (s, 18H, C(CH₃)₃), 1.18 (s, 18H, C(CH₃)₃), 3.47-3.51 (m, 4H, OCH₂CH₂O), 3.57-3.61 (OCH₂CH₂O) ppm.

8.4 Reagents required for ligand application studies.

8.4.1 Tsuji-Trost allylation.

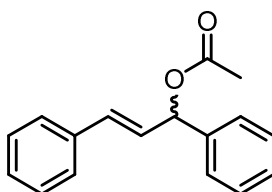
8.4.1.1 (*E*)-1,3-diphenylprop-2-en-1-ol.⁵

Magnesium turnings (4.60 g, 191 mmol, 1.3 equiv) were added to dry Et₂O (50 ml). Bromo benzene (20.0 ml, 131 mmol, 1.3 equiv) was diluted with Et₂O (50 ml). This mixture was then added to the Mg/Et₂O mixture at 20 ml/h. Once the addition was complete, the reaction mixture was heated to reflux for 45 min. The reaction mixture was then cooled (0 °C) and cinnamaldehyde (18.5 ml, 147 mmol) was added dropwise at 20 ml/h. The reaction mixture was allowed to warm to room temperature and stirred overnight. The reaction was finally quenched with sat. NH₄Cl. The organic layer was washed with H₂O (100 ml), dried over MgSO₄ and the excess solvent was removed under reduced pressure, yielding a yellow semi-solid as the crude product. Purification was achieved by recrystallization from pentane, affording the alcohol product as yellow needle-like crystals (12.3 g, 30%).

The characterisation data collected for this compound compared well with the reported literature values.⁵

Chapter 8: Additional Supporting information

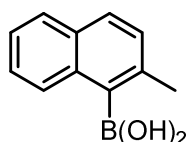
^1H NMR (300 MHz, CHLOROFORM-*d*) δ 2.07 (d, $J = 3.7$ Hz, 1H, ArCHCH), 6.34 (dd, $J = 6.0, 3.7$ Hz, 1H, ArCHCH), 6.64 (d, $J = 15.9$ Hz, 1H, ArCHO), 7.16-7.40 (m, 10H, ArH).

8.4.1.2 *(E)-1,3-diphenylallyl acetate.*⁶

1,3-diphenyl alcohol (3.00 g, 14.3 mmol) was added to freshly distilled DCM (80 ml) and cooled (0 °C). Acetic anhydride (4.00 ml, 28.6 mmol, 2.0 equiv) and DMAP (cat) were then added. The reaction was allowed to warm to room temperature and TLC analysis confirmed the completion of the reaction after 20 min. The contents of the flask was transferred to a separating funnel. The organic layer was washed with sat. NaHCO_3 (50 ml), brine (50 ml) and dried over MgSO_4 . The excess solvent was removed under reduced pressure, yielding a yellow oil as the crude product. Purification was achieved by silica gel column chromatography, (EtOAc:PET, 5:95), yielding a colourless oil (3.24 g, 90%).

The characterisation data collected for this compound compared well with the reported literature values.⁶

^1H NMR (300 MHz, CHLOROFORM-*d*) δ 2.09 (s, 3H, OCH_3), 6.63 (dd, $J = 15.7, 6.8$ Hz, 1H, ArCHCH), 6.41 (d, $J = 6.8$ Hz, 1H, ArCHCH), 6.60 (d, $J = 15.6$ Hz, 1H, ArCHO), 7.19-7.40 (m, 10H, ArH) ppm.

8.4.1 *Asymmetric Suzuki cross-coupling.*8.4.1.1 *Synthesis of (2-methylnaphthalen-1-yl)boronic acid.*⁷

1-bromo-2-methylnaphthalene (2.00 g, 9.04 mmol) was added to freshly distilled THF (50 ml) under argon and cooled (-78 °C). *n*-BuLi (13.6 mmol, 1.5 equiv) was then carefully added, turning the colourless mixture a clear yellow colour. After stirring for 15 min, freshly distilled trimethyl borate (2.50 ml, 22.6 mmol, 2.5 equiv) was added. The reaction mixture was given time to warm to room temperature and stirred overnight. It was finally quenched with 1M HCl, after which the product was extracted with DCM. The organic layer was washed with an additional portion of 1M HCl (50 ml), dried over MgSO_4 , and the excess solvent was removed under reduced pressure. Purification was achieved via trituration from PET at room temperature. The white solid was collected via filtration (1.21 g, 72%).

The characterisation data collected for this compound compared well with the reported literature values.

8.6 References.

- (1) Perrin, D. D.; Armarego, W. L. F. *Purification of Laboratory Chemicals*; 3rd ed.; Pergamon Press: Oxford, 1988.
- (2) McKennon, M. J.; Meyers, A. I. *J. Org. Chem.* **1993**, *58*, 3568.
- (3) Mohler, D. L.; Shen, G. *Org. Biomol. Chem.* **2006**, *4*, 2082.
- (4) Herbert, S. A.; Castell, D. C.; Clayden, J.; Arnott, G. E. *Org. Lett.* **2013**, *15*, 3334.
- (5) Stoner, E. J.; Cothron, D. A.; Balmer, M. K.; Roden, B. A. *Tetrahedron* **1995**, *51*, 11043.
- (6) Leung, W.; Cosway, S.; Jones, R. H. V.; McCann, H.; Wills, M. J. *Chem. Soc., Perkin Trans. 1* **2001**, 2588.
- (7) Shin, M. G.; Kim, S. O.; Park, H. T.; Park, S. J.; Yu, H. S.; Kim, Y. H.; Kwon, S. K. *Dyes Pigm.* **2012**, *92*, 1075.